Model compounds for intermediates and transition states in Sonogashira and Negishi coupling: d8-d10 bonds in large heterobimetallic complexes are weaker than computational chemistry predicts.

Author(s):
Oeschger, Raphael; Bissig, Raphael; Chen, Peter

Publication date:
2022-06-15

Permanent link:
https://doi.org/10.3929/ethz-b-000554108

Originally published in:
Journal of the American Chemical Society 144(23), https://doi.org/10.1021/jacs.2c01641

Supporting Information

Model compounds for intermediates and transition states in Sonogashira and Negishi coupling: d^8-d^{10} bonds in large heterobimetallic complexes are weaker than computational chemistry predicts.

Raphael J. Oeschger, Raphael Bissig, Peter Chen*

Laboratorium für Organische Chemie, ETH Zürich, Vladimir-Prelog-Weg 2, 8093 Zürich, Switzerland

*peter.chen@org.chem.ethz.ch

Contents

1. Experimental

1.1. General Information

General: Unless otherwise stated, all reactions were carried out under an atmosphere of argon using standard Schlenk techniques or in a nitrogen filled glovebox. Reactions where Ag(I) was present were conducted with minimal sources of light present.

Solvents: All solvents were dried and distilled prior to use : dichloromethane (DCM) / acetonitrile (MeCN) / 1,2-difluorobenzene (DFB) over CaH_2; *n*-hexane, *n*-pentane, diethylether (Et_2O), tetrahydrofuran (THF) over Na/benzophenone with tetraethyleneglycoldimethylether (TEGDME); toluene over Na; MeOH over Mg. The solvents were stored over molecular sieves in a N_2-filled glovebox. Commercially available ethyl acetate (EtOAc, Acros Organics with Acroseal) was stored over molecular sieves prior to use. Deuterated solvents were dried by storing over molecular sieves for at least 3 days prior to use.

Commercial consumables: Syringe filters (PTFE, pore size 0.2 µm, diameter. 13 mm, Whatman or PTFE, pore size 0.45 µm, diameter 25 mm, CHROMAFIL) were dried using a vacuum oven at 60 °C for at least 3 days prior to use.

Commercially available compounds: *n*-Butyllithium in *n*-hexane solution (*n*-BuLi, 1.6 M in *n*-hexane, Sigma Aldrich) was titrated with *sec*-Butanol using 2,2'-bipyridine as an indicator prior to use. The following chemicals were purchased and used without further purifaction: *N,N,N',N'*-tetramethylethylenediamine (TMEDA, Aldrich ≥99.5%), allyl bromide (Acros, 99%), paraformaldehyde (Acros, 96%), hydrogen chloride solution 4M in 1,4-dioxane (Alfa Aesar), potassium *tert*-butoxide (KO^tBu, Sigma Aldrich), copper(I) chloride (CuCl, Fluka), Chloro[1,3-bis(2,6-diisopropylphenyl)imidazol-2-ylidene]copper(I) ([(IPr)CuCl], TCI), Chloro[1,3-bis(2,6-diisopropylphenyl)imidazol-2-ylidene]silver(I) ([(IPr)AgCl], TCI), Chloro[1,3-bis(2,6-diisopropylphenyl)imidazol-2-ylidene]gold(I) ([(IPr)AuCl], ABCR), Sodium tetrakis[3,5-bis(trifluoromethyl)phenyl]borate (NaBArF, Apollo), silver tetrafluoroborate ($AgBF_4$, ABCR) , silver trifluoromethanesulfonate (AgOTf, ABCR).

Reported compounds: *cis*-Bis(benzo[*h*]quinoline)palladium(II)[1] ($Pd(bhq)_2$), [(2,6-($^iPr_2PO)_2C_6H_3$)Pd(CCPh)][2] ([^{iPr}POCOP)Pd(CCPh)], Bis(2,6-diisopropylphenyl)butane-2,3-diimine[3] were synthesized according to literature.

Analytical instrumentation:

NMR spectra were recorded on a Bruker Ascend 500 MHz or Bruker Ascend 400 MHz and were analyzed using the MestReNova (v14.1.0-24037) software suite. The spectra were referenced to the specific residual solvent peak[4]: ^{1}H-NMR (CD_2Cl_2) δ = 5.32 ppm, ^{13}C-NMR (CD_2Cl_2) δ = 53.84 ppm. In ^{1}H-NMR spectra the peak integrals were normalized to a well separated and identifiable peak or so that the sum of compound peak integrals added up to the expected number of H nuclei.

XRD measurements were performed by the in-house service. Temperature sensitive compounds were transported in a pre-cooled (-35°C) dewar and immediately transferred onto a µChill coldhead[5] device using a pipette. The crystals were kept at low temperatures with a constant flow of cold inert gas during the preparation of the XRD measurement. Single crystals of the compound were selected and mounted on a XtaLAB Synergy, Dualflex, Pilatus 300K diffractometer (or on a Bruker Apex2 Duo (Mo) diffractometer). The crystals were kept at 100.0(1) K or 200(1) K during data collection. Using Olex2[6], the structure was solved with either the SHELXT[7] (or the XT[7]) structure solution program using Intrinsic Phasing and refined with the SHELXL[8] (or the XL[9]) refinement package using Least Squares minimization. The obtained data were analyzed using the Mercury software suite (Version 3.10.3).

Elemental Analysis, the quantitative measurement of the elemental composition of a compound with respect to specific elements was performed by the in-house service. For C, H, N, a LECO TruSpec Micro instrument was used, wherein the gaseous combustion products of C (CO_2) and H (H_2O) are quantified by means of infrared spectroscopy. Nitrogen is measured as N_2 with a thermal conductivity detector. Elemental compositions of the halides Cl and F were determined by digesting the sample using the Schöniger method, followed by capturing combustion products in an absorbing

solution with subsequent quantification by ion chromatography. Compounds were dried a few days before performing Elemental analysis.

Electrospray Ionisation (ESI) high resolution mass spectrometry (HR-MS) measurements for analytical purposes were performed by the in-house service on a Bruker Daltonics maXis ESI-QTOF Instrument.

Qualitative MS measurements:

Qualitative Electrospray Ionization Mass Spectrometry (ESI-MS) experiments were performed on a Thermo Finnigan TSQ Quantum triple quadrupole mass spectrometer. Gas-tight syringes were used for spray solution injection.

1.2. Synthesis of Pincer based Bimetallic Compounds

1.2.1. Overview and Additional Information

The synthesis of the here reported bimetallic complexes is summarized in Table SI-1. The complexes can be formed by combining a palladium pincer complex [(^{iPr}POCOP)Pd(CCPh)] with a cation, formally written as [(IPr)M]$^+$, derived from the corresponding salt. While the palladium complex is bench stable and easy to handle, this is not necessarily true for the [(IPr)MX] fragment. [(IPr)M]$^+$ can be generated from commercially available [(IPr)MCl] by halide cleavage. The preparation of the bimetallic complexes afforded side products, e.g. pseudo dimeric products [((^{iPr}POCOP)Pd(CCPh))$_2$Ag]X, [(IPr)$_2$AgX], [(IPr)Au(CCPh)·Au(IPr)]. The magnitude of these side products depended mainly on the order of addition and the stoichiometric precision. Crystallization, being the applied method of purification, leads to the observation of all these side products. Fractional crystallization resulted in different orders of crystallization of the mentioned compounds. In order to have a clean crystallization of the bimetallic compound, the desired species had to be dominant. In particular the synthesis of the [(IPr)Ag]$^+$ systems required specific conditions. A major side product stemming from the halide cleavage of [(IPr)AgCl] was [(IPr)$_2$Ag]$^+$, this being presumably a consequence from the transmetalation of an IPr-organyl from one [(IPr)Ag]$^+$ or [(IPr)AgCl] to another in a bimolecular process, hence it can be prevented by the slow addition of [(IPr)AgCl] to the cleavage ragent, e.g. AgX. The concentration of [(IPr)Ag]$^+$ being in substoichiometric amounts (compared to the palladium complex already present in the solution) lead to reduced amounts of the [(IPr)$_2$Ag]$^+$ pseudo-dimers.

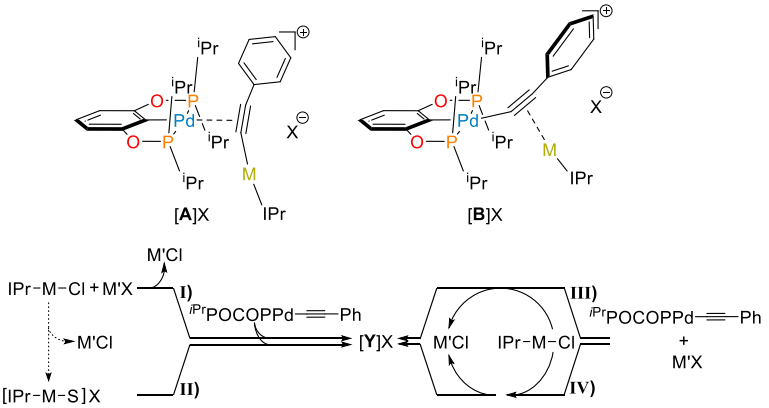

Pathway	M'	Conditions Solvents / *Added Solvent for Crys.*	Compound [**Y**]X [**A**]X	 [**B**]X
I)	Ag	THF / *Et$_2$O*	-	[**1**]BF$_4$
II)	-	DFB / *n*-hexane or THF / *Et$_2$O*	[**3**]BF$_4$	[**1**]BArF, [**3**]BArF
III)	Ag	DFB / THF/ *n*-hexane	[**3**]OTf[a]	[**2**]BF$_4$, [**2**]OTf
IV)	Na	1) CH_2Cl_2, 2) THF / *Et$_2$O* / *n*-hexane	-	[**2**]BArF

Table SI-1: Schematic overview for the bulk synthesis of the Pincer-based compounds. Equimolar stoichiometries for all reactions. I) Halide cleavage with subsequent filtration and addition to the Pd complex, II) simple addition, III) dropwise addition of [(IPr)MCl] with subsequent filtration, IV) dropwise addition of [(IPr)MCl] followed by solvent replacement and subsequent filtration. All compounds [Y]X were isolated by crystallization. All crystals were grown at -35°C. a) Contamination observed, was not obtained pure.

1.2.2. Synthesis of [(^{iPr}POCOP)Pd^{II}(CCPh)•Cu^{I}(IPr)]BF_4, [**1**]BF_4:

[(IPr)CuCl] (9.7 mg, 20 µmol, 1 eq.) and $AgBF_4$ (3.9 mg, 20 µmol, 1 eq.) were suspended in THF (1 mL) in a vial in the glovebox. After 5 min, the suspension was filtered through a syringe filter and added to a solution of [(^{iPr}POCOP)Pd(CCPh)] (11.0 mg, 20 µmol, 1 eq.) in THF (0.6 mL). The reaction mixture was filtered through a syringe filter to a new vial, the syringe filter was rinsed with THF (0.2 mL). This solution was layered with Et_2O (2 mL) and cooled to -35°C (crys. from solvent-mixture: THF approx. 1.8 mL, Et_2O approx. 2 mL). Crystals were kept at this temperature and formed after 2-3 days. The supernatant was removed and the crystals were crushed and dried by vacuum. A white powder was obtained (3 mg, 3.2 µmol, yield: 14 %, post-analytics).

^{1}H NMR (400 MHz, CD_2Cl_2) δ (ppm) 7.57 (t, 2H, *J*=7.8 Hz), 7.36 – 7.26 (m, 1H), 7.31 (d, *J* = 7.8 Hz, 4H), 7.22 (s, 2H), 7.16 (t, 2H, *J*=7.8 Hz), 6.99 (tt, 1H, *J*=8.0, 1.2 Hz), 6.71 – 6.63 (m, 2H), 6.55 (d, 2H, *J*=8.0 Hz), 2.54 (hept, 4H, *J*=6.9 Hz), 2.08 (hept, 4H, *J*=7.3 Hz), 1.18 (d, 12H, *J*=6.8 Hz), 1.16 – 1.09 (m, 12H), 1.09 (d, 12H, *J*=7.0 Hz), 1.07 – 0.98 (m, 12H)

^{13}C{^{1}H} NMR (101 MHz, CD_2Cl_2)[a] δ (ppm) 145.82, 134.89, 132.28, 131.33, 129.82 (d, *J*=2.8 Hz), 129.46, 125.15, 125.05, 106.13 (t, *J*=7.3 Hz), 29.64 (t, *J*=12.5 Hz), 29.19, 24.78, 24.23, 18.03 (t, *J*=3.4 Hz), 16.74 ppm

^{31}P{^{1}H} NMR (162 MHz, CD_2Cl_2) δ (ppm) 192.20

^{19}F{^{1}H} NMR (377 MHz, CD_2Cl_2)[b] δ (ppm) -153.53, -153.58

^{11}B NMR (128 MHz, CD_2Cl_2) δ (ppm) -1.16

(for NMR spectra see Section 3.1.1)

ESI-HRMS Positive mode: calculated for $C_{53}H_{72}CuN_2O_2P_2Pd^+$ [M^+] 999.3410 m/z; found 999.3402 m/z. Negative mode: calculated for BF_4^- [M^-] 87.0035 m/z; found 87.0037 m/z.

Crystal Data for $C_{65}H_{96}BCuF_4N_2O_5P_2Pd$ (*M* =1304.12 g/mol): monoclinic, space group $P2_1/c$ (no. 14), *a* = 12.49750(10) Å, *b* = 23.21590(10) Å, *c* = 22.65500(10) Å, *β* = 90.4240(10)°, *V* = 6572.96(7) Å^3, *Z* = 4, *T* = 100.0(1) K, µ(Cu Kα) = 3.544 mm^{-1}, *Dcalc* = 1.318 g/cm^3, 93018 reflections measured (7.074° ≤ 2Θ ≤ 159.708°), 14123 unique (R_{int} = 0.0488, R_{sigma} = 0.0269) which were used in all calculations. The final R_1 was 0.0403 (I > 2σ(I)) and wR_2 was 0.1147 (all data).

(for further information on crystal structure see Section 3.3.1)

1.2.3. Synthesis of [(IPr)Cu^{I}(THF)]BArF:

In a vial, [(IPr)CuCl] (152 mg, 0.3 mmol, 1 eq.) and NaBArF (276 mg, 0.3 mmol, 1 eq.) were combined and suspended in THF (extra dry, 2 mL). The suspension was stirred at r.t. overnight. The solvent was evaporated and the remaining solid was suspended in dichloromethane (extra dry, 3 mL). The suspension was filtered through a syringe filter and the solvent was subsequently removed by vacuum evaporation to afford the product (white powder, 384.57 mg). This compound was used without further purification.

1.2.4. Synthesis of [(^{iPr}POCOP)Pd^{II}(CCPh)•Cu^{I}(IPr)]BArF, [**1**]BArF:

a) The bimetallic complex was prepared by dissolving [(^{iPr}POCOP)Pd(CCPh)] (13.5 mg, 25 µmol, 1 eq.) and [(IPr)Cu(THF)]BArF (32.5 mg) in 1,2-$C_6H_4F_2$ (1.5 mL) in a vial in the glovebox. The solution was filtered through a syringe filter twice, layered with *n*-hexane (2 mL), and cooled to -35 °C (crys. from solvent-mixture: 1,2-$C_6H_4F_2$ approx. 1.5 mL, *n*-hexane approx. 2 mL). Crystals were formed after 3 days. The supernatant was removed and the crystals were washed with *n*-hexane (1 mL), crushed and dried by vacuum and a white powder was obtained (19.05 mg, 10 µmol, yield: 42 %).

^{1}H NMR (400 MHz, CD_2Cl_2) δ (ppm) 7.75 – 7.69 (m, 8H), 7.60 – 7.52 (m, 2H), 7.56 (s, 4H), 7.34 – 7.27 (m, 1H), 7.30 (d, *J* = 7.8 Hz, 4H), 7.19 (s, 2H), 7.18 – 7.11 (m, 2H), 7.03 – 6.94 (m, 1H), 6.70 – 6.63 (m, 2H), 6.55 (d, 2H, *J*=8.0 Hz), 2.53 (hept, 4H, *J*=6.9 Hz), 2.08 (hept, 4H, *J*=7.1 Hz), 1.17 (d, 12H, *J*=6.8 Hz), 1.16 – 1.09 (m, 12H), 1.09 (d, 12H, *J*=7.0 Hz), 1.08 – 0.97 (m, 12H)

---

[a] ^{13}C{^{1}H}-NMR peak-assignments not comprehensive.

[b] ^{19}F{^{1}H}-NMR of compounds with BF_4^- counterion show two peaks. This observation can be explained by the effect of two different boron isotopes ^{10}B (abund. 19.9 %) and ^{11}B (abund. 80.1 %) in close proximity to the ^{19}F nuclei. The different isotopes lead to the two observed chemical shifts in ^{19}F NMR (^{10}B downfield shift, ^{11}B upfield shift).

$^{13}C\{^1H\}$ NMR (101 MHz, CD_2Cl_2)[a] δ (ppm) 145.81, 135.21, 134.87, 132.28, 131.34, 129.86, 129.80, 129.45, 126.36, 125.07, 125.05, 117.88, 106.14, 29.64 (t, *J*=12.4 Hz), 29.19, 24.76, 24.20, 18.02 (t, *J*=3.3 Hz), 16.73

$^{31}P\{^1H\}$ NMR (162 MHz, CD_2Cl_2) δ (ppm) 192.12

$^{19}F\{^1H\}$ NMR (377 MHz, CD_2Cl_2) δ (ppm) -62.89

(for NMR spectra see Section 3.1.2)

ESI-HRMS Positive mode: calculated for $C_{53}H_{72}CuN_2O_2P_2Pd^+$ [M^+] 999.3410 m/z; found 999.3399 m/z. Negative mode: calculated for $C_{32}H_{12}BF_{24}^-$ [M^-] 863.0660 m/z; found 863.0662 m/z.

Elemental Analysis: Calc: C: 54.76 %, H: 4.54 %, N: 1.50 %. Found C: 54.74 %, H: 4.40 %, N: 1.88 %.

b) The bimetallic complex was prepared by dissolving ($^{i\text{Pr}}$POCOP)PdCCPh (5.5 mg, 10 mmol) and (IPr)Cu(THF)]BArF (13 mg, 10 mmol) in 1,2-$C_6H_4F_2$ (0.6 mL) in a vial in the glovebox. The solution was filtered through a syringe filter, layered with *n*-hexane (0.8 mL), and cooled to -35 °C. Crystals were formed after 2 days.

Crystal Data for $C_{85}H_{84}BCuF_{24}N_2O_2P_2Pd$ (*M* =1864.23 g/mol): triclinic, space group P-1 (no. 2), *a* = 15.71856(6) Å, *b* = 16.47461(7) Å, *c* = 18.04887(8) Å, *α* = 105.5135(4)°, *β* = 107.5009(4)°, *γ* = 97.1043(3)°, *V* = 4187.85(3) Å^3, *Z* = 2, *T* = 100.0(1) K, μ(CuKα) = 3.299 mm^{-1}, *Dcalc* = 1.478 g/cm^3, 165102 reflections measured (5.71° ≤ 2Θ ≤ 159.234°), 17788 unique (R_{int} = 0.0334, R_{sigma} = 0.0168) which were used in all calculations. The final R_1 was 0.0267 (I > 2σ(I)) and wR_2 was 0.0698 (all data).

(for further information see Section 3.3.2)

1.2.5. Synthesis of [($^{i\text{Pr}}$POCOP)Pd$^{\text{II}}$(CCPh)•Ag$^{\text{I}}$(IPr)]BF4, [**2**]BF_4:

a) [($^{i\text{Pr}}$POCOP)Pd(CCPh)] (19.9 mg, 36 μmol) and $AgBF_4$ (7.1 mg, 36 μmol) were combined and suspended with 1,2-$C_6H_4F_2$ (1 mL). [(IPr)AgCl] (20.2 mg, 38 μmol) was dissolved in THF (1 mL) and diluted with 1,2-$C_6H_4F_2$ (1 mL) and added dropwise (over 3 min) to the reaction mixture. The mixture was stirred for 5 min, filtered through a syringe filter. The clear solution was stepwise layered with *n*-hexane in the subsequent 10 days and kept at -35°C. When the mixture contained 1,2-$C_6H_4F_2$ (2 mL), THF (1 mL) and *n*-hexane (2 mL) in total, the solution was filtered using a syringe filter. The clear solution was layered with *n*-hexane (2 mL) and kept at -35 °C (crys. from solvent-mixture: 1,2-$C_6H_4F_2$ approx. 2 mL, THF approx. 1 mL, *n*-hexane approx. 4 mL). Crystals were observed after 5 days. The supernatant was removed and the crystals were crushed, washed with *n*-hexane (2 x 1 mL) and dried under vacuum and a white powder was obtained (8.4 mg, 7 μmol, yield: 20 %)

^1H NMR (400 MHz, CD_2Cl_2) δ (ppm) 7.53 (t, 2H, *J*=7.8 Hz), 7.38 – 7.32 (m, 1H), 7.31 – 7.25 (m, 6H), 7.25 – 7.18 (m, 2H), 6.99 (tt, 1H, *J*=8.0, 1.2 Hz), 6.83 (dt, 2H, *J*=8.3, 1.2 Hz), 6.55 (d, 2H, *J*=8.0 Hz), 2.53 (hept, 4H, *J*=6.9 Hz), 2.14 (hept, 4H, *J*=7.3 Hz), 1.18 (d, 12H, *J*=6.8 Hz), 1.16 – 1.08 (m, 24H), 1.05 – 0.96 (m, 12H) ppm

$^{13}C\{^1H\}$ NMR (101 MHz, CD_2Cl_2)[a] δ (ppm) 166.44, 145.86, 134.96, 132.80, 132.76, 131.37, 129.79, 129.73, 129.17, 125.30, 125.23, 124.96, 106.20, 106.13, 106.06, 29.71 (t, *J*=12.5 Hz), 29.10, 24.77, 24.21, 17.93 (t, *J*=3.2 Hz), 16.79

$^{31}P\{^1H\}$ NMR (162 MHz, CD_2Cl_2) δ (ppm) 192.75

$^{19}F\{^1H\}$ NMR (377 MHz, CD_2Cl_2)[b] δ (ppm) -153.49, -153.52 – -153.56 (m)

^{11}B NMR (128 MHz, CD_2Cl_2) δ (ppm) -1.17

(for NMR spectra see Section 3.1.3)

ESI-HRMS Positive mode: calculated for $C_{53}H_{72}AgN_2O_2P_2Pd^+$ [M^+] 1043.3149 m/z; found 1043.3164 m/z. Negative mode: calculated for BF_4^- [M^-] 87.0035 m/z; found 87.0031 m/z.

b) [(IPr)AgCl] (5.3 mg, 10 μmol) and $AgBF_4$ (2.0 mg, 10 μmol) were dissolved in THF (0.5 mL) in a vial in the glovebox. After 15 min, the suspension was filtered through a syringe filter and added to a solution of [($^{i\text{Pr}}$POCOP)Pd(CCPh)] (5.5 mg, 10 μmol) in THF (0.3 mL). This solution was layered with Et_2O (0.5 mL) and cooled to -35 °C. Crystals were formed after 4 days.

Crystal Data for $C_{61}H_{88}AgBF_4N_2O_4P_2Pd$ (*M* =1276.35 g/mol): triclinic, space group P-1 (no. 2), *a* = 11.22300(10) Å, *b* = 12.2171(3) Å, *c* = 23.2541(3) Å, *α* = 78.442(2)°, *β* = 83.5370(10)°, *γ* = 89.622(2)°, *V* = 3103.51(9) Å^3, *Z* = 2, *T* = 100.0(1) K, μ(CuKα) = 5.819 mm^{-1}, *Dcalc* = 1.366 g/cm^3, 114002 reflections measured (7.386° ≤ 2Θ ≤ 159.51°), 13209 unique (R_{int} = 0.0575, R_{sigma} = 0.0267) which were used in all calculations. The final R_1 was 0.0365 (I > 2σ(I)) and wR_2 was 0.0983 (all data).

(for further information see Section 3.3.3)

1.2.6. Synthesis of [($^{i\text{Pr}}$POCOP)Pd$^{\text{II}}$(CCPh)•Ag$^{\text{I}}$(IPr)]OTf, [**2**]OTf:

a) [($^{i\text{Pr}}$POCOP)Pd(CCPh)] (20.3 mg, 37 µmol) and AgOTf (9.5 mg, 37 µmol) were combined and suspended with 1,2-$C_6H_4F_2$ (1 mL). (IPr)AgCl (19.3 mg, 36 µmol) was dissolved in THF (1 mL) and diluted with 1,2-$C_6H_4F_2$ (1 mL) and added dropwise to the reaction mixture. The mixture was stirred for 5 min, filtered through a syringe filter. The clear solution was stepwise layered with *n*-hexane in the subsequent 6 days and kept at -35°C. When the mixture contained 1,2-$C_6H_4F_2$ (2 mL), THF (1 mL) and *n*-hexane (4 mL) in total, the solution was filtered using a syringe filter. The clear solution was layered with *n*-hexane (2 mL) and kept at -35 °C (crys. from solvent-mixture: 1,2-$C_6H_4F_2$ approx. 2 mL, THF approx. 1 mL, *n*-hexane approx. 6 mL). Crystals were observed after 2 days. The supernatant was removed and the crystals were crushed, washed with *n*-hexane (2 x 1 mL) and dried under vacuum and a white powder was obtained (24.3 mg, 20.3 µmol Yield: 55 %)

^{1}H NMR (400 MHz, CD_2Cl_2) δ (ppm) 7.53 (t, 2H, *J*=7.8 Hz), 7.35 (t, 1H, *J*=7.5 Hz), 7.32 – 7.25 (m, 6H), 7.22 (dd, 2H, *J*=8.4, 7.0 Hz), 6.99 (tt, 1H, *J*=8.0, 1.2 Hz), 6.84 (d, 2H, *J*=7.2 Hz), 6.55 (d, 2H, *J*=8.0 Hz), 2.53 (hept, 4H, *J*=6.9 Hz), 2.14 (hept, 4H, *J*=7.1 Hz), 1.18 (d, 12H, *J*=6.9 Hz), 1.16 – 1.07 (m, 24H), 1.02 (td, 12H, *J*=9.2, 7.0 Hz)

^{13}C{^{1}H} NMR (101 MHz, CD_2Cl_2)[a] δ (ppm) 166.51, 166.45, 166.39, 145.86, 134.96, 132.78, 131.36, 129.77, 129.17, 125.32, 125.25, 124.95, 106.19, 106.12, 106.04, 29.70 (t, *J*=12.6 Hz), 29.09, 24.77, 24.20, 17.92 (t, *J*=3.3 Hz), 16.79

^{31}P{^{1}H} NMR (162 MHz, CD_2Cl_2) δ (ppm) 192.78

^{19}F{^{1}H} NMR (377 MHz, CD_2Cl_2) δ (ppm) -78.94

(for NMR spectra see section 3.1.4)

ESI-HRMS Positive mode: calculated for $C_{53}H_{72}AgN_2O_2P_2Pd^+$ [M^+] 1043.3149 m/z; found 1043.3155 m/z.

Elemental Analysis: Calc: C: 54.30 %, H: 6.08 %, N: 2.35 %. Found C: 54.18 %, H: 5.98 %, N: 2.61 %.

b) [(IPr)AgCl] (7.1 mg, 13 µmol) and AgOTf (3.4 mg, 13 µmol) were dissolved in THF (0.7 mL) in a vial in the glovebox. After 20 min, the suspension was filtered through a syringe filter and added to a solution of [($^{i\text{Pr}}$POCOP)Pd(CCPh)] (7.4 mg, 13 µmol) in THF (0.2 mL). This solution was layered with Et_2O (1.5 mL) and cooled to -35 °C. Crystals were formed after 4-5 days.

Crystal Data for $C_{56}H_{76}AgF_3N_2O_{5.5}P_2PdS$ (M =1230.45 g/mol): triclinic, space group P-1 (no. 2), a = 13.06490(10) Å, b = 13.77990(10) Å, c = 18.7504(2) Å, α = 73.4020(10)°, β = 79.1420(10)°, γ = 71.1830(10)°, V = 3044.85(5) Å3, Z = 2, T = 200.0(1) K, µ(CuKα) = 6.222 mm-1, Dcalc = 1.342 g/cm3, 63178 reflections measured (7.188° ≤ 2Θ ≤ 159.192°), 12961 unique (Rint = 0.0423, Rsigma = 0.0285) which were used in all calculations. The final R1 was 0.0314 (I > 2σ(I)) and wR2 was 0.0939 (all data).

(for further information see Section 3.3.4)

1.2.7. Synthesis of [($^{i\text{Pr}}$POCOP)Pd$^{\text{II}}$(CCPh)•Ag$^{\text{I}}$(IPr)]BArF, [**2**]BArF:

NaBArF (32.5 mg, 37 µmol, 1 eq.) and [($^{i\text{Pr}}$POCOP)Pd(CCPh)] (20.03 mg, 36 µmol, 1 eq.) were suspended with dichloromethane (1.5 mL). [(IPr)AgCl] (19.7 mg, 37 µmol, 1 eq.) was dissolved in dichloromethane (2mL) and added to the reaction mixture dropwise. The mixture was stirred for 1h at r.t. and filtered using syringe filter (PTFE). The filtrate was dried using vacuum and a white foamy solid was obtained. The solid was then redissolved in THF (0.4 mL) and layered with Et_2O (4 mL) and *n*-hexane (5 mL). Crystals formed after 7 days. The supernatant was removed and the crystals were crushed, washed with *n*-hexane (2 x 1 mL) and dried by vacuum and a powder was obtained (20.61 mg, 11 µmol yield: 30 %).

^{1}H NMR (400 MHz, CD_2Cl_2) δ (ppm) 7.76 – 7.68 (m, 8H), 7.56 (s, 4H), 7.52 (t, 2H, *J*=7.8 Hz), 7.33 (dddd, 1H, *J*=8.0, 7.0, 2.4, 1.2 Hz), 7.28 (d, 4H, *J*=7.8 Hz), 7.26 (d, 2H, *J*=1.8 Hz), 7.21 (t, 2H, *J*=7.7 Hz), 6.99 (tt, 1H, *J*=8.0, 1.2 Hz), 6.83 (dq, 2H, *J*=7.4, 1.2 Hz), 6.55 (d, 2H, *J*=8.0 Hz), 2.52 (hept, 4H, *J*=6.9 Hz), 2.13 (hept, 4H, *J*=7.1 Hz), 1.17 (d, 12H, *J*=6.9 Hz), 1.15 – 1.08 (m, 12H), 1.10 (d, 12H, *J*=6.9 Hz), 1.05 – 0.97 (m, 12H)

^{13}C{^{1}H} NMR (101 MHz, CD_2Cl_2)[a] δ (ppm) 145.89, 135.20, 131.42, 129.84, 129.75, 129.18, 125.24, 125.17, 124.99, 123.65, 117.86, 106.17, 29.74 (t, *J*=12.6 Hz), 29.13, 24.76, 24.21, 17.95 (t, *J*=3.3 Hz), 16.81

$^{31}P\{^{1}H\}$ NMR (162 MHz, CD_2Cl_2) δ (ppm) 192.62 (d, *J* = 0.9 Hz)
$^{19}F\{^{1}H\}$ NMR (377 MHz, CD_2Cl_2) δ (ppm) -62.89
^{11}B NMR (128 MHz, CD_2Cl_2) δ (ppm) -6.61
(for NMR spectra see Section 3.1.5)
ESI-HRMS Positive mode: calculated for $C_{53}H_{72}AgN_2O_2P_2Pd^+$ [M^+] 1043.3165 m/z; found 1043.3133 m/z.
Negative mode: calculated for $C_{32}H_{12}BF_{24}^-$ [M^-] 863.0660 m/z; found 863.0662 m/z.
Elemental Analysis: Calc: C: 53.49 %, H: 4.44 %, N: 1.47 %. Found C: 53.37 %, H: 4.22 %, N: 1.76 %.
Crystal Data for $C_{85}H_{84}AgBF_{24}N_2O_2P_2Pd$ (*M* =1908.56 g/mol): triclinic, space group P-1 (no. 2), *a* = 15.70660(10) Å, *b* = 16.49960(10) Å, *c* = 18.15710(10) Å, *α* = 105.2690(10)°, *β* = 107.8080(10)°, *γ* = 97.3030(10)°, *V* = 4209.95(5) Å^3, *Z* = 2, *T* = 100.0(1) K, μ(Cu Kα) = 4.836 mm^{-1}, *Dcalc* = 1.506 g/cm^3, 163544 reflections measured (5.396° ≤ 2Θ ≤ 160.242°), 17959 unique (R_{int} = 0.0418, R_{sigma} = 0.0205) which were used in all calculations. The final R_1 was 0.0257 (I > 2σ(I)) and wR_2 was 0.0627 (all data).
(for further information see Section 3.3.5)

1.2.8. Synthesis of [(^{iPr}POCOP)Pd^{II}•(PhCC)Au^{I}(IPr)]BF_4, [**3**]BF_4:

a) The bimetallic complex was prepared by dissolving [(^{iPr}POCOP)Pd(CCPh)] (20.1 mg, 37 μmol) and [(IPr)Au(MeCN)]BF_4 (26.4 mg, 37 μmol) in 1,2-$C_6H_4F_2$ (1.5 mL) in a vial in the glovebox. The solution was filtered through a syringe filter, layered with *n*-hexane (0.9 mL), and cooled to -35 °C. Crystals were formed after 4 days. The supernatant was removed and the crystals were crushed, washed with *n*-hexane (2 x 1 mL) and dried by vacuum and a powder was obtained (24.4 mg, 20 μmol yield: 55 %)
^{1}H NMR (400 MHz, CD_2Cl_2)[c] δ (ppm) 7.58 (dd, 2H, *J*=8.1, 7.5 Hz), 7.36 (d, 5H, *J*=7.9 Hz), 7.34 (s, 2H), 7.32 – 7.29 (m, 4H), 7.02 (tt, 1H, *J*=8.1, 1.2 Hz), 6.54 (d, 2H, *J*=8.0 Hz), 2.63 (hept, 4H, *J*=6.9 Hz), 2.01 (hept, 4H, *J*=7.0 Hz), 1.30 (d, 12H, *J*=6.9 Hz), 1.23 (d, 12H, *J*=6.9 Hz), 1.12 – 1.02 (m, 13H), 0.90 – 0.80 (m, 12H)
$^{13}C\{^{1}H\}$ NMR (101 MHz, CD_2Cl_2)[a] δ (ppm) 185.71, 166.34, 146.20, 134.41, 132.55, 131.27, 130.41, 129.82, 129.10, 125.16, 125.11, 124.77, 122.85, 106.60, 29.42, 29.33, 29.30, 29.19, 24.49, 24.29, 17.09, 16.49
$^{31}P\{^{1}H\}$ NMR (162 MHz, CD_2Cl_2) δ (ppm) 188.05 ppm
$^{19}F\{^{1}H\}$ NMR (377 MHz, CD_2Cl_2)[b,c] δ (ppm)-153.49, -153.54 (d, *J*=1.8 Hz)
^{11}B NMR (128 MHz, CD_2Cl_2) δ (ppm) -1.17 ppm
(for NMR spectra see Section 3.1.6)
b) The bimetallic complex was prepared by dissolving [(^{iPr}POCOP)Pd(CCPh)] (16 mg, 29 μmol) and [(IPr)Au(MeCN)]BF_4 (20.6 mg, 29 μmol) in THF (2.5 mL) in a vial in the glovebox. The solution was filtered through a syringe filter, layered with Et_2O (2 mL), and cooled to -35 °C. Crystals were formed after 1 day.
ESI-HRMS Positive mode: calculated for $C_{53}H_{72}AuN_2O_2P_2Pd^+$ [M^+] 1133.3783 m/z; found 1133.3779 m/z.
Negative mode: calculated for BF_4^- [M^-] 87.0035 m/z; found 87.0034 m/z.
Crystal Data for $C_{57}H_{80}AuBF_4N_2O_3P_2Pd$ (*M* =1293.34 g/mol): monoclinic, space group $P2_1/m$ (no. 11), *a* = 10.83380(10) Å, *b* = 15.88720(10) Å, *c* = 17.4029(2) Å, *β* = 106.8160(10)°, *V* = 2867.28(5) Å^3, *Z* = 2, *T* = 100.0(1) K, μ(CuKα) = 8.254 mm^{-1}, *Dcalc* = 1.498 g/cm^3, 38250 reflections measured (5.304° ≤ 2Θ ≤ 159.418°), 6366 unique (R_{int} = 0.0601, R_{sigma} = 0.0359) which were used in all calculations. The final R_1 was 0.0427 (I > 2σ(I)) and wR_2 was 0.1109 (all data).
(for further information see Section 3.3.6)

1.2.9. Synthesis of [(^{iPr}POCOP)Pd^{II}•(PhCC)Au^{I}(IPr)]OTf, [**3**]OTf:

a) [(^{iPr}POCOP)Pd(CCPh)] (59.9 mg, 110 μmol) and AgOTf (28.1 mg, 110 μmol) were combined and suspended with 1,2-$C_6H_4F_2$ (2 mL). (IPr)AuCl (68.1 mg, 36 μmol) was dissolved in THF (2.5 mL) and diluted with 1,2-$C_6H_4F_2$ (1 mL) and added dropwise (8 min) to the reaction mixture. The mixture was stirred for 10 min, filtered through a syringe filter. The clear solution was stepwise layered with *n*-hexane in the subsequent 4 days and kept at -35°C (crys. from solvent-mixture: 1,2-$C_6H_4F_2$ approx. 3 mL, THF approx. 2.5 mL, *n*-hexane approx. 5 mL). The supernatant was discarded and the crystals were crushed, washed with *n*-hexane (2 x 1 mL) and dried by vacuum and a powder was obtained. This solid was re-dissolved

[c] Contamination observed, assumed to be 1,2-$C_6H_4F_2$.

with THF (1 mL), 1,2-$C_6H_4F_2$ (1 mL) and layered with *n*-hexane (1.5 mL) and kept at -35°C for 5 days. The supernatant was removed and the crystals were crushed, washed with *n*-hexane (2 x 1 mL) and dried by vacuum and a powder was obtained. This solid was recrystallized from 1,2-$C_6H_4F_2$ (0.6 mL) and *n*-hexane (0.8 mL) at -35°C. After 1 day crystals were observed. The supernatant was removed and the crystals were crushed, washed with *n*-hexane (2 x 1 mL) and dried by vacuum and a powder was obtained. (18.9 mg, not pure)[a]

^{1}H NMR (400 MHz, CD_2Cl_2)[a] δ (ppm) 7.58 (dd), 7.37 (d), 7.35 (s, 2H), 7.32 – 7.29 (m, 4H), 7.02 (tt, 1H), 6.55 (d, 2H, *J*=8.0 Hz), 2.63 (hept), 2.01 (hept, 4H, *J*=7.0 Hz), 1.31 (d, *J*=6.89 Hz), 1.23 (d, *J*=6.86 Hz), 1.12 – 1.02 (m, 12H), 0.90 – 0.80 (m, 12H)

^{31}P{^{1}H} NMR (162 MHz, CD_2Cl_2)[a] δ (ppm) 188.03

^{19}F{^{1}H} NMR (377 MHz, CD_2Cl_2)[a] δ (ppm) -78.92

(for NMR spectra see Section 3.1.7)

ESI-HRMS Positive mode: calculated for $C_{53}H_{72}AuN_2O_2P_2Pd^+$ [M^+] 1133.3764 m/z; found 1133.3760 m/z. Negative mode: calculated for CF_3O_3S [M^-] 148.9526 m/z; found 148.9526 m/z.

Elemental Analysis: Calc: C: 50.53 %, H: 5.65 %, N: 2.18 %. Found C: 51.37 %, H: 5.81 %, N: 2.51 %.

b) The bimetallic complex was prepared by dissolving [($^{i\text{Pr}}$POCOP)Pd(CCPh)] (5.5 mg, 10 µmol) and [(IPr)Au(OTf)] (7.4 mg, 10 µmol) in 1,2-$C_6H_4F_2$ (0.6 mL) in a vial in the glovebox. The solution was filtered through a syringe filter, layered with *n*-hexane (0.8 mL), and cooled to -35 °C. Crystals were formed after 2 days.

Crystal Data for $C_{55}H_{74}AuCl_2F_3N_2O_5P_2PdS$ (*M* =1368.42 g/mol): monoclinic, space group $P2_1/m$ (no. 11), *a* = 10.8130(5) Å, *b* = 15.7986(8) Å, *c* = 17.8785(9) Å, *β* = 107.1730(10)°, *V* = 2918.0(2) Å^3,*Z* = 2, *T* = 100.0(1) K, µ(MoKα) = 3.057 mm^{-1}, *Dcalc* = 1.557 g/cm^3, 71777 reflections measured (3.512° ≤ 2Θ ≤ 61.062°), 9157 unique (R_{int} = 0.0748, R_{sigma} = 0.0543) which were used in all calculations. The final R_1 was 0.0332 (I > 2σ(I)) and wR_2 was 0.0691 (all data).

(for further information see Section 3.3.7)

1.2.10. Synthesis of [(IPr)Au$^{\text{I}}$(MeCN)]BArF:

[(IPr)AuCl] (186.5 mg, 0.3 mmol) and NaBArF (268.5 mg, 0.3 mmol) were combined and suspended with MeCN (8 mL). The reaction mixture was stirred over night at r.t. The reaction mixture was dried by vacuum and the obtained solid was suspended with dichloromethane (8 mL). The suspension was filtered using a syringe filter (PTFE), the filtrate was dried by vacuum evaporation and a white powder was obtained (353.2 mg, 79 % Yield).

^{1}H NMR (400 MHz, CD_2Cl_2) δ (ppm) 7.75-7.68 (m, 8H), 7.61-7.53 (m, 2H), 7.56 (s, 4H), 7.39-7.33 (m, 6H), 2.45 (hept, 4H, *J*=6.9 Hz), 2.21 (s, 3H), 1.29 (d, 12H, *J*=6.9 Hz), 1.24 (d, 12H, *J*=6.9 Hz)

^{13}C{^{1}H} NMR (101 MHz, CD_2Cl_2) δ (ppm) 162.90, 161.91, 146.11, 145.73, 135.20, 131.70, 131.42, 126.35, 125.20, 124.98, 124.64, 124.50, 123.65, 117.87, 117.83, 29.30, 29.00, 24.78, 24.30, 24.10, 23.95, 3.3

^{19}F{^{1}H} NMR (377 MHz, CD_2Cl_2) δ (ppm) -62.88

^{11}B NMR (128 MHz, CD_2Cl_2) δ (ppm) -6.61 (p, *J*=2.9 Hz)

(for NMR spectra see Section 3.1.8)

ESI-HRMS Positive mode: calculated for $C_{29}H_{39}AuN_3^+$ [M^+] 626.2804 m/z; found 626.2806 m/z. Negative mode: calculated for $C_{32}H_{12}BF_{24}$ [M^-] 863.0660 m/z; found 863.0659 m/z.

Elemental Analysis: Calc: C: 49.18 %, H: 3.45 %, N: 2.82 %, Cl: 0 %, F: 30.6 %. Found C: 49.11 %, H: 3.40 %, N: 2.70 %, Cl: 0.18 %, F: 26.95 %.

1.2.11. Synthesis of [($^{i\text{Pr}}$POCOP)Pd$^{\text{II}}$(CCPh)• Au$^{\text{I}}$(IPr)]BArF, [**3**]BArF:

The bimetallic complex was prepared by dissolving [($^{i\text{Pr}}$POCOP)Pd(CCPh)] (13.5 mg, 25 µmol) and [(IPr)Au(MeCN)]BArF (37.07 mg, 25 µmol) in 1,2-$C_6H_4F_2$ (0.5 mL) and *n*-hexane (0.5 mL) in a vial in the glovebox. The solution was filtered through a syringe filter, layered with *n*-hexane (3.5 mL), and cooled to -35 °C. Crystals were formed after 16 days. The supernatant was removed and the crystals were crushed, washed with *n*-hexane (1 mL) and dried by vacuum and a grey-white powder was obtained (36.94 mg, 19 µmol Yield: 75 %)

^{1}H NMR (400 MHz, CD_2Cl_2) δ (ppm) 7.74 – 7.70 (m, 8H), 7.61 – 7.53 (m, 2H), 7.56 (s, 4H), 7.39 – 7.33 (m, 1H), 7.36 (d, 4H, *J*=7.8 Hz), 7.32 – 7.28 (m, 2H), 7.31 (d, 4H, *J*=5.4 Hz), 7.01 (tt, 1H, *J*=8.1, 1.2 Hz), 6.54

(d, 2H, *J*=8.0 Hz), 2.62 (hept, 4H, *J*=6.9 Hz), 2.00 (hept, 4H, *J*=7.1 Hz), 1.30 (d, 12H, *J*=6.9 Hz), 1.22 (d, 12H, *J*=6.9 Hz), 1.11 – 1.03 (m, 12H), 0.89 – 0.80 (m, 12H)

$^{13}C\{^{1}H\}$ NMR (101 MHz, CD_2Cl_2)[a] δ (ppm) 185.81, 146.19, 135.18, 134.39, 132.55, 131.28, 130.43, 129.81, 129.08, 126.33, 124.77, 124.69, 123.62, 117.85, 106.61, 106.53, 29.42, 29.34, 29.30, 29.18, 24.46, 24.27, 17.08, 16.47

$^{31}P\{^{1}H\}$ NMR (162 MHz, CD_2Cl_2) δ (ppm) 187.95

$^{19}F\{^{1}H\}$ NMR (377 MHz, CD_2Cl_2) δ (ppm) -62.87

^{11}B NMR (128 MHz, CD_2Cl_2) δ (ppm) -6.61

(for NMR spectra see Section 3.1.9)

ESI-HRMS Positive mode: calculated for $C_{53}H_{72}AuN_2O_2P_2Pd^+$ [M^+] 1133.3783 m/z; found 1133.3750 m/z. Negative mode: calculated for $C_{32}H_{12}BF_{24}^-$ [M^-] 863.0660 m/z; found 863.0647 m/z.

Elemental Analysis: Calc: C: 51.10 %, H: 4.24 %, N: 1.40 %. Found C: 51.14 %, H: 3.99 %, N: 1.67 %.

Crystal Data for $C_{85}H_{84}AuBF_{24}N_2O_2P_2Pd$ (*M* =1997.65 g/mol): triclinic, space group P-1 (no. 2), *a* = 15.73380(10) Å, *b* = 16.5046(2) Å, *c* = 18.12680(10) Å, *α* = 105.1640(10)°, *β* = 107.8150(10)°, *γ* = 97.3110(10)°, *V* = 4213.93(7) Å^3, *Z* = 2, *T* = 100.00(10) K, μ(Mo Kα) = 2.091 mm^{-1}, *Dcalc* = 1.574 g/cm^3, 140167 reflections measured (4.768° ≤ 2Θ ≤ 69.54°), 31908 unique (R_{int} = 0.0351, R_{sigma} = 0.0340) which were used in all calculations. The final R_1 was 0.0285 (I > 2σ(I)) and wR_2 was 0.0642 (all data).

(for further information see Section 3.3.8)

1.3. Synthesis of the Bimetallic Compound [4a]BArF

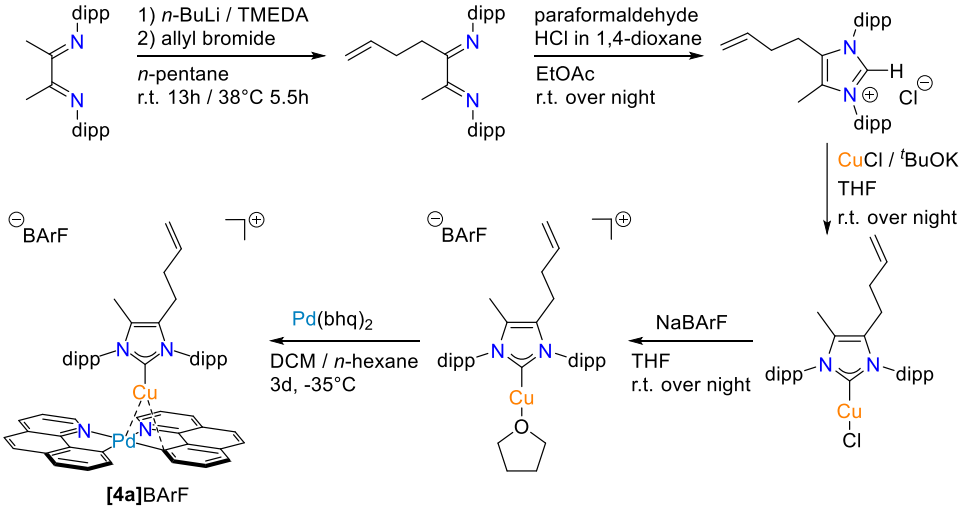

Figure SI-1: Synthesis of complex [**4a]BArF**, showing attachment of the 3-butenyl function to the remote site of the IPr ligand.

1.3.1. Synthesis of Bis(2,6-diisopropylphenyl)hept-6-ene-2,3-diimine, $^{Me,but\text{-}3\text{-}en\text{-}1\text{-}yl,dipp_2}$DAB:

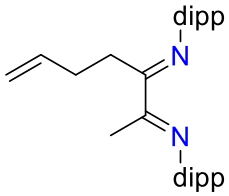

To a solution of Bis(2,6-diisopropylphenyl)butane-2,3-diimine (3 g, 7.4 mmol) in pentane (13 mL) was added a solution of *n*-BuLi (4.5 mL, 7.4 mmol, 1.65 M in *n*-hexane) and TMEDA (2.3 mmol, 1.12 mL) in pentane (19.5 mL) at r.t. The reaction mixture was stirred overnight. Allyl bromide (2.6 mL, 30 mmol) was added and the reaction mixture was heated to 38 °C for 6 h. Excess allyl bromide was removed under vacuum and the residue was suspended in pentane, filtered and evaporated. Recrystallization from hot MeOH afforded the product as yellow crystals. (2.453 g, 5.5 mmol, Yield: 74 %)

^{1}H NMR (400 MHz, CD_2Cl_2) δ (ppm) 7.17 (t, 4H, *J*=7.7 Hz), 7.13 – 7.03 (m, 2H), 5.71 (ddt, 1H, *J*=16.9, 10.1, 6.6 Hz), 4.97 – 4.86 (m, 2H), 2.82 – 2.67 (m, 4H), 2.67 – 2.58 (m, 2H), 2.28 (dt, 2H, *J*=8.1, 6.5 Hz), 2.05 (s, 3H), 1.25 (d, 6H, *J*=6.9 Hz), 1.20 (d, 6H, *J*=6.9 Hz), 1.16 (d, 6H, *J*=6.8 Hz), 1.12 (d, 6H, *J*=6.8 Hz)

$^{13}C\{^{1}H\}$ NMR (101 MHz, CD_2Cl_2) δ (ppm) 170.86, 168.39, 146.60, 146.08, 138.06, 135.59, 135.31, 124.17, 124.07, 123.36, 123.21, 115.04, 54.31, 30.86, 29.35, 28.84, 28.83, 23.43, 23.41, 23.19, 22.78, 22.17, 17.19, 1.18

(for NMR spectra see Section 3.2.1)

Elemental Analysis: Calc: C: 83.73 %, H: 9.97 %, N: 6.30 %. Found C: 83.45 %, H: 9.52 %, N: 6.21 %.

1.3.2. Synthesis of $^{Me,but-3-en-1-yl}$IPrHCl•MeOH:

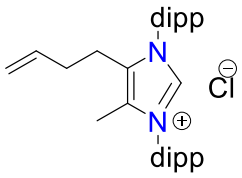

a) Bis(2,6-diisopropylphenyl)hept-6-ene-2,3-diimine (1 g, 2.25 mmol) was dissolved in dry EtOAc (6 mL) under Ar. A solution of paraformaldehyde (90 mg, 3 mmol) in HCl in 1,4-dioxane (0.9 mL, 4M, 3.6 mmol) was prepared in a vial (by means of a sonification bath) and added to the reaction mixture at 0 °C. The reaction was stirred overnight at r.t. and then filtered through a frit (Por 4). The obtained solid was dissolved in MeOH and precipitated with Et_2O. This precipitation was repeated 3 times and an off-white solid was obtained. The solid was dried using vaccum and the product was obtained as a powder (290.7 mg, Yield: 26 %)

^{1}H NMR[d] (400 MHz, CD_2Cl_2) δ (ppm) 11.41 (d, 1H, J=0.6 Hz), 7.69 – 7.58 (m, 2H), 7.46 – 7.37 (m, 4H), 5.72 (ddt, 1H, J=17.1, 10.2, 6.9 Hz), 5.08 – 5.00 (m, 1H), 4.96 (dq, 1H, J=17.1, 1.5 Hz), 3.28 (d, J=0.7 Hz)[d], 2.55 (t, 2H, J=7.4 Hz), 2.39 – 2.19 (m, 4H), 2.15 (qt, 2H, J=7.4, 1.3 Hz), 2.04 (s, 3H), 1.33 (d, 6H, J=6.8 Hz), 1.30 – 1.18 (m, 18H) ppm

^{13}C{^{1}H} NMR[d] (101 MHz, CD_2Cl_2) δ (ppm) 145.87, 145.74, 139.58, 135.98, 132.45, 132.32, 131.54, 129.64, 128.34, 128.30, 125.21, 125.18, 117.22, 50.22[d], 32.36, 29.61, 29.52, 26.19, 25.43, 25.33, 23.09, 22.96, 22.65, 9.63

^{1}H NMR[d] (400 MHz, DMSO-d^6) δ (ppm) 10.04 (dq, 1H, J=4.1, 2.0 Hz), 7.76 – 7.64 (m, 2H), 7.56 (dd, 4H, J=7.8, 6.4 Hz), 5.78 (ddt, 1H, J=17.1, 10.2, 6.9 Hz), 5.01 (dt, 1H, J=10.1, 1.4 Hz), 4.92 (dq, 1H, J=17.2, 1.5 Hz), 4.19 (s)[d], 3.16 (s)[d], 2.63 (t, 2H, J=7.1 Hz), 2.30 (dp, 4H, J=24.1, 6.7 Hz), 2.12 (q, 2H, J=7.1 Hz), 2.07 (s, 3H), 1.32 (d, 6H, J=6.7 Hz), 1.25 (d, 6H, J=6.7 Hz), 1.12 (t, 12H, J=6.7 Hz) ppm

^{13}C{^{1}H} NMR[d] (101 MHz, DMSO-d^6) δ (ppm) 145.20, 145.17, 137.02, 136.35, 132.27, 132.13, 131.39, 129.98, 127.69, 127.65, 125.09, 125.02, 116.53, 31.50, 28.57, 28.50, 25.50, 24.71, 22.66, 22.18, 21.63, 8.99

(for NMR spectra see Section 3.2.2)

ESI-HRMS Positive mode: calculated for $C_{32}H_{45}N_2^+$ [M^+] 457.3577 m/z; found 457.3571 m/z.

Elemental Analysis: Calculated for $^{Me,but-3-en-1-yl}$IPrHCl•MeOH: C: 75.47 %, H: 9.40 %, N: 5.33 %. Found C: 75.41 %, H: 9.56 %, N: 5.63 %.

b) The compound can be recrystallized by vapour diffusion crystallization DCM/Et_2O. An XRD-measurement was conducted.

(for further information see Section 3.4.1)

1.3.3. Synthesis of [($^{Me,but-3-en-1-yl}$IPr)Cu^{I}Cl]:

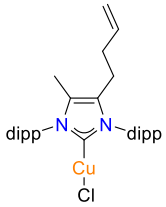

The imidazolium salt (100.4 mg, 0.2 mmol), KO^{t}Bu (27.4 mg, 0.24 mmol) and CuCl (19.94 mg, 0.2 mmol) were suspended in THF (5 mL). The mixture was stirred under Ar for 16 h at r.t. The reaction mixture was filtered through celite and evaporated to dryness. The solid residue was dissolved in dichloromethane (4.5 mL) and filtered (syringe filter). The solution was reduced to 1/3 of the volume by applying N_2-flow. The vial was put into a bigger flask, *n*-pentane (5 mL) was poured into the outer compartment. This vapour diffusion crystallization was kept at -20 °C for 3 days. Transparent crystals were observed, the supernatant was discarded and the crystals were washed with *n*-pentane (2x1 2mL), crushed to a fine solid and dried using vacuum. (85.71 mg, Yield: 76 %)

^{1}H NMR (400 MHz, CD_2Cl_2) δ (ppm) 7.60 – 7.49 (m, 2H), 7.39 – 7.30 (m, 4H), 5.71 (ddt, 1H, *J*=17.1, 10.3, 6.8 Hz), 5.03 – 4.88 (m, 2H), 2.54 – 2.35 (m, 6H), 2.19 – 2.08 (m, 2H), 1.93 (s, 3H), 1.32 – 1.20 (m, 24H)

^{13}C{^{1}H} NMR (101 MHz, CD_2Cl_2) δ (ppm) 177.17, 146.55, 146.43, 136.89, 133.23, 133.20, 130.79, 130.72, 130.68, 129.90, 127.51, 124.69, 124.64, 116.33, 32.77, 29.01, 28.97, 26.44, 25.50, 23.72, 23.33, 23.05, 10.07

(for NMR spectra see Section 3.2.3)

---

[d] In ^{1}H NMR (400 MHz, CD_2Cl_2) a peak at 3.28 ppm and in ^{13}C NMR a peak at 50.22 ppm were observed, those peaks were assigned to **CH**$_3$OH.

Elemental Analysis: Calc: C: 69.16 %, H: 7.98 %, N: 5.04 %. Found C: 69.21 %, H: 8.04 %, N: 5.24 %.

1.3.4. Synthesis of [($^{Me,but-3-en-1-yl}$IPr)Cu^{I}(THF)]BArF:

[($^{Me,but-3-en-1-yl}$IPr)CuCl] (50.4 mg, 90 µmol) was combined with NaBArF (81.12 mg, 90 µmol) and dissolved with THF (1.2 mL) and stirred over night at r.t. The reaction mixture was filtered using syringe filter and subsequently dried by vacuum. The obtained powder was suspended in dichloromethane (2 mL) and filtered using syringe filter (PTFE). The solution was dried using vacuum, giving an off-red powder (132.75 mg) that was used without further purification.

1.3.5. Synthesis of [($^{Me, but-3-en-1-yl}$IPr)Cu^{I}•Pd^{II}(bhq)$_2$]BArF , [**4a**]BArF:

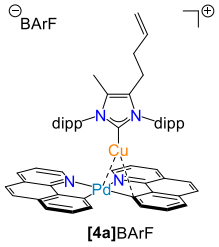

The bimetallic complex was prepared by adding a solution of [$^{Me,but-3-en-1-yl}$IPrCu(THF)]BArF (31.12 mg) in dichloromethane (1.2 mL) to Pd(bhq)$_2$ (10 mg, 22 µmol) in a vial in the glovebox. The solution was filtered (syringe filter), the filter was washed with dichloromethane (0.5 mL). After repeated addition of dichloromethane and layering with *n*-hexane, keeping the mixture at -35 °C , crystals were formed after 2 days (final solvent mixture: dichloromethane 2.3 mL / *n*-hexane 4 mL). (21.6 mg, 12 µmol, yield: 54 %)

^{1}H NMR (500 MHz, CD_2Cl_2) δ (ppm) 8.69 (dd, 2H, *J*=5.1, 1.4 Hz), 8.45 (dd, 2H, *J*=8.0, 1.4 Hz), 7.86 (dd, 4H, *J*=8.1, 6.8 Hz), 7.78 – 7.69 (m, 14H), 7.56 (q, 4H, *J*=1.5 Hz), 7.35 – 7.28 (m, 3H), 7.21 (t, 1H, *J*=7.7 Hz), 6.98 (d, 2H, *J*=7.7 Hz), 6.89 (d, 2H, *J*=7.7 Hz), 5.57 (ddt, 1H, *J*=17.0, 10.2, 6.7 Hz), 4.86 (ddd, 1H, *J*=10.2, 1.7, 1.1 Hz), 4.82 (dq, 1H, *J*=17.1, 1.5 Hz), 2.20 (dd, 2H, *J*=8.9, 6.6 Hz), 2.11 – 1.95 (m, 6H), 1.74 (s, 3H), 0.99 (d, 6H, *J*=6.8 Hz), 0.95 (d, 6H, *J*=6.9 Hz), 0.55 (t, 12H, *J*=6.7 Hz)

^{13}C{^{1}H} NMR (126 MHz, CD_2Cl_2) δ (ppm)[c] 153.00, 147.88, 145.87, 145.75, 144.22, 140.45, 138.92, 137.08, 136.56, 135.21, 134.83, 132.84, 130.88, 130.20, 130.12, 130.01, 127.92, 127.82, 127.04, 126.09, 124.64, 124.34, 124.15, 123.93, 122.60, 117.88, 116.32, 54.27, 54.06, 53.84, 53.62, 53.41, 32.30, 28.69, 25.58, 24.60, 23.63, 23.28, 23.05, 10.01.

^{19}F{^{1}H} NMR (471 MHz, CD_2Cl_2) δ (ppm) -62.87

(for NMR spectra see Section 3.2.4)

ESI-HRMS Positive mode: calculated for $C_{58}H_{60}CuN_4Pd^+$ [M^+] 981.3160 m/z; found 981.3127 m/z. Negative mode: calculated for $C_{32}H_{12}BF_{24}$[M^-] 863.0660 m/z; found 863.0650 m/z.

Elemental Analysis: Calc: C: 58.55 %, H: 3.93 %, N: 3.03 %. Found C: 59.10 %, H: 3.53 %, N: 3.41 %.

Crystal Data for $C_{90}H_{72}BCuF_{24}N_4Pd$ (*M* =1846.26 g/mol): triclinic, space group P-1 (no. 2), *a* = 12.6056(2) Å, *b* = 16.5906(2) Å, *c* = 22.0168(2) Å, *α* = 104.2570(10)°, *β* = 105.8030(10)°, *γ* = 94.5440(10)°, *V* = 4240.82(10) Å^3, *Z* = 2, *T* = 100.0(1) K, µ(CuKα) = 2.900 mm^{-1}, *Dcalc* = 1.446 g/cm^3, 163181 reflections measured (6.028° ≤ 2Θ ≤ 159.516°), 18092 unique (R_{int} = 0.0522, R_{sigma} = 0.0237) which were used in all calculations. The final R_1 was 0.0561 (I > 2σ(I)) and wR_2 was 0.1196 (all data).

(for further information see Section 3.4.2)

1.4. Mass Spectrometry, Collision-Induced Dissociation Experiments

1.4.1. Dissociations of the Pincer based Bimetallic Compounds

Solutions for ESI-MS experiments were prepared by mixing the Pd-complex with [(IPr)M]X or by dissolving the bimetallic complex directly. For ESI-MS experiments acetonitrile or dichloromethane were used as spraying solvents.

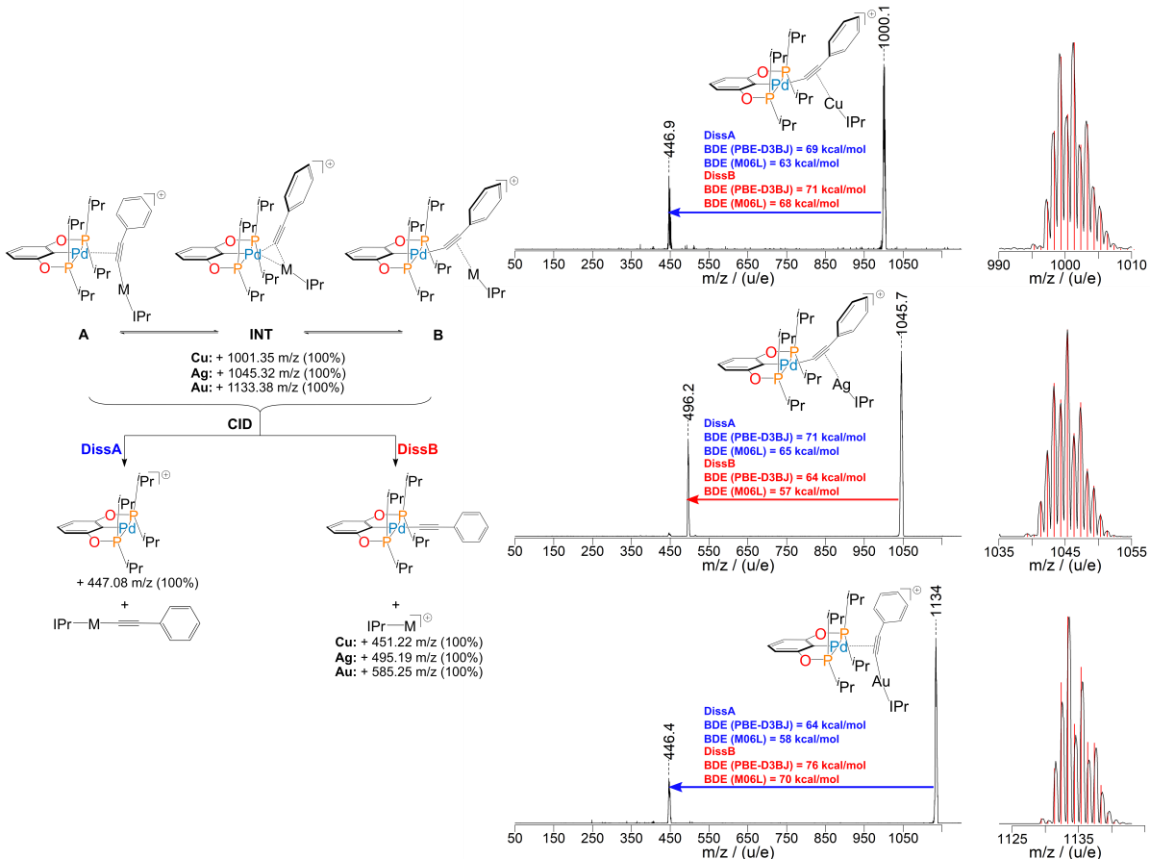

Figure SI-2: Overview ESI-MS CID experiment. Left) Schematic representation of the dissociation process, right) Experimentally obtained ESI-MS CID spectra for the shown ions [(^{iPr}POCOP)Pd(CCPh)M(IPr)] M=Cu (1001 m/z), Ag (1045 m/z), Au (1133 m/z) with Q2-gas Ar (0.2 mTorr) and collision offset of 60 eV.. The bond dissociation energies were calculated using the following methods: PBE-D3BJ/Def2-QZVP//PBE-D3BJ/Def2-SVP and M06L/Def2-QZVP//PBE-D3BJ/Def2-SVP (see section 2.4).

1.4.2. Cleavage of a Remote C-C Bond in the Bimetallic Compound [**4a**]BArF

Spray solutions of the bimetallic complex was prepared by mixing [($^{Me,but-3-en-1-yl}$IPr)CuCl] (0.6 mg, 1 µmol and $AgBF_4$ (0.2 mg, 1 µmol) in dichloromethane (0.2 mL) in a vial in the glovebox. After 5 min, the suspension was filtered through a syringe filter and added to a solution of $Pd(bhq)_2$ (0.5 mg, 10 µM) in dichloromethane (0.2 mL). 10 µL of this solution were added to 2 mL of acetonitril and used immediately.

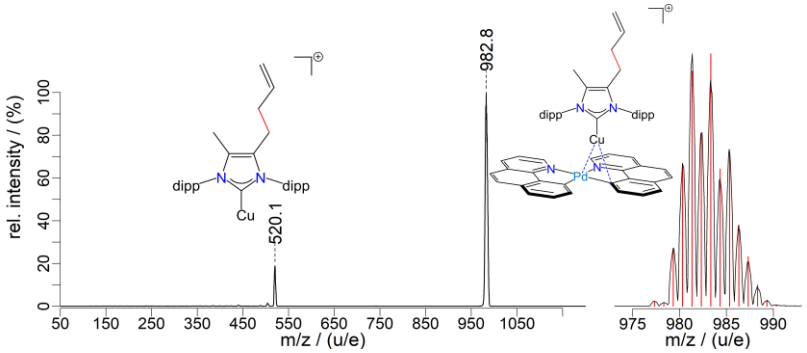

Figure SI-3: left) CID spectrum of Pd/Cu complex (m/z = 983) with Ar (0.1 mTorr), right) isotope peak pattern overlaied with the corresponding simulated isotope peak pattern.

2. Computational Information

2.1. General Introduction

Assuming a reaction mechanism as represented in Figure SI-4 it is evident that both the σ-π-σ rearrangement aswell as the dissociation asymptotes are subject to conformational isomerism.
The energetic span of internal rearrangements is expected to be minor compared to the dissociation processes. In order to investigate relative bond dissociation energies it is necessary to find the lowest lying ground state structure within the σ-π-σ rearrangement reaction system, aswell as the lowest lying ground state structures for the dissociation asymptotes. Rearrangement preceding dissociation can in principle have an influence on the measured relative dissociation rates, if the rearrangement is slow enough, therefore not only the lowest lying ground state but also the knowledge about the potential energy surface is required, e.g. validate and quantify the fast pre-equilibria.
As for comparison of the computational results with solid state structures, only the conformational space within the σ-π-σ rearrangement is of relevance.

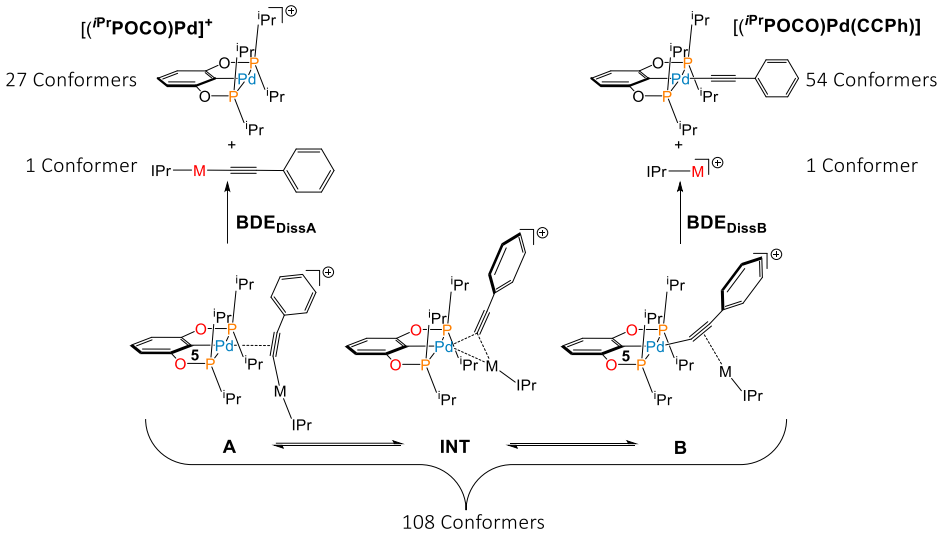

Figure SI-4: Proposed reaction mechanism for the σ-π-σ rearrangement and the dissociation asymptotes. The number of starting structures in the conformational search for every molecule is noted. The molecular structures and processes are labeled.

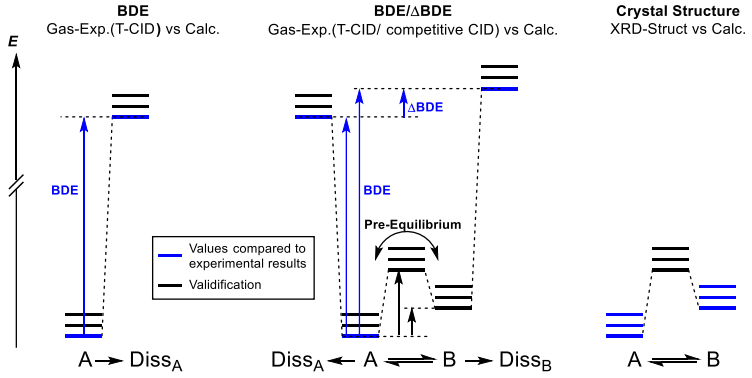

Figure SI-5: Schematic representation of the relevance of different aspects of the computational investigation.

2.2. Conformational Search

A conformational search was conducted for the following structures: [(^{iPr}POCOP)Pd]$^+$, [(^{iPr}POCOP)Pd(CCPh)] (see section 2.2.1) and the bimetallic pincer complex [(^{iPr}POCOP)Pd(CCPh)M(IPr)]$^+$ (see section 2.2.2). The dissociation fragments [(IPr)M(CCPh)] and [(IPr)M]$^+$, as well as the backbone ligand of the Pd-complex (^{iPr}POCOP), were not further investigated, they are assumed to be rigid and therefore their conformational space is expected to be constrained in structure and energy. Sets of conformers were generated manually according to the observed features (by XRD), these were used as starting geometries for subsequent optimizations.

Computational Specifications:

Optimizations : The calculations for the conformational search were performed using ORCA 4.0.1. Geometry optimizations were performed using the PBE functional together with the def2-SVP[10] basis set; for Pd,Ag and Au Def2-ECP[11–18] was used, and Grimme's D3 dispersion correction was used (with Becke-Johnson damping).[19,20] For all calculations Grid5 DFT integration grid was used. SCF convergency criteria were set to TightSCF and optimization convergency criteria were set to TightOpt (TolE = 1e-6, TolRMSG = 3e-5, TolMaxG = 1e-4, TolRMSD = 6e-4, TolMaxD = 1e-3). For all calculations, Coulomb fitting was employed with general Weigend J auxiliary basis set.[21] The structures for [(^{iPr}POCOP)Pd(CCPh)] were optimized using cartesian coordinates.

Single Point Calculations : All single point calculations were performed based on the optimized structures (PBE-D3BJ/def2-SVP) as described above. Single point calculations were performed using the same settings as in the optimizations but with the larger basis set Def2-QZVP.[10]

Evaluation of the structural parameters: All structural parameters were read from the xyz-files and processed (calculation of angles and dihedral angles) using a home-built R code (see section 2.5.4).

Comparison of conformers with XRD structures by RMSD evaluation: The obtained structures from the conformational search were compared to the corresponding XRD structures using an open-source program to determine the RMSD[22] value. Default settings were used, hence the Kabsch algorithm was used.[23]

2.2.1. Conformational search of the Dissociation Asymptotes.

In this section the conformational search on the dissociation asymptotes is reported, in particular the following complexes were treated: [(^{iPr}POCOP)Pd]$^+$, [(^{iPr}POCOP)Pd(CCPh)]. In both cases the conformat ional space is span by the ^{i}Pr groups located on the phosphorus atoms, in the later case an additional rotation of the acetylide group was considered. Assuming that every ^{i}Pr group is located in one of three potential wells results in 3^4 (81) possible conformers (see Figure SI-8) for [(^{iPr}POCOP)Pd]$^+$. The obtained structures were compared and for all structures that were interconvertible by one of the following symmetry operations σ_{xz}, σ_{yz} or a C_2-rotation a single representative was choosen. Hence the conformational space was reduced to 27 structures by symmetry. For [(^{iPr}POCOP)Pd(CCPh)] an additional structural parameter was considered, namely the rotation of the phenylacetylide moiety, setting this either perpendicular or in-plane with respect to the complex plane, leading to 54 structural conformers. This combinatioric evaluation lead to the construction of starting guesses for subsequent quantum chemical calculations (see Figure SI-8).

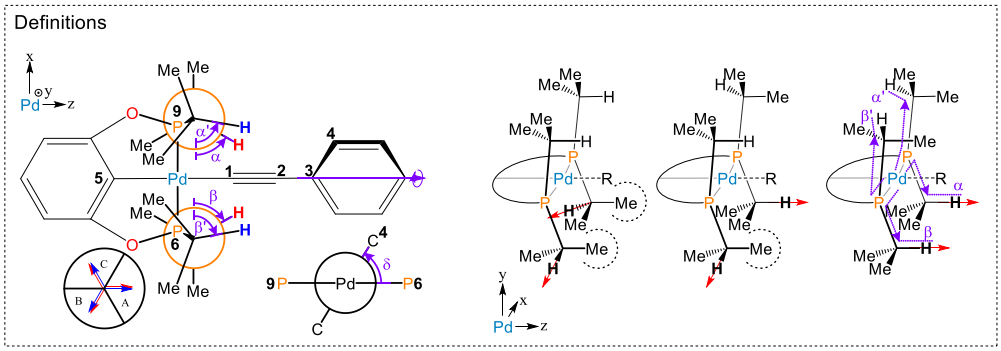

Figure SI-6: Definitions of structural parameters for [(^{iPr}POCOP)Pd(CCPh)]. [(^{iPr}POCOP)Pd]$^+$ is treated in the same way.

In the following notation the conformation space regarding the iso-propyl groups (located on ^{iPr}POCOP) is written as sequence of 4 letters, e.g. AAAA. Every letter represents an *i*Pr group and also shows in which 120° sector the hydrogen –C**H**Me_2 (according to the α',α,β,β' and in that order) is lying as defined in Figure SI-6.

The initial conformational structures did retain their structure regarding the *i*Pr group while optimizing by DFT, hence all of the structures optimized into a local energetic pit. The optimization of the [(^{iPr}POCOP)Pd(CCPh)] structures showed that arrangement of the Ph ring (in plane /out of plane) are retained during the optimization. The relative energies of the conformers range up to 7.3 kcal/mol[e] for [(^{iPr}POCOP)Pd]$^+$ and 7.7 kcal/mol[h] for [(^{iPr}POCOP)Pd(CCPh)]. The energetic difference between the conformations is assumed to stem from an interaction between the *i*Pr groups. In the following it is assumed that the remote ^{i}Pr located on different phosphorus atoms do not interact while the ^{i}Pr located on the same phosphorus atom do. Treating the ^{i}Pr-P-^{i}Pr groups as distinct sub units of the molecule it is possible to determine their energetic influence on the system. A set of 6 possible distinct ^{i}Pr-P-^{i}Pr conformations can be found, see Figure SI-7. The energies of all calculated structures were referenced to the lowest energy structure. Selecting all structures that are composed of two identical ^{i}Pr-P-^{i}Pr sub units and subsequently divide their relative energy by 2 lead to an energy term that can be assigned to a particular ^{i}Pr-P-^{i}Pr conformer shown in Figure SI-7. Using these energies in an additive manner allows to estimate the destabilization of a specific overall-conformer with respect to the lowest energy structure. The relative energy of any conformer can be determined by adding up the interaction energies of the participating local ^{i}Pr-P-^{i}Pr conformers. The residual energy contribution (actual relative energy – recalculated relative energy) that is not accounted with the additivity scheme is below 0.16 kcal/mol[h]. This small residual energy contribution validates the assumption that the remote isopropyl groups do almost not interact and can be treated as separate entities.

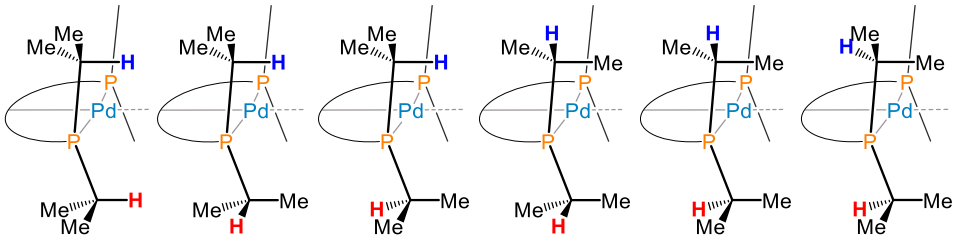

Figure SI-7: Interaction energies (PBE-D3BJ/Def2-QZVP//PBE-D3BJ/Def2-SVP) between neighboring ^{i}Pr groups (^{i}Pr-P-^{i}Pr) located on the phosphorus atoms. The relative energy of a specific [(^{iPr}POCOP)Pd-X]$^{+z}$ conformer can be estimated by adding up the corresponding interaction energies.

[e] PBE-D3BJ/Def2-QZVP // PBE-D3BJ/Def2-SVP

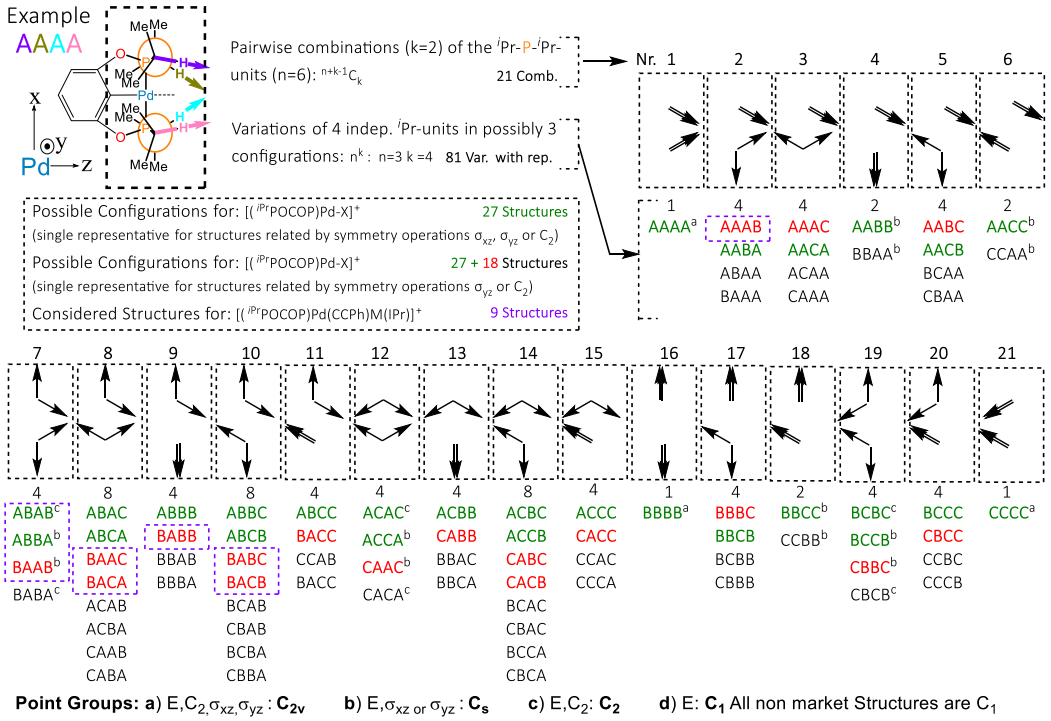

Figure SI-8: Overview of combinatorics regarding the ^{i}Pr conformational space. A conformer is described by 4 letters, each represents an ^{i}Pr group according to the example. A,B,C show the orientation of the -C**H**Me$_2$ hydrogen, specifically in which 120° sector the **H** lies. In green all local conformations that were treated in the conformational search of [(^{iPr}POCOP)Pd]$^+$ and [(^{iPr}POCOP)Pd(CCPh)]. In purple all local conformations are listed that were used for the conformational search of [(^{iPr}POCOP)Pd(CCPh)M(IPr)]$^+$.

2.2.2. Conformational Search on the σ -π-σ Rearrangement

The investigation of the σ-π-σ rearrangement system requires a more thorough conformational search. The potential energy surface between A, INT and B spans an energy range of a few kcal/mol, discussion of structural motifs within that range requires consideration of a broader range of conformers.

The reported bimetallic complexes can be studied by partitioning the molecule into four main components, the palladium side with its chelating pincer-ligand (*(^{iPr}POCOP)Pd*-△), the metal-IPr (*(IPr)M*-△) and the acetylide bridging group (*(PhCC)*-△), the fourth component being the structural arrangement of the previously mentioned components (*Pd•CC•M*:△).

The manual search for conformers, according to the geometric parameters defined here (also see Figure SI-10), produced starting guesses for the subsequent optimizations, as well as criteria for classifying the optimized structures once the calculations were done. Furthermore these classifications are then used as criteria to identify the most resembling conformer with respect to the XRD structures.

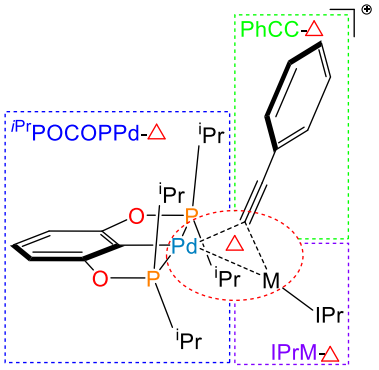

Scheme SI-9: Partition of [(^{iPr}POCOP)Pd•(CCPh)•M(IPr)]$^+$

The *(^{iPr}POCOP)Pd*-△ component was treated analogous to the [(^{iPr}POCOP)Pd]$^+$ as described in section 2.2.1. The obtained structures (81 *i*Pr conformers) were compared and for all structures that were interconvertible by one of the following symmetry operations: σ_{yz} or a C_2-rotation, a single representative was choosen. Different from the case for [(^{iPr}POCOP)Pd]$^+$ conformers that interconverted by σ_{xz} can not be removed, because the later introduced ligand [(IPr)M(CCPh)] is not symmetric with respect to this mirror plane. This evaluation lead to 45 conformers regarding the *(^{iPr}POCOP)Pd*-△) component.

In order to reduce the computational effort only conformers where at least one of the local conformer ^{i}Pr-P-^{i}Pr AB was present and the "A"-part was located on the lower side (on the IPr side) namely:[f] ABAB (0 kcal/mol, asym), ABBA (0 kcal/mol, exo), BAAB (0 kcal/mol, endo), BABB (1 kcal/mol), BACB (1.3 kcal /mol), BABC (1.3 kcal /mol), BAAC (3 kcal/mol) BACA (3 kcal/ mol) ,AAAB (3.1 kcal/mol).
In the *(IPr)M*-△ component the IPr group was placed either in-plane or perpendicular with respect to the pincer backbone structure.
The *(PhCC)*-△component was treated in the same way as in the case of [(^{iPr}POCOP)Pd(CCPh)] as described in section 2.2.1. The phenyl group was placed either in-plane or perpendicular with respect to the pincer backbone structure.
The △ component originated from the XRD structures for conformations A and B. For the Intermediate case, a pre-calculation with the approximate arrangement was conducted which was then used as the template.

In total the conformational space for [(^{iPr}POCOP)Pd(CCPh)M(IPr)]$^{+}$ is span by 108 (9*3*2*2) initial conformers.

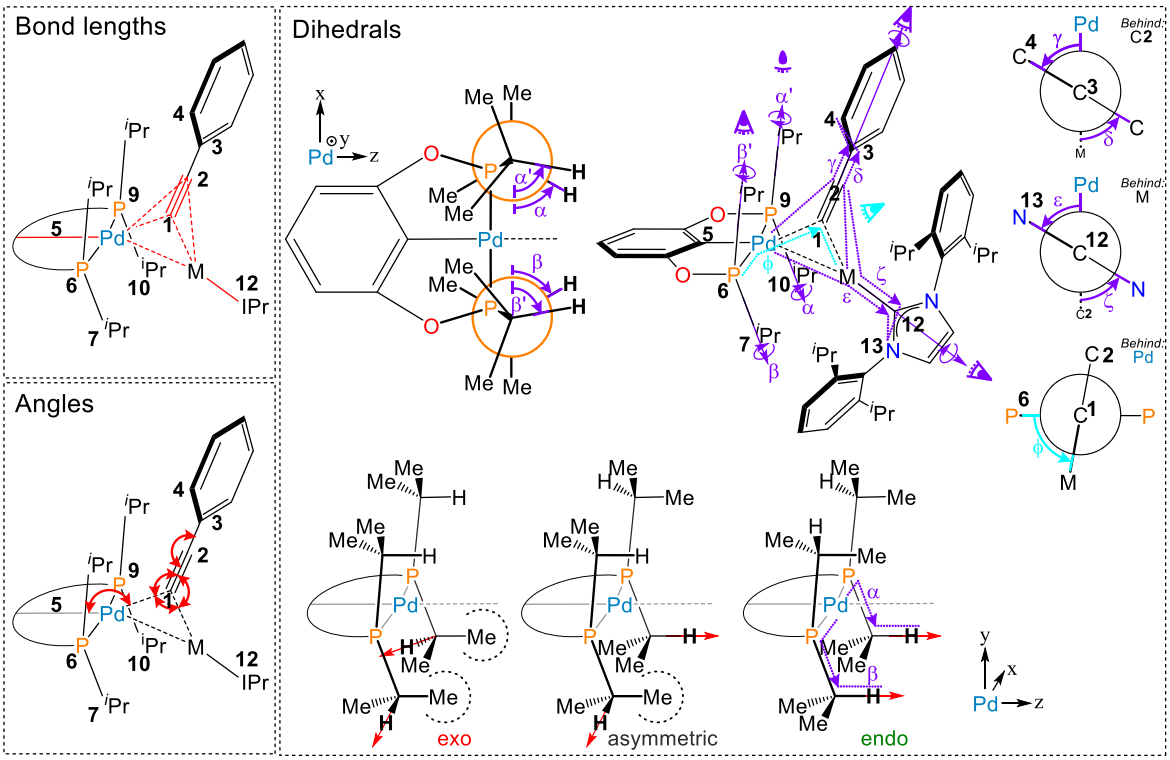

Figure SI-10: Overview of selected structural parameters. The experimentally observed local conformations of the ^{i}Pr-P-^{i}Pr are shown (endo, asym, exo).

As mentioned in the introduction, the pincer-based bimetallic complex can be dissected into 4 parts (*(^{iPr}POCOP)Pd* -△, *(IPr)M* -△, *(PhCC)*-△, △). In the following section, the conformations of all parts are defined and evaluated based on specific structural parameters.

Definition of the core-structure △ (*Pd•CC•M):* In order to classify the conformational structures to A, INT or B a proper definition was required. A major difference between the named conformational families is their differing structural arrangement in the Pd-C1(C2)-M core part of the complex. For example the Pd-C1-C2 angle can be used as a metric for the structural change along the transmetalation reaction. This parameter is as close to the true reaction coordinate as one can, using only a single internal coordinate. While this parameter allows to differentiate between conformational families A and B it

[f] Energy values in paranthesis are derived from the results in section 2.2.1. These values show to what extend a specific arrangement of the ^{i}Pr-P-^{i}Pr groups destabilizes the conformation with respect to the lowest lying ground state.

does not differentiate easily between INT and B. In order to differentiate INT from the other conformational families, the Metal(Pd)-Metal(Cu,Ag,Au) distance was chosen as the structural parameter and compared to the sum of van der Waals radii.[24] For the definitions see Table SI-2.

If	b(Pd-M) < ($r^{V.D.W}$(Pd) + $r^{V.D.W}$(M))[a]	→	INT
elseif	a(Pd-C1-C2) < 120°	→	A
elseif	a(Pd-C1-C2) > 120°	→	B

Table SI-2: Definition of the conformational families A, INT and B. The test-variables a(Pd-C1-C2)/ (°) and b(Pd-M) / (Å) are structural parameters as defined in SI-10. The variable $r^{V.D.W}$ denotes the van der Waals radii according to literature.[24]

Evaluation of the obtained optimized structures using this classification allows the assignment of the descriptors A, Int or B to any conformer. In Figure SI-11 the obtained structural parameters of the conformational space are plotted with respect to the two dimensions that were used for the criteria (Table SI-2) and it can be observed that the conformational families are grouping together satisfactory except for Ag where the differentiation of Int and B is not as clear.

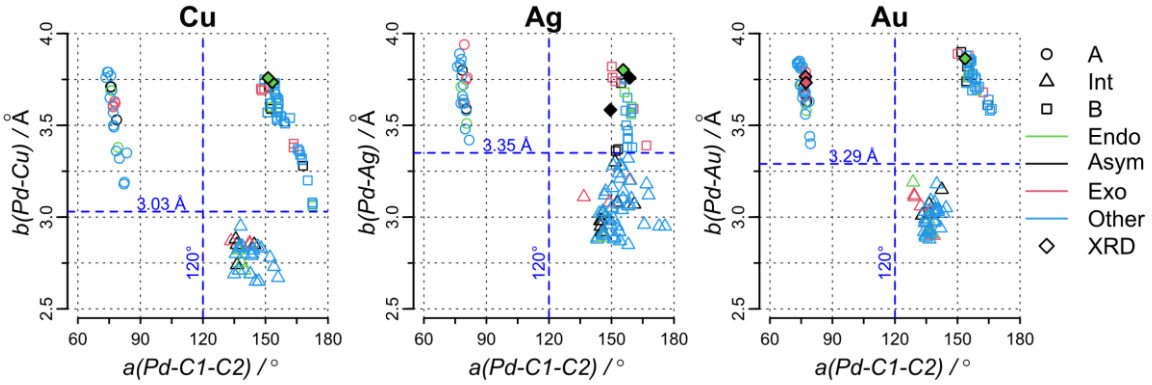

Figure SI-11: Results of the conformational space for [(^{iPr}POCOP)Pd(CCPh)M(IPr)]$^+$ (M= Cu, Ag, Au) according to the bond length b(Pd-M) / (Å) and the angle a(Pd-C1-C2) / (°). In order to classify the structures into A, INT and B, the two dimensions were used, the corresponding classification criteria (see Table SI-2) are shown (dashed blue lines). Additionally the structural parameters obtained from the XRD structures are noted.

Definition and categorization of the pheripherial structure (^{iPr}POCOP)Pd -△ (^{i}Pr-groups): Reading out the dihedrals from the obtained structures can be misleading, while the absolute magnitude is intuitively accessible it can be hard to go beyond that, e.g. the rotational sense is often hard to imagine. Hence the structural parameters were modified so that they represent the values expected according to the definitions in Figure 10.

If d(Pd-P9-C10-H11)	> 0° →	α = 360° -d(Pd-P9-C10-H11)	→ α ∈ [0°,360°]
	< 0° →	α = -d(Pd-P9-C10-H11)	
If d(Pd-P9-C-H)	< 0° →	α' = 360°+d(Pd-P9-C-H)	→ α' ∈ [0°,360°]
	> 0° →	α' = d(Pd-P9-C-H)	
If d(Pd-P6-C7-H8)	< 0° →	β = 360° +d(Pd-P6-C7-H8)	→ β ∈ [0°,360°]
	> 0° →	β = d(Pd-P6-C7-H8)	
If d(Pd-P6-C-H)	> 0° →	β' = 360°-d(Pd-P6-C-H)	→ β' ∈ [0°,360°]
	< 0° →	β' = -d(Pd-P6-C-H)	

Table SI-3: Definitions for α,α',β and β'. Dihedral angles that were obtained from the evaluation of the structures are transformated according to the definitions shown in SI-10.

The [(^{iPr}POCOP)Pd(CCPh)M(IPr)]$^+$ conformer structures were classified according to the three experimentally observed conformational families, endo, asym and exo. For the conformational search, more conformations were investigated (as explained above), those were found to be neither present in the lowest energy conformations nor were they observed in the crystal structures. Hence they are collapsed into one additional conformational family (Other Conf.)

If	α' ∈ [135°,255°] & α ∈ [0°,135°] & β ∈ [0°,135°] & β' ∈ [135°,255°]	→ endo (BAAB)
elseif	α' ∈ [0°,135°] & α ∈ [135°,255°] & β ∈ [0°,135°] & β' ∈ [135°,255°]	→ asym (ABAB)
elseif	α' ∈ [135°,255°] & α ∈ [0°,135°] & β ∈ [135°,255°] & β' ∈ [0°,135°]	→ asym (BABA)
elseif	α' ∈ [0°,135°] & α ∈ [135°,255°] & β ∈ [135°,255°] & β' ∈ [0°,135°]	→ exo (ABBA)
else		→ Other Conf.

Table SI-4: Definition of the conformational families endo, asym, exo and other conformations.

The *i*Pr space is span by the 4 dimensions α,α',β and β' as described above and therefore a multi dimensional figure would be required. In Figure SI-12 the structural parameters α and β are plotted because these parameters can be assigned to the iso-propyl groups in close proximity to the IPr Ligand which are expected to be affected the most by steric interactions. The results show that the conformers are grouping satisfactory with respect to the conformational families Endo, Asym, Exo and the other conformers.

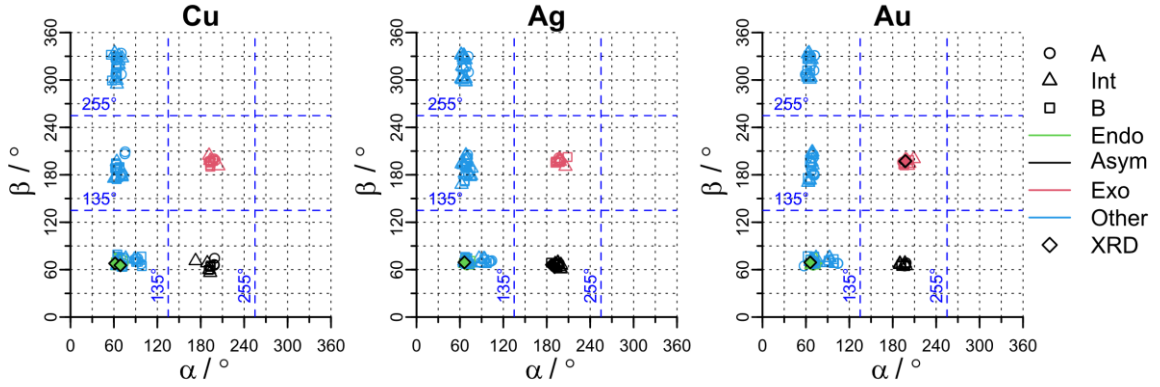

Figure SI-12: Results of the conformational search for [(^{iPr}POCOP)Pd(CCPh)M(IPr)]$^+$, the structures were optimized at the level of theory PBE-D3BJ/Def2-SVP using ORCA 4.0.1. Characterization of the conformational spaces for [(^{iPr}POCOP)Pd(CCPh)M(IPr)]$^+$ (M= Cu, Ag, Au) according to the angles α and β. The definition of the markers can be found in the legend on the right side.

Definition and categorization of the pheripherial structures PhCC-△ and IPrM-△: As already mentioned above, the dihedral angles were modified prior to evaluation for the sake of intuitive accessibility (see table SI-5). For both components two angles were defined respectively (see Figure SI-10). Dihedral angles have to be taken cautiously when the atoms are almost aligned, which is the case for the choosen descriptors for these components. In order to have a better representation of the actual rotation of these pheripheral structures the choice of the dihedral angle to be evaluated was based on the a(Pd-C1-C2) angle. For a(Pd-C1-C2) being below the arbitraty chosen angle of 120° γ and ε were choosen as the metrices for the evaluation of the rotation of the named components (see Table SI-6). Based on these modified dihedral angles, for both components two classes were defined the perpendicular classes (i and I) and the in-plane classes (ii and II) (see also Figure SI-13).

If d(Pd-C2-C3-C4)	∈ [-45°,45°]	→	γ = d(Pd-C2-C3-C4)	γ ∈ [-90°,90°]
	∈ [45°,90°]	→	γ = d(Pd-C2-C3-C4)	
	∈ [90°,135°]	→	γ = d(Pd-C2-C3-C4) – 180 °	
	∈ [-135°,180°]	→	γ = d(Pd-C2-C3-C4) – 180 °	
	∈ [-180°,-135°]	→	γ = d(Pd-C2-C3-C4) + 180 °	
	∈ [-135°,-90°]	→	γ = d(Pd-C2-C3-C4) + 180 °	
	∈ [-90°,-45°]	→	γ = d(Pd-C2-C3-C4)	

Table SI-5: Definitions for γ δ ε ζ dihedral angles, derived from d(Pd-C2-C3-C4), d(M-C2-C3-C4), d(Pd-M-C12-N13), d(C2-M-C12-N13) respectively. Dihedral angles that were obtained from the evaluation of the structures are transformated along the definition shown in SI-10.

If a(Pd-C1-C2)	< 120 °	→	γ/ δ = γ	γ ∈ [-90°,90°]
			ε/ζ = ε	γ ∈ [-90°,90°]
	> 120 °	→	γ/ δ = δ	γ ∈ [-90°,90°]
			ε/ζ = ζ	γ ∈ [-90°,90°]

Table SI-6: Definitions of γ/δ and ε/ζ. Depending on the a(Pd-C1-C2) angle, one of the two angles is a better representation.

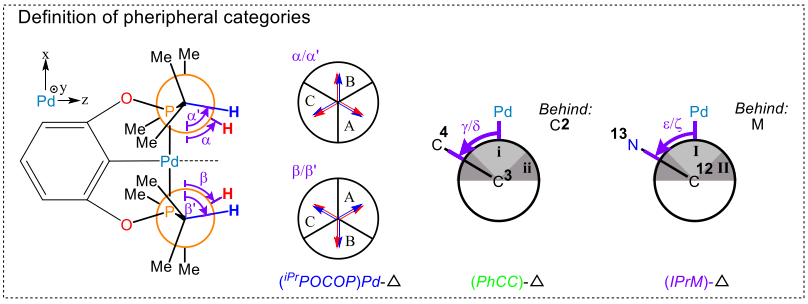

Figure SI-13: Classifications of the pheripheral conformations.

If γ/ δ	∈ [-45°,45°]	→	i
	∈ [-90°,-45°] or [45°,90°]	→	ii
If ε/ζ	∈ [-45°,45°]	→	I
	∈ [-90°,-45°] or [45°,90°]	→	II

Table SI-7: Categorization of the pheripheral conformations of PhCC and (IPr)M.

As can be seen in Figure SI-14, the conformational space with respect to the components *PhCC-△ and (IPr)M-△* are not as well defined.

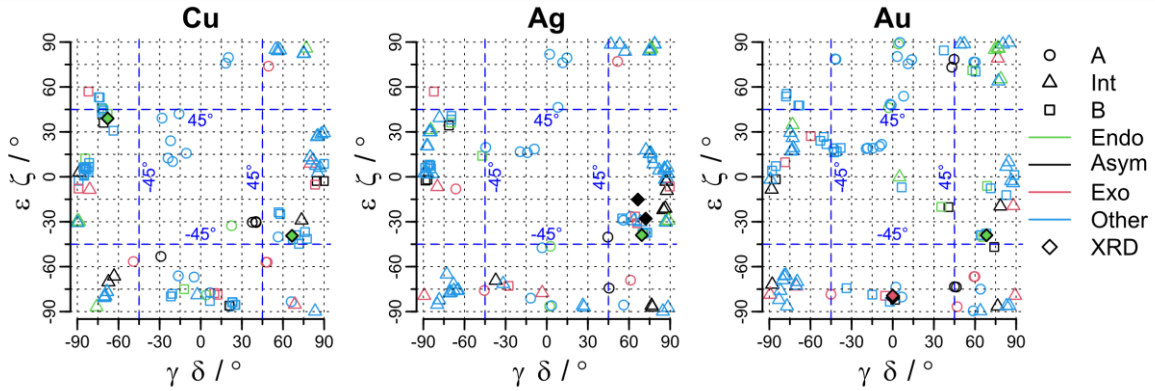

Figure SI-14: Results of the conformational search for [(iPrPOCOP)Pd(CCPh)M(IPr)]+, the structures were optimized at the level of theory PBE-D3BJ/Def2-SVP using ORCA 4.0.1. Characterization of the conformational spaces for [(iPrPOCOP)Pd(CCPh)M(IPr)]+ (M= Cu, Ag, Au) according to the angles γ/δ and ε/ζ. The definition of the markers can be found in the legend on the right side.

2.2.3. Comparison of Conformational Space with XRD Structures

The comparison of the obtained conformational structures with the observed XRD structures is inherently difficult and arbitrary. Using RMSD as a metric for comparison can be misleading, e.g. the influence of the core part on the RMSD value is supressed because it consists of just a few atoms and also the displacements are rather small compared to the peripheral displacements. The phenyl-acetylid group aswell as the IPr Ligand reaching out of the molecule act as leavers and therefore show larger displacements compared to the core part, hence those structural motives dominate the RMSD comparison. It is possible to conduct RMSD evaluation on a subset of atoms, however in case of the here described molecule it is not possible to capture all structural features in a single meaningful RMSD value. The comparison of the XRD structures with the obtained conformational space proceeds in two steps: the conformations with the same categorizations (A, INT, B, Endo, Asym, Exo, i,ii, I,II) as the XRD

structures are filtered out and in a subsequent step the remaining conformers are compared to the XRD structures by RMSD (without hydrogens, see Figure SI-15) and the most resembling structure is chosen. The pre-selected (by comparison of the categorized components) list of conformers are already quite similar in structure, hence the RMSD is not as affected as much by peripheral displacements and therefore was used to pin-point to a single most resembling structure.

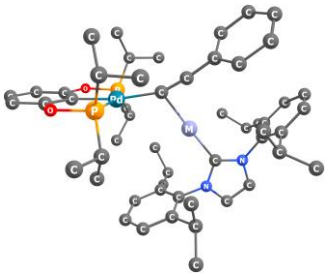

Figure SI-15: Schematic representation of the considered atoms in the RMSD evaluation. Molecule without hydrogens.

Correction 1: As mentioned above, the computational conformational space was reduced by symmetry, e.g. the local conformers ABAB were calculated whereas BABA were not. In case of the XRD structure [(^{iPr}POCOP)Pd(CCPh)•Ag(IPr)]OTf a local conformer of BABA was observed, since there is no local conformer BABA in the calculated conformational space this structure was mirrored prior to the entire analysis including the RMSD evaluation.

Correction 2: The RMSD value is calculated by comparing every atom position in an index-list pairwise manner, therefore both structures have to be listed/labelled in the same way. Occasionally it happend that the Phenyl or IPr moieties did rotate off in different directions counter-/clockwise (in the conformational space), this can lead to wrong RMSD evaluations. In order to overcome this error, the crystal structures Ph and IPr moieties were relabeled in all possible manners how these moieties could have rotated (see Figure SI-16). The conformere was compared to all re-labeled crystal structures and the lowest RMSD value was chosen.

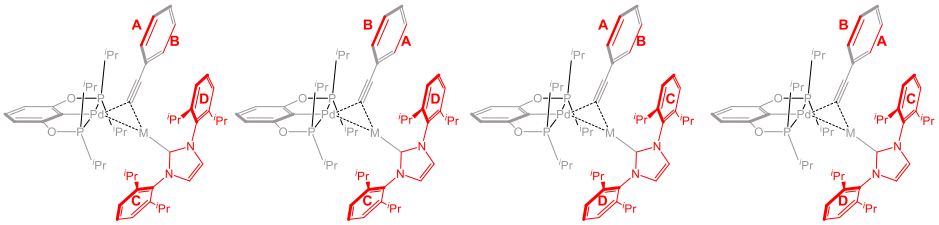

Figure SI-16: Correction of the RMSD evaluation. The Ph and IPr moieties were re-labeled in 4 different ways and subsequently the structures were compared by RMSD. The lowest RMSD was taken.

Correction 3: In case of [(^{iPr}POCOP)Pd(CCPh)•Au(IPr)]BF_4 and [(^{iPr}POCOP)Pd(CCPh)•Au(IPr)]OTf no conformation matched all 4 criteria (categorizations of the components mentioned above). The next best matching structure was taken, this structure did not match the classification regarding the Phenyl moieties.

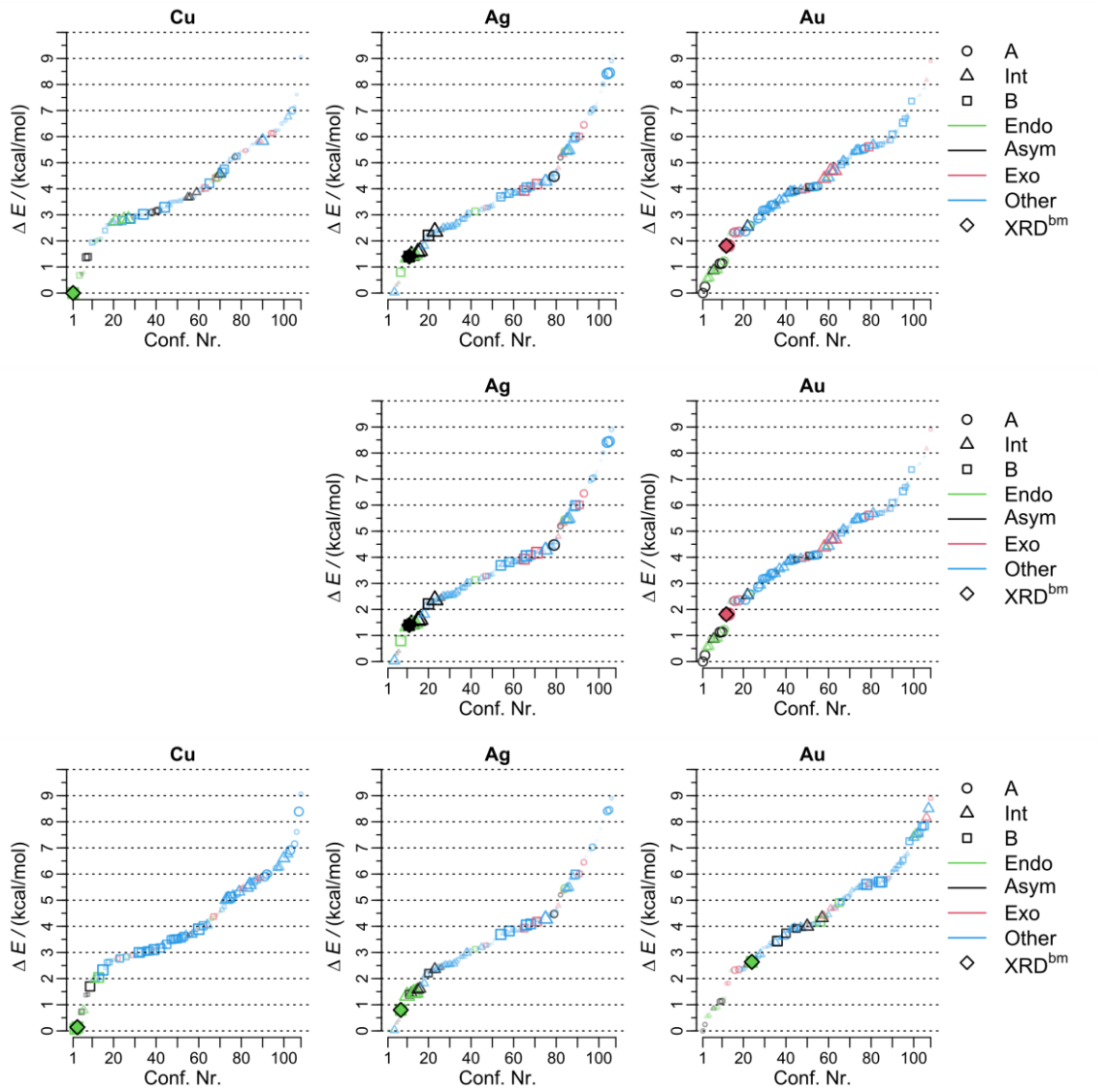

Figure SI-17: Results of RMSD calculations. Top) Countrion BF_4^- Middle) Counterion OTf^- Bottom) Counterion $BArF^-$. The marker size and marker transparency are scaled according to the following equation: $NRMSD_{conf}=1-(RMSD_{conf.}-RMSD_{conf.,min})/(RMSD_{conf.,max}-RMSD_{conf.,min})$. The conformer which matched the XRD structure the most is also marked (bm =best match).

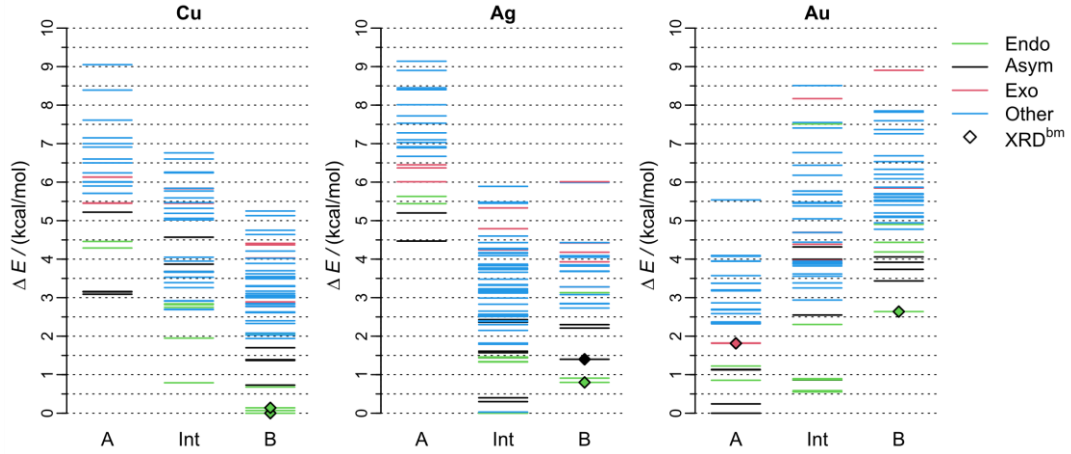

Figure SI-18: Energy of the obtained conformations classified into the structural classification A, Int and B. The level of theory was PBE-D3BJ/Def2-QZVP//PBE-D3BJ/Def2-SVP. Classification according to Endo (green), Asym (black) and Exo (red) are represented in color. The conformer which matched the XRD structure the most is also marked (bm =best match).

2.3. Potential Energy Surface of the σ -π-σ Rearrangement and the Transition State search

In order to find transition state structures, 2D relaxed surface scans were performed. Two internal degrees of freedom were selected and a 2 dimensional grid of possible value-combinations was constructed. Subsequently the 2D PES was sampled by constrained optimizations (two internal coordinates) at the pre-determined grid points. Based on the obtained 2D PES, the transition states were identified and submitted to transition state optimization calculations. The energetically lowest lying conformation was chosen as the base structure for the 2D relaxed surface scan.

2.3.1. 2D Potential Energy Surface of the σ -π-σ Rearrangement

Computational Specifications:

Constrained Optimizations: At every grid point the molecular structure was optimized (2 constrained internal coordinates) using xtb (Version 6.2 RC2) with otherwise default settings.[24–31] The resulting structures were reoptimized by DFT using ORCA 4.0.1. For the reoptimization (2 constrained internal coordinates) the same computational settings were used as for the conformational search except the integration grid was set to Grid 4.

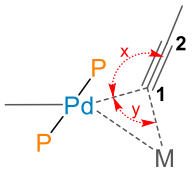

Figure SI-19: Schematic representation of the dynamic structural range of the Pd-C1(C2)-M core part. The parameters that were scanned are denoted as x and y for the angles a(Pd-C1-C2) and a(Pd-C1-M) respectively.

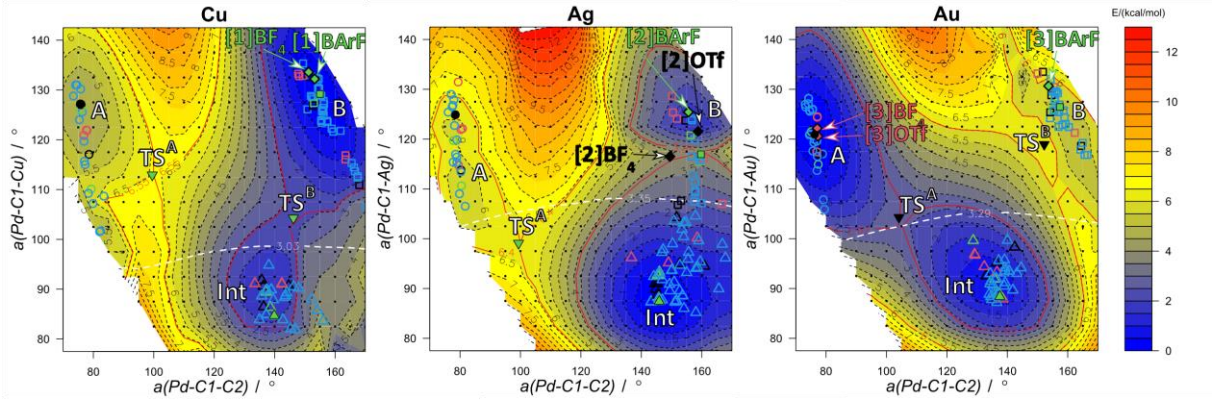

Figure SI-20: Contour plot (R Version 1.4.1103) of the 2D potential energy surface for the proposed transmetalation step. The underlying grid (black points) is spanned by two angles a(Pd-C1-C2) and a(Pd-C1-M), with the increment in both dimensions chosen to be 5°. The lowest lying conformer (from conformational search) was reoptimized at every grid-point (2D constraints), first by xtb (Version 6.2 RC2) and then by DFT. The DFT calculations were performed on ORCA (Program Version 4.0.1) and the level of theory was PBE-D3BJ/Def2-SVP with TightSCF and a Grid 4. The conformers from the conformational search (○:A,△:Int, □:B, ▽:TS) and XRD structures (◇) were superimposed based on their respective structural parameters. Additional contour lines are plotted, in red the approximate energy level for the transition states and in white one of the cut off criteria for the A, Int, B assignment (see Table SI-2) is shown.

The 2D PES of Cu and Au look similar but "inverted". For both Cu and Au the calculated conformers fall into their respective local energetic pit; this shows that the chosen scanned parameters are actually good criteria to distinguish between the different conformational families. In case of Ag a clear distinction between A and INT can be observed, however between INT and B this is not obvious.

When calculating the 2D PES from the energetic lowest lying conformer it appeared that the structural feature regarding the *i*Pr groups on the phosphorus atoms did not change, e.g. the endo, asym and exo conformation stayed intact throughout the entire 2D scans. Assuming that the optimization scheme chosen does not overcome certain conformational barriers leads to the conclusion that the 2D PES for other conformers than the chosen one might look different.

Not only does the 2D relaxed surface scan provide access to the transition states but also it allows to look at the conformational families, A, INT, and B from another perspective. In particular the Ag case is special, as the conformers between INT and B spread along the direction of the a(Pd-C1-Ag) angle. It can be seen that some conformers are assigned to B even though they are located closer to the energetic minimum of INT. This might imply that there is a low intrinsic barrier computationally and that therefore other conformations (peripheral) gain in importance, hence the molecule optimizes into a local and most likely shallow minimum.

2.3.2. Transition states

Computational specifications:

Transition state optimizations: The transition state optimizations were performed at the same level of theory as the calculation of the bond dissociation energies. In order to verify the presence of a unique imaginary frequency along the proposed reaction mechanism, frequency calculations were performed at the optimized transition state structures.

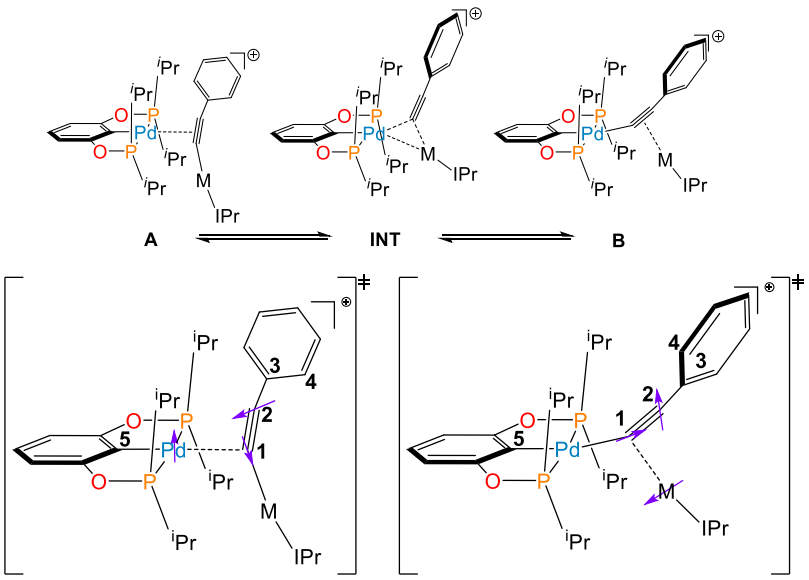

Figure SI-21: Schematic representation of the transition state structures for TS^A and TS^B. The approximate and schematic displacement vectors corresponding to vibration modes with imaginary frequencies are are shown (purple arrows). Displacement vectors of the other atoms are omitted for clarity.

	TS^A		TS^B	
	b(Pd-M) / (Å)	Imaginary frequencies / [cm^{-1}]	b(Pd-M) / (Å])	Imaginary frequencies / [cm^{-1}]
Cu	3.40	-50.07	3.15	-30.72
Ag	3.22	-43.06	NA	NA
Au	3.33	-41.44	3.59	-36.97

Table SI-7: Summarizing the imaginary frequencies as well as the bond length of the Pd-M for the found transition states.

2.4. Bond Dissociation Energies of the Pincer based Bimetallic Compounds

In order to calculate the bond dissociation energies, the following structures were considered: $[(^{iPr}POCOP)Pd]^+$, $[(^{iPr}POCOP)Pd(CCPh)]$, $[(IPr)M^+]$, $[(IPr)M(CCPh)]$ and the bimetallic pincer complex $[(^{iPr}POCOP)Pd(CCPh)\bullet M(IPr)]^+$. For $[(^{iPr}POCOP)Pd]^+$, $[(^{iPr}POCOP)Pd(CCPh)]$ and $[(^{iPr}POCOP)Pd(CCPh)M(IPr)]^+$ the energetically lowest lying conformers were chosen from the conformational search (see section 2.2)

Computational specifications:

Optimizations: The involved structures were optimized according to the computational method described above in the conformational search (see section 2.2.1). In order to validate the ground state nature of the molecular structure, and also to obtain zero point energies, frequency calculations were performed on the same level of theory as the optimization (PBE-D3/Def2-SVP) .

*Single Point Calculations:*The optimized structures were then recalculated by single point calculations of various levels of theory , using ORCA 4.0.1 as well as the ADF suite (ADF Version).

ORCA: The PBE functional was employed together with and without Grimme's D3 dispersion correction (with Becke-Johnson damping), whereas for M06-L was corrected with and without d3zero dispersion correction.[33] The calculations were performed for increasingly large basis sets Def2-SVP / Def2-TZVP / Def2-QZVP.

ADF[34]**:** Single point calculations were performed on top of the structures optimized in ORCA (PBE-D3/def2-SVP). Energies were computed using the M06-L functional and a TZP basis-set without frozen core. Relativistic effects including spin-orbit coupling were treated via the Zero Order Regular Approximation (ZORA) formalism.

BSSE correction: The dissociation limits were corrected for the basis set superposition error by applying the particular counterpoise correction. All calculations were performed according to the described single point calculation settings.

For AB $\rightarrow$ A + B

BDE_{noBSSE} $= E^{A}{}_{A}(A) + E^{B}{}_{B}(B) - E^{AB}{}_{AB}(AB)$

ΔE_{BSSE} $=[E^{AB}{}_{A}(A) - E^{AB}{}_{A}(AB) + E^{AB}{}_{B}(B) - E^{AB}{}_{B}(AB)]$

$BDE_{BSSEcorr}$ $= BDE_{noBSSE} - \Delta E_{BSSE}$

$E^{Y}{}_{X}(Z)$ represents the energy of fragment X at the optimized geometry of fragment Y with the basis set of Z.

In order to calculate the bond dissociation energy, the lowest energy conformations (based on the PBE-D3BJ/Def2-QZVP//PBE-D3BJ/Def2-SVP calculations) of both the asymptotes as well as the σ-π-σ rearrangement were chosen.

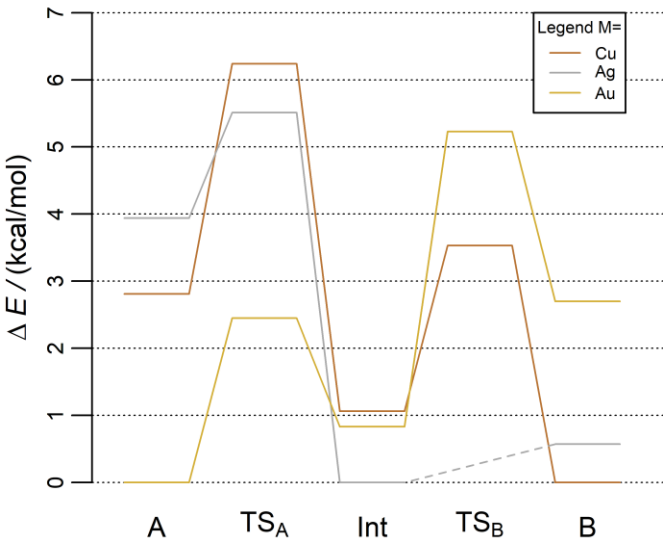

Figure SI-22: Potential Energy surface for the transmetalation step in the $[(^{iPr}POCOP)Pd(CCPh)M(IPr)]^+$ (M= Cu, Ag, Au) system. The energy values were obtained from PBE-D3BJ/Def2-QZVP//PBE-D3BJ/Def2-SVP calculations with zero point energy correction.

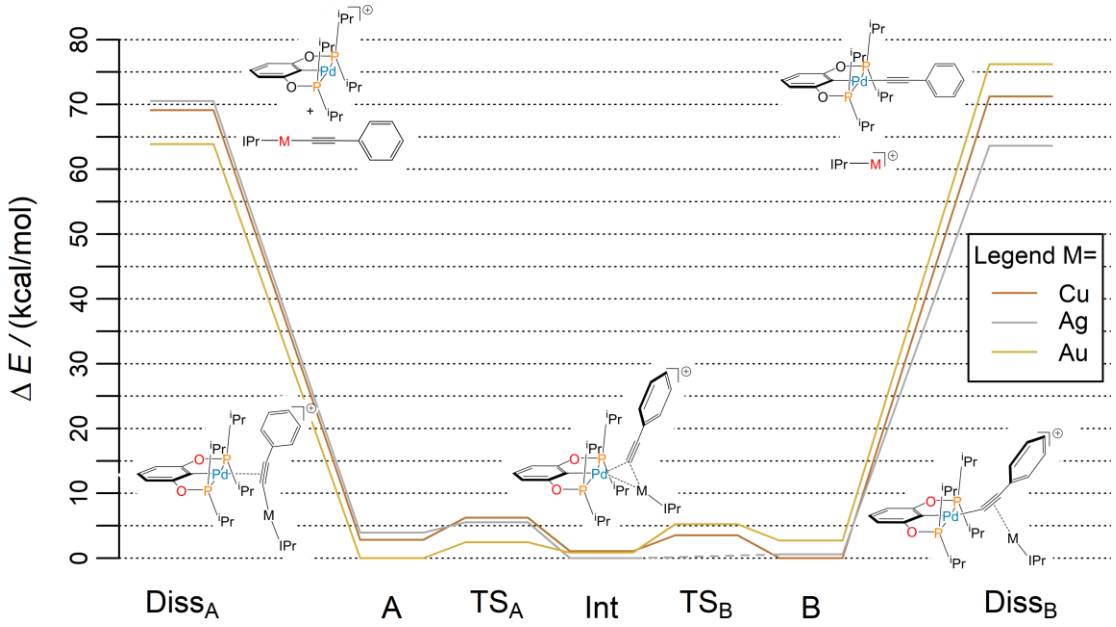

Figure SI-23: Potential Energy surface for the σ-π-σ rearrangement and the dissociation pathways in the [(^{iPr}POCOP)Pd(CCPh)M(IPr)]$^+$ (M= Cu, Ag, Au) system. The energy values were obtained from PBE-D3BJ/Def2-QZVP//PBE-D3BJ/Def2-SVP calculations with zero point energy correction. The dissociation asymptotes were additionally corrected for BSSE using the CP correction method.

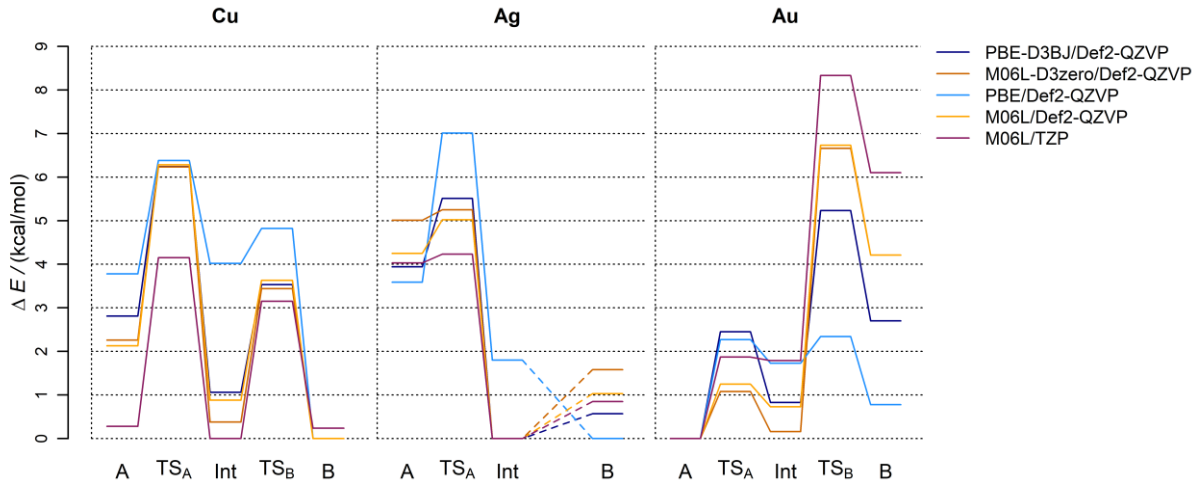

Figure SI-24: Potential Energy surface for the σ-π-σ rearrangement in the [(^{iPr}POCOP)Pd(CCPh)M(IPr)]$^+$ (M= Cu, Ag, Au) system. The structures were all optimized using PBE-D3BJ/Def2-SVP, zero point energies were obtained at the same level of theory. Single point calculations were performed at different levels of theory, e.g. PBE-D3BJ/Def2-QZVP, M06L-D3zero/Def2-QZVP and relativistic calculations M06L/TZP. The values for the non-dispersion-corrected energies were obtained by subtracting the dispersion correction.

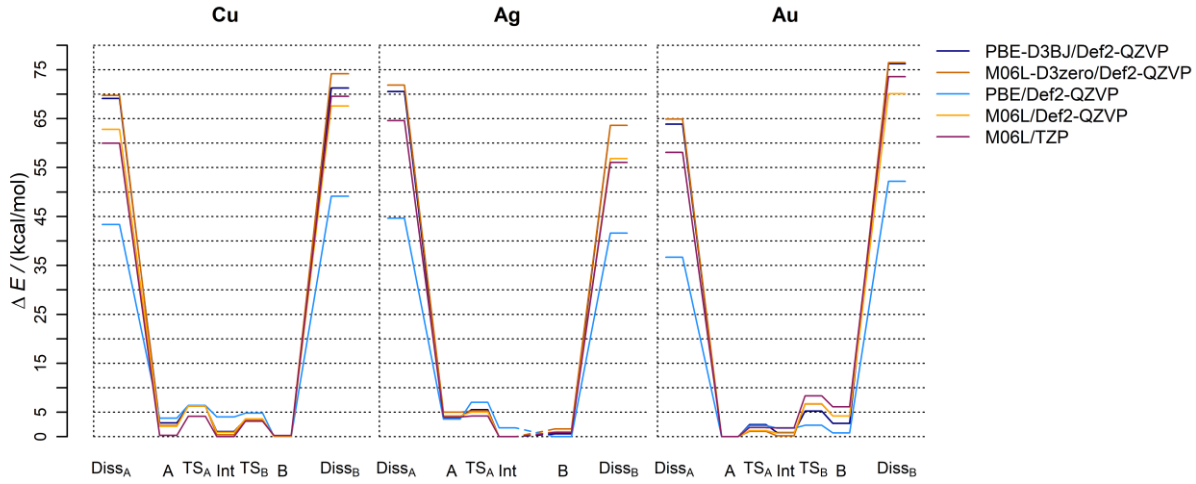

Figure SI-25: Potential Energy surface for the σ-π-σ rearrangement and the dissociation pathways in the [(^{iPr}POCOP)Pd(CCPh)M(IPr)]$^+$ (M= Cu, Ag, Au) system. The structures were all optimized using PBE-D3BJ/Def2-SVP, zero point energies were obtained at the same level of theory. Single point calculations were performed at different levels of theory, e.g. PBE-D3BJ/Def2-QZVP, M06L-D3zero/Def2-QZVP and relativistic calculations M06L/TZP. The values for the non-dispersion-corrected energies were obtained by subtracting the dispersion correction. The dissociation asymptotes were additionally corrected for BSSE using the CP correction.

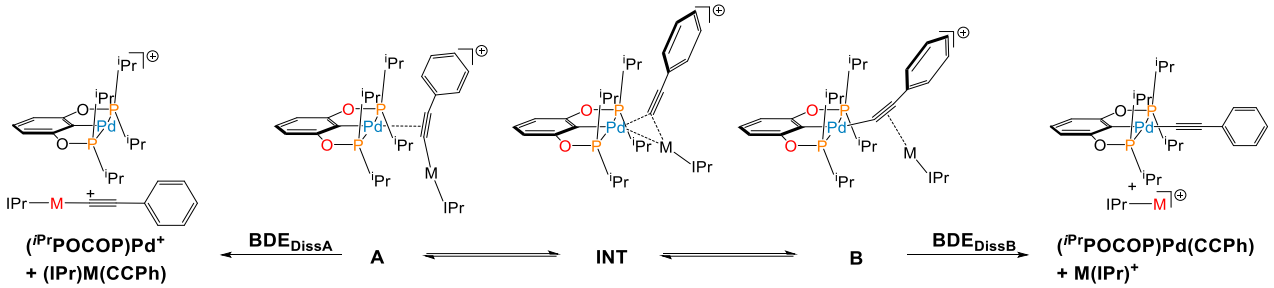

			Program			ORCA												ADF
			Functional			PBE-D3BJ			M06-L-D3zero			PBE			M06-L			M06-L
			Basis Set			Def2-SVP[a]	Def2-TZVP	Def2-QZVP	Def2-SVP	Def2-TZVP	Def2-QZVP	Def2-SVP	Def2-TZVP	Def2-QZVP	Def2-SVP	Def2-TZVP	Def2-QZVP	TZP
M	**Index**		**Structure Name**	**chrg**	**mult**													
Cu	BDE_{DissA}	$Diss_A$	[(iPrPOCOP)Pd]+ + [(IPr)Cu(CCPh)]	1,0	1,1	69.23	67.83	69.13	68.94	68.52	69.75	43.46	42.06	43.36	61.99	61.96	62.80	59.97
		A	[(iPrPOCOP)Pd(CCPh)•Cu(IPr)]+	1	1	2.94	2.41	2.81	2.43	1.79	2.26	3.91	3.39	3.78	2.30	1.60	2.13	0.28
		TS_A	[(iPrPOCOP)Pd(CCPh)-Cu(IPr)]+	1	1	6.31	5.85	6.24	6.26	5.79	6.23	6.45	5.99	6.38	6.31	5.77	6.28	4.15
	$E_{\sigma\text{-}\pi\text{-}\sigma}$	Int	[(iPrPOCOP)Pd(CCPh)Cu(IPr)]+	1	1	0.72	0.77	1.06	0.20	**0.00**	0.38	3.68	3.74	4.02	0.69	0.43	0.88	**0.00**
		TS_B	[(iPrPOCOP)Pd-(PhCC)Cu(IPr)]+	1	1	2.73	3.23	3.53	2.95	3.20	3.44	4.01	4.51	4.82	3.14	3.32	3.63	3.15
		B	[(iPrPOCOP)Pd•(PhCC)Cu(IPr)]+	1	1	**0.00**	**0.00**	**0.00**	**0.00**	0.07	**0.00**	**0.00**	**0.00**	**0.00**	**0.00**	**0.00**	**0.00**	0.24
	BDE_{DissB}	$Diss_B$	[(iPrPOCOP)Pd(CCPh)] + [(IPr)Cu]+	0,1	1,1	67.28	70.64	71.24	70.36	73.56	74.19	45.18	48.54	49.14	63.75	67.00	67.58	69.56
Ag	BDE_{DissA}	$Diss_A$	[(iPrPOCOP)Pd]+ + [(IPr)Ag(CCPh)]	1,0	1,1	69.24	69.42	70.54	71.04	71.80	71.86	44.26	43.62	44.66	63.77	64.53	64.59	64.61
		A	[(iPrPOCOP)Pd(CCPh)•Ag(IPr)]+*	1	1	4.10	3.90	3.94	5.23	5.05	5.01	3.26	3.42	3.59	4.47	4.29	4.25	4.03
		TS_A	[(iPrPOCOP)Pd(CCPh)-Ag(IPr)]+	1	1	5.37	5.39	5.51	5.19	5.40	5.25	6.39	6.77	7.01	4.95	5.16	5.02	4.23
	$E_{\sigma\text{-}\pi\text{-}\sigma}$	Int	[(iPrPOCOP)Pd(CCPh)Ag(IPr)]+	1	1	**0.00**	**0.00**	**0.00**	**0.00**	**0.00**	**0.00**	1.32	1.69	1.80	**0.00**	**0.00**	**0.00**	**0.00**
		TS_B	[(iPrPOCOP)Pd-(PhCC)Ag(IPr)]+	1	1													
		B	[(iPrPOCOP)Pd•(PhCC)Ag(IPr)]+	1	1	1.06	0.69	0.57	2.03	1.74	1.58	**0.00**	**0.00**	**0.00**	1.48	1.19	1.03	0.85
	BDE_{DissB}	$Diss_B$	[(iPrPOCOP)Pd(CCPh)] + [(IPr)Ag]+	0,1	1,1	61.75	63.05	63.61	62.19	63.93	63.61	39.85	41.04	41.59	55.43	57.16	56.85	56.05
Au	BDE_{DissA}	$Diss_A$	[(iPrPOCOP)Pd]+ + [(IPr)Au(CCPh)]	1,0	1,1	63.01	62.95	63.86	64.30	64.93	64.91	35.81	35.75	36.66	57.58	58.16	58.14	58.10
		A	[(iPrPOCOP)Pd(CCPh)•Au(IPr)]+	1	1	**0.00**	**0.00**	**0.00**	0.12	**0.00**	**0.00**	**0.00**	**0.00**	**0.00**	**0.00**	**0.00**	**0.00**	**0.00**
		TS_A	[(iPrPOCOP)Pd(CCPh)-Au(IPr)]+	1	1	2.36	2.32	2.45	1.21	0.89	1.08	2.18	2.14	2.27	1.26	1.07	1.25	1.87
	$E_{\sigma\text{-}\pi\text{-}\sigma}$	Int	[(iPrPOCOP)Pd(CCPh)Au(IPr)]+	1	1	0.62	0.77	0.83	**0.00**	0.02	0.16	1.53	1.67	1.73	0.45	0.59	0.73	1.79
		TS_B	[(iPrPOCOP)Pd-(PhCC)Au(IPr)]+	1	1	6.03	5.29	5.23	6.95	6.68	6.66	3.15	2.41	2.34	6.90	6.75	6.73	8.33
		B	[(iPrPOCOP)Pd•(PhCC)Au(IPr)]+	1	1	3.44	2.83	2.70	4.70	4.38	4.21	1.52	0.90	0.78	4.58	4.39	4.21	6.10
	BDE_{DissB}	$Diss_B$	[(iPrPOCOP)Pd(CCPh)] + [(IPr)Au]+	0,1	1,1	74.30	76.25	76.22	73.72	76.98	76.43	50.28	52.23	52.19	68.10	70.65	70.10	73.57

Table SI-8: The energies are referenced to the lowest energy structure found with the specified method. DissA and DissB denote the dissociated products stemming from a dissociation process from A or B respectively; BSSE denotes that the energy has been corrected for basis set superposition error by applying the counterpoise correction. All energies are zero-point energy corrected. *small imaginary frequency observed (-4.61 cm^{-1}).

2.5. Input Templates and Codes

Keyword	Description:
<RUNTYPE>	Various runtypes were used: **sp** (single point calculation), **opt** (optimization using internal coordinates, w/o constraints), **copt** (optimization using cartesian coordinates), **freq** (analytical frequencies), **NumFreq** (numerical frequencies). For transition state optimizations **optts** was used.
<F>	Keyword for the choice of the electron-correlation-energy-functional, e.g. **pbe** (GGA functional) or **m06l** (meta-GGA).
<B>	Keyword for the choice of the basis set, e.g. **def2-SVP**, **def2-TZVP**, **def2-QZVP**
<Disp>	Grimme's D3 dispersion correction with Becke-Johnson damping) **d3bj** was employed together with PBE, whereas for M06-L **d3zero** dispersion correction was used.
<CHRG>	Charge value (integer value), necessary molecule specific input parameter.
<M>	Multiplicity value (integer value), necessary molecule specific input parameter.
<XYZ>	Filename of the xyz-coordinate file, e.g. the XMOL (Symbol X Y Z) format.
<OUT_FILENAME>	The filename for the calculation output.
<NP>	Number of processors requested for the calculation.
<MEM>	Memory requested for the calculation (per core).
<IDxN>	Index of the atom in the atomic-list, has to be provided for constrained calculations.
$E^{Y}_{X}(Z)$	represents the energy of fragment X at the optimized geometry of fragment Y with the basis set of Z.

2.5.1. XTB Input Files

The xtb calculations were submitted according to the following command line along with the following additional files:

bsub xtb --input *.inp <XYZ> -chrg <CHRG> -opt > <OUT_FILENAME>.log

Constrained optimization/ *Input file for xtb. "*.inp"* *File form.: "*.inp"*	$constrain angle: <IDx1>,<IDx2>, <IDx3>, <Value1> angle: <IDx4>,<IDx5>, <IDx6>, <Value2> $end
Coordination file (XMOL format) / *External input file. <XYZ>* *File form.: "*.xyz"*	Number-of-Atoms Header Symbol X Y Z . . .

Table SI-9: Input files used for xtb calculations.

2.5.2. ORCA Input Files

Single-point-/ Optimization-/ Frequency-/ Transition state optimization calculations *Input file for Orca.* *File form.: "*.inp"*	!RKS <F> <Disp> RI <B> def2/J TightOPT TightSCF Grid5 NoFinalGrid NoMOPrint Printbasis %pal nprocs <NP> end %maxcore <MEM> %base "<OUT_FILENAME_opt>" %geom Calc_Hess true TolE=1e-6 TolRMSG=3e-5 TolMaxG=1e-4 TolRMSD=6e-4 TolMaxD=1e-3 end *xyzfile <CHRG> <M> <XYZ>

Constrained optimization/ *Input file for Orca File form.: "*.inp"*

```
!RKS <F>  <Disp> RI <B> def2/J opt TightSCF Grid4 NoFinalGrid NoMOPrint Printbasis
%pal nprocs <NP> end
%maxcore <MEM>
%scf maxiter 1000 end
%base "<OUT_FILENAME_opt>"

%geom maxiter 1000
      constraints
      {A <IDx1> <IDx2> <IDx3> <Value1> C}
      {A <IDx4> <IDx5> <IDx6> <Value2> C}
      end
end

*xyzfile <CHRG>  <M>  <XYZ>
```

Coordination file (XMOL format) / *External input file. <XYZ> File form.: "*.xyz"*

```
Number-of-Atoms
Header
Symbol X Y Z
.
.
.
```

BSSE CP correction calculations
Input file for Orca File form.: ".inp"*

ORCA ΔE_{BSSE} = $[E^{AB}_{A}(A) - E^{AB}_{A}(AB) + E^{AB}_{B}(B) - E^{AB}_{B}(AB)]$

$E^{AB}_{AB}(AB)$

```
#-------------------------------------------------------
# After the Orca calculation you will get two "inter-
# action energies" at the end of the output file. The
# difference is the negative BSSE.
#
# The script will set the orbital guess "PModel" for
# jobs 2-5 since Orca will try to use the .gbw-files of
# the earlier calculations which does not work for jobs
# 2 and 3 and does not help for jobs 4 and 5.
#-------------------------------------------------------
#
#-------------------------
#    First the dimer
#-------------------------
!RKS <F>  <Disp> RI <B> def2/J sp TightSCF Grid5 NoFinalGrid NoMOPrint Printbasis PModel
%pal nprocs <NP>  end
%maxcore <MEM>
%base "<OUT_FILENAME_sp_E-AB >"

%id "dimer"

* xyz <CHRG_Dimer>  <M_Dimer >
Symbol X Y Z
.
.
.
*
```

$E^{AB}_{A}(A)$

```
#-------------------------
#   Now the fragments at
#     dimer-geometry
#-------------------------

$new_job
!RKS <F>  <Disp> RI <B> def2/J sp TightSCF Grid5 NoFinalGrid NoMOPrint Printbasis PModel
%pal nprocs <NP>  end
%maxcore <MEM>
%base "<OUT_FILENAME_sp_A >"

%id "fragment"

%scf guess PModel end

* xyz <CHRG_FragA>  <M_FragA >
Symbol X Y Z
.
.
.

*
```

E^{AB}_{B}(B)	$new_job !RKS <F> <Disp> RI <B> def2/J sp TightSCF Grid5 NoFinalGrid NoMOPrint Printbasis PModel %pal nprocs <NP> end %maxcore <MEM> %base "<OUT_FILENAME_sp_B >" %id "fragment" %scf guess PModel end * xyz <CHRG_FragB> <M_FragB> Symbol X Y Z . . . * #------------------------- # Now the fragments at # dimer-geometry with # the dimer-basis #-------------------------
E^{AB}_{A}(AB)	$new_job !RKS <F> <Disp> RI <B> def2/J sp TightSCF Grid5 NoFinalGrid NoMOPrint Printbasis PModel %pal nprocs <NP> end %maxcore <MEM> %base "<OUT_FILENAME_sp_ABg >" %id "ghost" %scf guess PModel end * xyz <CHRG_FragA> <M_FragA> Symbol X Y Z . . . Symbol : X Y Z . . . * $new_job !RKS <F> <Disp> RI <B> def2/J sp TightSCF Grid5 NoFinalGrid NoMOPrint Printbasis PModel %pal nprocs <NP> end %maxcore <MEM> %base "<OUT_FILENAME_sp_AgB >" %id "ghost" %scf guess PModel end * xyz <CHRG_FragB> <M_FragB> Symbol : X Y Z . . . Symbol X Y Z . . . *
E^{AB}_{B}(AB)	

Table SI-10: Input files used for orca calculations.

2.5.3. ADF Input Files

Single-point-calculations
Input file for ADF.
File form.: ".inp"*

```
#nproc=<NP>
#mem=<MEM>

$ADFBIN/adf << eor
title  <OUT_FILENAME>

atoms
inline <XYZ>
end

charge <CHRG>

Basis
Type ZORA/TZP
Core None
end

Symmetry NOSYM

xc
 MetaGGA M06L
end

relativistic SpinOrbit ZORA


end input
eor
mv TAPE21 <OUT_FILENAME>.t21
mv logfile <OUT_FILENAME>.log
```

Coordination file (XMOL format) / *External input file. <XYZ>*
File form.: ".xyz"*

```
Number-of-Atoms
Header
Symbol X Y Z
.
.
.
```

BSSE CP correction calculations
Input file for ADF
File form.: ".inp"*

ORCA ΔE_{BSSE} = $[E^{AB}_{A}(A) - E^{AB}_{A}(AB) + E^{AB}_{B}(B) - E^{AB}_{B}(AB)] / E^{AB}_{A}(A)$

$E^{AB}_{B}(B)$

```
$ADFBIN/adf << eor
title  <OUT_FILENAME>_AB_A_A

atoms
Symbol X Y Z
.
.
.
end

charge <CHRG_FragA>

Basis
Type ZORA/TZP
Core None
end

Symmetry NOSYM

xc
 MetaGGA M06L
end

relativistic SpinOrbit ZORA


end input
eor
mv TAPE21 <OUT_FILENAME>_AB_A_A.t21
mv logfile <OUT_FILENAME>_AB_A_A.log
$ADFBIN/adf << eor
title  <OUT_FILENAME>_AB_B_B
```

	atoms Symbol X Y Z . . . end charge <CHRG_FragB> Basis Type ZORA/TZP Core None end Symmetry NOSYM xc MetaGGA M06L end relativistic SpinOrbit ZORA end input eor mv TAPE21 <OUT_FILENAME>_AB_B_B.t21 mv logfile <OUT_FILENAME>_AB_B_B.log
$E^{AB}_{A}(AB)$	$ADFBIN/adf << eor title <OUT_FILENAME>_AB_A_AB atoms Symbol X Y Z . . . Gh.Symbol X Y Z . . . end charge <CHRG_FragA> Basis Type ZORA/TZP Core None end Symmetry NOSYM xc MetaGGA M06L end relativistic SpinOrbit ZORA end input eor mv TAPE21 <OUT_FILENAME>_AB_A_AB.t21 mv logfile <OUT_FILENAME>_AB_A_AB.log
$E^{AB}_{B}(AB)$	$ADFBIN/adf << eor title <OUT_FILENAME>_AB_B_AB atoms Gh.Symbol X Y Z . . . Symbol X Y Z . .

```
.
end
charge <CHRG_FragB>

Basis
Type ZORA/TZP
Core None
end

Symmetry NOSYM

xc
  MetaGGA M06L
end

relativistic SpinOrbit ZORA


end input
eor
mv TAPE21 <OUT_FILENAME>_AB_B_AB.t21
mv logfile <OUT_FILENAME>_AB_B_AB.log
```

Table SI-11: Collection of Input files used for ADF calculations.

2.5.4. R-Script for Analysis of xyz data files

`External coordination file for BSSE calculations <XYZ>:`

```
# Script for extraction of structural parameters from .xyz files
library(pracma)
rm(list = ls())
path='./'
# -------------------------INPUT and DESCRIPTION-----------------------------------------------------------------------
# IMPORTANT DESCRIPTION:
# INPUT: Replace the <INPUT.xyz> with the file name of the *.xyz file that is supposed to be analyzed.
#       Multiple structures can be contained in the *.xyz file. They have to be organized according to the following rules:
# Header Line 1: Number of Atoms                  (this is not important for this code but it might be for ORCA calculations)
# Header Line 2: "Name = NAME Energy(a.u.) = ENERGY"  (Energy values can be passed onto the code via replacement of "ENERGY" with a value
#                                     The length of Header-Line 2 has to be either 3 or 6)
# Symbol X Y Z

xyzFileName <- '<INPUT.xyz>' # Here goes the filename of the *xyz
txtOutputFileName <- "<OUTPUT.txt>" # Output filename (*.txt)
# Specification of the parameters to be extracted. b_para for bond distances, a_para for angles, and d_para for dihedrals.
#   The numbers that have to be supplied represent the labels (starting at 1 for the first atom) of the correspoding atoms.
#   Example used for structural parameter extraction used for most of the otherwise appended *.xyz in this publication:
b_para= rbind(c(1,55),c(1,56),c(1,57),c(1,14),c(55,56),c(55,57),c(55,69),c(56,57))
a_para=rbind(c(1,56,55),c(1,56,57),c(14,1,56),c(55,56,57),c(56,57,58))
d_para=rbind(c(1,2,15,19),c(1,2,16,28),c(1,3,17,37),c(1,3,18,46),c(1,56,57,59),c(1,55,69,75),c(3,1,56,55),c(57,56,69,105),c(55,56,57,59))

# ---------------------------------------------------------------------------------------------------------------------
outfilename <- paste(c(lapply(sub(pattern = "(.*)\\..*$", replacement = "\\1",basename(xyzFileName)),as.character),txtOutputFileName), collapse="")
if (length(grep('Name',readLines(xyzFileName)))==0){
  print("NO NAME PATTERN PRESENT, second line has to start with 'Name'")
}else {
  Lines <- c(grep('Name',readLines(xyzFileName))-1,length(readLines(xyzFileName)))
  for (Line_Nr in 1:(length(Lines)-1)){
    XYZ=read.table(file=paste(path,xyzFileName, sep=''),skip=Lines[Line_Nr]+1,nrows=Lines[Line_Nr+1]-Lines[Line_Nr]-2)#read.table(file=paste(path,file, sep=''), header=F, skip=2,
sep="")
    colnames(XYZ)=c('AtomType','x','y','z')
    Header <- read.table(file=paste(path,xyzFileName, sep=''),skip=Lines[Line_Nr],nrows=1)#readLines(paste(path,xyzFileName, sep=''), n = Lines[Line_Nr]+1)
    # Calculation of the structural parameters that are supposed to be extracted.
    b_value<-vector()
    for (i in 1:length(b_para[,1])){
      #Calculate bond distances
      b_value[i]=norm(as.matrix(XYZ[b_para[i,2],2:4]-XYZ[b_para[i,1],2:4]),type="2")
    }
    a_value<-vector()
    for (i in 1:length(a_para[,1])){
      temp_vec1=as.matrix(XYZ[a_para[i,1],2:4]-XYZ[a_para[i,2],2:4])
      temp_vec2=as.matrix(XYZ[a_para[i,3],2:4]-XYZ[a_para[i,2],2:4])
      #Calculate angles
      a_value[i]=acos(dot(temp_vec1,temp_vec2) / (norm(temp_vec1,type="2") *
norm(temp_vec2,type="2")))*180/pi#norm(cross(temp_vec1,temp_vec2)),dot(temp_vec1,temp_vec2))
    }
    d_value<-vector()
    for (i in 1:length(d_para[,1])){
      temp_vec1=as.matrix(XYZ[d_para[i,2],2:4]-XYZ[d_para[i,1],2:4])
      temp_vec2=as.matrix(XYZ[d_para[i,3],2:4]-XYZ[d_para[i,2],2:4])
      temp_vec3=as.matrix(XYZ[d_para[i,4],2:4]-XYZ[d_para[i,3],2:4])
      #Calculate dihedrals

d_value[i]=atan2d(dot(cross(cross(temp_vec1,temp_vec2),cross(temp_vec2,temp_vec3)),temp_vec2/norm(temp_vec2,type="2")),dot(cross(temp_vec1,temp_vec2),cross(temp_vec
2,temp_vec3)))#norm(cross(temp_vec1,temp_vec2)),dot(temp_vec1,temp_vec2))
    }

    # OUTPUT
    Name <- Header[3]
```

```
   if (length(Header)==3){
     print("No Energies detected")
     # WRITE Column LABELS, no energy column
     if (Line_Nr==1){

write.table(paste(c("Struc_Nr","Name",apply(cbind((apply(cbind(as.character(XYZ[b_para[,1],1]),b_para[,1]),1,paste,collapse="")),(apply(cbind(as.character(XYZ[b_para[,2],1]),b_p
ara[,2]),1,paste,collapse=""))),1,paste,collapse="_"),apply(cbind((apply(cbind(as.character(XYZ[a_para[,1],1]),a_para[,1]),1,paste,collapse="")),(apply(cbind(as.character(XYZ[a_para
[,2],1]),a_para[,2]),1,paste,collapse=""))),(apply(cbind(as.character(XYZ[a_para[,3],1]),a_para[,3]),1,paste,collapse=""))),1,paste,collapse="_"),apply(cbind((apply(cbind(as.character(
XYZ[d_para[,1],1]),d_para[,1]),1,paste,collapse="")),(apply(cbind(as.character(XYZ[d_para[,2],1]),d_para[,2]),1,paste,collapse="")),(apply(cbind(as.character(XYZ[d_para[,3],1]),d_p
ara[,3]),1,paste,collapse="")),(apply(cbind(as.character(XYZ[d_para[,4],1]),d_para[,4]),1,paste,collapse=""))),1,paste,collapse="_")),collapse="\t"), outfilename, append = TRUE,
sep="\t",row.names = FALSE, col.names = FALSE,quote = FALSE)
     }
     x <- c(Line_Nr,lapply(Name,as.character),b_value,a_value,d_value)#
     write.table(paste(x, collapse="\t"), outfilename, append = TRUE, sep="\t",row.names = FALSE, col.names = FALSE,quote = FALSE)
   }else {
     Energies <- as.numeric(Header[6])
     # WRITE Column LABELS
     if (Line_Nr==1){
     write.table(paste(c("Struc_Nr","Name",
"Energy",apply(cbind((apply(cbind(as.character(XYZ[b_para[,1],1]),b_para[,1]),1,paste,collapse="")),(apply(cbind(as.character(XYZ[b_para[,2],1]),b_para[,2]),1,paste,collapse=""))),
1,paste,collapse="_"),apply(cbind((apply(cbind(as.character(XYZ[a_para[,1],1]),a_para[,1]),1,paste,collapse="")),(apply(cbind(as.character(XYZ[a_para[,2],1]),a_para[,2]),1,paste,col
lapse="")),(apply(cbind(as.character(XYZ[a_para[,3],1]),a_para[,3]),1,paste,collapse=""))),1,paste,collapse="_"),apply(cbind((apply(cbind(as.character(XYZ[d_para[,1],1]),d_para[,1])
,1,paste,collapse="")),(apply(cbind(as.character(XYZ[d_para[,2],1]),d_para[,2]),1,paste,collapse="")),(apply(cbind(as.character(XYZ[d_para[,3],1]),d_para[,3]),1,paste,collapse="")),(
apply(cbind(as.character(XYZ[d_para[,4],1]),d_para[,4]),1,paste,collapse=""))),1,paste,collapse="_")),collapse="\t"), outfilename, append = TRUE, sep="\t",row.names = FALSE,
col.names = FALSE,quote = FALSE)
     }
     x <- c(Line_Nr,lapply(Name,as.character),Energies,b_value,a_value,d_value)#
     write.table(paste(x, collapse="\t"), outfilename, append = TRUE, sep="\t",row.names = FALSE, col.names = FALSE,quote = FALSE)
   }
  } # END OF LOOP through LINE_Nr
 } # END IF "NAME" is present
```

Table SI-12: R-Code for analysis of the resulting structures.

3. Additional Information

3.1. NMR-Spectra of the Pincer based Bimetallic Compounds

3.1.1. NMR spectra of [(^{iPr}POCOP)Pd^{II}(CCPh)•Cu^{I}(IPr)]BF_4, [**1**]BF_4:

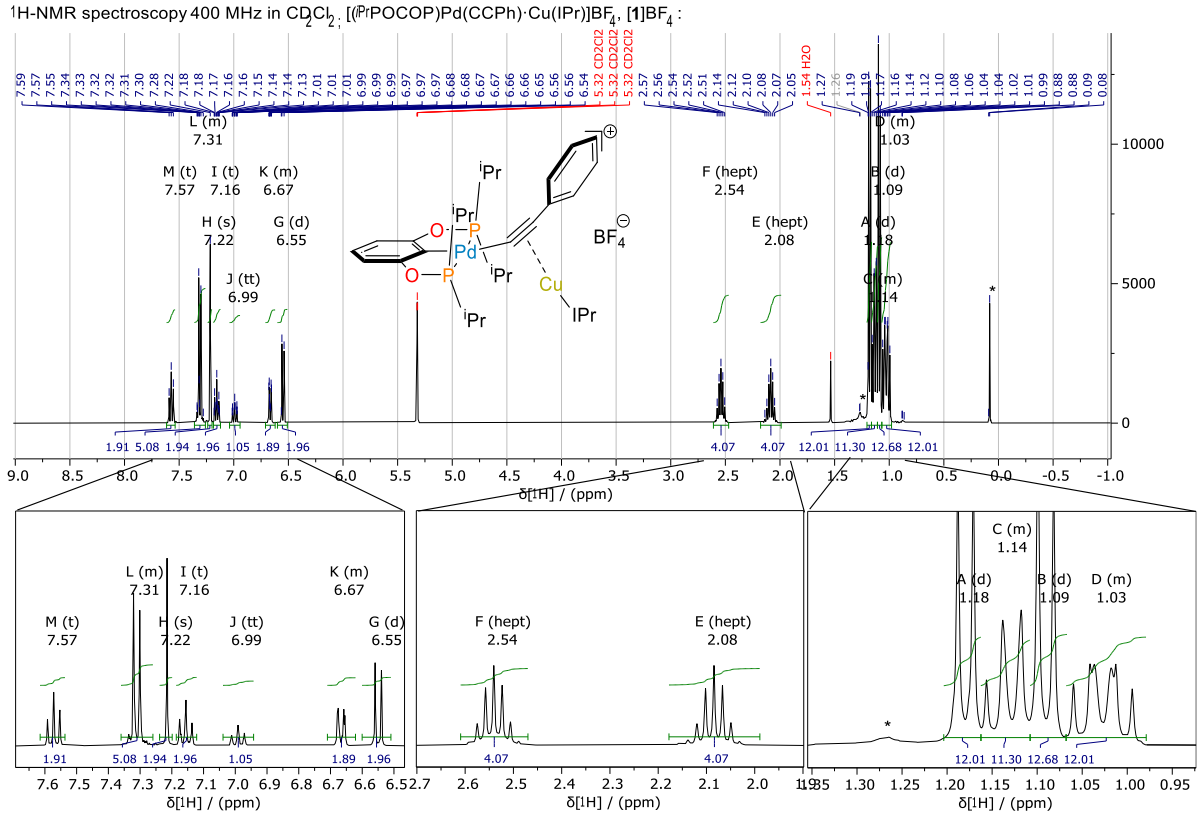

Figure SI-26: ^{1}H-NMR (400 MHz) spectrum of compound [(^{iPr}POCOP)Pd(CCPh)•Cu(IPr)]BF_4, [**1**]BF_4 , in CD_2Cl_2 measured at r.t. The spectrum was referenced to the residual solvent peak: ^{1}H-NMR (CD_2Cl_2) δ = 5.32 ppm. Impurities are marked with an asterisk*. *Top)* the full ^{1}H-NMR spectrum. *Bottom)* expansions of selected sections of the ^{1}H-NMR spectrum with arbitrary scaling of intensity.

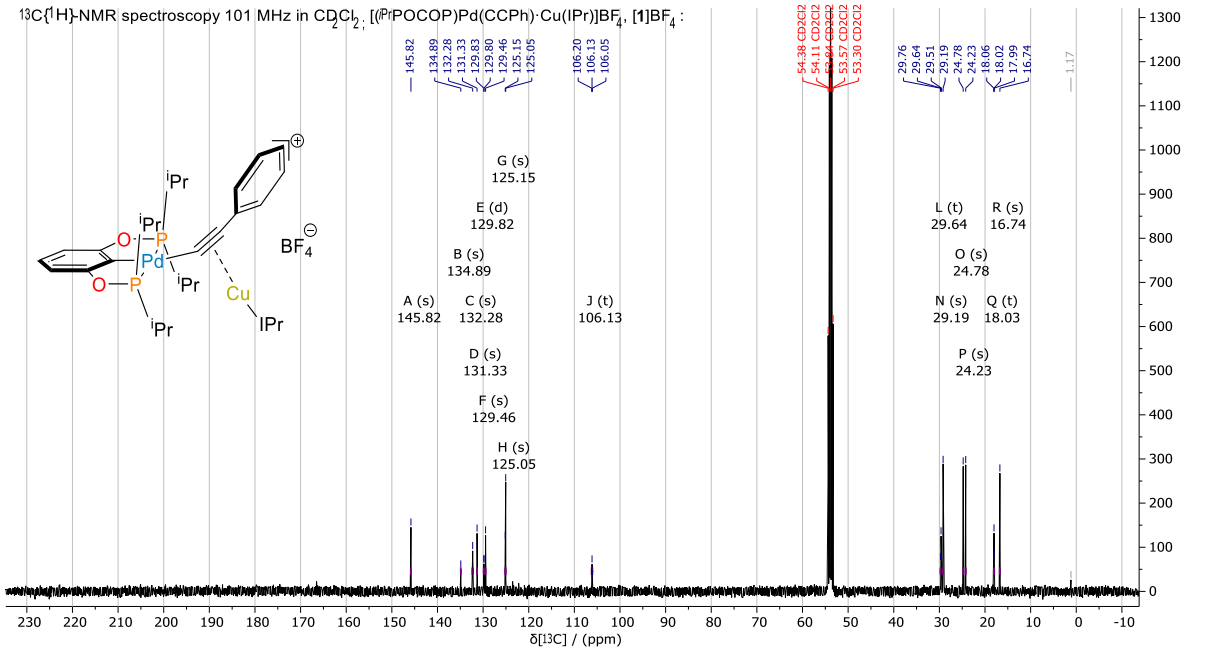

Figure SI-27: ^{13}C{^{1}H}-NMR (101 MHz) spectrum of compound [(^{iPr}POCOP)Pd(CCPh)•Cu(IPr)]BF_4, [**1**]BF_4 , in CD_2Cl_2 measured at r.t. The spectrum was referenced to the residual solvent peak: ^{13}C -NMR (CD_2Cl_2) δ = 53.84 ppm.

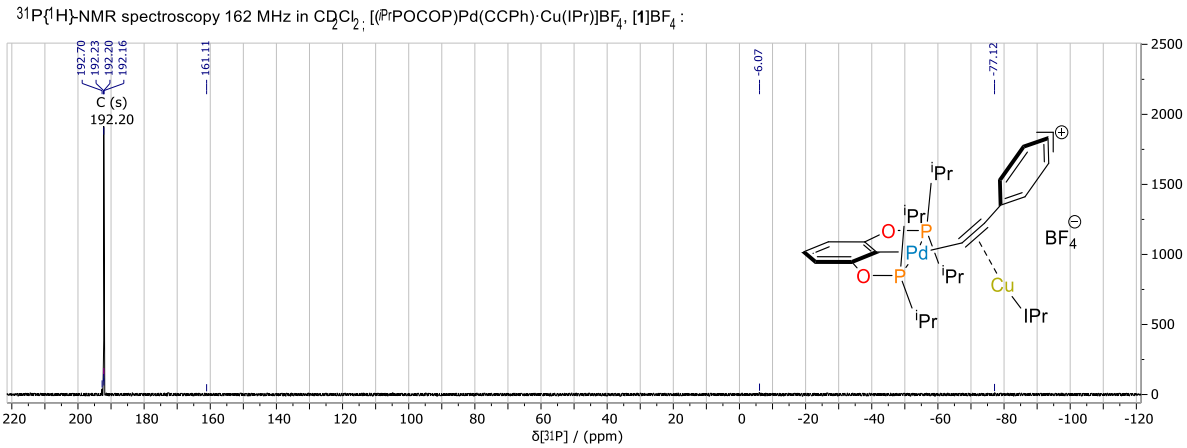

Figure SI-28: $^{31}P\{^{1}H\}$-NMR (162 MHz) spectrum of compound [(^{iPr}POCOP)Pd(CCPh)•Cu(IPr)]BF_4, [**1**]BF_4, in CD_2Cl_2 measured at r.t.

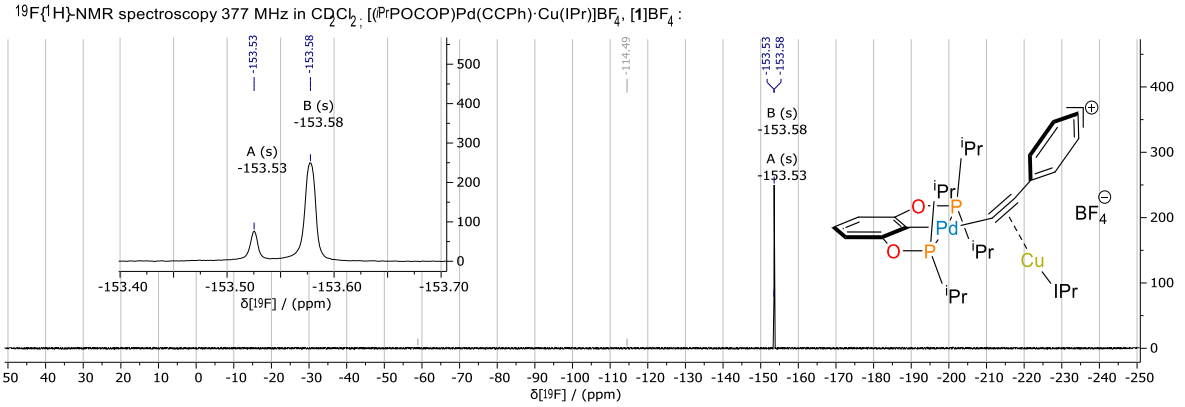

Figure SI-29: $^{19}F\{^{1}H\}$-NMR (377 MHz) spectrum of compound [(^{iPr}POCOP)Pd(CCPh)•Cu(IPr)]BF_4, [**1**]BF_4, in CD_2Cl_2 measured at r.t. *Inset)* expansions of selected section of the $^{19}F\{^{1}H\}$-NMR spectrum with arbitrary scaling of intensity.

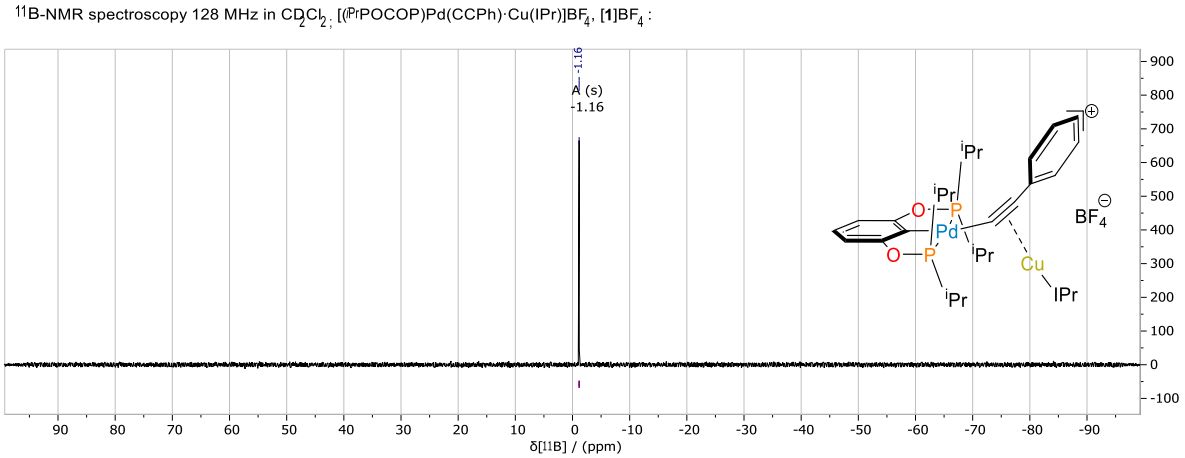

Figure SI-30: ^{11}B-NMR (128 MHz) spectrum of compound [(^{iPr}POCOP)Pd(CCPh)•Cu(IPr)]BF_4, [**1**]BF_4, in CD_2Cl_2 measured at r.t.

3.1.2. NMR spectra of [($^{i\text{Pr}}$POCOP)Pd$^{\text{II}}$(CCPh)•Cu$^{\text{I}}$(IPr)]BArF, [**1**]BArF:

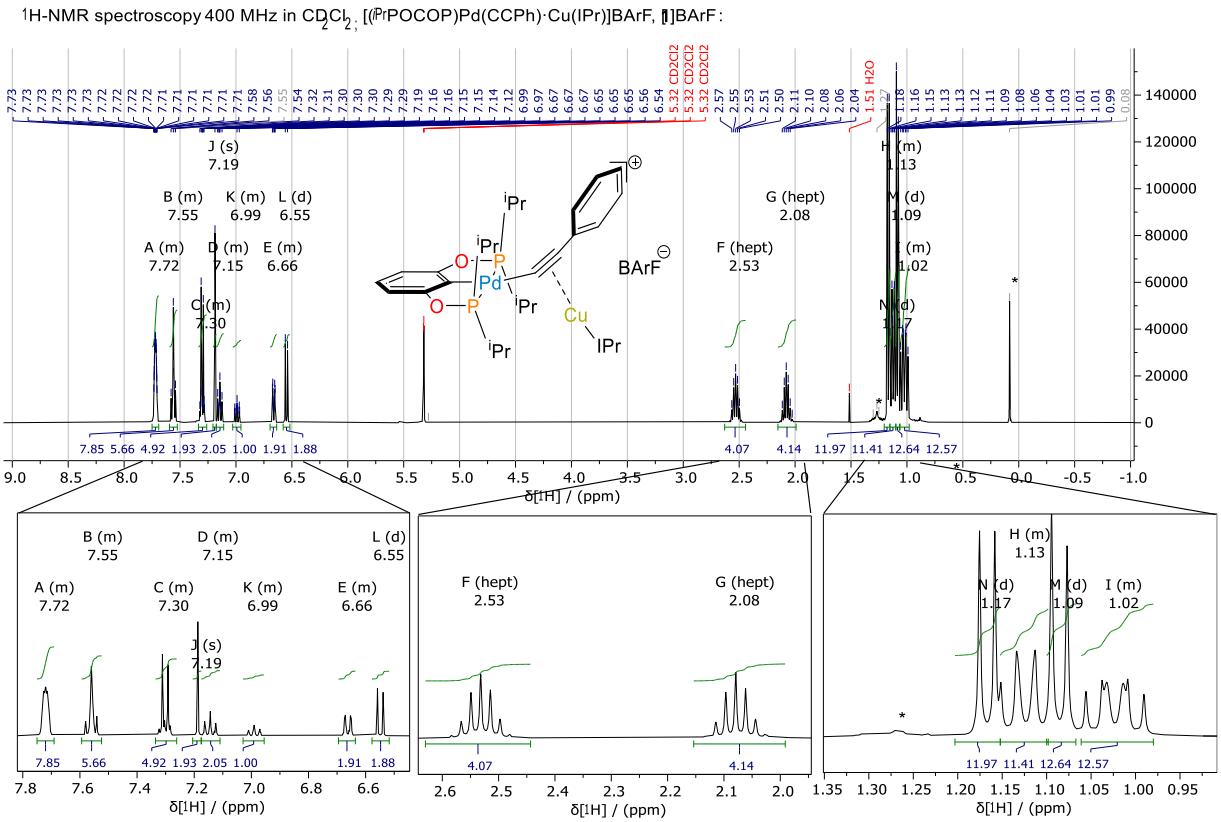

Figure SI-31: ^{1}H-NMR (400 MHz) spectrum of compound [($^{i\text{Pr}}$POCOP)Pd(CCPh)•Cu(IPr)]BArF, [**1**]BArF , in CD_2Cl_2 measured at r.t. The spectrum was referenced to the residual solvent peak: ^{1}H-NMR (CD_2Cl_2) δ = 5.32 ppm. Impurities are marked with an asterisk*. *Top)* the full ^{1}H-NMR spectrum. *Bottom)* expansions of selected sections of the ^{1}H-NMR spectrum with arbitrary scaling of intensity.

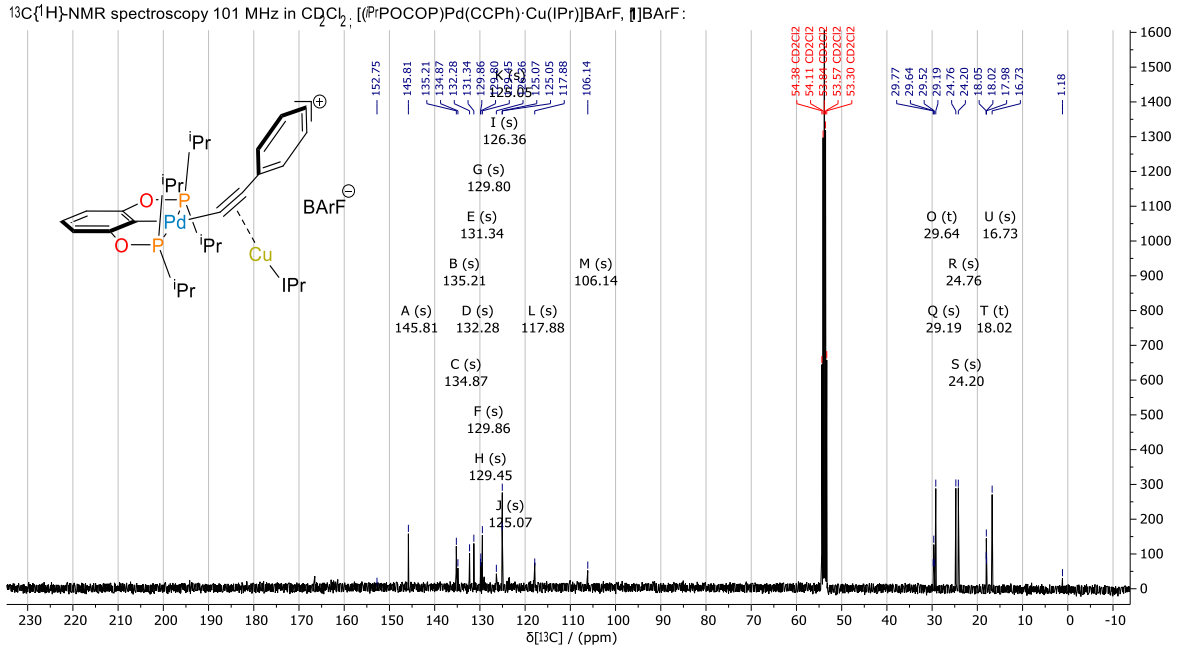

Figure SI-32: ^{13}C{^{1}H}-NMR (101 MHz) of compound [($^{i\text{Pr}}$POCOP)Pd(CCPh)•Cu(IPr)]BArF, [**1**]BArF , in CD_2Cl_2 measured at r.t. The spectrum was referenced to the residual solvent peak: ^{13}C -NMR (CD_2Cl_2) δ = 53.84 ppm.

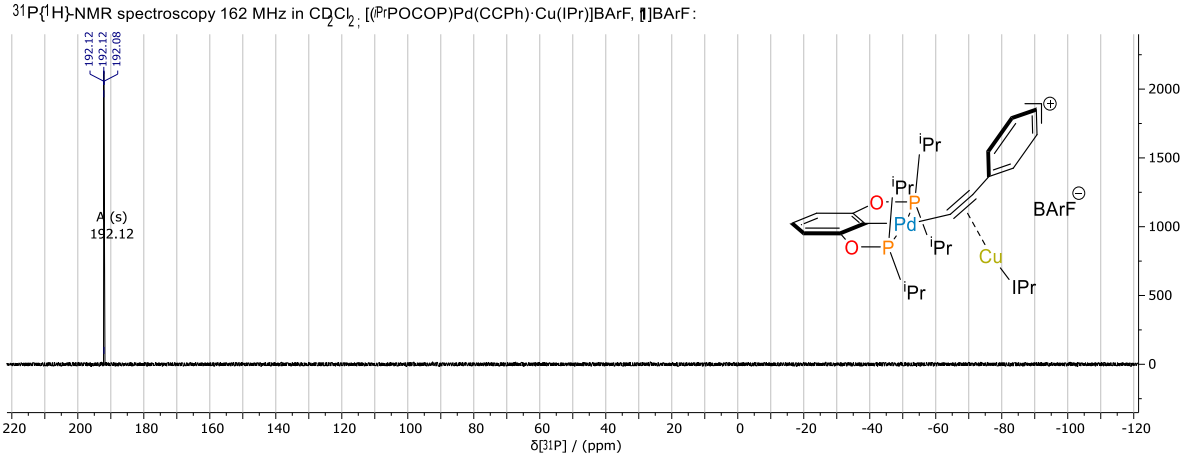

Figure SI-33: $^{31}P\{^{1}H\}$-NMR (162 MHz) spectrum of compound [(^{iPr}POCOP)Pd(CCPh)•Cu(IPr)]BArF, [**1**]BArF , in CD_2Cl_2 measured at r.t.

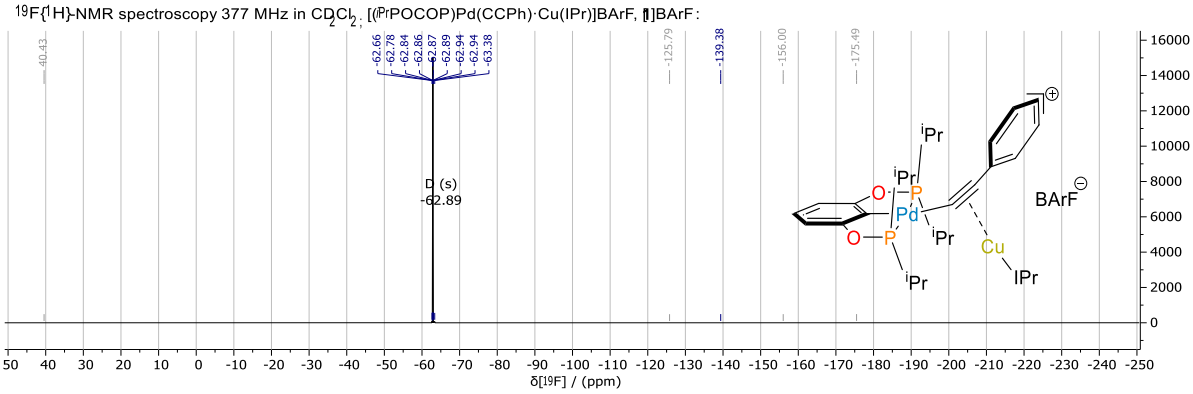

Figure SI-34: $^{19}F\{^{1}H\}$-NMR (377 MHz) spectrum of compound [(^{iPr}POCOP)Pd(CCPh)•Cu(IPr)]BArF, [**1**]BArF , in CD_2Cl_2 measured at r.t.

3.1.3. NMR spectra of [($^{i\text{Pr}}$POCOP)Pd$^{\text{II}}$(CCPh)•Ag$^{\text{I}}$(IPr)]BF4, [**2**]BF_4:

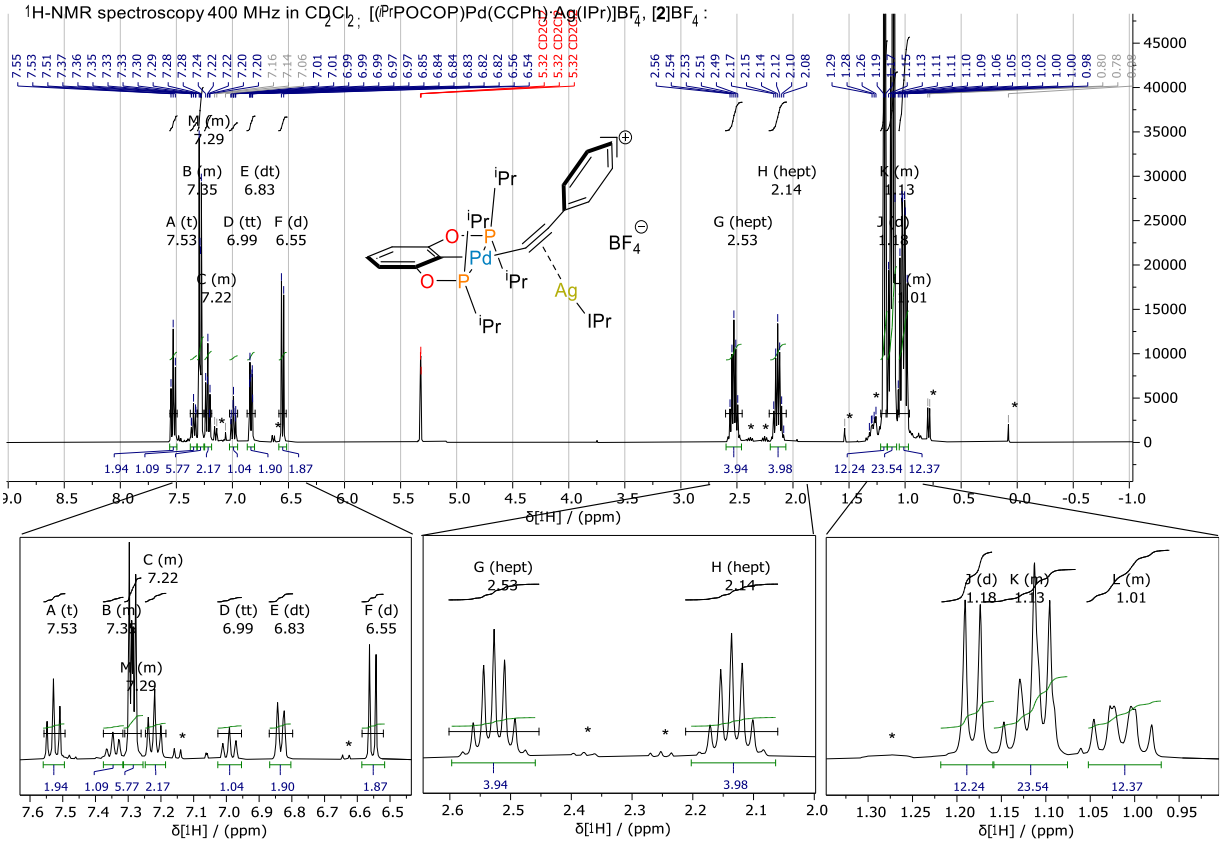

Figure SI-35: ¹H-NMR (400 MHz) spectrum of compound [($^{i\text{Pr}}$POCOP)Pd(CCPh)•Ag(IPr)]BF_4, [**2**]BF_4 , in CD_2Cl_2 measured at r.t. The spectrum was referenced to the residual solvent peak: ¹H-NMR (CD_2Cl_2) δ = 5.32 ppm. Impurities are marked with an asterisk*. *Top)* the full ¹H-NMR spectrum. *Bottom)* expansions of selected sections of the ¹H-NMR spectrum with arbitrary scaling of intensity.

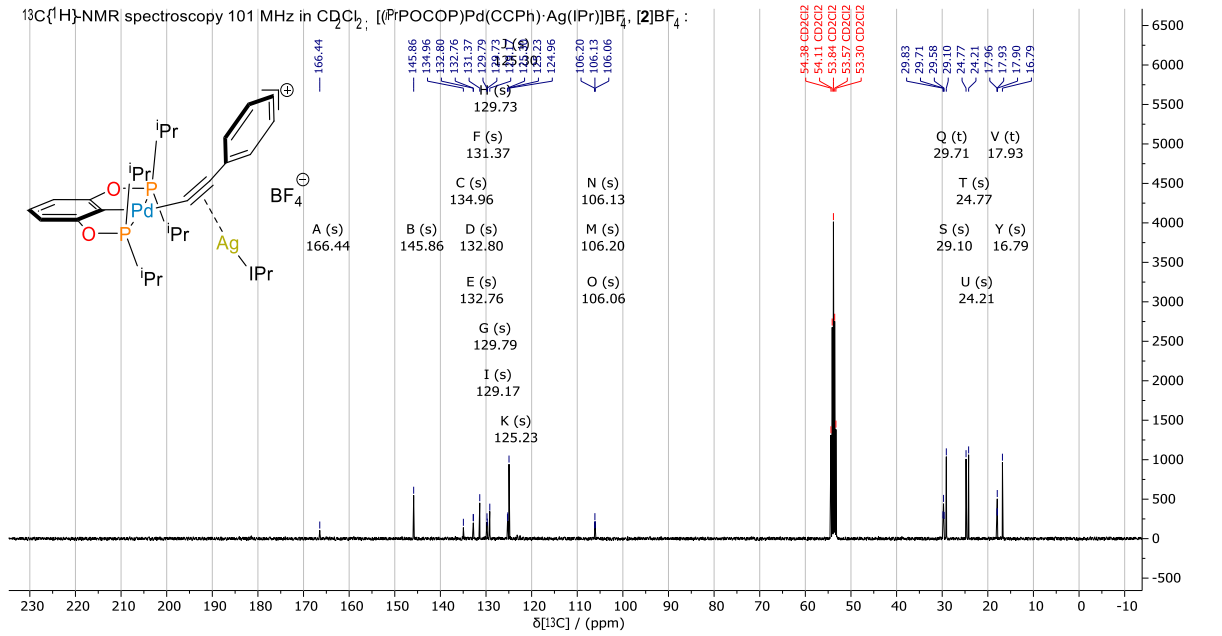

Figure SI-36: :$^{13}C\{^1H\}$-NMR (101 MHz) spectrum of compound [($^{i\text{Pr}}$POCOP)Pd(CCPh)•Ag(IPr)]BF_4, [**2**]BF_4 , in CD_2Cl_2 measured at r.t. The spectrum was referenced to the residual solvent peak: ^{13}C -NMR (CD_2Cl_2) δ = 53.84 ppm.

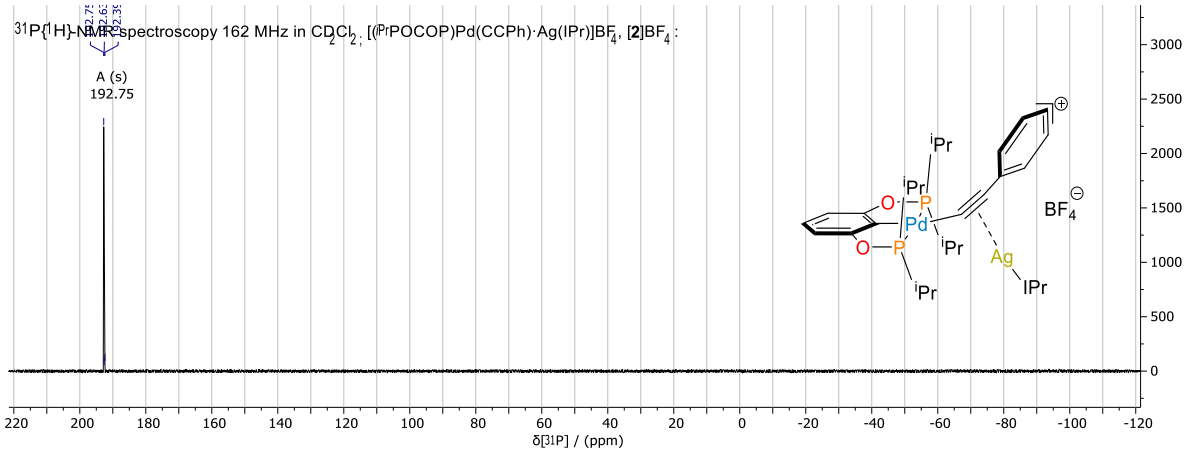

Figure SI-37 **:** $^{31}P\{^{1}H\}$-NMR (162 MHz) spectrum of compound [(^{iPr}POCOP)Pd(CCPh)•Ag(IPr)]BF_4, [**2**]BF_4 , in CD_2Cl_2 measured at r.t.

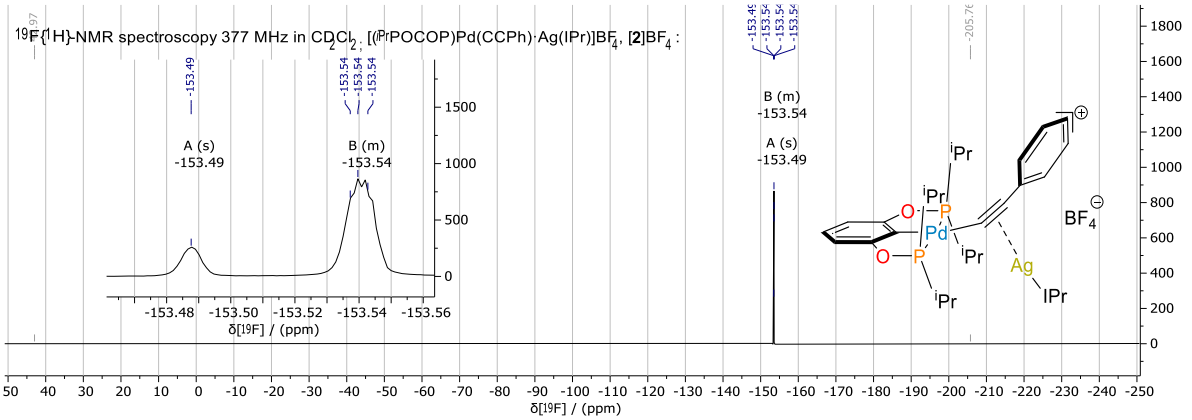

Figure SI-38: $^{19}F\{^{1}H\}$-NMR (377 MHz) spectrum of compound [(^{iPr}POCOP)Pd(CCPh)•Ag(IPr)]BF_4, [**2**]BF_4 , in CD_2Cl_2 measured at r.t. *Inset)* expansions of selected section of the $^{19}F\{^{1}H\}$-NMR spectrum with arbitrary scaling of intensity.

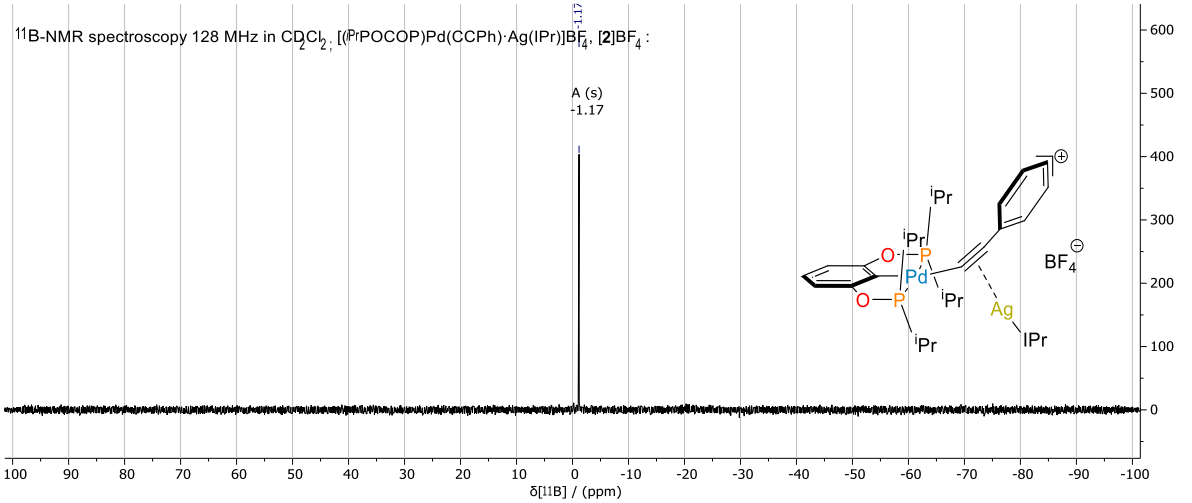

Figure SI-39: ^{11}B-NMR (128 MHz) spectrum of compound [(^{iPr}POCOP)Pd(CCPh)•Ag(IPr)]BF_4, [**2**]BF_4 , in CD_2Cl_2 measured at r.t.

3.1.4. NMR spectra of [($^{i\text{Pr}}$POCOP)Pd$^{\text{II}}$(CCPh)•Ag$^{\text{I}}$(IPr)]OTf, [**2**]OTf:

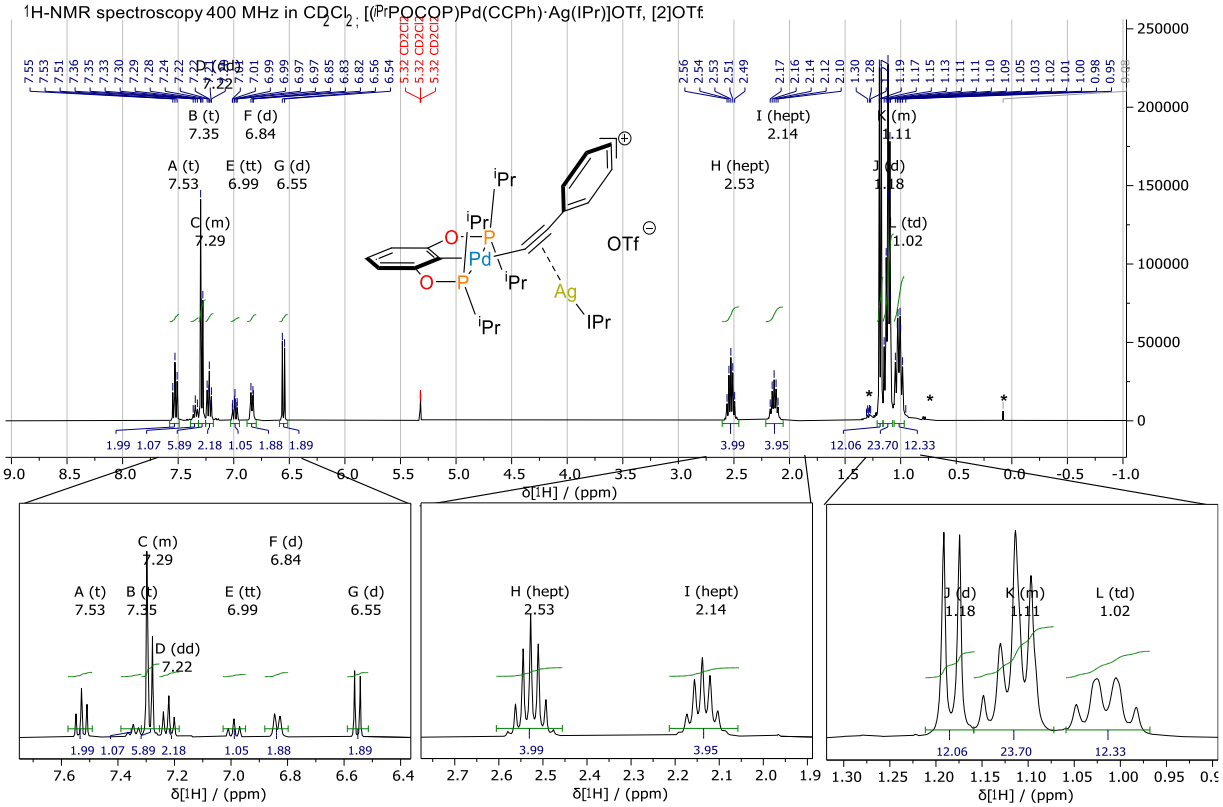

Figure SI-40: ^{1}H-NMR (400 MHz) spectrum of compound [($^{i\text{Pr}}$POCOP)Pd(CCPh)•Ag(IPr)]OTf, [**2**]OTf, in CD_2Cl_2 measured at r.t. The spectrum was referenced to the residual solvent peak: ^{1}H-NMR (CD_2Cl_2) δ = 5.32 ppm. Impurities are marked with an asterisk*. *Top)* the full ^{1}H-NMR spectrum. *Bottom)* expansions of selected sections of the ^{1}H-NMR spectrum with arbitrary scaling of intensity.

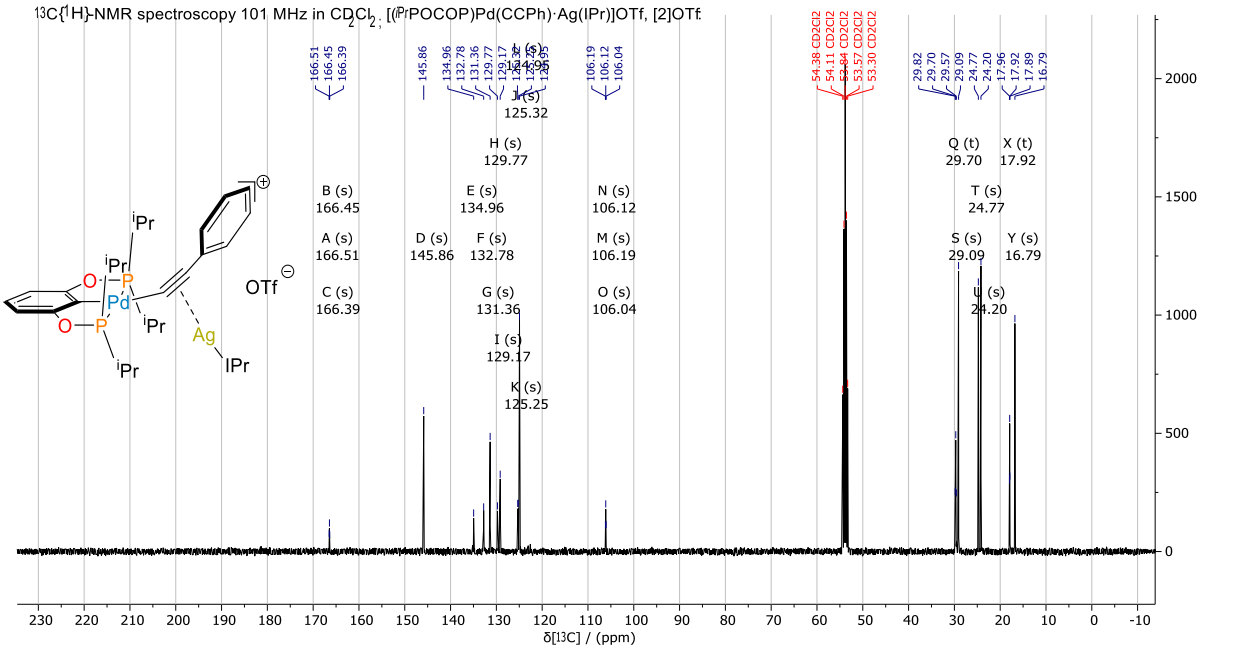

Figure SI-41: ^{13}C{^{1}H}-NMR (101 MHz) spectrum of compound [($^{i\text{Pr}}$POCOP)Pd(CCPh)•Ag(IPr)]OTf, [**2**]OTf, in CD_2Cl_2 measured at r.t. The spectrum was referenced to the residual solvent peak: ^{13}C -NMR (CD_2Cl_2) δ = 53.84 ppm.

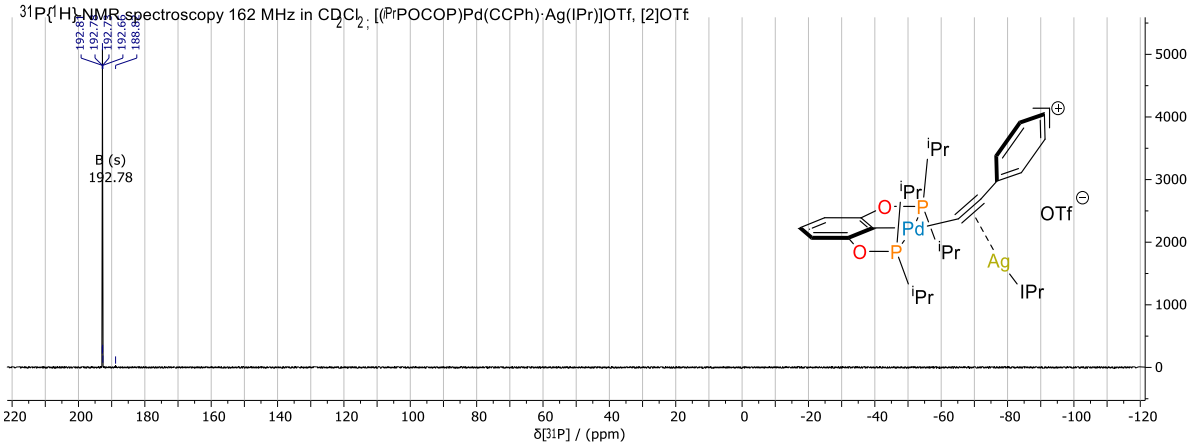

Figure SI-42: $^{31}P\{^{1}H\}$-NMR (162 MHz) spectrum of compound [(^{iPr}POCOP)Pd(CCPh)•Ag(IPr)]OTf, [**2**]OTf, in CD_2Cl_2 measured at r.t.

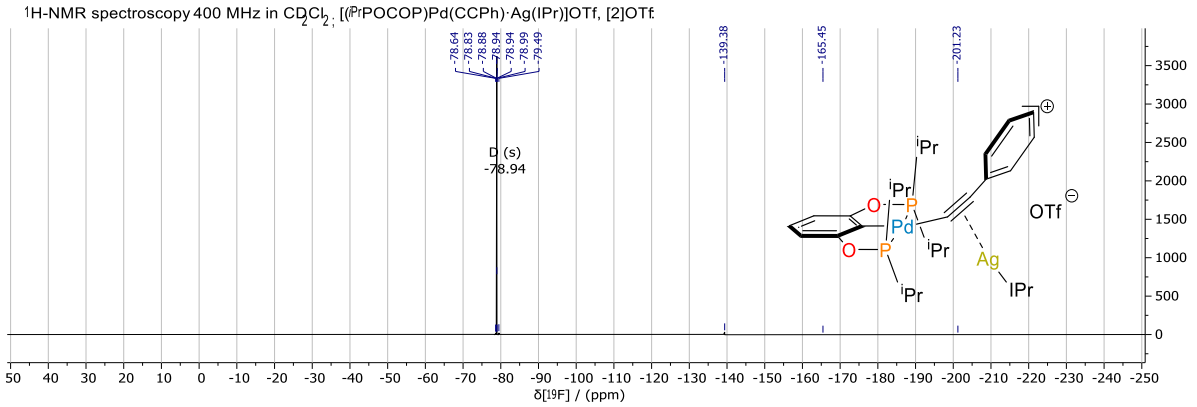

Figure SI-43: $^{19}F\{^{1}H\}$-NMR (377 MHz) spectrum of compound [(^{iPr}POCOP)Pd(CCPh)•Ag(IPr)]OTf, [**2**]OTf, in CD_2Cl_2 measured at r.t.

3.1.5. NMR spectra of [($^{i\text{Pr}}$POCOP)Pd$^{\text{II}}$(CCPh)•Ag$^{\text{I}}$(IPr)]BArF, [**2**]BArF:

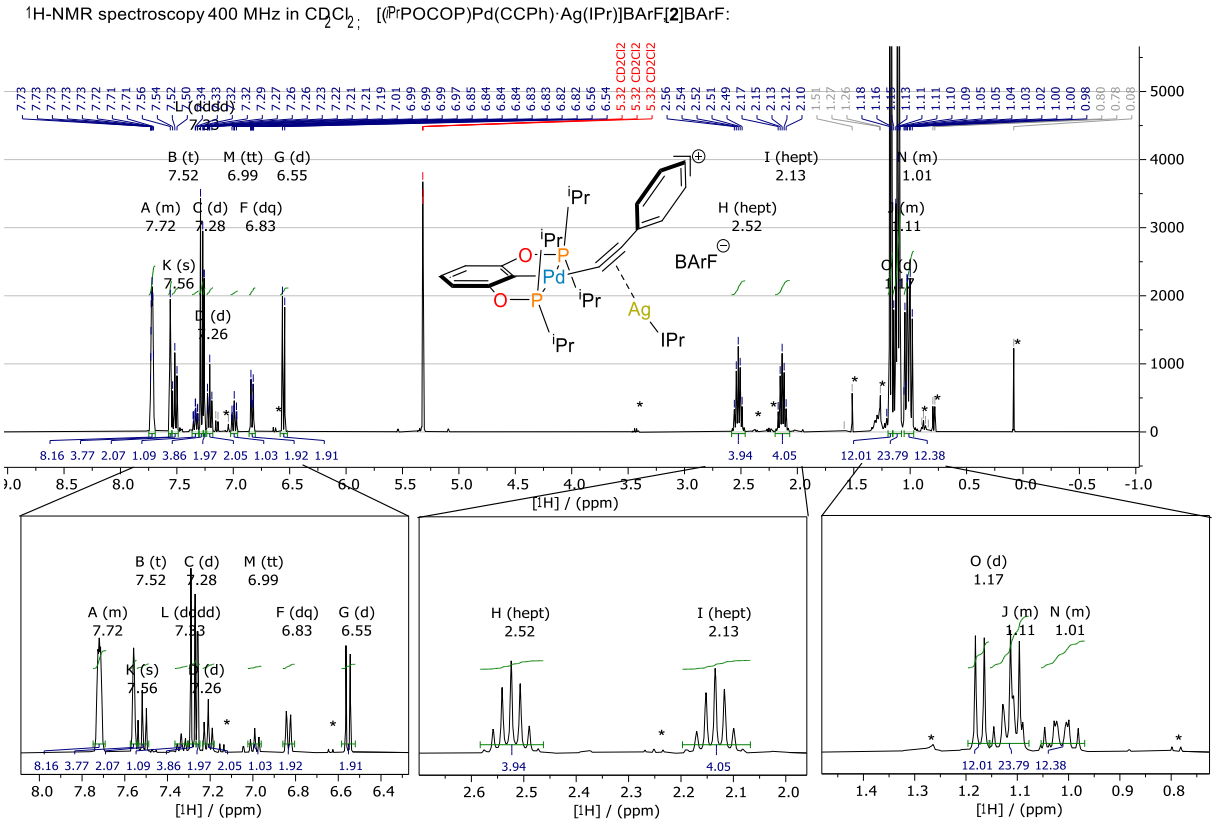

Figure SI-44: ^{1}H-NMR (400 MHz) spectrum of compound [($^{i\text{Pr}}$POCOP)Pd(CCPh)•Ag(IPr)]BArF, [**2**]BF_4, in CD_2Cl_2 measured at r.t. The spectrum was referenced to the residual solvent peak: ^{1}H-NMR (CD_2Cl_2) δ = 5.32 ppm. Impurities are marked with an asterisk*. *Top)* the full ^{1}H-NMR spectrum. *Bottom)* expansions of selected sections of the ^{1}H-NMR spectrum with arbitrary scaling of intensity.

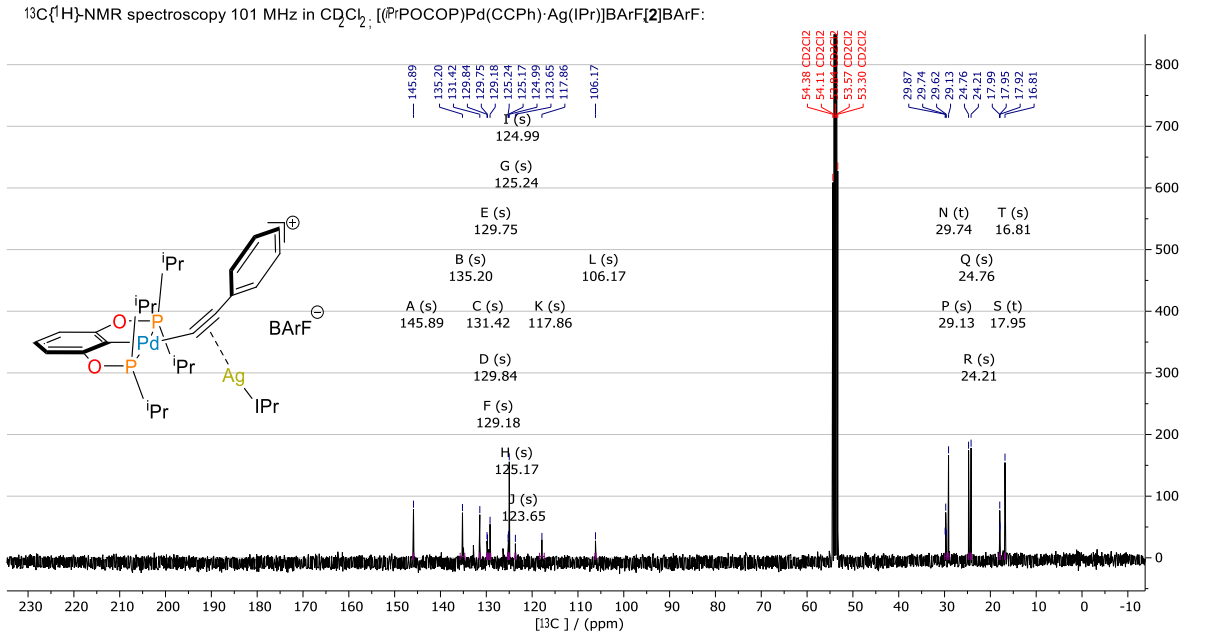

Figure SI-45: ^{13}C{^{1}H}-NMR (101 MHz) spectrum of compound [($^{i\text{Pr}}$POCOP)Pd(CCPh)•Ag(IPr)]BArF, [**2**]BF_4, in CD_2Cl_2 measured at r.t. The spectrum was referenced to the residual solvent peak: ^{13}C -NMR (CD_2Cl_2) δ = 53.84 ppm.

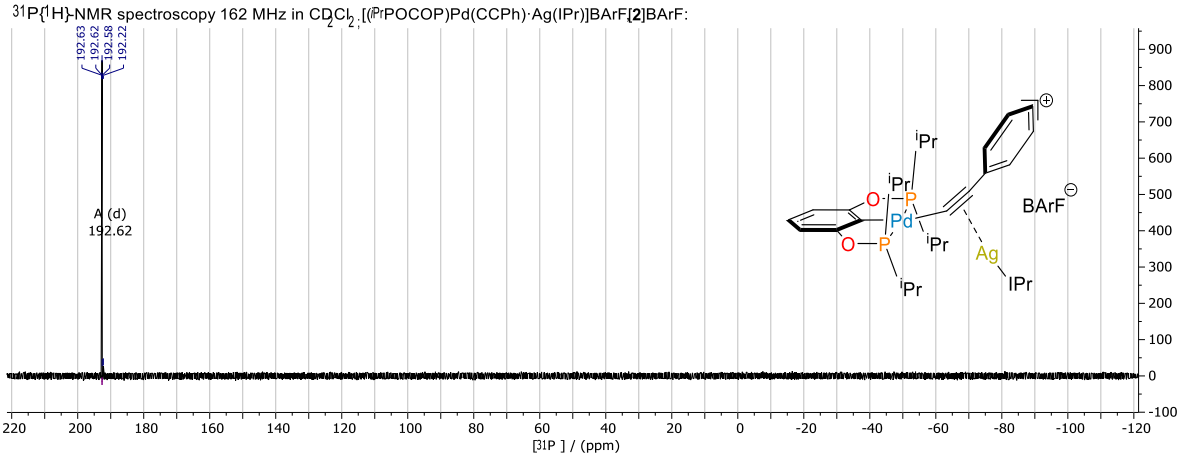

Figure SI-46: $^{31}P\{^{1}H\}$-NMR (162 MHz) spectrum of compound [(^{iPr}POCOP)Pd(CCPh)•Ag(IPr)]BArF, [**2**]BF_4, in CD_2Cl_2 measured at r.t.

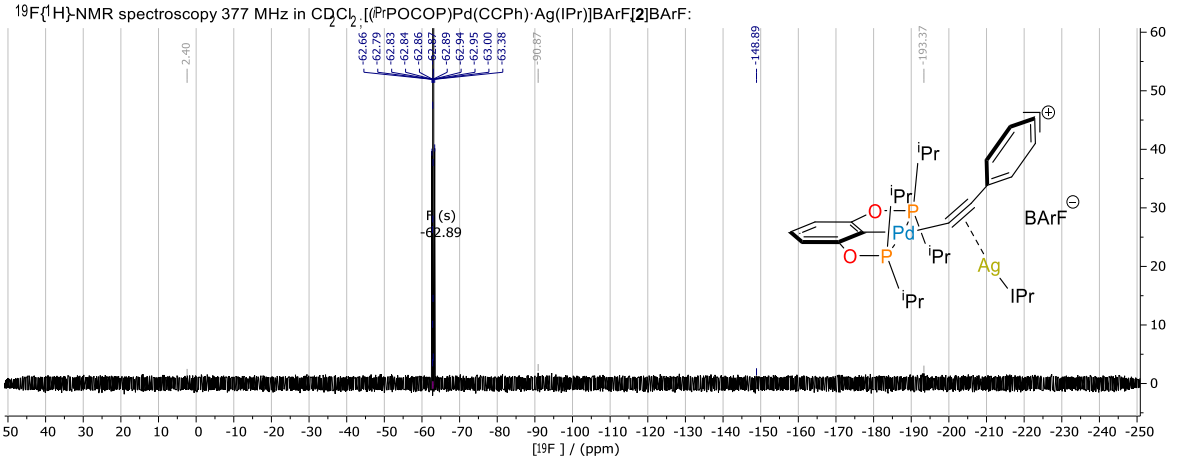

Figure SI-47: $^{19}F\{^{1}H\}$-NMR (377 MHz) spectrum of compound [(^{iPr}POCOP)Pd(CCPh)•Ag(IPr)]BArF, [**2**]BF_4, in CD_2Cl_2 measured at r.t.

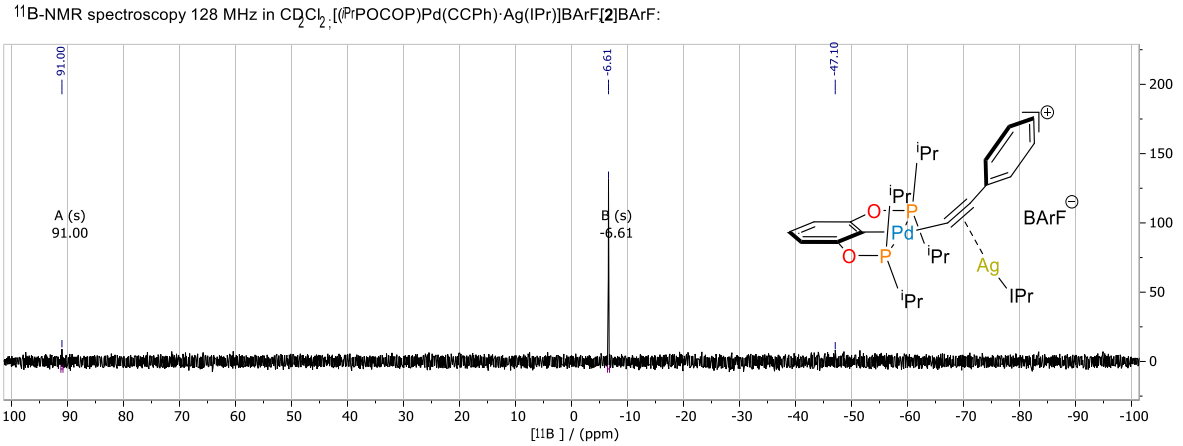

Figure SI-48: ^{11}B-NMR (128 MHz) spectrum of compound [(^{iPr}POCOP)Pd(CCPh)•Ag(IPr)]BArF, [**2**]BF_4, in CD_2Cl_2 measured at r.t.

3.1.6. NMR spectra of [($^{i\text{Pr}}$POCOP)Pd$^{\text{II}}$•(PhCC)Au$^{\text{I}}$(IPr)]BF_4, [**3**]BF_4:

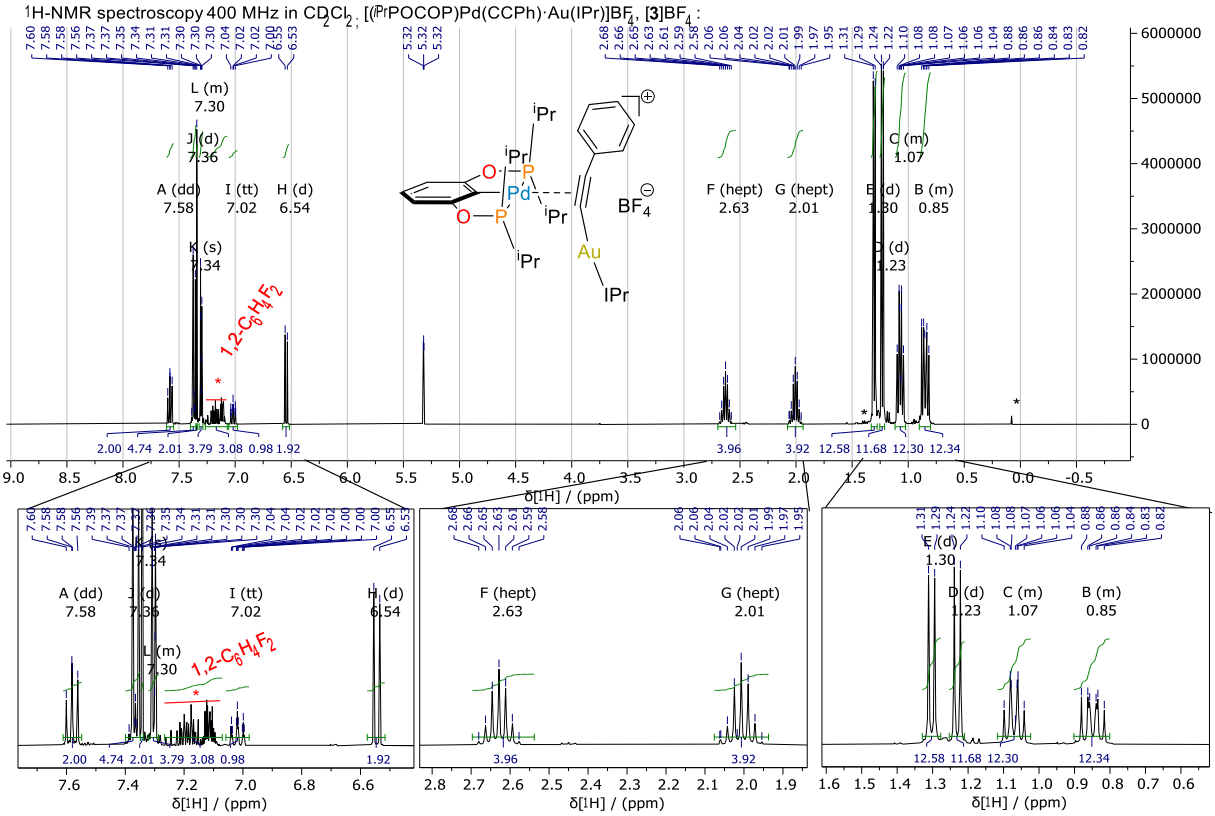

Figure SI-49: ^{1}H-NMR (400 MHz) spectrum of compound [($^{i\text{Pr}}$POCOP)Pd•(PhCC)Au(IPr)]BF_4, [**3**]BF_4, in CD_2Cl_2 measured at r.t. The spectrum was referenced to the residual solvent peak: ^{1}H-NMR (CD_2Cl_2) δ = 5.32 ppm. Impurities are marked with an asterisk*. *Top)* the full ^{1}H-NMR spectrum. *Bottom)* expansions of selected sections of the ^{1}H-NMR spectrum with arbitrary scaling of intensity.

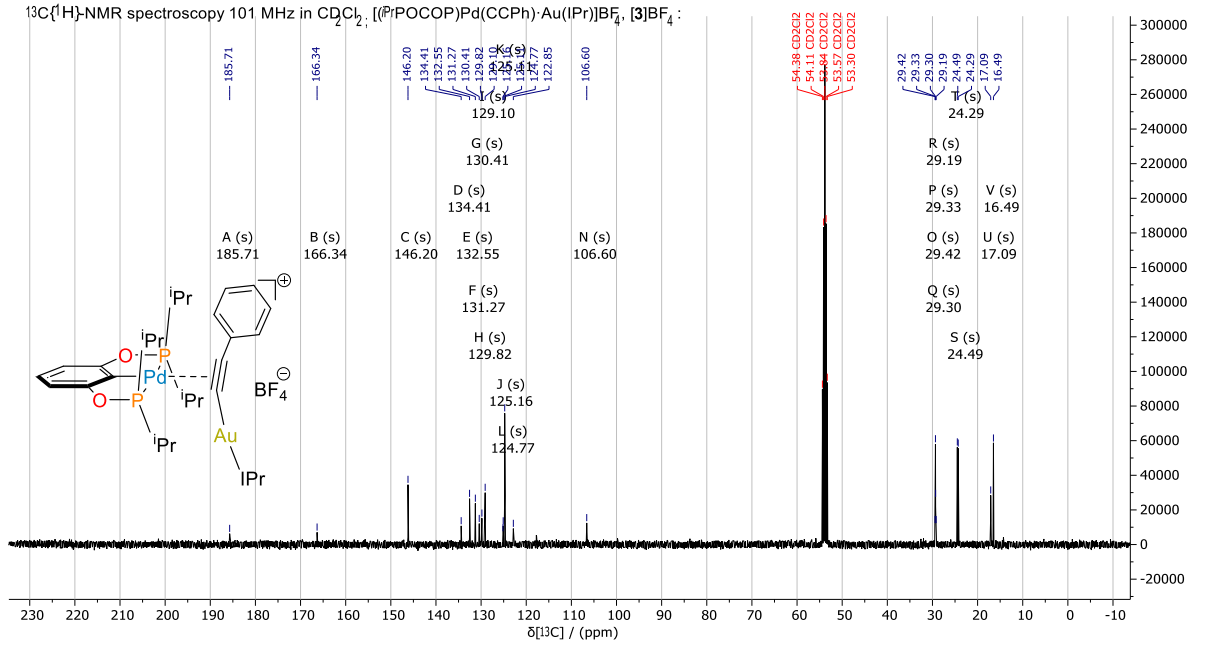

Figure SI-50: ^{13}C{^{1}H}-NMR (101 MHz) spectrum of compound [($^{i\text{Pr}}$POCOP)Pd•(PhCC)Au(IPr)]BF_4, [**3**]BF_4, in CD_2Cl_2 measured at r.t. The spectrum was referenced to the residual solvent peak: ^{13}C -NMR (CD_2Cl_2) δ = 53.84 ppm.

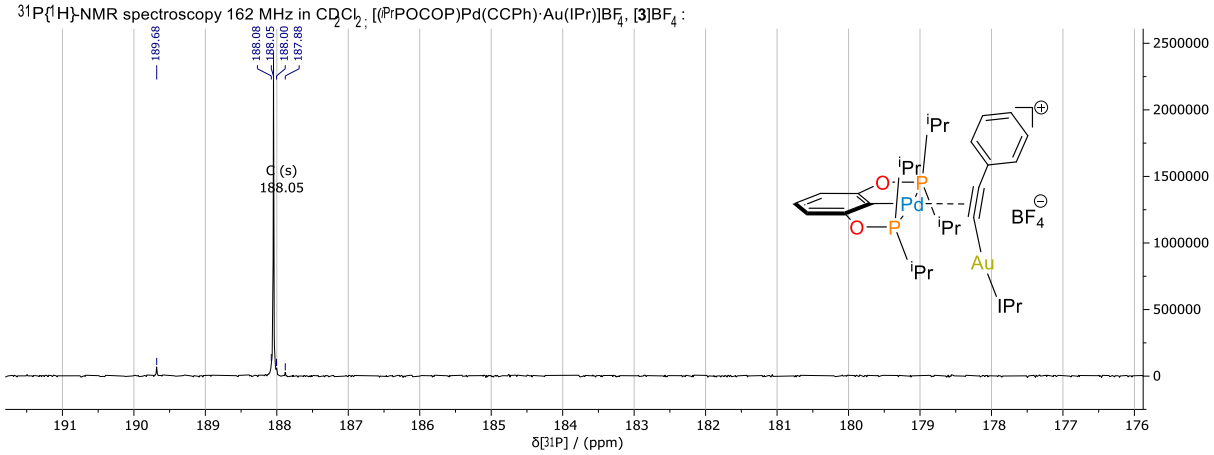

Figure SI-51: $^{31}P\{^{1}H\}$-NMR (162 MHz) spectrum of compound [(^{iPr}POCOP)Pd•(PhCC)Au(IPr)]BF_4, [**3**]BF_4 , in CD_2Cl_2 measured at r.t.

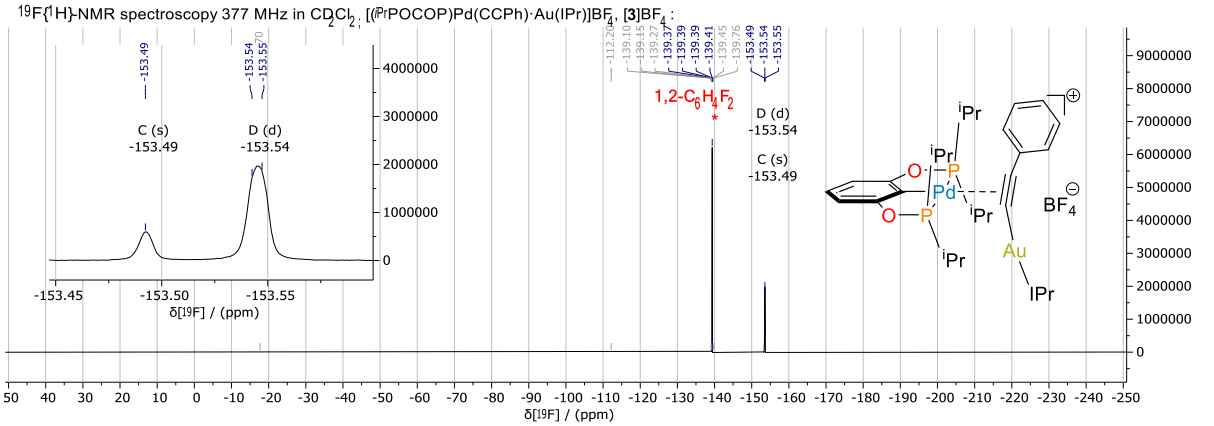

Figure SI-52: $^{19}F\{^{1}H\}$-NMR (377 MHz) of compound [(^{iPr}POCOP)Pd•(PhCC)Au(IPr)]BF_4, [**3**]BF_4 , in CD_2Cl_2 measured at r.t. *Inset)* expansions of selected section of the $^{19}F\{^{1}H\}$-NMR spectrum with arbitrary scaling of intensity.

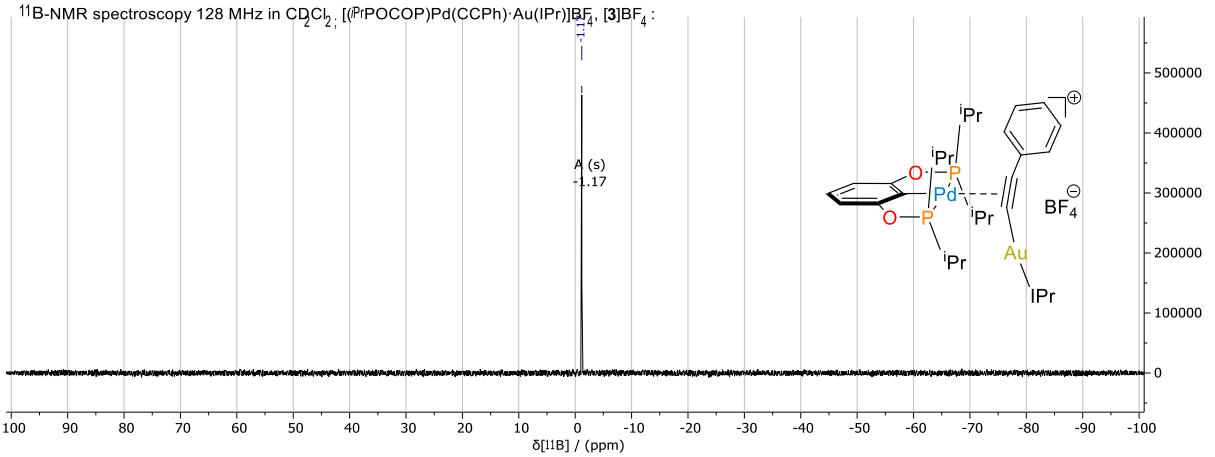

Figure SI-53: ^{11}B-NMR (128 MHz) spectrum of compound [(^{iPr}POCOP)Pd•(PhCC)Au(IPr)]BF_4, [**3**]BF_4 , in CD_2Cl_2 measured at r.t.

3.1.7. NMR spectra of [(*i*PrPOCOP)Pd^{II}•(PhCC)Au^{I}(IPr)]OTf, [**3**]OTf:

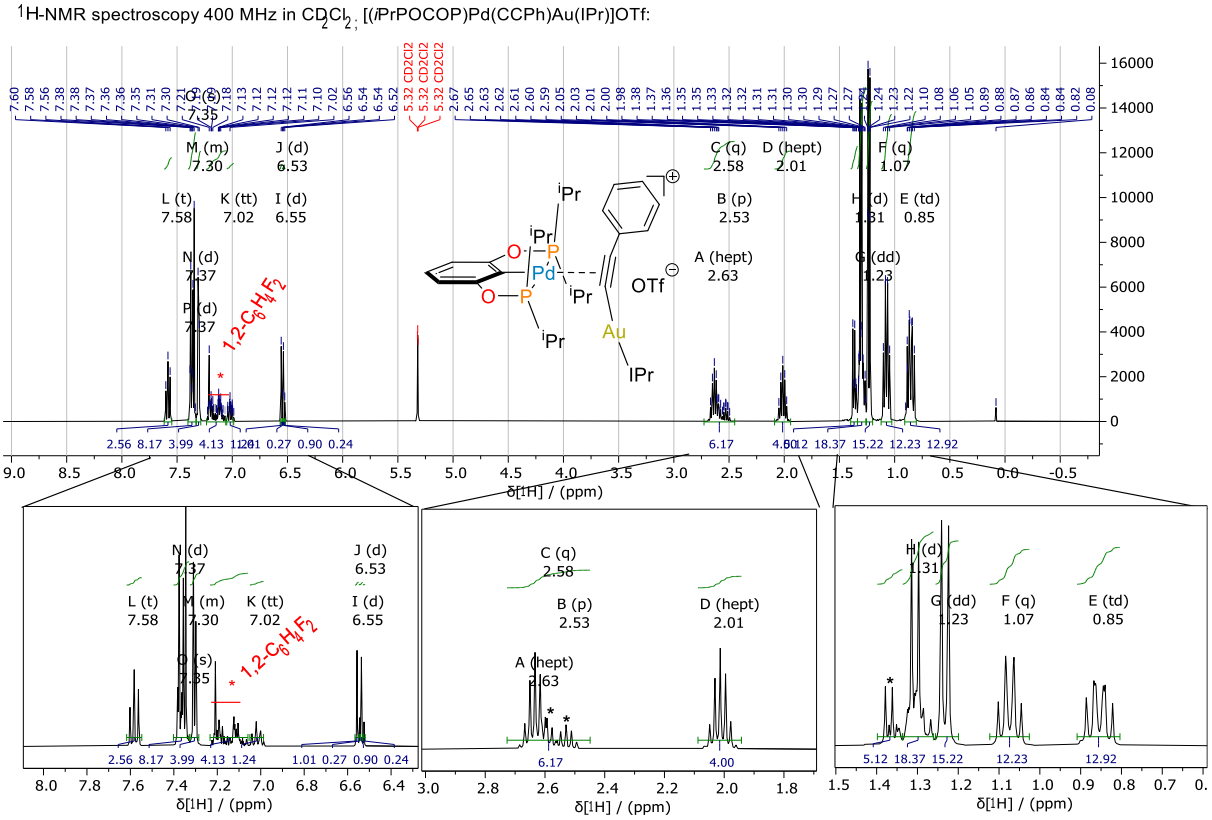

Figure SI-54: ^{1}H-NMR (400 MHz) spectrum of compound [(*i*PrPOCOP)Pd•(PhCC)Au(IPr)]OTf, [**3**]BF_4, in CD_2Cl_2 measured at r.t. The spectrum was referenced to the residual solvent peak: ^{1}H-NMR (CD_2Cl_2) δ = 5.32 ppm. Impurities are marked with an asterisk*. *Top)* the full ^{1}H-NMR spectrum. *Bottom)* expansions of selected sections of the ^{1}H-NMR spectrum with arbitrary scaling of intensity.

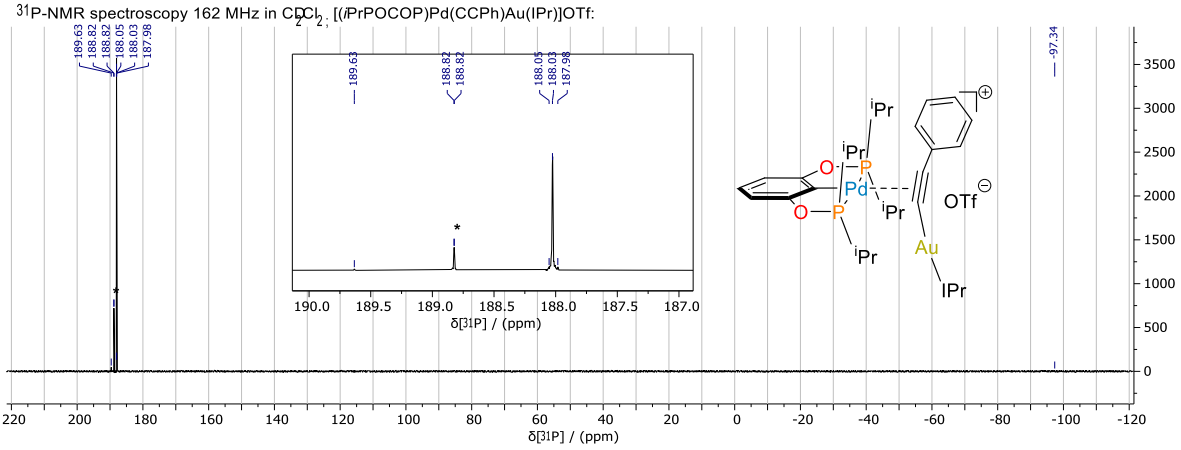

Figure SI-55: ^{31}P{^{1}H}-NMR (162 MHz) spectrum of compound [(*i*PrPOCOP)Pd•(PhCC)Au(IPr)]OTf, [**3**]BF_4, in CD_2Cl_2 measured at r.t.

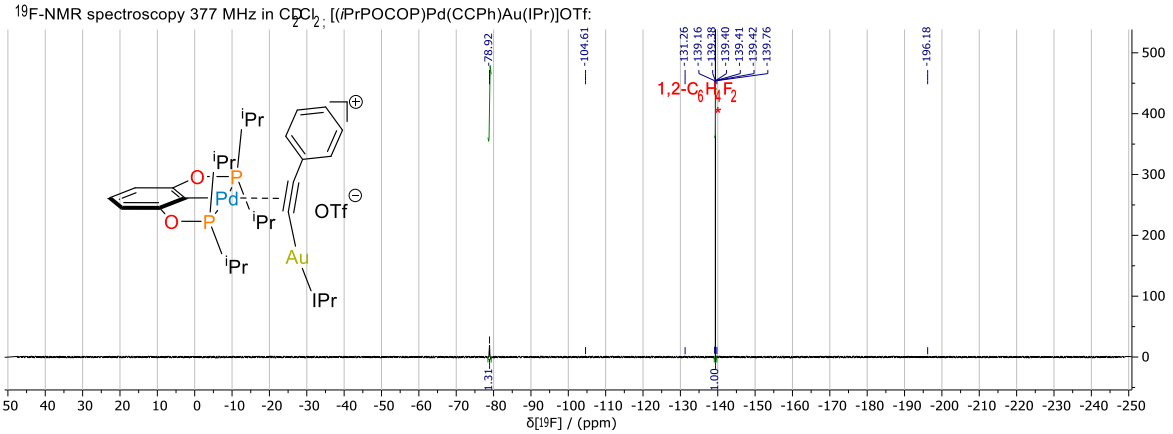

Figure SI-56: $^{19}F\{^{1}H\}$-NMR (377 MHz) spectrum of compound [(^{iPr}POCOP)Pd•(PhCC)Au(IPr)]OTf, [**3**]BF_4 , in CD_2Cl_2 measured at r.t.

3.1.8. NMR spectra of [(IPr)Au^{I}(MeCN)]BArF:

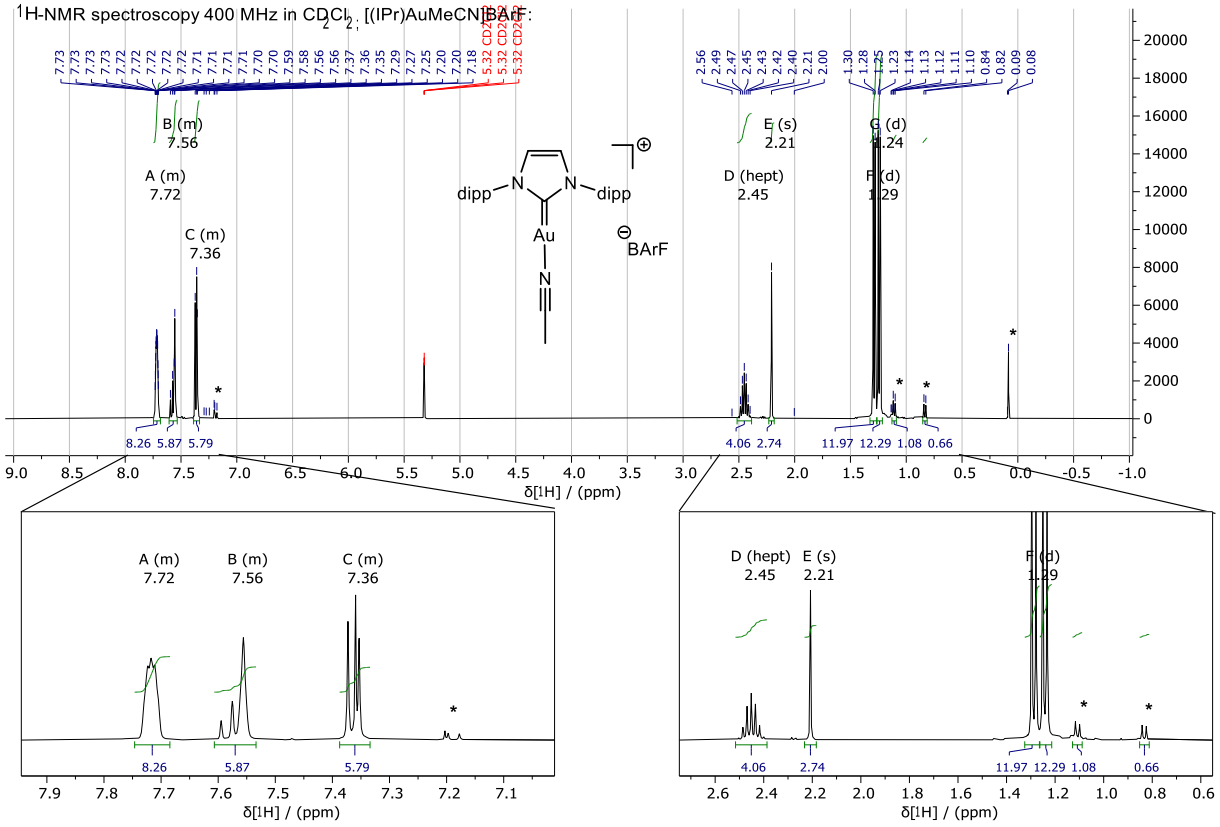

Figure SI-57: ^{1}H-NMR (400 MHz) spectrum of compound [(IPr)Au(MeCN)]BArF, in CD_2Cl_2 measured at r.t. The spectrum was referenced to the residual solvent peak: ^{1}H-NMR (CD_2Cl_2) δ = 5.32 ppm. Impurities are marked with an asterisk*. *Top)* the full ^{1}H-NMR spectrum. *Bottom)* expansions of selected sections of the ^{1}H-NMR spectrum with arbitrary scaling of intensity.

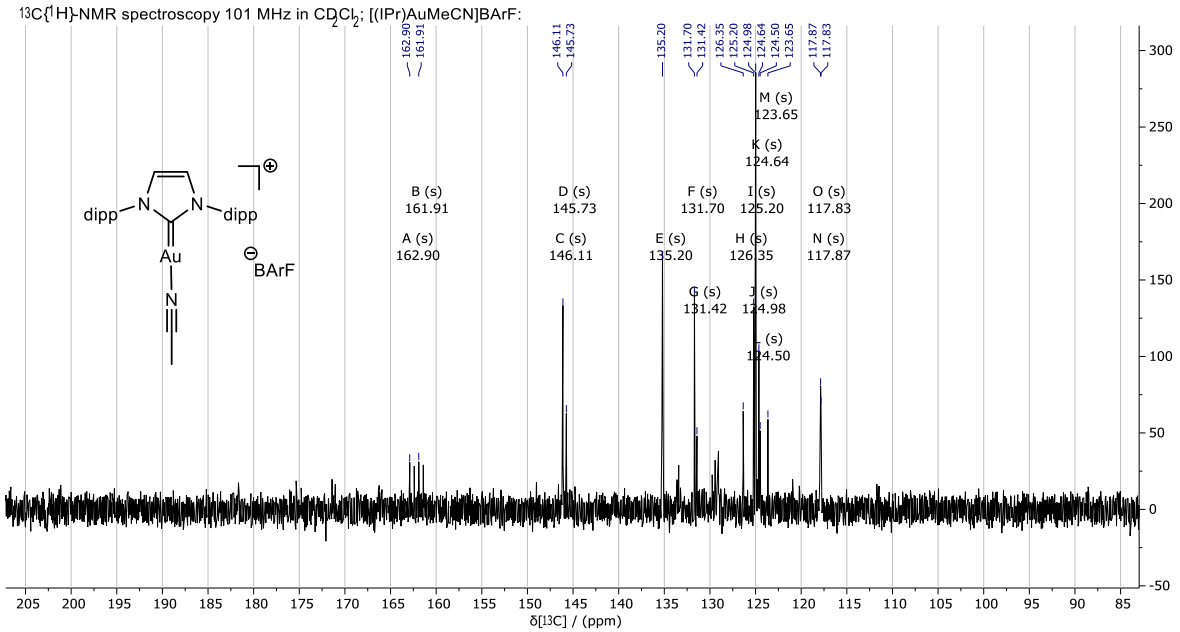

Figure SI-58: $^{13}C\{^{1}H\}$-NMR (101 MHz) spectrum of compound [(IPr)AuMeCN]BArF, in CD_2Cl_2 measured at r.t. The spectrum was referenced to the residual solvent peak: ^{13}C -NMR (CD_2Cl_2) δ = 53.84 ppm.

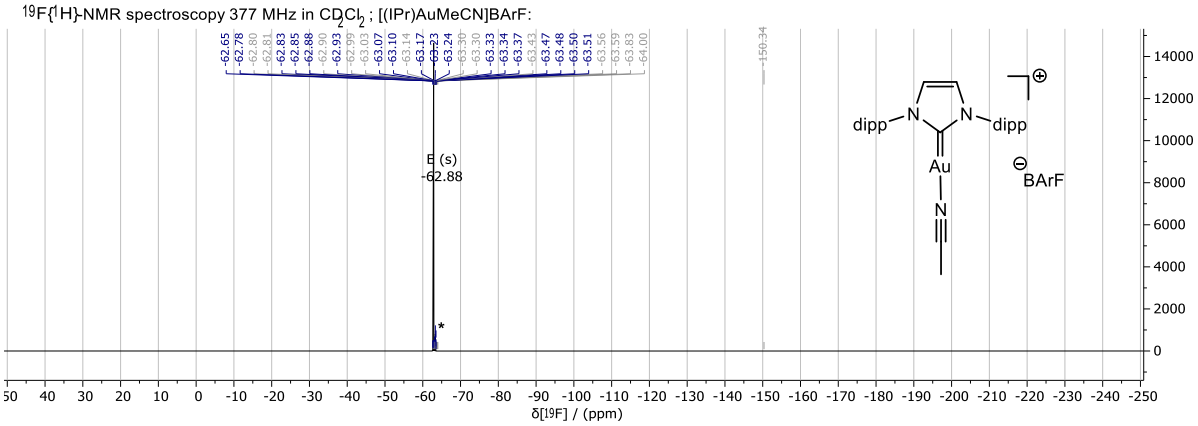

Figure SI-59: $^{19}F\{^{1}H\}$-NMR (377 MHz) spectrum of compound [(IPr)AuMeCN]BArF, in CD_2Cl_2 measured at r.t.

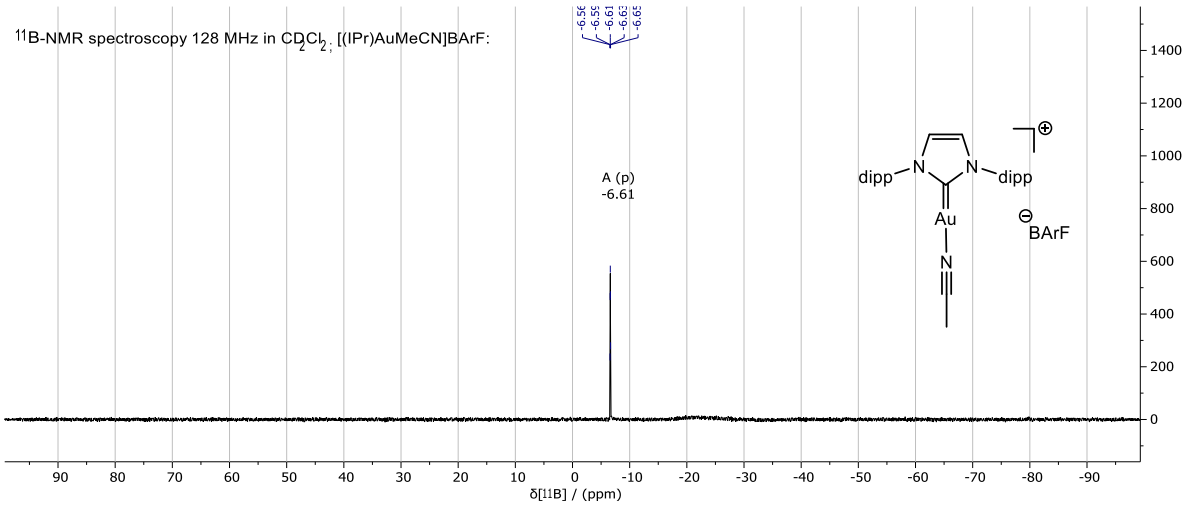

Figure SI-60: ^{11}B-NMR (128 MHz) spectrum of compound [(IPr)AuMeCN]BArF, in CD_2Cl_2 measured at r.t.

3.1.9. NMR spectra of [($^{i\text{Pr}}$POCOP)Pd$^{\text{II}}$•(PhCC)Au$^{\text{I}}$(IPr)]BArF, [**3**]BArF:

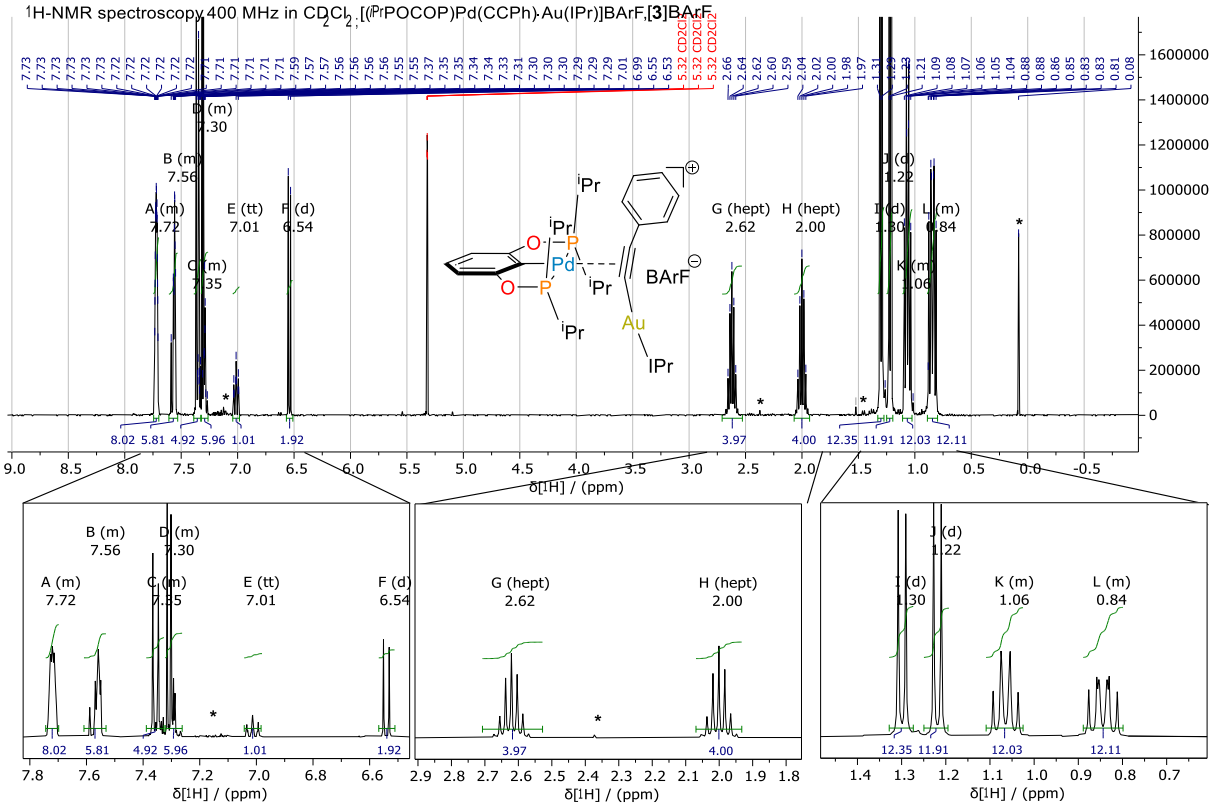

Figure SI-61: ^{1}H-NMR (400 MHz) of compound [($^{i\text{Pr}}$POCOP)Pd•(PhCC)Au(IPr)]BArF, [**3**]BArF , in CD_2Cl_2 measured at r.t. The spectrum was referenced to the residual solvent peak: ^{1}H-NMR (CD_2Cl_2) δ = 5.32 ppm. Impurities are marked with an asterisk*. *Top)* the full ^{1}H-NMR spectrum. *Bottom)* expansions of selected sections of the ^{1}H-NMR spectrum with arbitrary scaling of intensity.

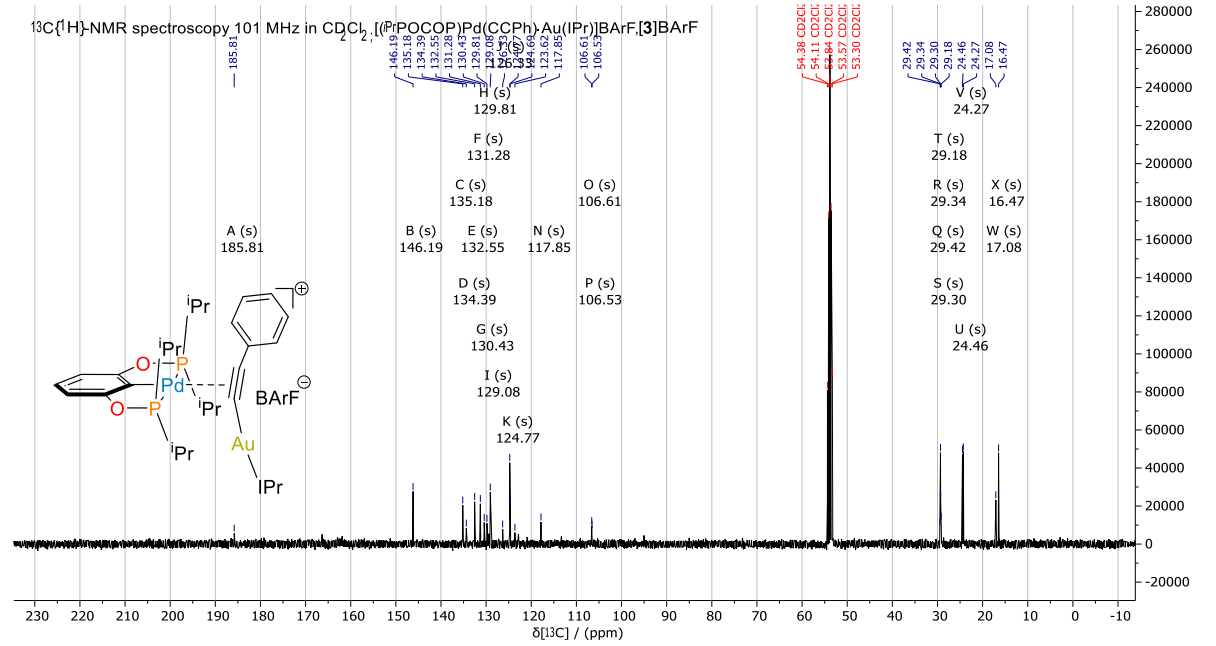

***Figure SI-62*:** ^{13}C{^{1}H}-NMR (101 MHz) spectrum of compound [($^{i\text{Pr}}$POCOP)Pd•(PhCC)Au(IPr)]BArF, [**3**]BArF , in CD_2Cl_2 measured at r.t. The spectrum was referenced to the residual solvent peak: ^{13}C -NMR (CD_2Cl_2) δ = 53.84 ppm.

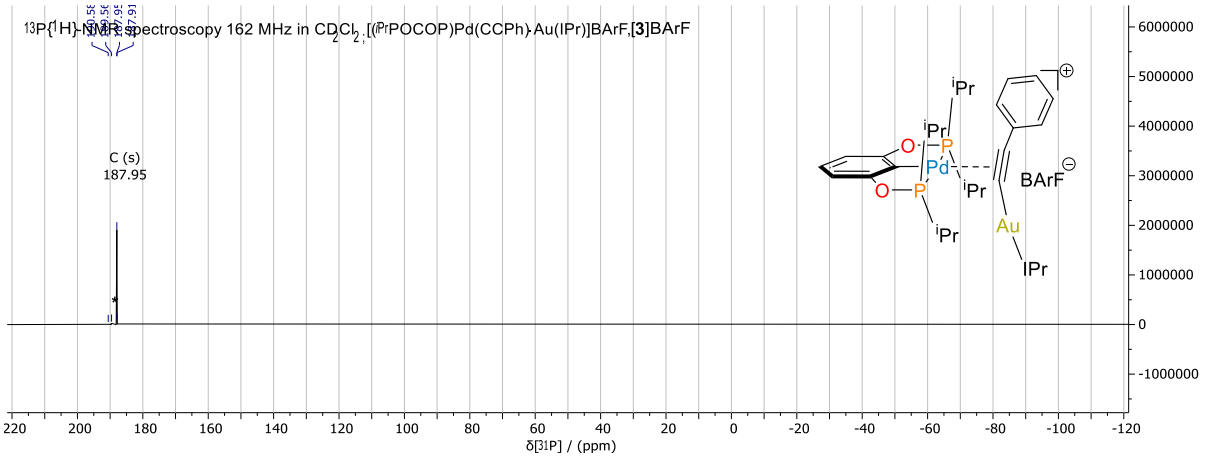

Figure SI-63: $^{31}P\{^{1}H\}$-NMR (162 MHz) spectrum of compound [(^{iPr}POCOP)Pd•(PhCC)Au(IPr)]BArF, [**3**]BArF , in CD_2Cl_2 measured at r.t.

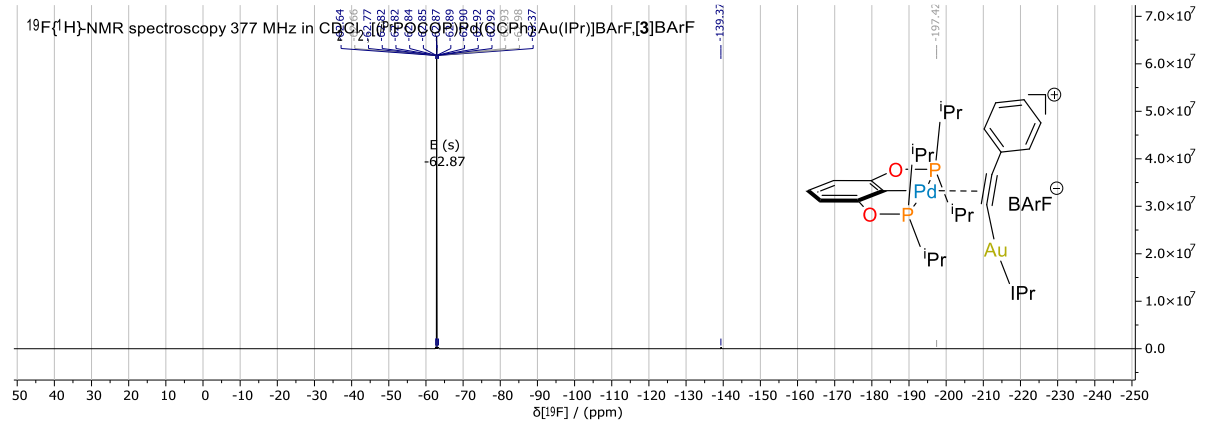

Figure SI-64: $^{19}F\{^{1}H\}$-NMR (377 MHz) spectrum of compound [(^{iPr}POCOP)Pd•(PhCC)Au(IPr)]BArF, [**3**]BArF , in CD_2Cl_2 measured at r.t.

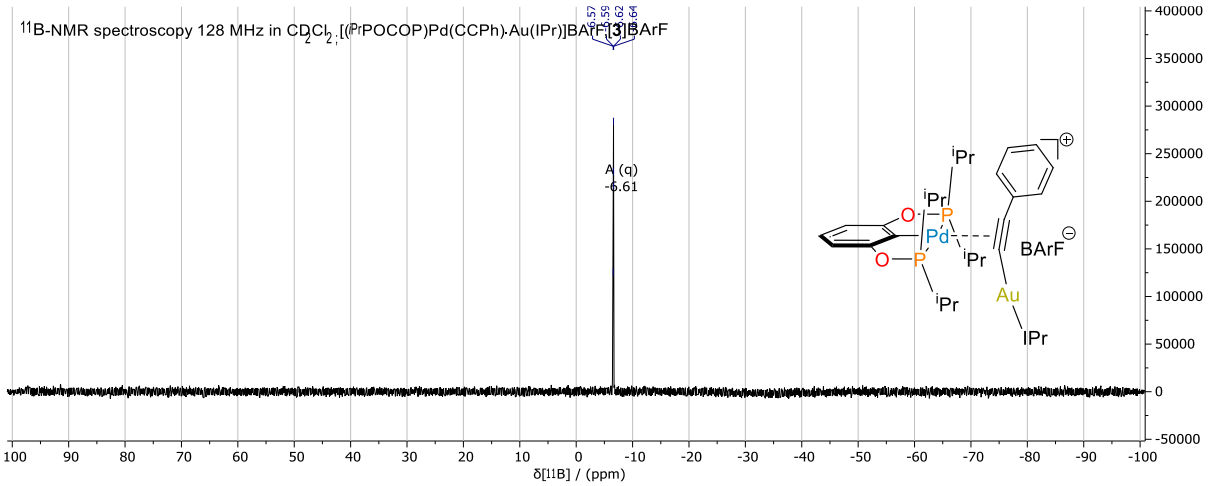

Figure SI-65: ^{11}B-NMR (128 MHz) spectrum of compound [(^{iPr}POCOP)Pd•(PhCC)Au(IPr)]BArF, [**3**]BArF , in CD_2Cl_2 measured at r.t.

3.2. NMR-spectra of Compounds within the Synthesis of [4a]BArF

3.2.1. NMR spectra of Bis(2,6-diisopropylphenyl)hept-6-ene-2,3-diimine, $^{Me,but\text{-}3\text{-}en\text{-}1\text{-}yl,dipp_2}$DAB:

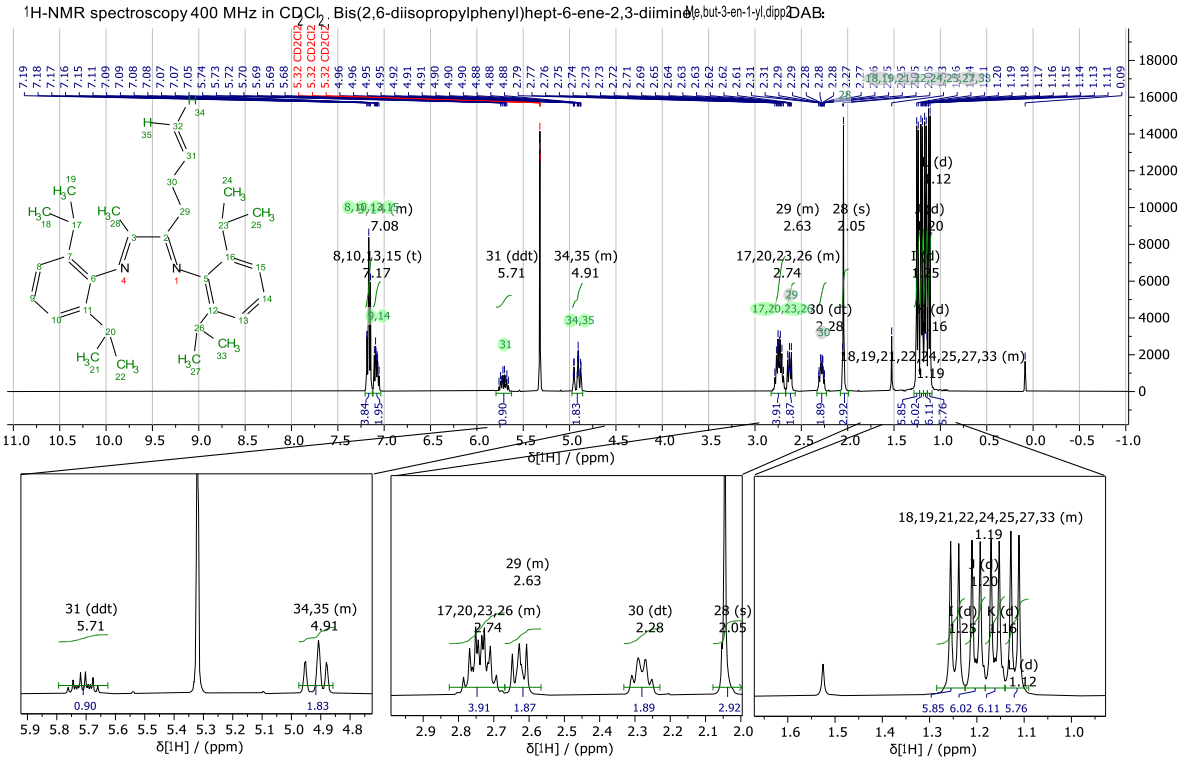

Figure SI-66: ^{1}H-NMR (400 MHz) of compound $^{Me,but\text{-}3\text{-}en\text{-}1\text{-}yl,dipp^2}$DAB, in CD_2Cl_2 measured at r.t. The spectrum was referenced to the residual solvent peak: ^{1}H-NMR (CD_2Cl_2) δ = 5.32 ppm. Impurities are marked with an asterisk*. *Top)* the full ^{1}H-NMR spectrum. *Bottom)* expansions of selected sections of the ^{1}H-NMR spectrum with arbitrary scaling of intensity.

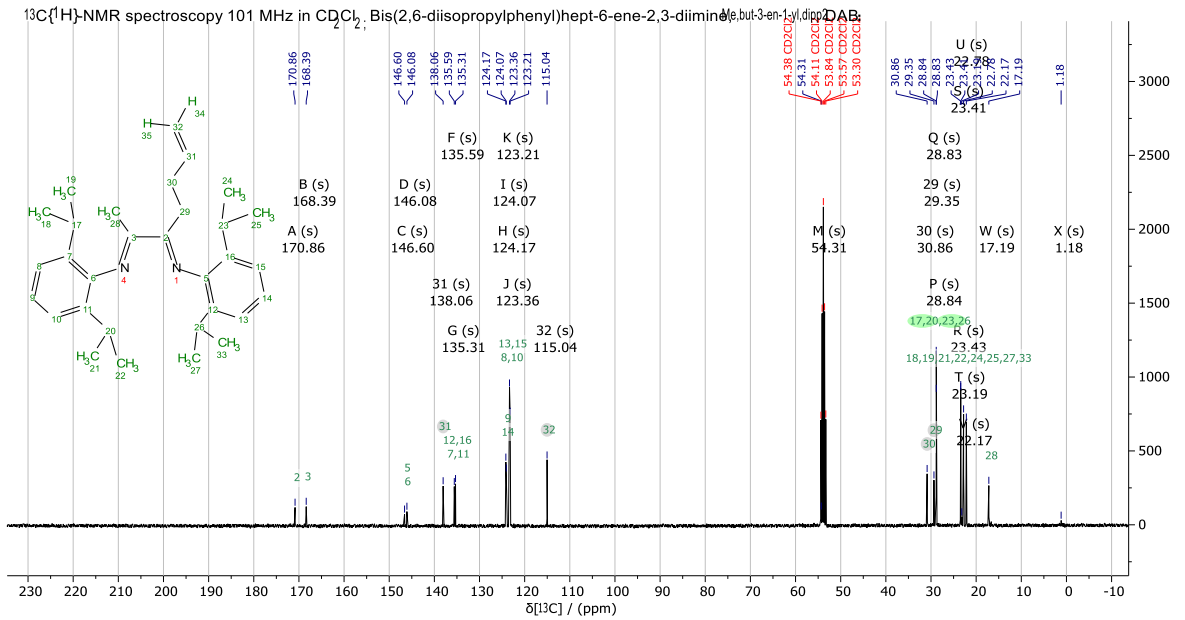

Figure SI-67: ^{13}C{^{1}H}-NMR (101 MHz) spectrum of compound $^{Me,but\text{-}3\text{-}en\text{-}1\text{-}yl,dipp^2}$DAB, in CD_2Cl_2 measured at r.t. The spectrum was referenced to the residual solvent peak: ^{13}C -NMR (CD_2Cl_2) δ = 53.84 ppm.

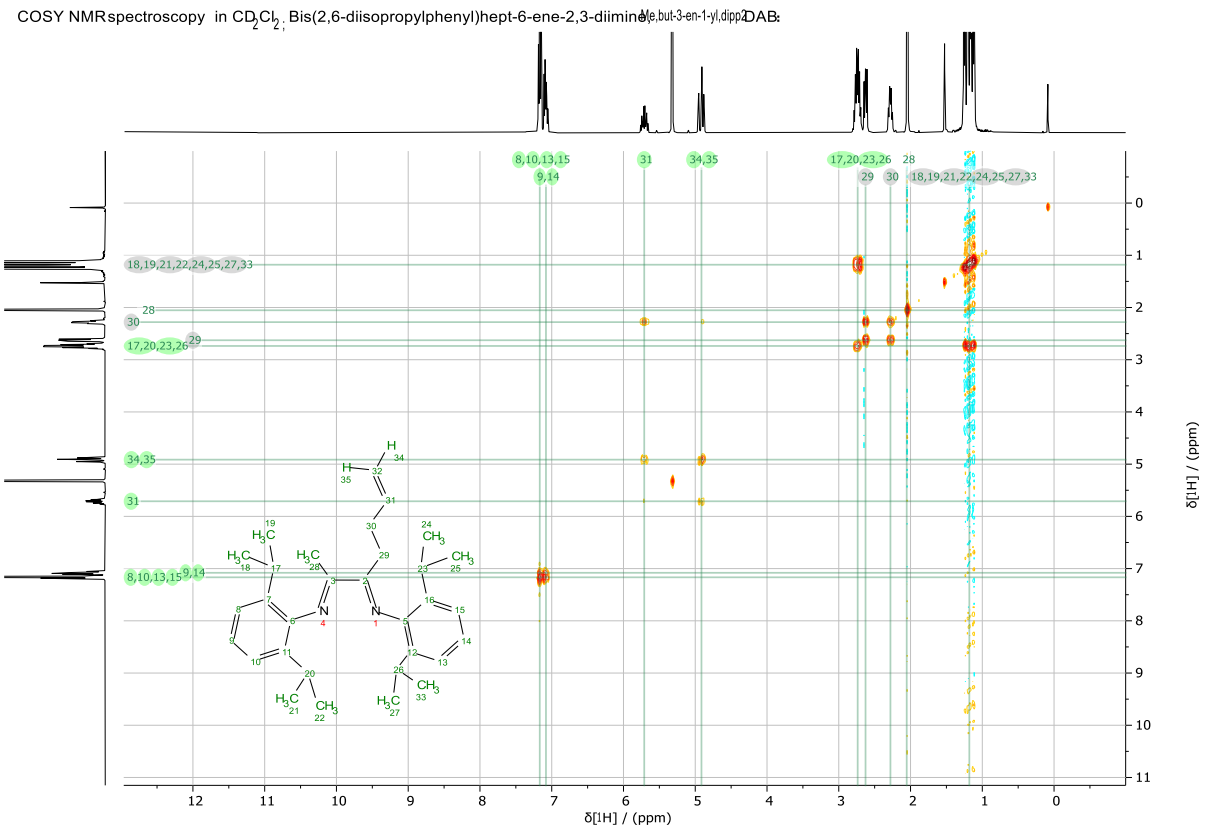

Figure SI-68: ^{1}H-^{1}H-COSY-NMR (400 MHz, 400 MHz) spectrum of compound $^{Me,but\text{-}3\text{-}en\text{-}1\text{-}yl,dipp2}$DAB, in CD_2Cl_2 measured at r.t.

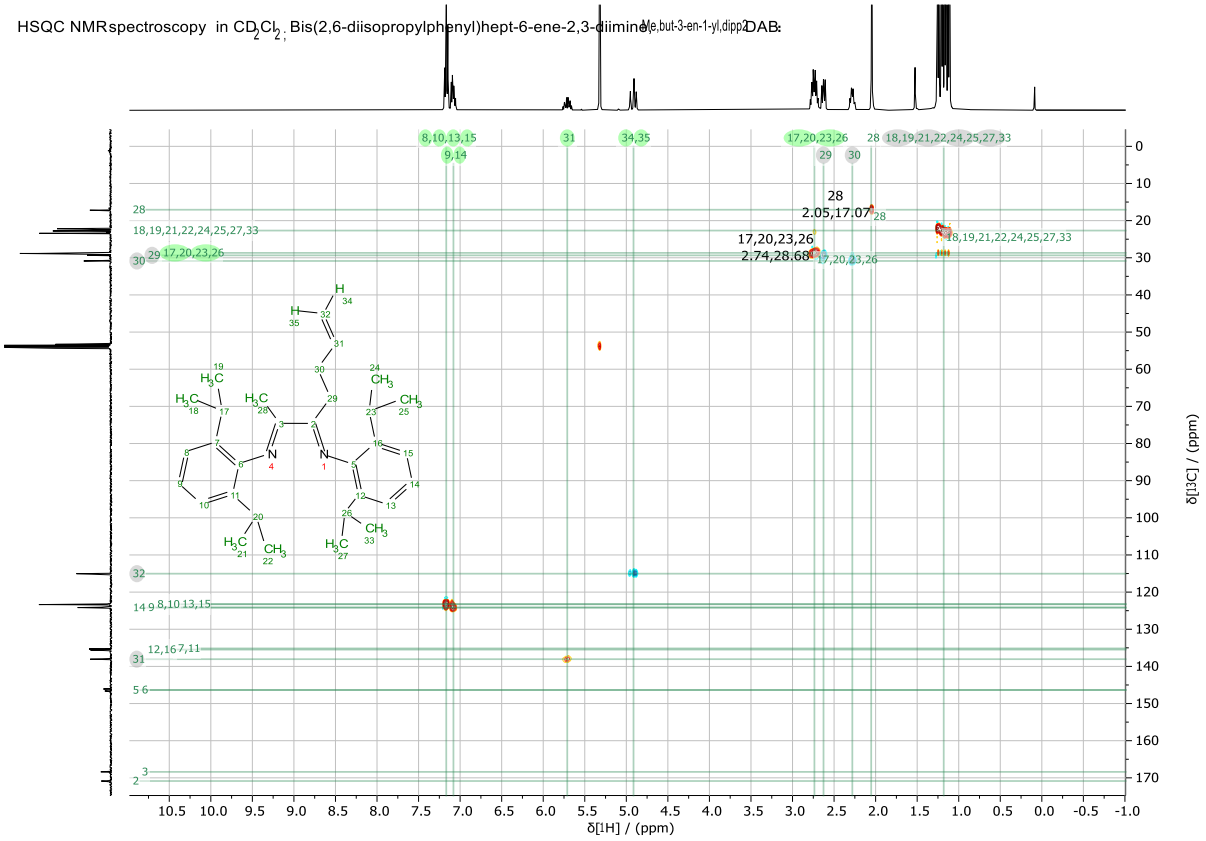

Figure SI-69: ^{1}H-^{13}C-HSQC-NMR (400 MHz, 101 MHz) spectrum of compound $^{Me,but\text{-}3\text{-}en\text{-}1\text{-}yl,dipp2}$DAB, in CD_2Cl_2 measured at r.t.

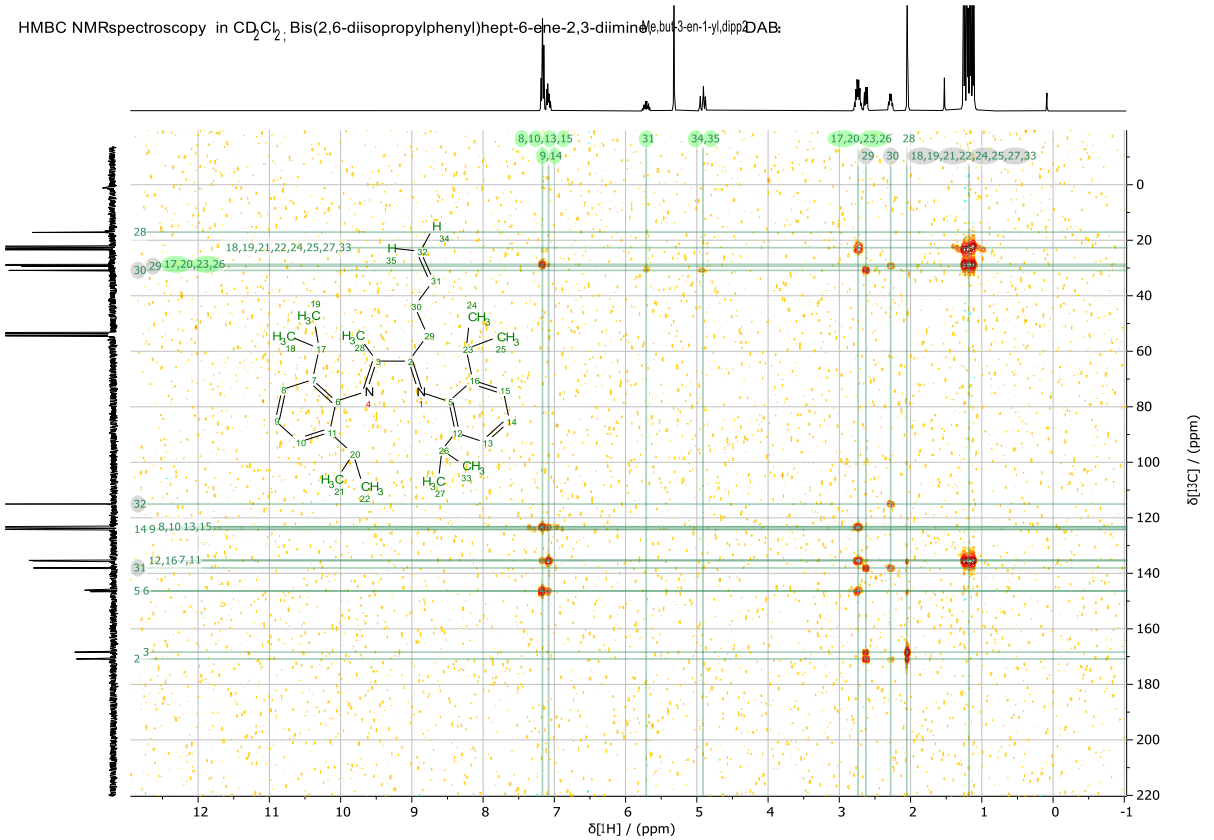

Figure SI-70: ^{1}H-^{13}C HMBC-NMR (400 MHz, 101 MHz) spectrum of compound $^{Me,but\text{-}3\text{-}en\text{-}1\text{-}yl,dipp2}$DAB, in CD_2Cl_2 measured at r.t.

3.2.2. NMR spectra of $^{Me,but\text{-}3\text{-}en\text{-}1\text{-}yl}$IPrHCl•MeOH:

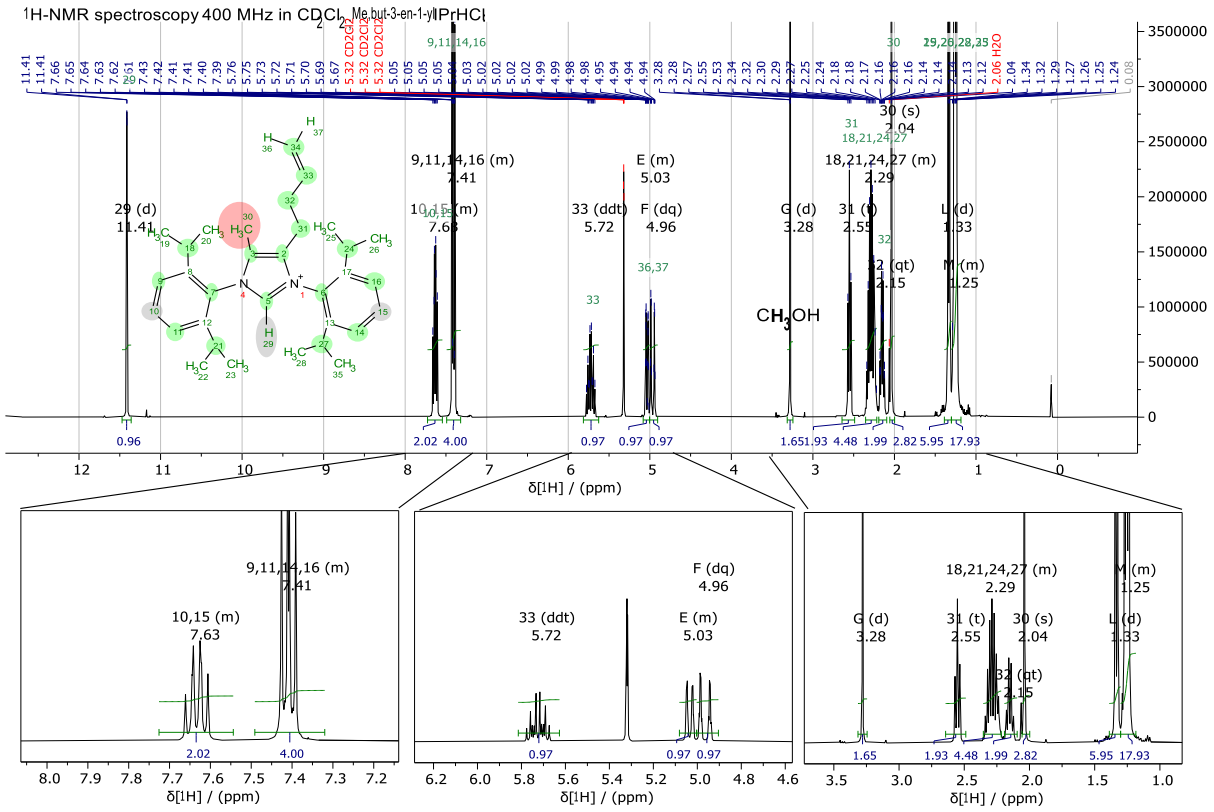

Figure SI-71: ^{1}H-NMR (400 MHz) of compound $^{Me,but\text{-}3\text{-}en\text{-}1\text{-}yl}$IPrHCl•MeOH, in CD_2Cl_2 measured at r.t. The spectrum was referenced to the residual solvent peak: ^{1}H-NMR (CD_2Cl_2) δ = 5.32 ppm. Impurities are marked with an asterisk*. *Top)* the full ^{1}H-NMR spectrum. *Bottom)* expansions of selected sections of the ^{1}H-NMR spectrum with arbitrary scaling of intensity.

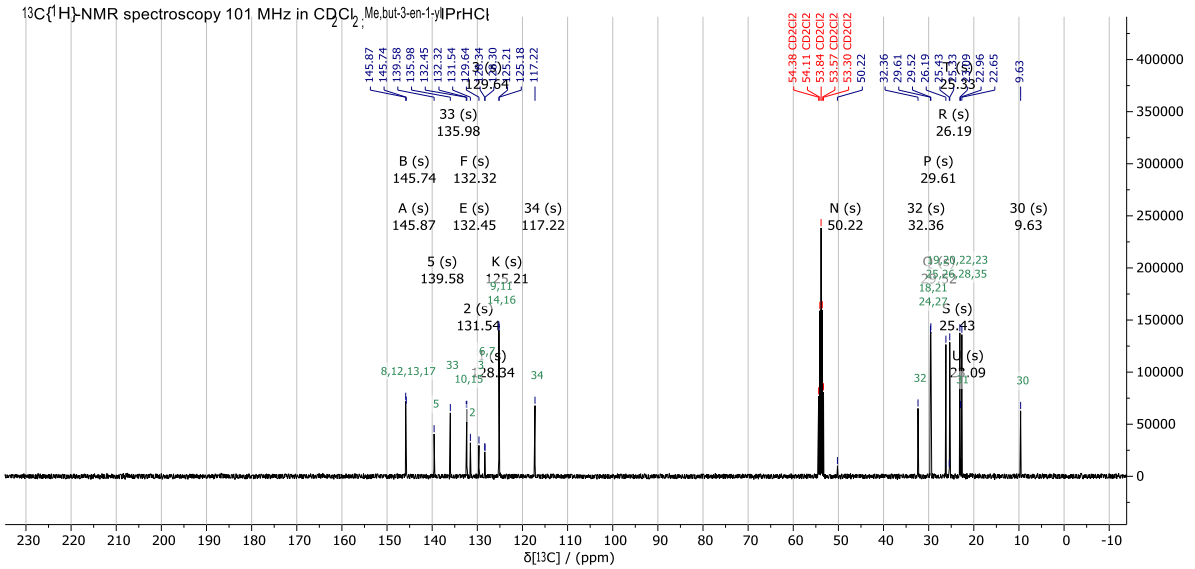

Figure SI-72: $^{13}C\{^1H\}$-NMR (101 MHz) spectrum of compound $^{Me,but\text{-}3\text{-}en\text{-}1\text{-}yl}$IPrHCl•MeOH, in CD_2Cl_2 measured at r.t.

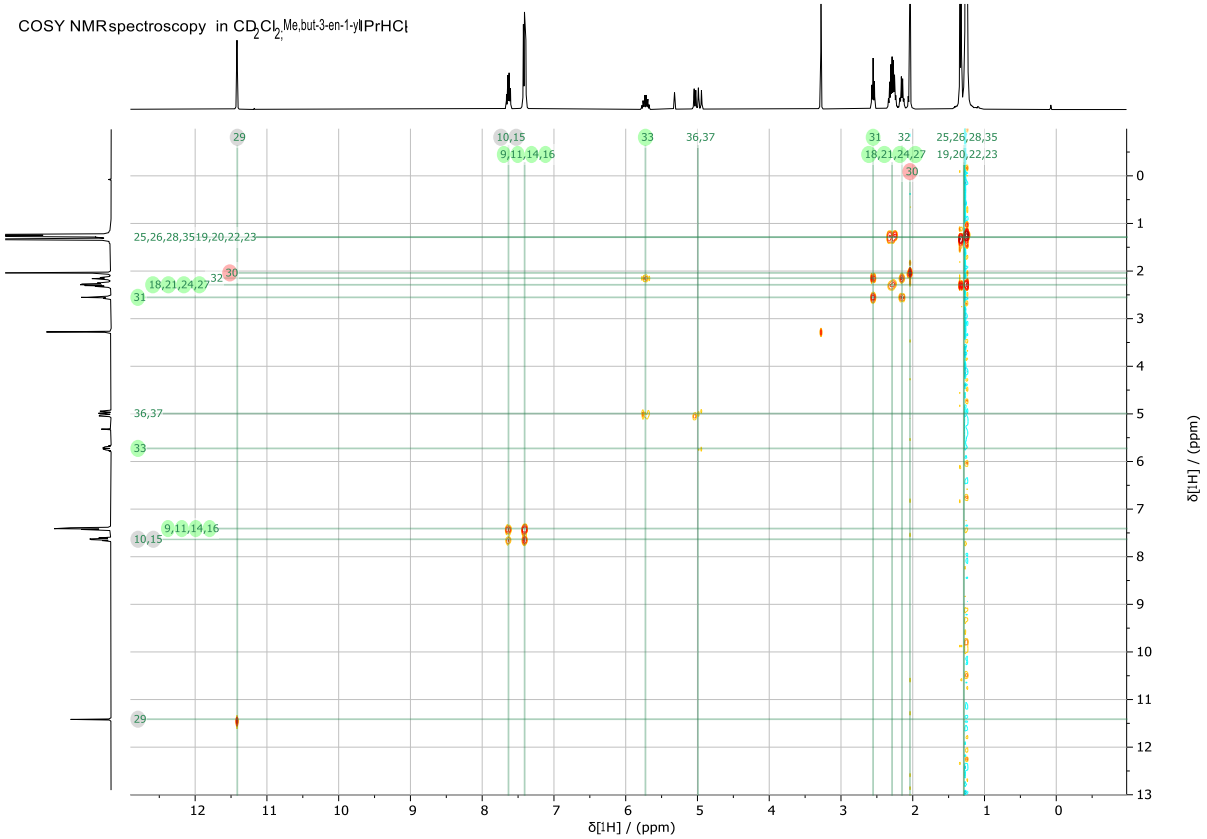

Figure SI-73: ^1H-^1H COSY-NMR (400 MHz, 400 MHz) of compound $^{Me,but\text{-}3\text{-}en\text{-}1\text{-}yl,dipp2}$DAB, in CD_2Cl_2 measured at r.t.

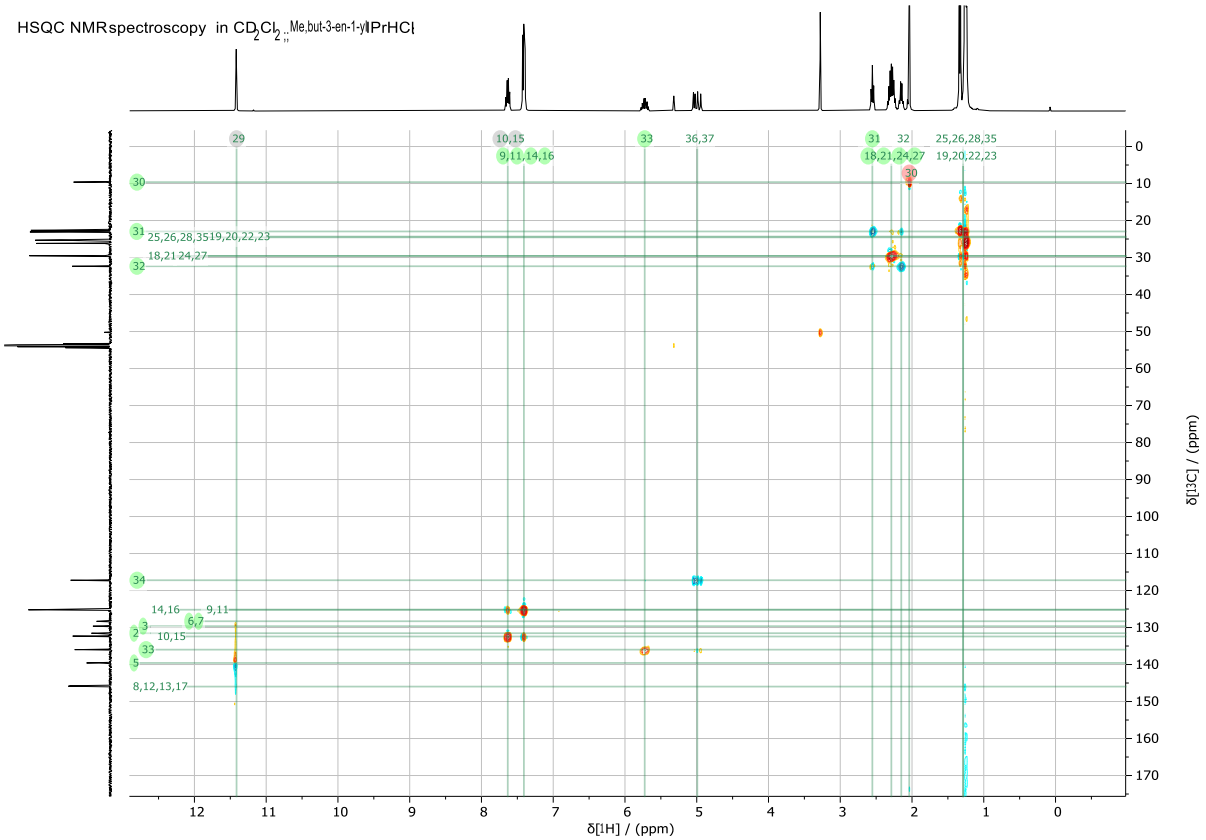

Figure SI-74: ^{1}H-^{13}C HSQC-NMR (400 MHz, 101 MHz) spectrum of compound $^{Me,but\text{-}3\text{-}en\text{-}1\text{-}yl,dipp2}$DAB, in CD_2Cl_2 measured at r.t.

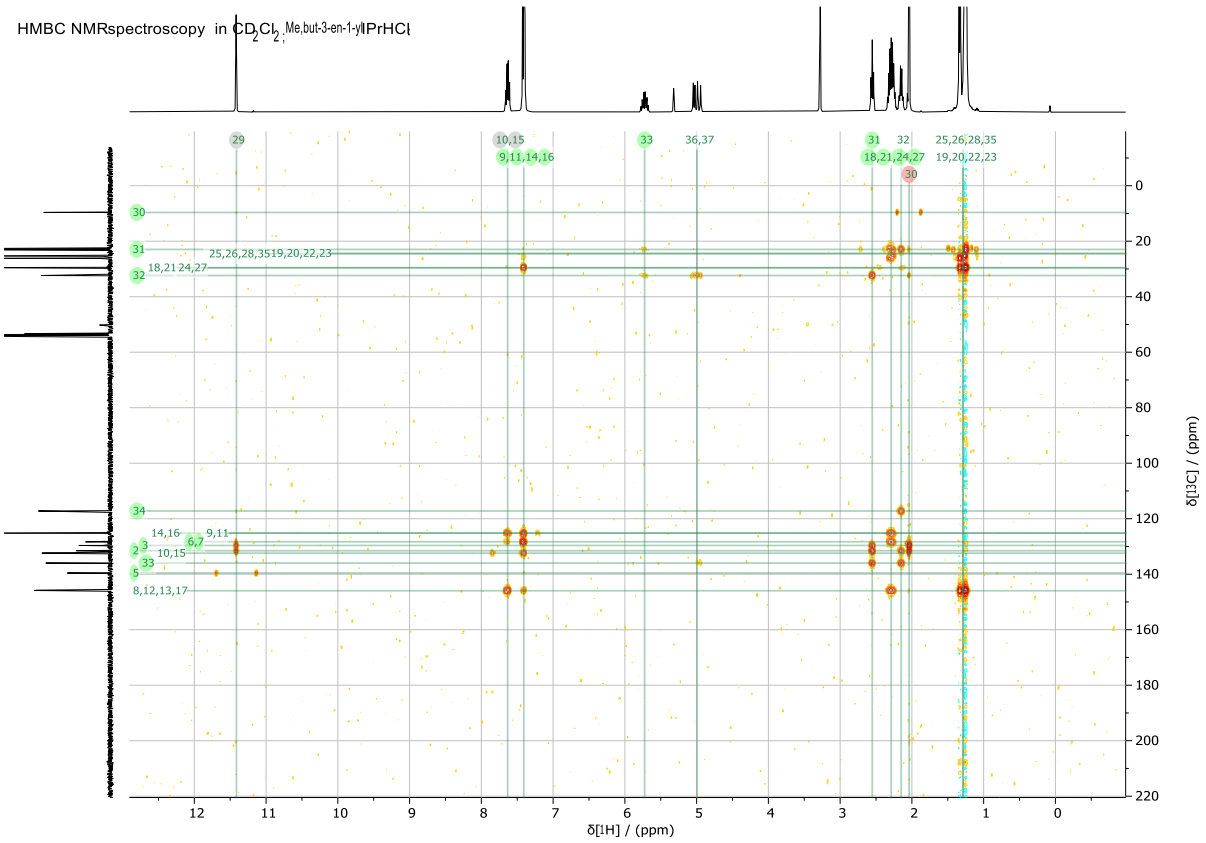

Figure SI-75: ^{1}H-^{13}C HMBC-NMR (400 MHz, 101 MHz) of compound $^{Me,but\text{-}3\text{-}en\text{-}1\text{-}yl,dipp2}$DAB, in CD_2Cl_2 measured at r.t.

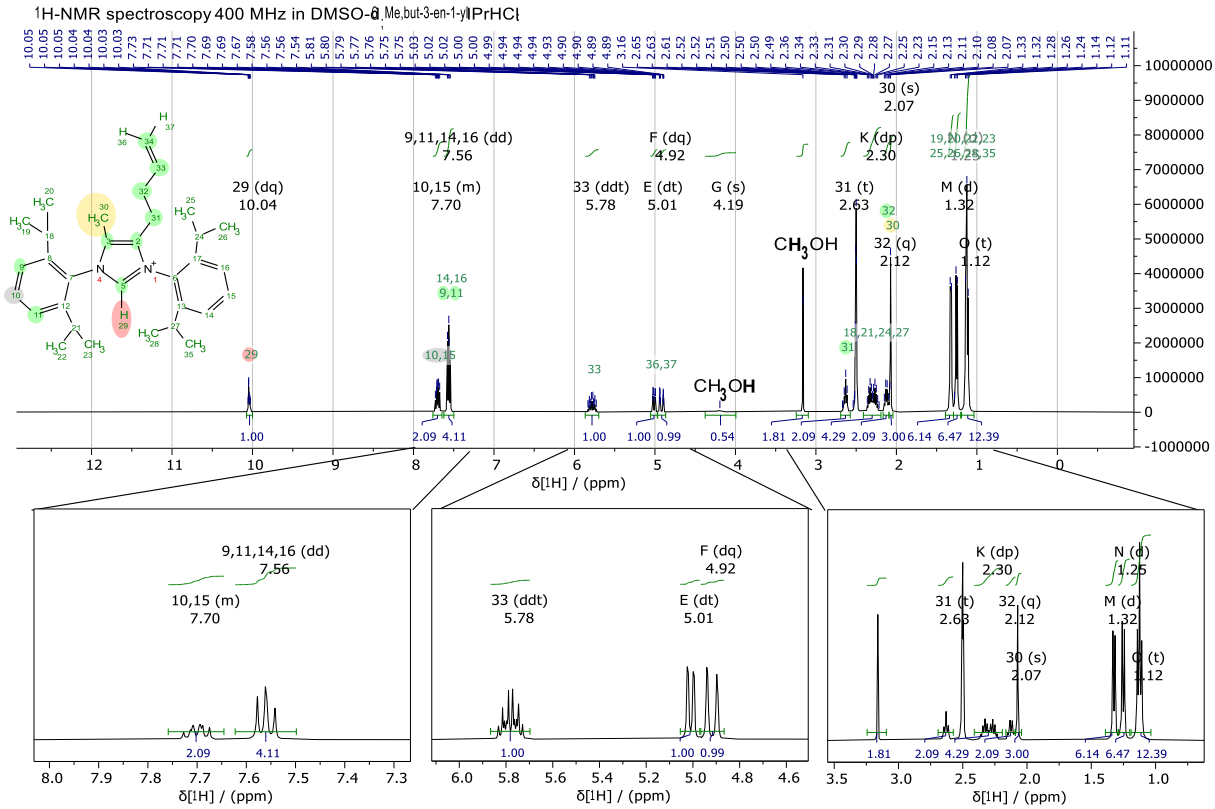

Figure SI-76: ^{1}H-NMR (400 MHz) of compound $^{Me,but\text{-}3\text{-}en\text{-}1\text{-}yl}$IPrHCl•MeOH, in DMSO-d^{6} measured at r.t. The spectrum was referenced to the residual solvent peak: ^{1}H-NMR (CD_2Cl_2) δ = 5.32 ppm. Impurities are marked with an asterisk*. *Top)* the full ^{1}H-NMR spectrum. *Bottom)* expansions of selected sections of the ^{1}H-NMR spectrum with arbitrary scaling of intensity.

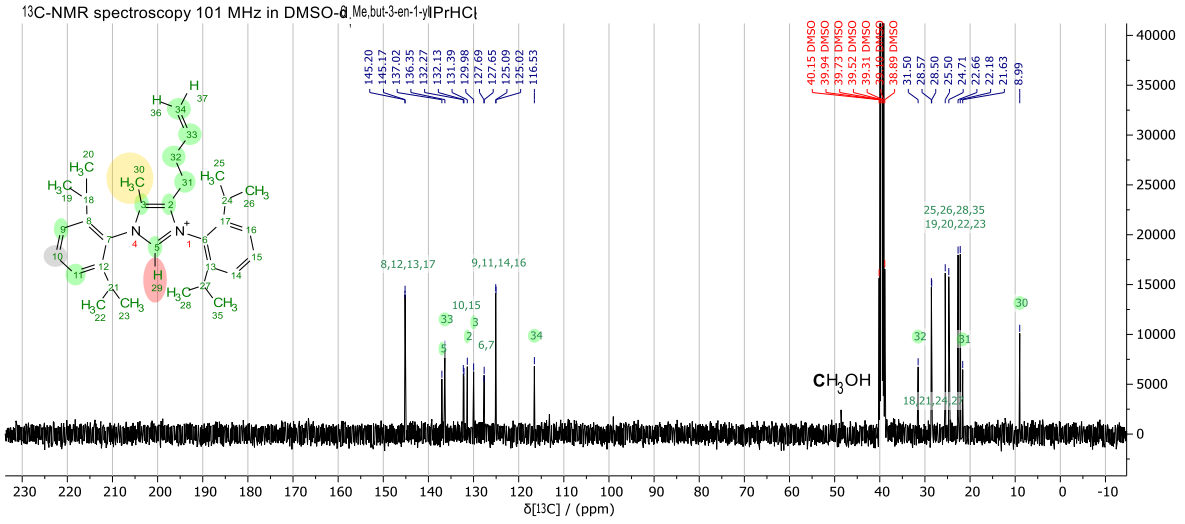

Figure SI-77: ^{13}C{^{1}H}-NMR (101 MHz) spectrum of compound $^{Me,but\text{-}3\text{-}en\text{-}1\text{-}yl}$IPrHCl•MeOH, in DMSO-d^{6} measured at r.t. The spectrum was referenced to the residual solvent peak: ^{13}C -NMR (CD_2Cl_2) δ = 53.84 ppm.

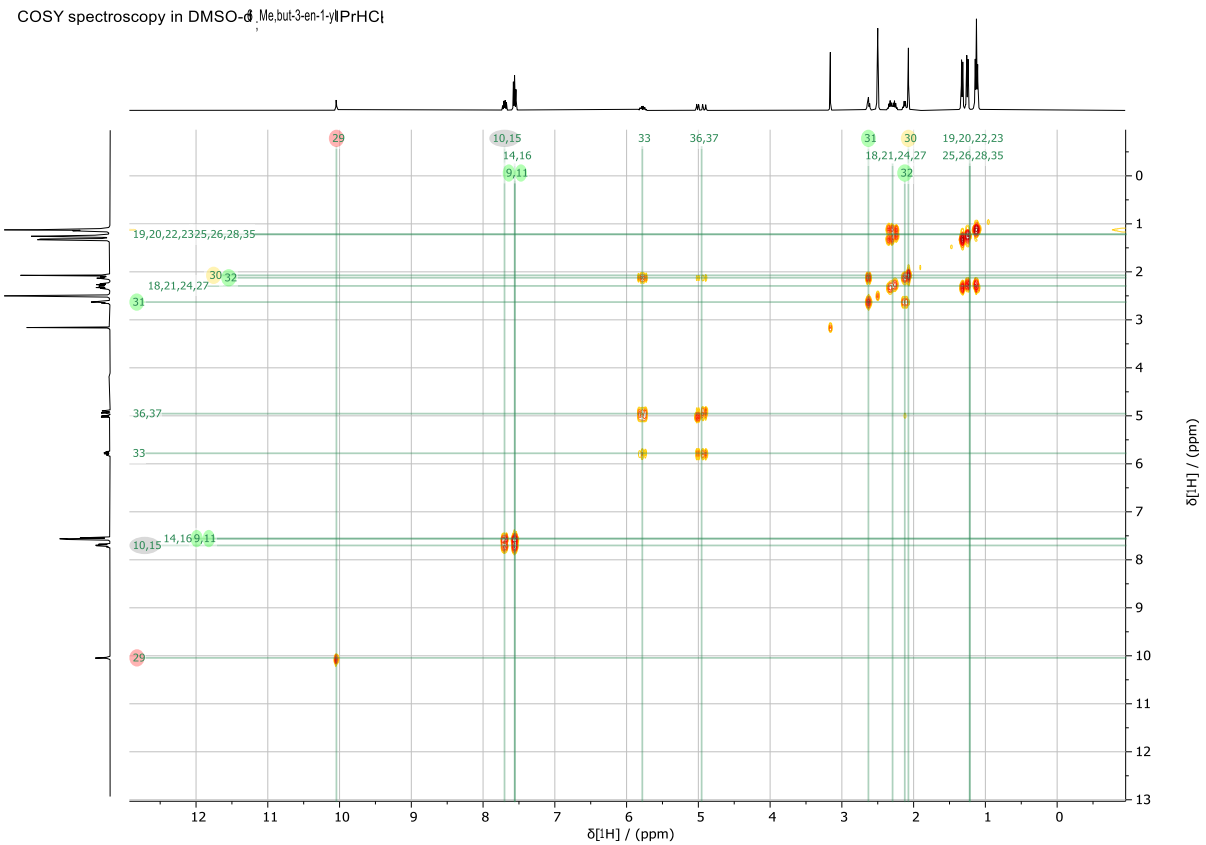

Figure SI-78: ^{1}H-^{1}H COSY-NMR (400 MHz, 400 MHz) spectrum of compound $^{Me,but\text{-}3\text{-}en\text{-}1\text{-}yl}$IPrHCl•MeOH, in DMSO-d^{6} measured at r.t.

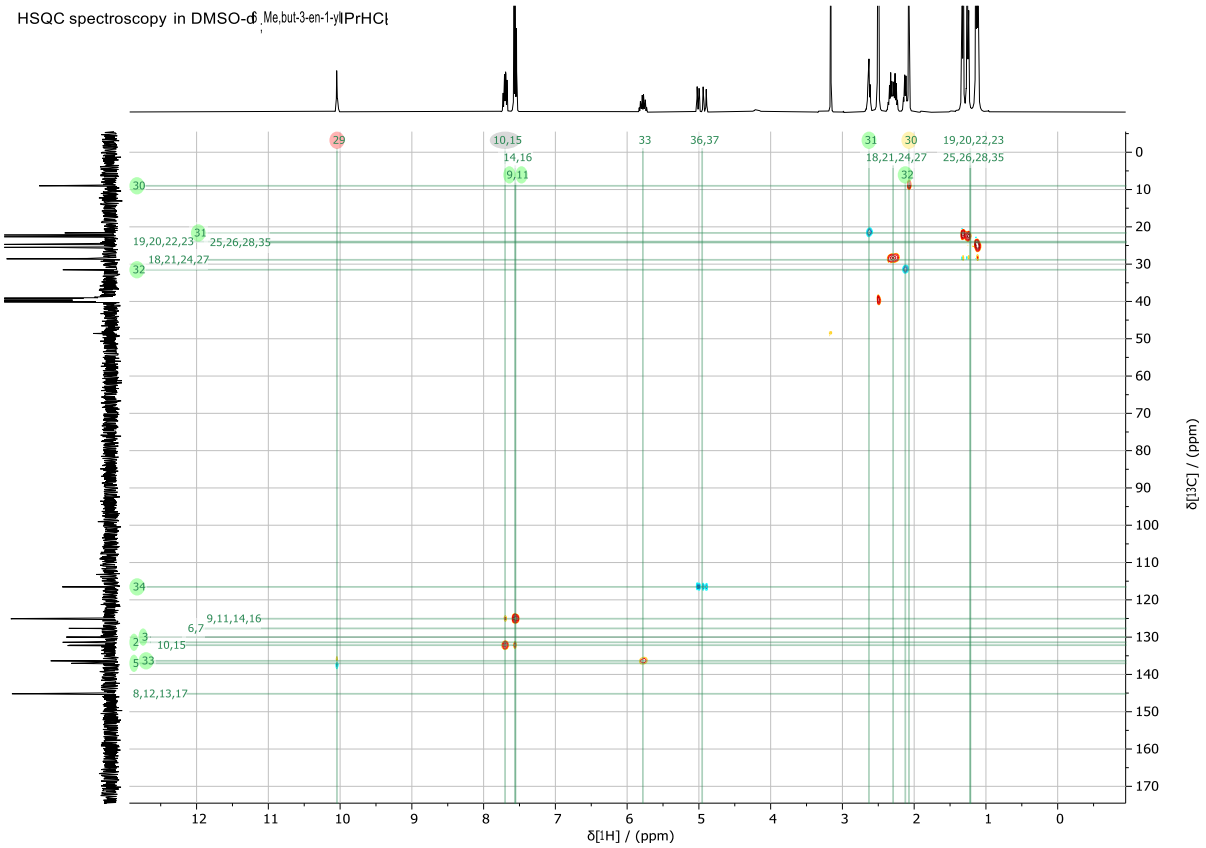

Figure SI-79: ^{1}H-^{13}C HSQC-NMR (400 MHz, 101 MHz) of compound $^{Me,but\text{-}3\text{-}en\text{-}1\text{-}yl}$IPrHCl•MeOH, in DMSO-d^{6} measured at r.t.

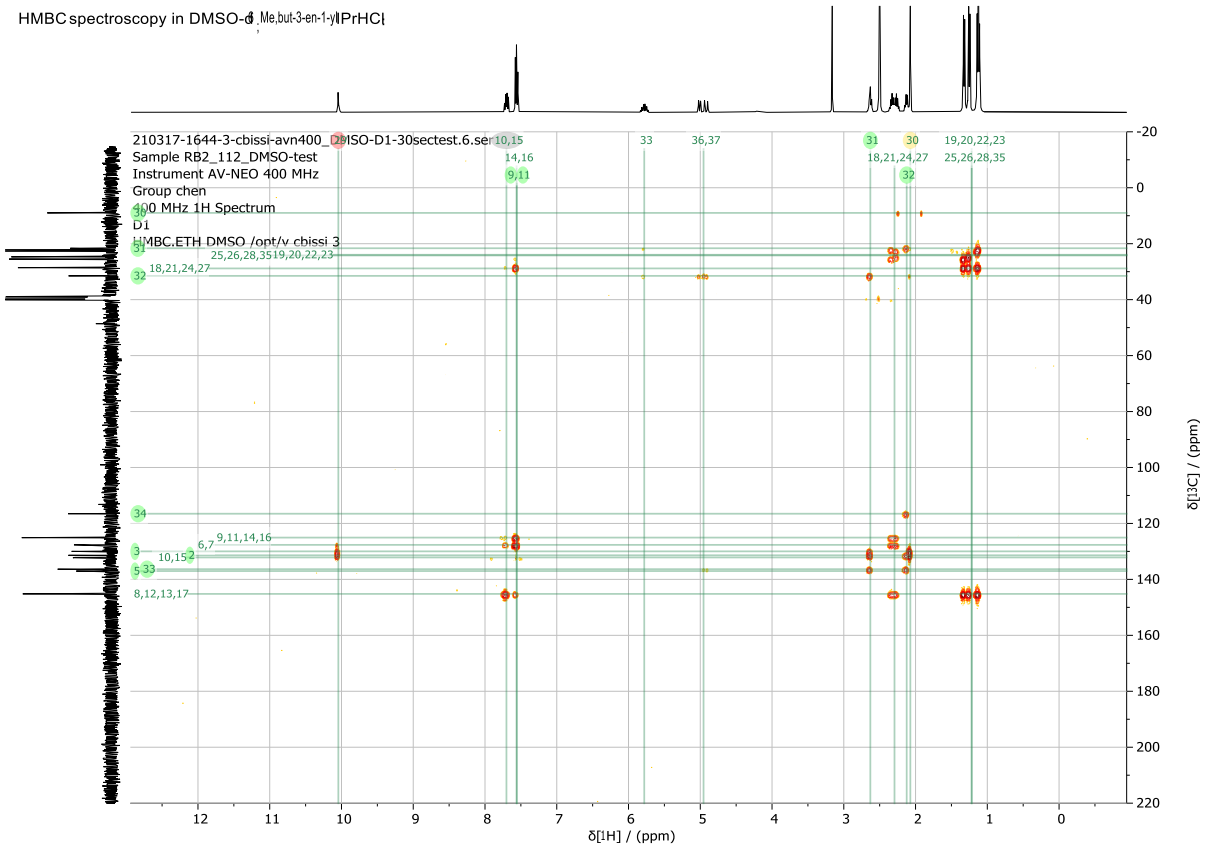

Figure SI-80: ^{1}H-^{13}C HMBC-NMR (400 MHz, 101 MHz) spectrum of compound $^{Me,but\text{-}3\text{-}en\text{-}1\text{-}yl}$IPrHCl•MeOH, in DMSO-$d^{6}$ measured at r.t.

3.2.3. NMR spectra of [($^{Me,but\text{-}3\text{-}en\text{-}1\text{-}yl}$IPr)$Cu^{I}$Cl]:

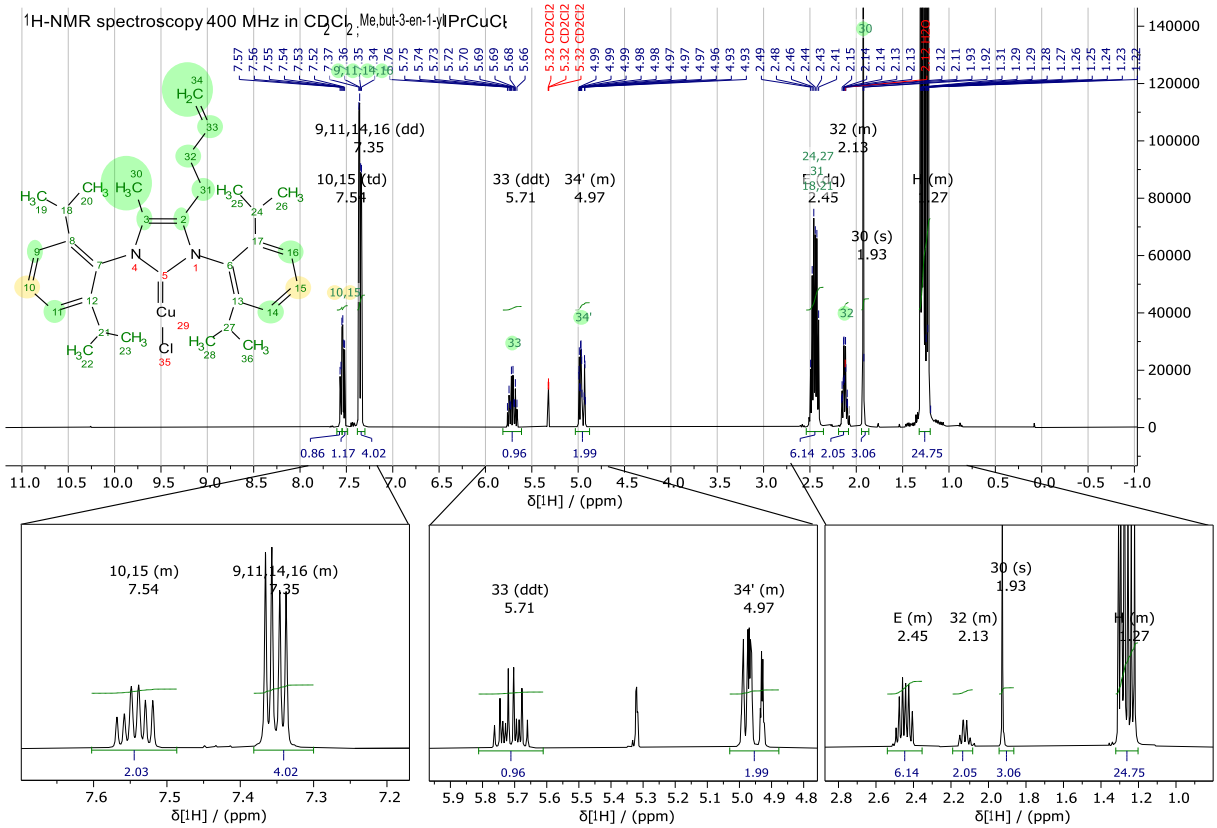

Figure SI-81: ^{1}H-NMR (400 MHz) of compound ($^{Me,but\text{-}3\text{-}en\text{-}1\text{-}yl}$IPr)CuCl, in CD_2Cl_2 measured at r.t. The spectrum was referenced to the residual solvent peak: ^{1}H-NMR (CD_2Cl_2) δ = 5.32 ppm. Impurities are marked with an asterisk*. *Top)* the full ^{1}H-NMR spectrum. *Bottom)* expansions of selected sections of the ^{1}H-NMR spectrum with arbitrary scaling of intensity.

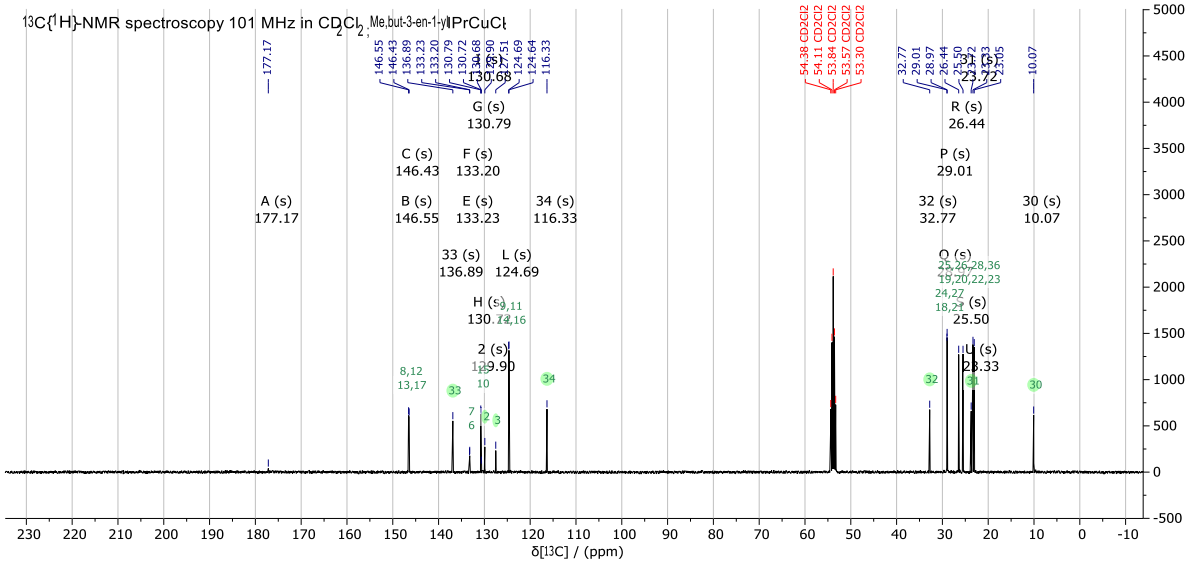

Figure SI-82: $^{13}C\{^{1}H\}$-NMR (101 MHz) spectrum of compound ($^{Me,but-3-en-1-yl}$IPr)CuCl, in CD_2Cl_2 measured at r.t. The spectrum was referenced to the residual solvent peak: ^{13}C -NMR (CD_2Cl_2) δ = 53.84 ppm.

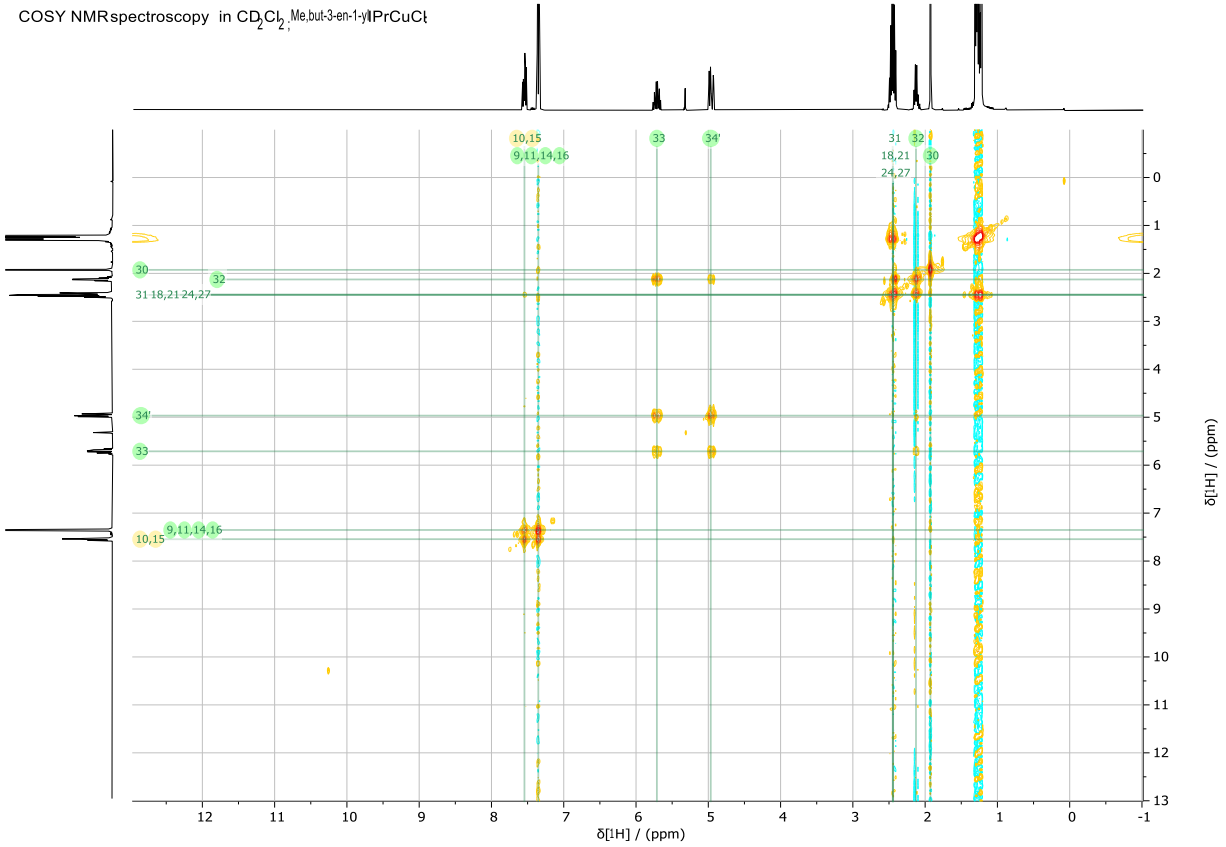

Figure SI-83: ^{1}H-^{1}H COSY-NMR (400 MHz, 400 MHz) spectrum of compound ($^{Me,but-3-en-1-yl}$IPr)CuCl, in CD_2Cl_2 measured at r.t.

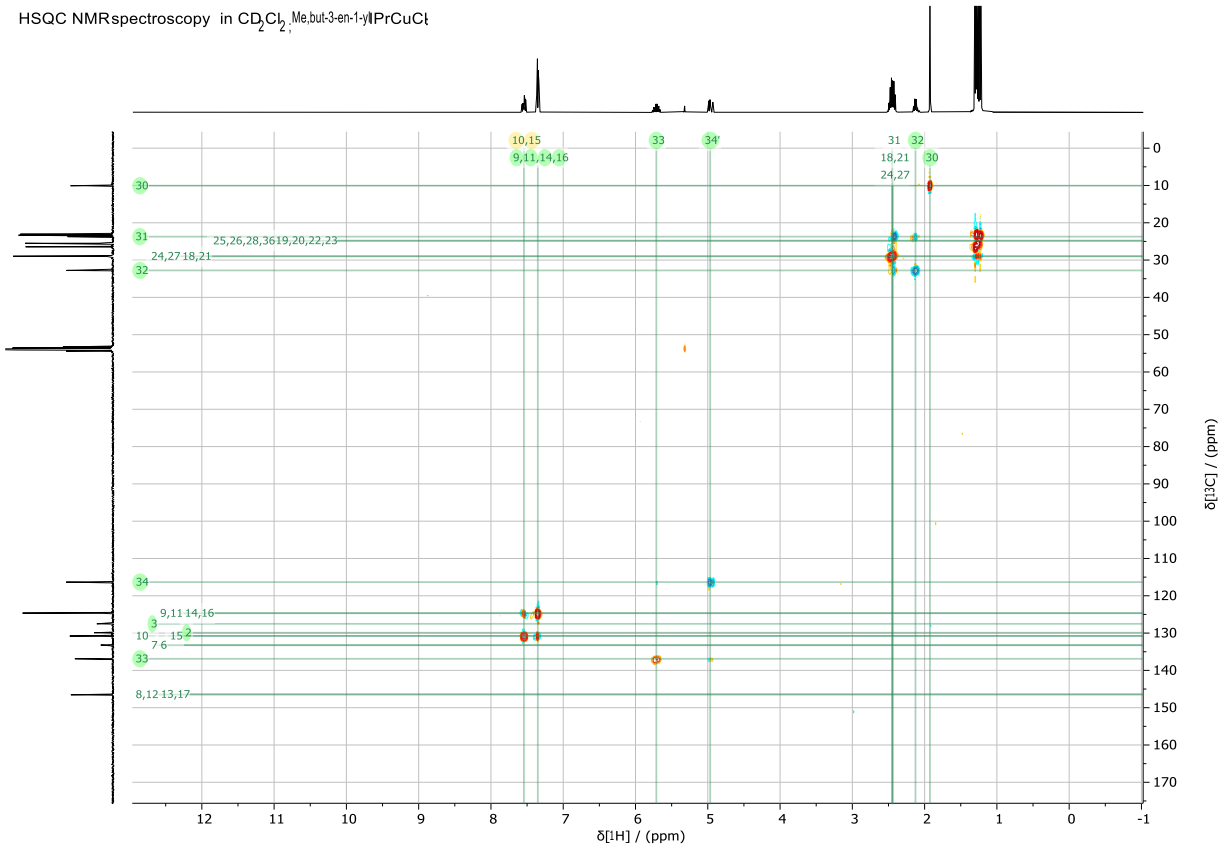

Figure SI-84: ^{1}H-^{13}C HSQC-NMR (400 MHz, 101 MHz) spectrum of compound ($^{Me,but\text{-}3\text{-}en\text{-}1\text{-}yl}$IPr)CuCl, in CD_2Cl_2 measured at r.t.

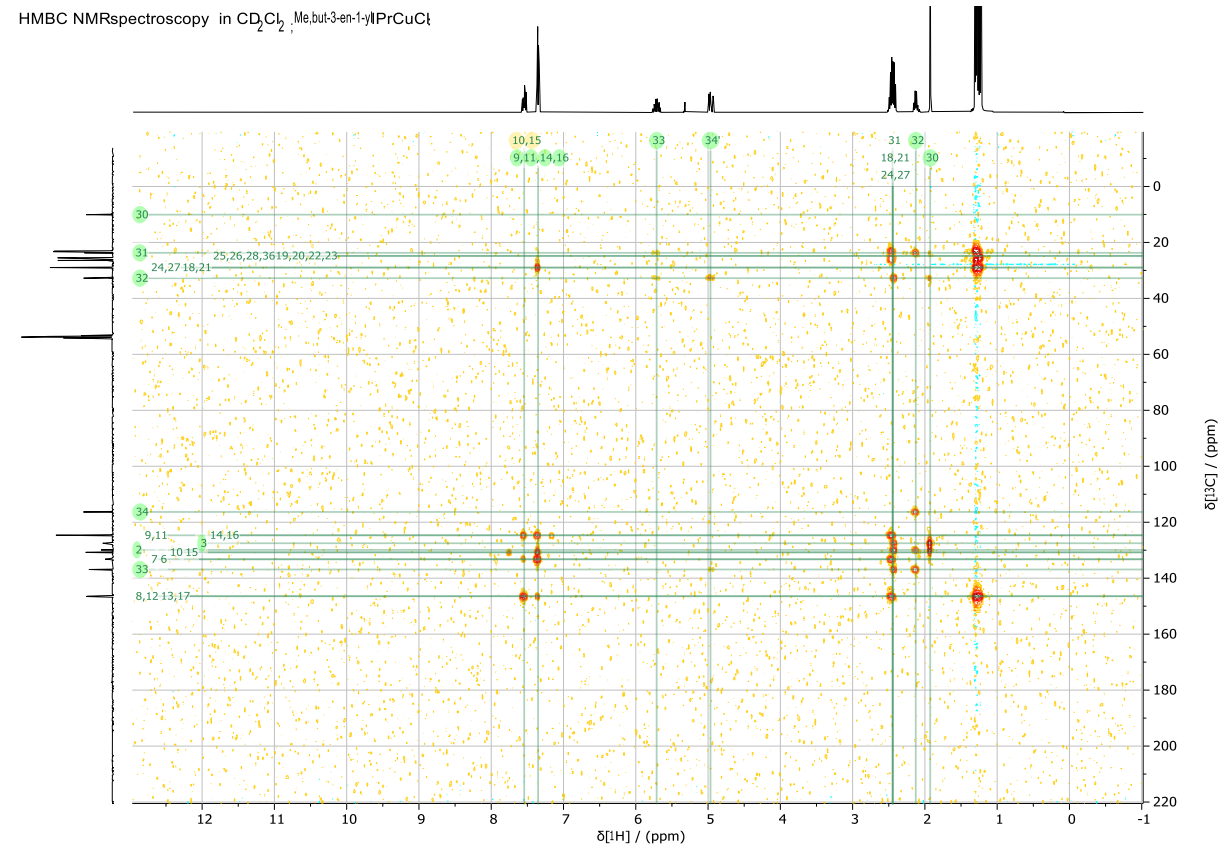

Figure SI-85: ^{1}H-^{13}C HMBC-NMR (400 MHz, 101 MHz) spectrum of compound ($^{Me,but\text{-}3\text{-}en\text{-}1\text{-}yl}$IPr)CuCl, in CD_2Cl_2 measured at r.t.

3.2.4. NMR spectra of [($^{Me, but-3-en-1-yl}$IPr)Cu^{I}•Pd^{II}(bhq)$_2$]BArF , [**4a**]BArF:

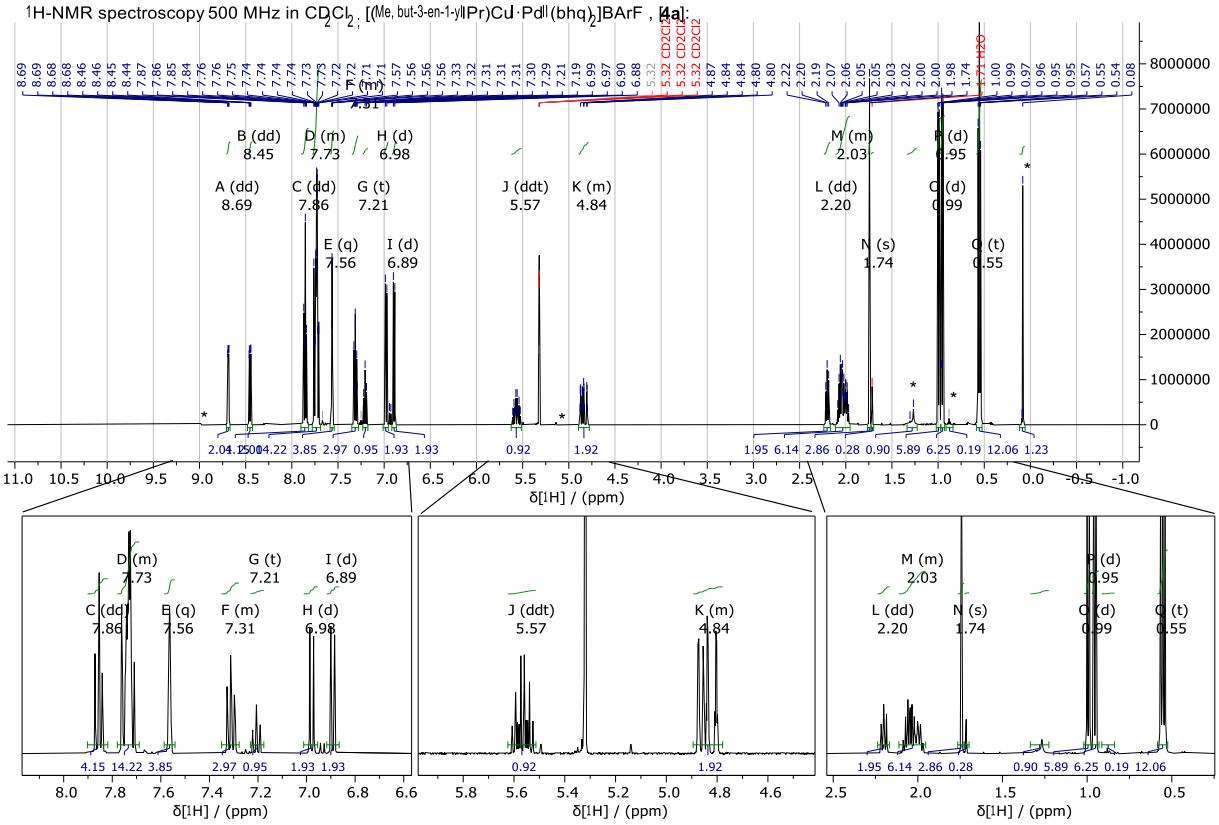

Figure SI-86: ^{1}H-NMR (500 MHz) of compound [($^{Me, but-3-en-1-yl}$IPr)Cu^{I}•Pd^{II}(bhq)$_2$]BArF, [**4a**]BArF, in CD_2Cl_2 measured at r.t. The spectrum was referenced to the residual solvent peak: ^{1}H-NMR (CD_2Cl_2) δ = 5.32 ppm. Impurities are marked with an asterisk*. *Top)* the full ^{1}H-NMR spectrum. *Bottom)* expansions of selected sections of the ^{1}H-NMR spectrum with arbitrary scaling of intensity.

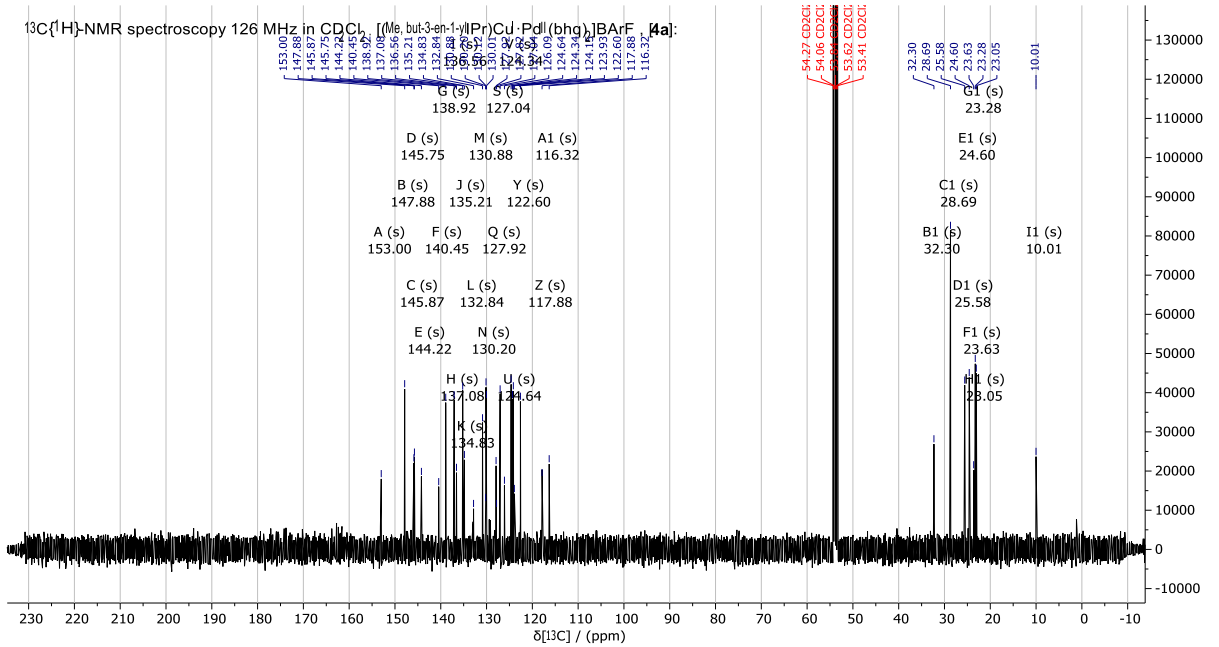

Figure SI-87: ^{13}C{^{1}H}-NMR (126 MHz) spectrum of compound [($^{Me, but-3-en-1-yl}$IPr)Cu^{I}•Pd^{II}(bhq)$_2$]BArF, [**4a**], in CD_2Cl_2 measured at r.t. The spectrum was referenced to the residual solvent peak: ^{13}C -NMR (CD_2Cl_2) δ = 53.84 ppm.

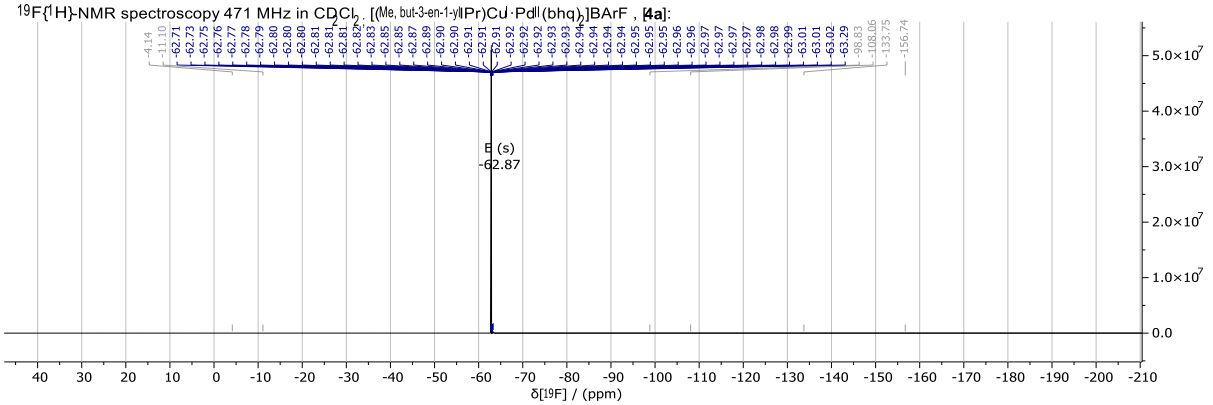

Figure SI-88: $^{19}F\{^{1}H\}$-NMR (471 MHz) spectrum of compound [($^{Me, but\text{-}3\text{-}en\text{-}1\text{-}yl}$IPr)$Cu^{I}$•$Pd^{II}(bhq)_2$]BArF, [**4a**], in CD_2Cl_2 measured at r.t.

3.3. Crystal Structure Determination of Pincer based Bimetallic Compounds [1]X,[2]X,[3]X

Chemical Formula	B 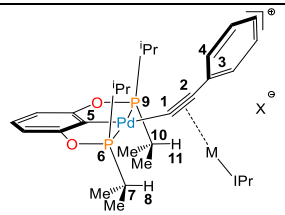					A 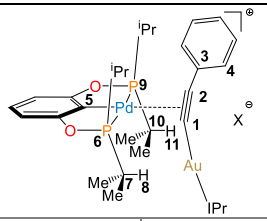		B 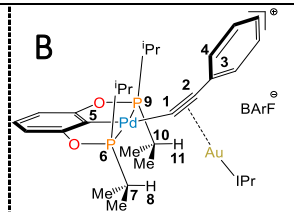
XRD –Structure[a)]	M= Cu, X= BF_4^- 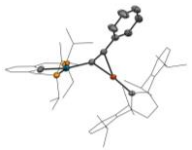	M= Cu, X= $BArF^-$ 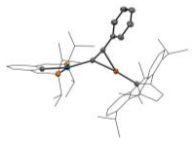	M= Ag, X= BF_4^- 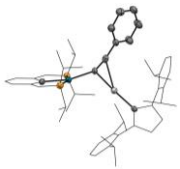	M= Ag, X= OTf^- 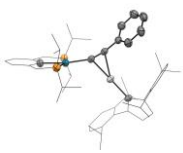	M= Ag, X= $BArF^-$ 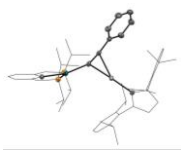	M= Au, X= BF_4^- 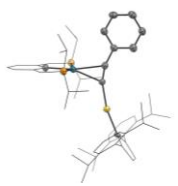	M= Au, X= OTf^- 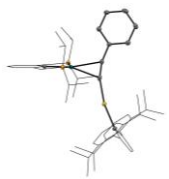	M= Au, X= $BArF^-$ 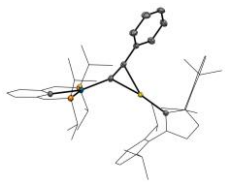
b(Pd-M)/(Å)	3.735	3.758	3.584	3.759	3.802	3.766	3.733	3.864
b(Pd-C1)/(Å)	2.057(2)	2.0626(15)	2.064(3)	2.056(2)	2.0515(16)	2.299(6)	2.298(4)	2.0516(17)
b(Pd-C2)/(Å)	3.207	3.193	3.170	3.221	3.207	2.347(6)	2.357(4)	3.210
b(Pd-C5)/(Å)	2.014(3)	2.0152(15)	2.010(3)	2.018(2)	2.0130(16)	2.010(6)	2.001(4)	2.0099(16)
b(M-C1)/(Å)	2.028(2)	2.0263(15)	2.151(3)	2.250(2)	2.2255(16)	1.999(6)	1.996(4)	2.1997(16)
b(M-C2)/(Å)	2.074(2)	2.0827(15)	2.542	2.354(2)	2.3254(16)	3.167	3.190	2.2419(16)
b(C1-C2)/(Å)	1.234(4)	1.227(2)	1.213(4)	1.217(3)	1.224(2)	1.210(9)	1.231(5)	1.240(2)
a(Pd-C1-M)/(°)	132.20(12)	133.58(8)	116.48(13)	121.53(11)	125.43(8)	122.2(3)	120.57(17)	130.66(8)
a(Pd-C1-C2)/(°)	153.2(2)	151.25(13)	149.5(2)	158.77(19)	155.60(14)	77.1(4)	77.3(3)	153.65(14)
a(C5-Pd-C1)/(°)	168.79(10)	165.81(6)	165.48(11)	171.84(9)	165.41(7)	159.9(2)	160.68(14)	165.94(7)
d(Pd-P6-C7-H8)/(°)	67.87	65.46	63.14	-172.96	69.21	-162.93	-162.54	69.14
d(Pd-P9-C10-H11)/(°)	-61.58	-68.93	169.15	-66.17	-66.24	162.93	162.54	-66.01
d(Pd-M-C12-N13)/(°)	-39.77	-141.96	-20.03	-153.24	-38.33	-99.17	-100.66	-39.44
d(Pd-C1-C2-C4)/(°)	51.89	96.05	49.06	100.41	58.19	180.00	180.00	54.38
d(M-C2-C3-C4)/(°)	-113.46	-67.97	-118.15	-72.18	-110.69	0.00	0.00	-111.63
d(P6-Pd-C1-M)/(°)	82.60	99.95	70.48	105.82	80.44	89.68	90.01	80.04
Cell *a | b | c* /(Å)	12.49750(10)|23.2159 0(10)|22.65500(10)	15.71856(6)|16.47461(7)|18.04887(8)	11.22300(10)|12.2171(3)|23.2541(3)	13.06490(10)|13.7799 0(10)|18.7504(2)	15.70660(10)|16.4996 0(10)|18.15710(10)	10.83380(10)|15.88720 (10)|17.4029(2)	10.8130(5)|15.7986(8) | 17.8785(9)	15.73380(10)|16.5046(2)|18.1 2680(10)
Cell *α | β | γ* /(°)	90|90.4240(10)|90	105.5135(4)|107.5009(4)|97.1043(3)	78.442(2)|83.5370(10) |89.622(2)	73.4020(10)|79.1420(1 0)|71.1830(10)	105.2690(10)|107.808 0(10)|97.3030(10)	90|106.8160(10)|90	90|107.1730(10)|90	105.1640(10)|107.8150(10)|9 7.3110(10)
Comment(asymetric unit):	Anion(1x),THF(3x) disordered			Anion(1x),THF(0.5x) disordered	Anion(1x) disordered	Crys.-graphic mirror. THF(1x) disordered		Anion(1x) disordered

Table SI-13: Summary table of XRD-structures of the bimetallic complexes. Values (b: bond length, a: angle, d: dihedral angle) without error were read out using the Mercury software suite (Version 3.10.3). a) Pictures of the XRD structure (ORTEP 50% probability ellipsoids), selected structural features are drawn as wireframe for clarity. Anions, hydrogens and co-crystallizing molecules omitted for clarity. Color-code as used in the chemical formula.

3.3.1. Crystal structure for [($^{i\text{Pr}}$POCOP)Pd$^{\text{II}}$(CCPh)•Cu$^{\text{I}}$(IPr)]BF_4, [**1**]BF_4:

Comment: The synthesis and crystallization procedure is described in experimental section 1.2.2. Three tetrahydrofuran molecules, as well as the anion are disordered within the asymmetric unit.

Crystal Data for $C_{65}H_{96}BCuF_4N_2O_5P_2Pd$ (*M* =1304.12 g/mol): monoclinic, space group $P2_1/c$ (no. 14), *a* = 12.49750(10) Å, *b* = 23.21590(10) Å, *c* = 22.65500(10) Å, *β* = 90.4240(10)°, *V* = 6572.96(7) Å^3, *Z* = 4, *T* = 100.0(1) K, μ(Cu Kα) = 3.544 mm^{-1}, *Dcalc* = 1.318 g/cm^3, 93018 reflections measured (7.074° ≤ 2Θ ≤ 159.708°), 14123 unique (R_{int} = 0.0488, R_{sigma} = 0.0269) which were used in all calculations. The final R_1 was 0.0403 (I > 2σ(I)) and wR_2 was 0.1147 (all data).

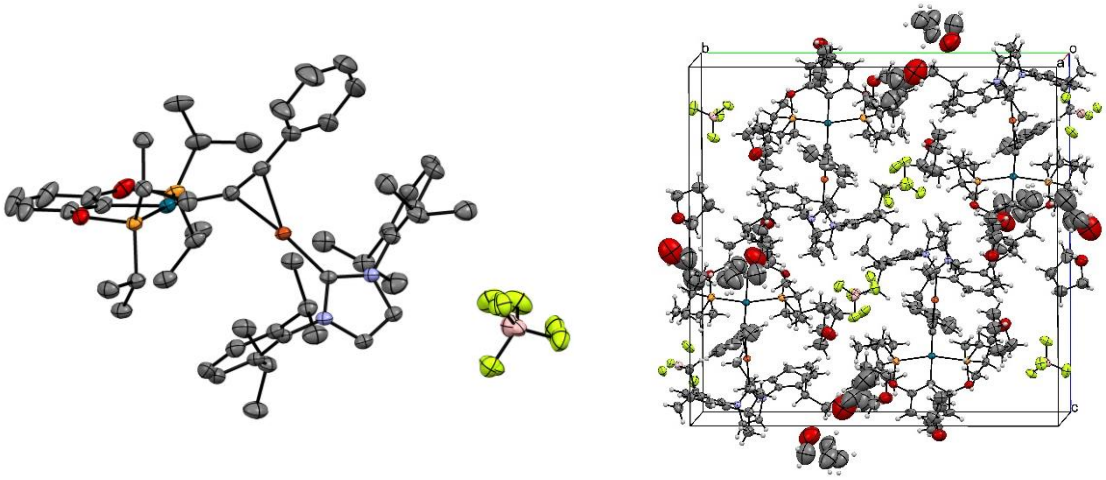

Figure SI-89: Representation of crystal structure from different perspectives. Colors-code: grey/carbon, red/oxygen, light-orange/phosphorus, dark-orange/Cu, yellow/fluorine, pink/boron, blue/nitrogen, teal/palladium. *Left)* XRD structure (ORTEP 50% probability ellipsoids), Hydrogens and co-crystallizing molecules omitted for clearity. *Right)* representation of the unit cell, crystal packing.

Table 1 Crystal data and structure refinement for c221019_2_2.

Identification code	c221019_2_2
Empirical formula	$C_{65}H_{96}BCuF_4N_2O_5P_2Pd$
Formula weight	1304.12
Temperature/K	100.0(1)
Crystal system	monoclinic
Space group	$P2_1/c$
a/Å	12.49750(10)
b/Å	23.21590(10)
c/Å	22.65500(10)
α/°	90
β/°	90.4240(10)
γ/°	90
Volume/Å^3	6572.96(7)
Z	4
ρ_{calc}g/cm^3	1.318
μ/mm^{-1}	3.544
F(000)	2744.0
Crystal size/mm^3	0.213 × 0.145 × 0.073
Radiation	Cu Kα (λ = 1.54184)
2Θ range for data collection/°	7.074 to 159.708
Index ranges	-15 ≤ h ≤ 11, -29 ≤ k ≤ 29, -28 ≤ l ≤ 28

Reflections collected	93018
Independent reflections	14123 [R_{int} = 0.0488, R_{sigma} = 0.0269]
Data/restraints/parameters	14123/727/883
Goodness-of-fit on F^2	1.024
Final R indexes [I>=2σ (I)]	R_1 = 0.0403, wR_2 = 0.1127
Final R indexes [all data]	R_1 = 0.0427, wR_2 = 0.1147
Largest diff. peak/hole / e $Å^{-3}$	0.68/-1.13

Table 2 Fractional Atomic Coordinates (×10^4) and Equivalent Isotropic Displacement Parameters ($Å^2$×10^3) for c221019_2_2. U_{eq} is defined as 1/3 of of the trace of the orthogonalised U_{IJ} tensor.

Atom	*x*	*y*	*z*	U(eq)
Pd1	5512.1(2)	6378.7(2)	1737.1(2)	24.53(6)
Cu1	6702.3(2)	6434.6(2)	3253.0(2)	23.22(8)
P1	5283.3(4)	7344.3(2)	1612.4(2)	24.99(11)
P2	5255.5(5)	5415.8(3)	1605.6(3)	32.11(13)
F4	8171(6)	6004(2)	6141(2)	44.7(12)
F1	6587(4)	5682(3)	6481(3)	53.1(15)
O1	4658.4(13)	7412.7(7)	967.8(7)	30.2(3)
O2	4547.5(16)	5354.5(8)	990.7(8)	41.1(4)
N1	5798.6(14)	6826.8(7)	4387.1(8)	23.1(3)
F3	8092(2)	5595(2)	7044.7(14)	52.8(10)
N2	6992.1(14)	6182.3(8)	4519.6(8)	24.1(3)
F2	7876(2)	5047.4(13)	6230(3)	61.0(13)
C45	4569(2)	6385.7(10)	1012.5(10)	31.2(5)
C11	5842.6(17)	6721.1(9)	4989.3(9)	26.8(4)
C9	6503.5(16)	6492.0(9)	4089.3(9)	23.1(4)
C24	7828.2(18)	5766.3(10)	4417.4(10)	27.7(4)
C12	5087.1(17)	7235.7(9)	4113.1(9)	24.8(4)
C1	6715.4(19)	6360.5(9)	2361.1(10)	28.0(5)
O1A	8473.2(19)	3486.7(12)	2239.9(12)	67.7(7)
C13	5432.9(18)	7807.2(10)	4049.8(10)	28.9(4)
C2	7660.8(19)	6325.5(10)	2517.8(10)	30.3(5)
C25	7532.8(19)	5205.1(10)	4265.0(10)	30.7(5)
C10	6598.3(18)	6315.6(10)	5072.6(10)	27.6(4)
C18	3731.1(19)	6425.2(10)	4031.7(11)	32.0(5)
C17	4070.6(17)	7044.1(10)	3941.0(9)	27.9(4)
C15	3722(2)	8011.0(11)	3585.8(11)	36.4(5)
C29	8894.6(18)	5944.4(11)	4488.3(11)	32.6(5)
C21	6528.1(19)	8005.0(10)	4269.9(11)	32.4(5)
C16	3396.2(19)	7448.1(11)	3672.9(10)	33.6(5)
C14	4728(2)	8186.3(10)	3776.7(11)	34.2(5)
C50	4281.4(19)	6897.0(11)	733.7(10)	33.9(5)
C00W	6375(2)	5020.2(10)	4205.6(11)	34.3(5)
C36	6440.9(18)	7813.0(10)	1520.3(10)	29.4(4)
C30	9183.9(19)	6562.0(12)	4653.7(12)	37.7(5)
C33	4347.5(18)	7710.0(10)	2103.7(10)	30.5(5)

C37	7258.4(19)	7517.3(11)	1122.0(11)	35.2(5)
C38	6928(2)	7956.8(11)	2126.6(11)	35.8(5)
C27	9424(2)	4977.5(11)	4221.3(12)	40.9(6)
C28	9686(2)	5533.1(12)	4381.4(12)	39.0(6)
C26	8368(2)	4812.5(11)	4164.7(11)	36.8(5)
C3	8807(2)	6282.4(12)	2590.2(12)	37.4(5)
C40	3308(2)	5402.7(11)	2133.6(12)	39.4(6)
C23	7315(2)	8059.0(11)	3757.8(12)	37.5(5)
C46	4231(2)	5876.5(11)	745.6(11)	38.7(6)
C34	3291.4(19)	7373.9(11)	2112.4(12)	35.8(5)
C20	3905(2)	6071.7(12)	3465.4(13)	42.4(6)
C35	4152(2)	8337.8(11)	1929.1(12)	38.2(5)
C39	4373(2)	5072.1(10)	2142.7(11)	34.5(5)
C49	3654(2)	6912.0(14)	226.4(12)	46.6(7)
C01E	6110(2)	4849.0(12)	3571.0(12)	41.5(6)
C19	2568(2)	6371.7(13)	4228.8(15)	45.5(7)
C22	6453(2)	8571.2(12)	4618.6(14)	44.5(6)
C32	10003(2)	6584.5(13)	5156.9(13)	44.6(6)
C8	9284(2)	5818.2(14)	2867.5(12)	48.3(7)
C31	9571(2)	6891.2(13)	4108.1(14)	45.9(6)
C47	3605(3)	5867.6(15)	236.4(12)	53.9(8)
C41	4182(3)	4432.2(11)	2031.6(13)	45.4(7)
C42	6377(2)	4942.1(11)	1436.5(13)	42.9(6)
C44	7015(3)	4782.5(13)	1992.2(15)	53.0(7)
C48	3319(3)	6391.7(15)	-12.2(13)	59.4(10)
C01P	6101(3)	4539.1(13)	4639.5(15)	52.5(7)
C43	7075(3)	5242.3(13)	973.2(15)	52.4(8)
B1	7683(4)	5577.6(18)	6474(2)	33.4(10)
C4	9451(2)	6717.5(16)	2367.3(17)	58.6(8)
C7	10402(3)	5787.1(18)	2910.6(14)	64.1(10)
C1A	9286(3)	3231(2)	1905.2(17)	68.1(10)
C6	11013(3)	6213(2)	2681.7(18)	69.8(11)
C2A	10303(3)	3270(2)	2252.6(17)	68.2(10)
C3A	9904(3)	3350(2)	2889.4(17)	68.2(10)
C4A	8908(3)	3691.5(18)	2787.1(19)	67.9(10)
C5	10556(3)	6671(2)	2415(2)	79.1(12)
O2A	9847(5)	4691(2)	9219(2)	78.6(16)
O3A	275(4)	1773(2)	5243(2)	75.1(15)
C6A	9568(6)	5241(3)	8379(3)	62.8(16)
C7A	8874(7)	5491(3)	8903(4)	72(2)
C8A	8956(7)	5044(3)	9382(4)	79(2)
C9A	855(6)	1656(5)	4715(4)	75(2)
C10A	166(6)	1807(4)	4201(4)	69.6(19)
C5A	9801(6)	4662(3)	8595(3)	64.8(17)
C12A	-782(6)	1608(4)	5096(3)	78(2)
C11A	-989(6)	1746(4)	4462(4)	76(2)
C7B	9011(15)	5188(11)	8707(9)	195(6)

O2B	9458(12)	5837(7)	9487(9)	232(6)
C8B	8731(12)	5335(8)	9323(10)	178(6)
C5B	10441(11)	5615(8)	9219(8)	176(6)
C6B	10240(14)	5245(10)	8718(8)	190(6)
C9B	-478(14)	1845(7)	4246(10)	166(6)
O3B	363(13)	1772(7)	4692(7)	183(5)
C12B	987(12)	1311(6)	4449(8)	136(5)
C10B	-714(13)	1223(8)	4123(10)	166(6)
C11B	369(12)	968(8)	4070(8)	145(5)
F1A	6580(20)	5757(15)	6484(11)	37(5)
B1A	7610(19)	5569(8)	6380(9)	40(6)
F4A	8230(30)	6033(9)	6204(13)	42(6)
F3A	8046(16)	5326(14)	6883(11)	65(6)
F2A	7590(20)	5158(8)	5940(12)	62(6)

Table 3 Anisotropic Displacement Parameters ($Å^2×10^3$) for c221019_2_2. The Anisotropic displacement factor exponent takes the form: $-2\pi^2[h^2a^{*2}U_{11}+2hka^*b^*U_{12}+...]$.

Atom	U_{11}	U_{22}	U_{33}	U_{23}	U_{13}	U_{12}
Pd1	28.06(10)	23.78(9)	21.84(9)	-0.62(5)	5.34(6)	-1.11(5)
Cu1	23.77(16)	24.41(16)	21.58(16)	0.32(11)	6.27(12)	1.78(11)
P1	25.2(3)	25.2(3)	24.6(2)	2.99(19)	3.9(2)	-0.7(2)
P2	41.8(3)	25.7(3)	29.0(3)	-4.6(2)	10.0(2)	-2.6(2)
F4	42.6(19)	51(2)	40.7(17)	15.2(14)	-2.2(14)	-13.9(17)
F1	27.6(15)	58(3)	73(3)	2.9(19)	7.2(15)	4.0(15)
O1	29.0(8)	34.0(8)	27.6(8)	5.9(6)	2.1(6)	-3.2(6)
O2	57.9(11)	36.0(9)	29.3(8)	-7.4(7)	8.3(8)	-11.8(8)
N1	21.1(8)	24.3(8)	24.1(8)	0.0(7)	5.5(6)	-0.4(6)
F3	50.1(12)	67(2)	41.4(13)	17.8(13)	-3.0(10)	-6.1(13)
N2	23.1(8)	24.2(8)	25.0(8)	-0.1(7)	4.5(7)	1.1(7)
F2	51.7(14)	39.1(12)	92(3)	-12.0(15)	0.8(15)	5.4(10)
C45	34.5(12)	37.6(13)	21.6(10)	0.5(8)	5.9(9)	-7.6(9)
C11	26.9(10)	28.7(10)	24.8(10)	-1.9(8)	6.0(8)	-1.4(8)
C9	20.8(9)	22.5(9)	26.1(10)	-1.2(8)	4.6(8)	-1.9(7)
C24	26.5(10)	29.7(11)	27.1(10)	1.5(8)	4.3(8)	5.6(8)
C12	24.7(10)	26.5(10)	23.4(9)	-0.1(8)	5.9(8)	3.4(8)
C1	31.9(12)	27.0(11)	25.1(11)	1.8(8)	4.4(9)	1.5(8)
O1A	44.9(12)	81.1(17)	77.1(17)	-21.3(14)	-8.9(12)	8.4(12)
C13	32.2(11)	29.4(11)	25.2(10)	-0.2(8)	7.2(8)	0.9(9)
C2	31.7(12)	33.0(11)	26.3(11)	1.7(8)	8.2(9)	4.0(9)
C25	35.8(12)	28.1(11)	28.3(11)	2.4(9)	5.9(9)	5.1(9)
C10	27.5(11)	30.5(11)	25.0(10)	1.4(8)	4.0(8)	-0.8(8)
C18	22.1(11)	37.3(13)	36.6(13)	-1.1(9)	2.9(9)	-2.7(8)
C17	24.1(10)	35.5(11)	24.3(10)	-1.8(8)	6.5(8)	2.8(8)
C15	36.3(12)	43.5(13)	29.5(11)	3.4(10)	3.6(9)	14.8(10)
C29	27.4(11)	37.2(12)	33.1(11)	-1.3(9)	3.9(9)	5.4(9)

C21	33.2(12)	30.0(11)	33.9(12)	2.8(9)	4.0(9)	-3.8(9)
C16	26.8(11)	45.1(13)	29.0(11)	-1.9(10)	1.9(9)	6.5(10)
C14	40.2(13)	28.4(11)	34.0(12)	4.3(9)	7.7(10)	3.4(9)
C50	32.7(12)	43.0(13)	26.0(11)	4.4(9)	4.4(9)	-12.2(10)
C00W	36.9(12)	26.3(11)	39.7(13)	-0.3(9)	8.9(10)	-2.5(9)
C36	27.9(10)	27.9(11)	32.5(11)	5.5(9)	2.2(9)	-2.1(9)
C30	23.9(11)	41.1(13)	48.3(15)	-5.2(11)	5.4(10)	-0.2(10)
C33	30.5(11)	30.8(11)	30.3(11)	2.1(9)	6.6(9)	1.7(9)
C37	28.8(11)	38.4(13)	38.5(13)	7.1(10)	8.1(9)	-0.4(9)
C38	35.7(12)	32.8(12)	38.8(13)	3.1(10)	-2.6(10)	-4.6(10)
C27	40.6(14)	41.3(14)	40.8(14)	0.7(11)	4.0(11)	19.4(11)
C28	26.4(11)	47.5(14)	43.2(14)	-0.7(11)	2.8(10)	8.8(10)
C26	44.6(14)	30.2(11)	35.7(12)	-0.6(10)	3.7(10)	8.4(10)
C3	28.9(12)	50.1(14)	33.2(12)	-1.7(11)	6.2(9)	8.0(10)
C40	45.0(14)	33.2(12)	40.2(13)	-3.0(10)	13.2(11)	-5.0(10)
C23	32.9(12)	37.5(13)	42.3(13)	-1.3(10)	9.3(10)	-1.7(10)
C46	49.1(14)	42.4(14)	24.5(11)	-0.6(10)	7.3(10)	-17.1(11)
C34	31.2(12)	37.6(13)	38.5(13)	2.1(10)	10.5(10)	-0.8(10)
C20	36.3(13)	43.0(14)	48.2(15)	-12.2(12)	5.8(11)	-6.8(11)
C35	37.7(13)	31.3(12)	45.9(14)	2.4(10)	8.3(11)	3.4(10)
C39	46.3(14)	26.3(11)	31.1(11)	-3.5(9)	10.9(10)	-1.8(10)
C49	47.6(15)	61.5(18)	30.7(12)	15.3(12)	-5.0(11)	-20.3(13)
C01E	41.9(14)	35.5(13)	47.1(15)	-4.6(11)	1.7(11)	-5.7(11)
C19	29.3(13)	53.6(17)	53.9(17)	-4.4(12)	11.0(12)	-7.0(11)
C22	43.7(15)	42.3(15)	47.7(16)	-9.1(11)	10.5(12)	-10.6(11)
C32	36.3(13)	51.0(16)	46.6(15)	-5.4(13)	4.1(11)	-9.6(12)
C8	45.0(15)	61.4(18)	38.5(14)	-0.6(13)	4.1(11)	21.5(13)
C31	41.0(14)	41.9(14)	54.8(17)	4.6(12)	0.3(12)	2.2(11)
C47	72(2)	62.2(19)	27.4(12)	-1.9(12)	-1.1(12)	-35.4(16)
C41	59.8(17)	27.8(12)	48.9(15)	-4.2(11)	20.8(13)	-5.9(11)
C42	50.4(15)	30.2(12)	48.4(15)	-10.7(11)	18.7(12)	0.3(11)
C44	57.3(18)	39.9(15)	61.9(19)	-6.8(13)	11.4(15)	12.4(13)
C48	72(2)	77(2)	29.3(14)	13.9(13)	-11.6(14)	-39.3(17)
C01P	60.1(18)	41.1(15)	56.5(18)	11.9(13)	17.3(14)	-5.7(13)
C43	55.9(17)	43.7(15)	57.9(18)	-13.4(13)	29.3(14)	-2.1(13)
B1	28.7(18)	32.7(19)	39(2)	7.7(15)	3.8(15)	2.7(14)
C4	29.8(14)	70(2)	76(2)	16.5(18)	9.1(14)	1.1(13)
C7	53.5(19)	95(3)	44.0(16)	-8.5(17)	-3.0(14)	40.9(19)
C1A	49.0(18)	97(3)	59(2)	-6.4(19)	1.3(15)	0.2(18)
C6	28.9(15)	118(3)	62(2)	-8(2)	3.8(14)	16.0(18)
C2A	47.0(18)	88(3)	70(2)	-7(2)	7.4(16)	-4.1(18)
C3A	52.3(19)	90(3)	62(2)	-8(2)	-1.5(16)	-9.7(19)
C4A	52(2)	74(2)	78(3)	-27(2)	1.1(18)	0.5(17)
C5	31.4(16)	105(3)	101(3)	15(3)	11.5(18)	-0.6(18)
O2A	96(4)	81(3)	58(3)	-1(2)	3(3)	32(3)
O3A	75(3)	87(4)	63(3)	0(3)	-4(2)	-16(3)
C6A	59(4)	78(4)	51(3)	2(3)	0(3)	-5(3)

C7A	77(5)	63(4)	76(4)	-25(3)	-18(4)	28(4)
C8A	84(5)	65(5)	89(5)	-8(4)	43(4)	0(4)
C9A	56(4)	91(6)	77(5)	26(4)	-1(3)	-21(4)
C10A	59(4)	85(5)	64(4)	0(4)	1(3)	-9(4)
C5A	70(4)	71(4)	54(3)	-7(3)	4(3)	12(3)
C12A	61(4)	111(6)	63(4)	-17(4)	1(3)	-17(4)
C11A	56(4)	88(5)	83(5)	4(4)	5(3)	-14(4)
C7B	178(10)	209(13)	198(12)	29(11)	14(11)	33(11)
O2B	145(10)	259(14)	292(14)	42(10)	-10(10)	-15(9)
C8B	189(12)	134(13)	212(14)	4(13)	35(12)	34(10)
C5B	183(12)	186(16)	159(14)	57(10)	17(11)	28(11)
C6B	177(10)	195(13)	196(13)	60(10)	-3(11)	5(11)
C9B	134(13)	155(10)	208(15)	-12(12)	6(11)	7(10)
O3B	179(11)	198(10)	172(11)	-48(8)	-8(8)	40(8)
C12B	150(10)	121(10)	135(11)	-32(8)	4(9)	26(8)
C10B	138(9)	168(11)	192(14)	-53(11)	40(10)	-13(9)
C11B	142(10)	152(11)	141(11)	-15(9)	34(9)	-12(8)
F1A	47(8)	27(7)	36(10)	-4(6)	0(6)	-1(5)
B1A	45(8)	35(8)	39(8)	5(5)	-3(6)	1(6)
F4A	46(10)	33(8)	47(11)	7(7)	-5(8)	-1(7)
F3A	68(8)	66(12)	61(9)	29(9)	-9(7)	6(8)
F2A	81(11)	43(7)	61(10)	-12(7)	13(8)	3(7)

Table 4 Bond Lengths for c221019_2_2.

Atom	Atom	Length/Å	Atom	Atom	Length/Å
Pd1	P1	2.2773(6)	C00W	C01E	1.525(4)
Pd1	P2	2.2776(6)	C00W	C01P	1.529(4)
Pd1	C45	2.014(3)	C36	C37	1.531(3)
Pd1	C1	2.057(2)	C36	C38	1.535(3)
Cu1	C9	1.917(2)	C30	C32	1.527(4)
Cu1	C1	2.028(2)	C30	C31	1.535(4)
Cu1	C2	2.074(2)	C33	C34	1.533(3)
P1	O1	1.6587(17)	C33	C35	1.529(3)
P1	C36	1.823(2)	C27	C28	1.379(4)
P1	C33	1.829(2)	C27	C26	1.379(4)
P2	O2	1.651(2)	C3	C8	1.380(4)
P2	C39	1.831(2)	C3	C4	1.389(4)
P2	C42	1.825(3)	C40	C39	1.536(4)
F4	B1	1.389(4)	C46	C47	1.390(4)
F1	B1	1.390(4)	C39	C41	1.525(3)
O1	C50	1.390(3)	C49	C48	1.387(4)
O2	C46	1.389(3)	C8	C7	1.401(4)
N1	C11	1.387(3)	C47	C48	1.386(5)
N1	C9	1.358(3)	C42	C44	1.531(5)
N1	C12	1.438(3)	C42	C43	1.537(4)

F3	B1	1.387(5)	C4	C5	1.389(4)
N2	C9	1.353(3)	C7	C6	1.356(6)
N2	C24	1.443(3)	C1A	C2A	1.492(5)
N2	C10	1.385(3)	C6	C5	1.348(6)
F2	B1	1.372(4)	C2A	C3A	1.541(5)
C45	C50	1.391(3)	C3A	C4A	1.492(5)
C45	C46	1.392(3)	O2A	C8A	1.433(8)
C11	C10	1.346(3)	O2A	C5A	1.416(7)
C24	C25	1.397(3)	O3A	C9A	1.428(10)
C24	C29	1.403(3)	O3A	C12A	1.413(8)
C12	C13	1.403(3)	C6A	C7A	1.587(9)
C12	C17	1.399(3)	C6A	C5A	1.459(9)
C1	C2	1.234(4)	C7A	C8A	1.505(10)
O1A	C1A	1.404(4)	C9A	C10A	1.485(10)
O1A	C4A	1.431(4)	C10A	C11A	1.570(9)
C13	C21	1.524(3)	C12A	C11A	1.492(10)
C13	C14	1.388(3)	C7B	C8B	1.481(13)
C2	C3	1.444(3)	C7B	C6B	1.541(14)
C25	C00W	1.515(3)	O2B	C8B	1.522(13)
C25	C26	1.405(3)	O2B	C5B	1.469(13)
C18	C17	1.513(3)	C5B	C6B	1.444(14)
C18	C20	1.540(4)	C9B	O3B	1.462(13)
C18	C19	1.529(3)	C9B	C10B	1.499(13)
C17	C16	1.397(3)	O3B	C12B	1.436(12)
C15	C16	1.383(4)	C12B	C11B	1.399(13)
C15	C14	1.388(4)	C10B	C11B	1.483(14)
C29	C30	1.525(4)	F1A	B1A	1.381(13)
C29	C28	1.397(3)	B1A	F4A	1.385(13)
C21	C23	1.532(3)	B1A	F3A	1.379(13)
C21	C22	1.537(3)	B1A	F2A	1.382(13)
C50	C49	1.387(3)			

Table 5 Bond Angles for c221019_2_2.

Atom	Atom	Atom	Angle/˚	Atom	Atom	Atom	Angle/˚
P1	Pd1	P2	158.84(2)	C49	C50	C45	122.7(2)
C45	Pd1	P1	79.56(7)	C25	C00W	C01E	111.0(2)
C45	Pd1	P2	79.65(7)	C25	C00W	C01P	111.6(2)
C45	Pd1	C1	168.79(10)	C01E	C00W	C01P	111.6(2)
C1	Pd1	P1	101.30(6)	C37	C36	P1	109.47(16)
C1	Pd1	P2	99.86(6)	C37	C36	C38	111.3(2)
C9	Cu1	C1	172.97(9)	C38	C36	P1	109.69(16)
C9	Cu1	C2	151.86(10)	C29	C30	C32	111.8(2)
C1	Cu1	C2	34.98(10)	C29	C30	C31	110.2(2)
O1	P1	Pd1	105.15(6)	C32	C30	C31	111.8(2)
O1	P1	C36	102.17(9)	C34	C33	P1	109.02(16)

O1	P1	C33	101.08(10)	C35	C33	P1	112.73(16)
C36	P1	Pd1	120.18(8)	C35	C33	C34	110.6(2)
C36	P1	C33	107.70(11)	C28	C27	C26	120.7(2)
C33	P1	Pd1	117.49(8)	C27	C28	C29	121.2(2)
O2	P2	Pd1	105.60(7)	C27	C26	C25	121.1(2)
O2	P2	C39	101.62(11)	C8	C3	C2	122.0(3)
O2	P2	C42	100.29(12)	C8	C3	C4	118.9(3)
C39	P2	Pd1	115.19(8)	C4	C3	C2	119.0(3)
C42	P2	Pd1	120.75(9)	O2	C46	C45	118.9(2)
C42	P2	C39	110.14(12)	O2	C46	C47	118.4(2)
C50	O1	P1	114.17(14)	C47	C46	C45	122.7(3)
C46	O2	P2	114.28(15)	C40	C39	P2	107.42(17)
C11	N1	C12	124.14(17)	C41	C39	P2	114.14(17)
C9	N1	C11	111.48(18)	C41	C39	C40	110.5(2)
C9	N1	C12	124.37(17)	C48	C49	C50	117.9(3)
C9	N2	C24	124.30(18)	C3	C8	C7	119.9(3)
C9	N2	C10	111.82(18)	C48	C47	C46	117.8(3)
C10	N2	C24	123.88(18)	C44	C42	P2	111.69(19)
C50	C45	Pd1	121.66(17)	C44	C42	C43	112.1(3)
C50	C45	C46	116.8(2)	C43	C42	P2	108.1(2)
C46	C45	Pd1	121.40(19)	C47	C48	C49	122.0(3)
C10	C11	N1	106.53(19)	F4	B1	F1	108.6(3)
N1	C9	Cu1	128.32(16)	F3	B1	F4	108.9(4)
N2	C9	Cu1	127.86(15)	F3	B1	F1	110.0(4)
N2	C9	N1	103.72(18)	F2	B1	F4	110.0(4)
C25	C24	N2	118.3(2)	F2	B1	F1	109.6(4)
C25	C24	C29	123.5(2)	F2	B1	F3	109.8(3)
C29	C24	N2	118.2(2)	C3	C4	C5	119.6(3)
C13	C12	N1	118.57(19)	C6	C7	C8	120.0(3)
C17	C12	N1	117.89(19)	O1A	C1A	C2A	107.8(3)
C17	C12	C13	123.5(2)	C5	C6	C7	120.6(3)
Cu1	C1	Pd1	132.20(12)	C1A	C2A	C3A	102.8(3)
C2	C1	Pd1	153.2(2)	C4A	C3A	C2A	101.2(3)
C2	C1	Cu1	74.55(16)	O1A	C4A	C3A	105.6(3)
C1A	O1A	C4A	109.7(3)	C6	C5	C4	120.9(4)
C12	C13	C21	121.9(2)	C5A	O2A	C8A	104.9(6)
C14	C13	C12	116.8(2)	C12A	O3A	C9A	103.3(6)
C14	C13	C21	121.4(2)	C5A	C6A	C7A	101.2(5)
C1	C2	Cu1	70.47(15)	C8A	C7A	C6A	104.6(5)
C1	C2	C3	169.8(2)	O2A	C8A	C7A	105.0(6)
C3	C2	Cu1	119.71(18)	O3A	C9A	C10A	108.5(7)
C24	C25	C00W	122.5(2)	C9A	C10A	C11A	102.3(6)
C24	C25	C26	116.7(2)	O2A	C5A	C6A	107.4(5)
C26	C25	C00W	120.8(2)	O3A	C12A	C11A	108.9(6)
C11	C10	N2	106.45(19)	C12A	C11A	C10A	103.2(6)
C17	C18	C20	110.6(2)	C8B	C7B	C6B	102.0(8)
C17	C18	C19	112.7(2)	C5B	O2B	C8B	97.4(10)

C19	C18	C20	109.9(2)	C7B	C8B	O2B	105.1(13)
C12	C17	C18	121.3(2)	C6B	C5B	O2B	113.1(10)
C16	C17	C12	116.8(2)	C5B	C6B	C7B	103.4(8)
C16	C17	C18	121.9(2)	O3B	C9B	C10B	99.0(14)
C16	C15	C14	120.0(2)	C12B	O3B	C9B	102.2(10)
C24	C29	C30	121.9(2)	C11B	C12B	O3B	111.1(12)
C28	C29	C24	116.9(2)	C11B	C10B	C9B	102.7(14)
C28	C29	C30	121.2(2)	C12B	C11B	C10B	103.0(14)
C13	C21	C23	110.9(2)	F1A	B1A	F4A	109.0(12)
C13	C21	C22	111.6(2)	F1A	B1A	F2A	109.4(12)
C23	C21	C22	111.2(2)	F3A	B1A	F1A	110.5(12)
C15	C16	C17	121.3(2)	F3A	B1A	F4A	109.8(12)
C13	C14	C15	121.6(2)	F3A	B1A	F2A	108.5(12)
O1	C50	C45	118.4(2)	F2A	B1A	F4A	109.5(13)
C49	C50	O1	118.8(2)				

Table 6 Torsion Angles for c221019_2_2.

A	B	C	D	Angle/°	A	B	C	D	Angle/°
Pd1	P1	O1	C50	10.62(16)	C25	C24	C29	C30	179.9(2)
Pd1	P1	C36	C37	40.50(19)	C25	C24	C29	C28	1.9(4)
Pd1	P1	C36	C38	-81.88(17)	C10	N2	C9	Cu1	-176.09(16)
Pd1	P1	C33	C34	-49.41(19)	C10	N2	C9	N1	0.5(2)
Pd1	P1	C33	C35	-172.69(15)	C10	N2	C24	C25	95.7(3)
Pd1	P2	O2	C46	-4.53(18)	C10	N2	C24	C29	-83.0(3)
Pd1	P2	C39	C40	55.03(19)	C18	C17	C16	C15	-179.2(2)
Pd1	P2	C39	C41	177.89(18)	C17	C12	C13	C21	177.0(2)
Pd1	P2	C42	C44	80.6(2)	C17	C12	C13	C14	-2.9(3)
Pd1	P2	C42	C43	-43.3(2)	C29	C24	C25	C00W	178.5(2)
Pd1	C45	C50	O1	-0.2(3)	C29	C24	C25	C26	-1.8(3)
Pd1	C45	C50	C49	178.4(2)	C21	C13	C14	C15	-178.7(2)
Pd1	C45	C46	O2	0.6(3)	C16	C15	C14	C13	0.8(4)
Pd1	C45	C46	C47	-178.2(2)	C14	C13	C21	C23	-78.0(3)
Pd1	C1	C2	Cu1	178.8(4)	C14	C13	C21	C22	46.6(3)
Pd1	C1	C2	C3	3.4(17)	C14	C15	C16	C17	-1.3(4)
Cu1	C1	C2	C3	-175.3(14)	C50	C45	C46	O2	176.6(2)
Cu1	C2	C3	C8	67.4(3)	C50	C45	C46	C47	-2.2(4)
Cu1	C2	C3	C4	-113.4(3)	C50	C49	C48	C47	-0.9(5)
P1	O1	C50	C45	-7.7(3)	C00W	C25	C26	C27	-179.6(2)
P1	O1	C50	C49	173.6(2)	C36	P1	O1	C50	136.86(16)
P2	O2	C46	C45	3.0(3)	C36	P1	C33	C34	171.04(16)
P2	O2	C46	C47	-178.1(2)	C36	P1	C33	C35	47.8(2)
O1	P1	C36	C37	-75.27(17)	C30	C29	C28	C27	-178.8(2)
O1	P1	C36	C38	162.35(16)	C33	P1	O1	C50	-112.08(16)
O1	P1	C33	C34	64.30(17)	C33	P1	C36	C37	178.75(16)
O1	P1	C33	C35	-58.98(19)	C33	P1	C36	C38	56.38(19)

O1	C50	C49	C48	177.7(3)	C28	C29	C30	C32	-49.9(3)
O2	P2	C39	C40	-58.56(18)	C28	C29	C30	C31	75.1(3)
O2	P2	C39	C41	64.3(2)	C28	C27	C26	C25	0.3(4)
O2	P2	C42	C44	-164.2(2)	C26	C25	C00W	C01E	-64.2(3)
O2	P2	C42	C43	72.0(2)	C26	C25	C00W	C01P	60.9(3)
O2	C46	C47	C48	-178.3(3)	C26	C27	C28	C29	-0.2(4)
N1	C11	C10	N2	-0.3(2)	C3	C8	C7	C6	0.2(5)
N1	C12	C13	C21	-0.8(3)	C3	C4	C5	C6	-0.9(7)
N1	C12	C13	C14	179.21(19)	C46	C45	C50	O1	-176.2(2)
N1	C12	C17	C18	-0.8(3)	C46	C45	C50	C49	2.4(4)
N1	C12	C17	C16	-179.65(18)	C46	C47	C48	C49	1.1(5)
N2	C24	C25	C00W	-0.2(3)	C20	C18	C17	C12	-96.2(3)
N2	C24	C25	C26	179.6(2)	C20	C18	C17	C16	82.7(3)
N2	C24	C29	C30	-1.5(3)	C39	P2	O2	C46	116.04(18)
N2	C24	C29	C28	-179.5(2)	C39	P2	C42	C44	-57.7(2)
C45	C50	C49	C48	-0.9(4)	C39	P2	C42	C43	178.5(2)
C45	C46	C47	C48	0.5(5)	C19	C18	C17	C12	140.4(2)
C11	N1	C9	Cu1	175.88(15)	C19	C18	C17	C16	-40.8(3)
C11	N1	C9	N2	-0.7(2)	C8	C3	C4	C5	1.5(5)
C11	N1	C12	C13	89.2(3)	C8	C7	C6	C5	0.4(6)
C11	N1	C12	C17	-88.8(3)	C42	P2	O2	C46	-130.71(18)
C9	N1	C11	C10	0.6(2)	C42	P2	C39	C40	-164.21(18)
C9	N1	C12	C13	-91.5(3)	C42	P2	C39	C41	-41.4(2)
C9	N1	C12	C17	90.5(2)	C4	C3	C8	C7	-1.2(4)
C9	N2	C24	C25	-84.8(3)	C7	C6	C5	C4	-0.1(7)
C9	N2	C24	C29	96.5(3)	C1A	O1A	C4A	C3A	-22.6(5)
C9	N2	C10	C11	-0.1(3)	C1A	C2A	C3A	C4A	-33.4(4)
C24	N2	C9	Cu1	4.4(3)	C2A	C3A	C4A	O1A	34.4(4)
C24	N2	C9	N1	-179.06(19)	C4A	O1A	C1A	C2A	0.2(5)
C24	N2	C10	C11	179.4(2)	O3A	C9A	C10A	C11A	-25.1(10)
C24	C25	C00W	C01E	115.5(2)	O3A	C12A	C11A	C10A	19.2(10)
C24	C25	C00W	C01P	-119.4(3)	C6A	C7A	C8A	O2A	16.3(9)
C24	C25	C26	C27	0.6(4)	C7A	C6A	C5A	O2A	-30.7(8)
C24	C29	C30	C32	132.2(2)	C8A	O2A	C5A	C6A	43.3(8)
C24	C29	C30	C31	-102.8(3)	C9A	O3A	C12A	C11A	-35.0(9)
C24	C29	C28	C27	-0.8(4)	C9A	C10A	C11A	C12A	3.6(10)
C12	N1	C11	C10	-179.98(19)	C5A	O2A	C8A	C7A	-35.9(9)
C12	N1	C9	Cu1	-3.5(3)	C5A	C6A	C7A	C8A	8.2(8)
C12	N1	C9	N2	179.93(18)	C12A	O3A	C9A	C10A	37.7(9)
C12	C13	C21	C23	102.1(2)	O2B	C5B	C6B	C7B	-5(2)
C12	C13	C21	C22	-133.4(2)	C8B	C7B	C6B	C5B	-22(2)
C12	C13	C14	C15	1.2(3)	C8B	O2B	C5B	C6B	29(2)
C12	C17	C16	C15	-0.3(3)	C5B	O2B	C8B	C7B	-42(2)
C1	C2	C3	C8	-117.7(14)	C6B	C7B	C8B	O2B	41(2)
C1	C2	C3	C4	61.5(15)	C9B	O3B	C12B	C11B	-25(2)
O1A	C1A	C2A	C3A	21.3(5)	C9B	C10B	C11B	C12B	31(2)
C13	C12	C17	C18	-178.6(2)	O3B	C9B	C10B	C11B	-45(2)

C13	C12	C17	C16	2.5(3)	O3B	C12B	C11B	C10B	-4(2)
C2	C3	C8	C7	178.0(3)	C10B	C9B	O3B	C12B	42(2)
C2	C3	C4	C5	-177.7(3)					

Table 7 Hydrogen Atom Coordinates (Å×10^4) and Isotropic Displacement Parameters (Å^2×10^3) for c221019_2_2.

Atom	*x*	*y*	*z*	U(eq)
H11	5430.69	6895.99	5278.76	32
H10	6813.54	6156.4	5430.98	33
H18	4186.31	6260.52	4342.69	38
H15	3266.31	8271.77	3399.44	44
H21	6804.23	7708.75	4538.89	39
H16	2715.18	7336.47	3550.68	40
H14	4934.73	8567.03	3720.14	41
H00W	5929.16	5353.56	4303.86	41
H36	6206.44	8171.54	1331.16	35
H30	8530.42	6750.74	4791.61	45
H33	4652.32	7704.91	2503.5	37
H37A	7530.96	7179.36	1315.63	53
H37B	7837.2	7777.58	1043.95	53
H37C	6919.8	7409.39	756.7	53
H38A	6409.37	8157.39	2359.94	54
H38B	7547.15	8195.96	2075.89	54
H38C	7132.13	7606.85	2323.14	54
H27	9963.99	4711.31	4150.89	49
H28	10402.69	5635.98	4418.85	47
H26	8205.44	4435.38	4058.43	44
H40A	3445.78	5807.86	2171.49	59
H40B	2872.4	5276.51	2456.04	59
H40C	2940.12	5330.28	1767.55	59
H23A	7063.06	8346.68	3486.02	56
H23B	7369.69	7695.57	3558.14	56
H23C	8005.7	8168.54	3908.34	56
H34A	2981.86	7370.6	1723.37	54
H34B	2805.78	7555.17	2381.15	54
H34C	3425.58	6985.52	2238.2	54
H20A	3508.3	6242.51	3145.77	64
H20B	3661.41	5684.14	3526.26	64
H20C	4652.19	6068.08	3371.18	64
H35A	4814.96	8546.34	1947.99	57
H35B	3649.16	8507.88	2195.65	57
H35C	3870.33	8353.14	1534.13	57
H39	4696.4	5115.35	2535.59	41
H49	3463.75	7260.17	51.71	56
H01A	6554.22	4531.16	3456.57	62

H01B	6238.84	5170.03	3314	62
H01C	5371.73	4738.13	3543.19	62
H19A	2468.05	6588.23	4585.19	68
H19B	2402.91	5973.99	4299.73	68
H19C	2103.41	6519.34	3925.38	68
H22A	7141.97	8664.06	4782.86	67
H22B	5945.08	8528.1	4931.29	67
H22C	6225.12	8875.21	4359.33	67
H32A	9721.8	6389.49	5495.73	67
H32B	10150.02	6978.84	5256.05	67
H32C	10651.89	6399.42	5035.31	67
H8	8864.14	5526.57	3025.53	58
H31A	10180.31	6698.49	3945.02	69
H31B	9766.58	7276.22	4219.44	69
H31C	9006.6	6905.01	3818.37	69
H47	3384.34	5521.68	68.05	65
H41A	3883.36	4379.96	1643.75	68
H41B	3694.05	4285.2	2320.1	68
H41C	4849.12	4228.68	2061.2	68
H42	6091.63	4587.01	1262.42	51
H44A	7603.06	4537.85	1886.75	79
H44B	6558.62	4583.06	2262.93	79
H44C	7284.91	5126.51	2175.52	79
H48	2889.01	6394.38	-349.14	71
H01D	5353.44	4447.78	4606.18	79
H01E	6258.58	4664.07	5034.62	79
H01F	6517.64	4203.37	4550.37	79
H43A	7381.68	5585.25	1140.36	79
H43B	6643.2	5342.29	636.45	79
H43C	7637.59	4986.92	853.39	79
H4	9143.64	7037.94	2187.25	70
H7	10723.87	5474.03	3096.35	77
H1AA	9361.09	3431.06	1531.65	82
H1AB	9113.41	2831.53	1824.87	82
H6	11754.61	6189.38	2708.94	84
H2AA	10730.16	3596.2	2127.67	82
H2AB	10722.08	2920.71	2215.04	82
H3AA	9751.17	2983.31	3075.54	82
H3AB	10417.7	3560.95	3128.88	82
H4AA	8404.91	3631.18	3105.29	82
H4AB	9070.46	4099.24	2762.1	82
H5	10986.82	6960.02	2260.46	95
H6AA	9164.42	5230.78	8011.43	75
H6AB	10218.06	5462.41	8322.31	75
H7AA	9158.53	5857.61	9038.01	87
H7AB	8135.83	5545	8780	87
H8AA	9080.81	5223.27	9762.78	95

H8AB	8305.5	4817	9400.81	95
H9AA	1047.61	1251.7	4699.52	89
H9AB	1506.8	1882.57	4708.66	89
H10A	274.57	1542.43	3875.76	83
H10B	300.98	2197.12	4067.92	83
H5AA	9244.64	4396.91	8470.05	78
H5AB	10479.02	4528.59	8441.13	78
H12A	-1285.9	1813.05	5342.68	94
H12B	-874.48	1198.09	5162.15	94
H11A	-1387.63	2102.89	4421.32	91
H11B	-1382.89	1438.86	4268.28	91
H7BA	8688.06	5455.61	8429.41	234
H7BB	8791.16	4799.08	8607.57	234
H8BA	8859.5	5009.08	9583.05	214
H8BB	7984.96	5445.11	9350.37	214
H5BA	10878.16	5937.44	9093.76	211
H5BB	10843.48	5401.55	9513.78	211
H6BA	10579.22	4872.95	8770.08	227
H6BB	10497.31	5418.98	8356	227
H9BA	-220.04	2043.74	3898.94	199
H9BB	-1095.28	2045.22	4402.14	199
H12C	1585.82	1470.31	4233.14	163
H12D	1271.67	1075.26	4766.82	163
H10C	-1107.27	1048.7	4444.59	199
H10D	-1121.02	1178.54	3759.63	199
H11C	373.67	569.02	4195.95	174
H11D	624.33	991.4	3667.64	174

Table 8 Atomic Occupancy for c221019_2_2.

Atom	*Occupancy*	Atom	*Occupancy*	Atom	*Occupancy*
F4	0.850(16)	F1	0.850(16)	F3	0.850(16)
F2	0.850(16)	B1	0.850(16)	O2A	0.535(4)
O3A	0.535(4)	C6A	0.535(4)	H6AA	0.535(4)
H6AB	0.535(4)	C7A	0.535(4)	H7AA	0.535(4)
H7AB	0.535(4)	C8A	0.535(4)	H8AA	0.535(4)
H8AB	0.535(4)	C9A	0.535(4)	H9AA	0.535(4)
H9AB	0.535(4)	C10A	0.535(4)	H10A	0.535(4)
H10B	0.535(4)	C5A	0.535(4)	H5AA	0.535(4)
H5AB	0.535(4)	C12A	0.535(4)	H12A	0.535(4)
H12B	0.535(4)	C11A	0.535(4)	H11A	0.535(4)
H11B	0.535(4)	C7B	0.465(4)	H7BA	0.465(4)
H7BB	0.465(4)	O2B	0.465(4)	C8B	0.465(4)
H8BA	0.465(4)	H8BB	0.465(4)	C5B	0.465(4)
H5BA	0.465(4)	H5BB	0.465(4)	C6B	0.465(4)
H6BA	0.465(4)	H6BB	0.465(4)	C9B	0.465(4)

H9BA	0.465(4)	H9BB	0.465(4)	O3B	0.465(4)
C12B	0.465(4)	H12C	0.465(4)	H12D	0.465(4)
C10B	0.465(4)	H10C	0.465(4)	H10D	0.465(4)
C11B	0.465(4)	H11C	0.465(4)	H11D	0.465(4)
F1A	0.150(16)	B1A	0.150(16)	F4A	0.150(16)
F3A	0.150(16)	F2A	0.150(16)		

3.3.2. Crystal structure for [($^{i\text{Pr}}$POCOP)Pd$^{\text{II}}$(CCPh)•Cu$^{\text{I}}$(IPr)]BArF, [**1**]BArF$_4$:

Crystal Data for $C_{85}H_{84}BCuF_{24}N_2O_2P_2Pd$ (*M* =1864.23 g/mol): triclinic, space group P-1 (no. 2), *a* = 15.71856(6) Å, *b* = 16.47461(7) Å, *c* = 18.04887(8) Å, *α* = 105.5135(4)°, *β* = 107.5009(4)°, *γ* = 97.1043(3)°, *V* = 4187.85(3) Å^3, *Z* = 2, *T* = 100.0(1) K, μ(CuKα) = 3.299 mm^{-1}, *Dcalc* = 1.478 g/cm^3, 165102 reflections measured (5.71° ≤ 2Θ ≤ 159.234°), 17788 unique (R_{int} = 0.0334, R_{sigma} = 0.0168) which were used in all calculations. The final R_1 was 0.0267 (I > 2σ(I)) and wR_2 was 0.0698 (all data).

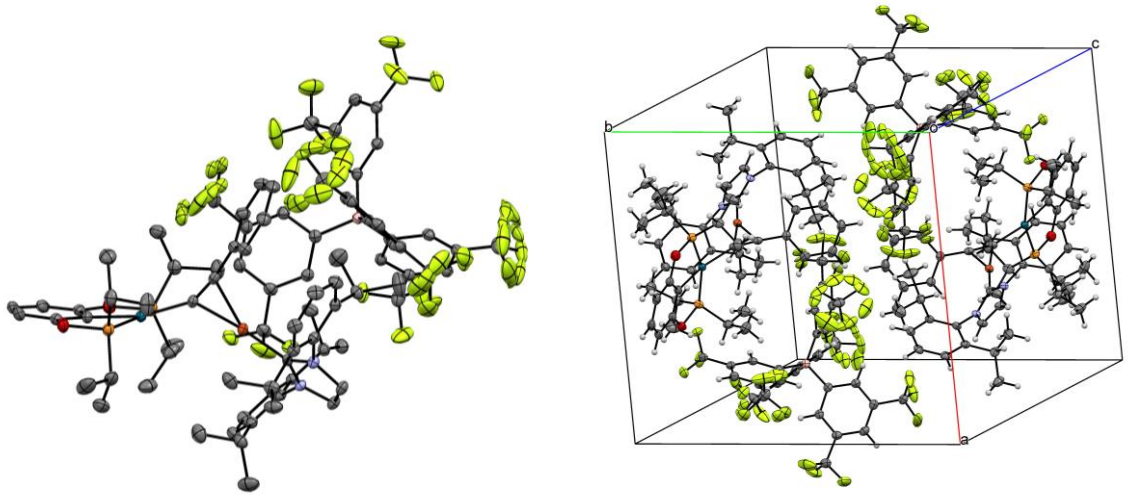

Figure SI-90: Representation of crystal structure from different perspectives. Color-code: grey/carbon, red/oxygen, light-orange/phosphorus, dark-orange/Cu, yellow/fluorine, pink/boron, blue/nitrogen, teal/palladium. Left) XRD structure (ORTEP 50% probability ellipsoids), hydrogens and co-crystallizing molecules omitted for clearity. Right) representation of the unit cell, crystal packing.

Table 1 Crystal data and structure refinement for c020717_4_2.

Identification code	c020717_4_2
Empirical formula	$C_{85}H_{84}BCuF_{24}N_2O_2P_2Pd$
Formula weight	1864.23
Temperature/K	100.0(1)
Crystal system	triclinic
Space group	P-1
a/Å	15.71856(6)
b/Å	16.47461(7)
c/Å	18.04887(8)
α/°	105.5135(4)
β/°	107.5009(4)
γ/°	97.1043(3)
Volume/Å^3	4187.85(3)
Z	2
ρ_{calc}g/cm^3	1.478
μ/mm^{-1}	3.299
F(000)	1900.0
Crystal size/mm^3	0.191 × 0.122 × 0.038
Radiation	CuKα (λ = 1.54184)
2Θ range for data collection/°	5.71 to 159.234
Index ranges	-19 ≤ h ≤ 19, -20 ≤ k ≤ 20, -23 ≤ l ≤ 22
Reflections collected	165102

Independent reflections	17788 [R_{int} = 0.0334, R_{sigma} = 0.0168]
Data/restraints/parameters	17788/945/1280
Goodness-of-fit on F^2	1.071
Final R indexes [I>=2σ (I)]	R_1 = 0.0267, wR_2 = 0.0692
Final R indexes [all data]	R_1 = 0.0279, wR_2 = 0.0698
Largest diff. peak/hole / e $Å^{-3}$	0.69/-0.50

Table 2 Fractional Atomic Coordinates (×10^4) and Equivalent Isotropic Displacement Parameters ($Å^2$×10^3) for c020717_4_2. U_{eq} is defined as 1/3 of of the trace of the orthogonalised U_{IJ} tensor.

Atom	*x*	*y*	*z*	U(eq)
Pd1	5620.1(2)	2485.4(2)	9788.0(2)	17.02(4)
Cu1	6601.1(2)	2889.6(2)	8226.9(2)	16.82(5)
P1	6873.4(3)	2873.3(3)	10953.9(2)	21.45(8)
P2	4177.7(3)	1803.5(3)	8894.3(2)	20.77(8)
F1A	1084.9(7)	-611.3(7)	5569.1(7)	35.7(2)
F19A	-1177.5(7)	-707.9(7)	2223.7(7)	35.6(2)
F2A	1191.4(9)	-693.5(7)	4396.3(8)	45.6(3)
O2	3623.8(8)	1496.6(8)	9450.8(7)	25.4(2)
F4A	105(6)	2944(5)	6610(7)	31.3(8)
F3A	2364.1(7)	-119.1(8)	5490.5(10)	53.6(4)
F7A	-277.1(11)	4989.7(8)	2919.6(7)	52.2(3)
O1	6488.4(8)	2687.3(8)	11661.9(7)	26.0(2)
F20A	-302(1)	-1152.8(7)	1571.3(10)	55.4(4)
F10A	-2839.6(8)	3159.3(9)	3977.9(10)	56.5(4)
F8A	514.0(9)	5588.3(8)	4170.6(9)	57.9(4)
N2	7767.6(8)	2884.9(8)	7205.4(8)	17.2(2)
F13A	4175(7)	2216(4)	3545(7)	26.1(17)
F21A	-1496.2(10)	-756.2(9)	970.8(8)	61.6(4)
F9A	-918.9(11)	5486.0(9)	3761.3(12)	72.2(5)
F14A	4013(8)	3341(6)	3182(5)	32.3(17)
F16B	2924(8)	5134(9)	6438(11)	44(3)
N1	6753.5(8)	1710.6(8)	6754.5(8)	16.8(2)
F11A	-2688.1(9)	1932.0(9)	3366.9(10)	58.2(4)
F12A	-2116.3(9)	2432.1(13)	4664.7(10)	74.1(5)
C18	7064.4(10)	2482.8(9)	7362.8(9)	16.3(3)
F15A	5076(6)	3433(8)	4307(7)	49(2)
C7	6249.4(10)	3867.9(10)	9001.6(9)	19.3(3)
C1	6088.4(10)	3189.5(10)	9145.4(9)	18.4(3)
F5A	131(3)	1863(3)	7012(3)	41.6(9)
C25	8279.6(10)	3763.3(10)	7651.2(9)	18.4(3)
C10A	175.4(10)	2933.8(10)	3955.7(9)	19.2(3)
C31	9059.1(10)	3915(1)	8343.3(10)	20.5(3)
F17B	3783(6)	4309(8)	6827(8)	43(2)
C27	6047.7(10)	1024.0(9)	6698.3(9)	17.3(3)

C18A	-415.5(11)	4206.5(10)	3803.3(10)	21.6(3)
F6A	1396(4)	2790(5)	7389(5)	75(3)
C13A	282.0(11)	3751.4(10)	3860.7(9)	20.3(3)
C8	4151.2(11)	1673.5(10)	10266.0(11)	23.0(3)
C6A	963.2(10)	1857(1)	4676.6(10)	19.7(3)
C19	6396.0(11)	4730.6(10)	8936.8(10)	20.6(3)
C36	9534.2(11)	4772.9(11)	8752.3(11)	24.7(3)
C33	6303.4(10)	485.2(10)	7169.3(9)	19.7(3)
C2	5075.7(11)	2070.1(10)	10535(1)	21.2(3)
C20A	3542.8(11)	3256.3(11)	4288.4(10)	23.5(3)
C26	7888.2(10)	2371.3(11)	6514.8(10)	21.8(3)
C11A	1992.4(10)	2932.5(10)	4313.2(10)	20.0(3)
C34	5157.9(10)	901.1(10)	6145.9(9)	18.7(3)
C32	7982.8(10)	4416.1(10)	7346.8(10)	20.5(3)
C28	7253.6(10)	1629.9(10)	6233.3(10)	21.1(3)
C42	4512.5(10)	200.4(10)	6080.6(10)	22.6(3)
C21A	3205.0(11)	4080.0(11)	5420.2(10)	23.1(3)
C3A	1230.9(10)	691.7(11)	5257.8(10)	22.1(3)
C23A	525.0(11)	1439.7(10)	1615.7(10)	22.1(3)
C22A	-247(1)	333(1)	1950.4(10)	21.3(3)
C43	4908.1(10)	1501(1)	5640.4(10)	21.1(3)
C22	7281.3(11)	5215.9(11)	9167.1(10)	23.9(3)
C15A	2646.6(11)	2761.6(10)	3946.4(10)	21.8(3)
C16A	68.1(10)	853.7(10)	2770.2(10)	20.0(3)
C4A	1198.8(10)	1057.8(10)	4639.6(10)	20.3(3)
C17A	828.6(11)	1961.6(10)	2432.5(10)	20.9(3)
C24A	-273.2(11)	5065.9(11)	3671.3(10)	24.9(3)
C12A	626.9(10)	1682.7(10)	3042.7(10)	19.3(3)
C44	9253.7(11)	5434.6(11)	8474.5(11)	27.3(4)
C49	4740.9(11)	-344.8(11)	6541.4(11)	25.6(3)
C30A	-14.1(11)	616.1(10)	1363.9(10)	21.6(3)
C37	9379.2(11)	3186.9(11)	8642.8(10)	24.9(3)
C2A	1462.0(11)	-175.8(12)	5178.7(12)	27.4(4)
C14A	-679.7(11)	2595.4(10)	3977.3(10)	21.2(3)
C40	5623.7(11)	-198.2(11)	7083(1)	24.2(3)
C19A	-1365.5(11)	3051.8(11)	3936.9(10)	23.2(3)
F18B	4291(5)	5304(6)	6423(8)	51(2)
C9	5568.1(11)	2274.5(11)	11366.7(11)	23.6(3)
C27A	3831.7(11)	3918.2(11)	5026.1(10)	24.6(3)
C38	8490.2(11)	5258.8(11)	7776.3(11)	25.0(3)
C25A	-1245.8(11)	3865.5(11)	3847.8(10)	24.1(3)
C1A	2306.1(11)	3610.8(11)	5063.1(10)	22.4(3)
C5	3399.7(11)	2384.1(12)	8390.3(11)	26.6(3)
C52	4046.6(12)	1088.7(11)	4880(1)	26.9(3)
C20	3727.4(12)	1473.2(11)	10788.9(12)	27.8(4)
C8A	795.9(11)	2276.2(11)	5387.6(10)	22.2(3)
C39	7135.1(11)	4235.4(11)	6591.3(10)	23.8(3)

C45	8982.7(12)	3054.7(13)	9290.8(12)	33.3(4)
C24	4248.9(13)	1711.8(12)	11614.9(12)	30.7(4)
C3	7486.7(11)	3996.3(12)	11468.9(10)	27.8(4)
C35	6668.9(14)	6382.8(11)	8809.6(12)	31.6(4)
C7A	850.6(11)	1925.3(11)	6016.3(10)	25.3(3)
C5A	1061.5(11)	1122.5(12)	5955.1(10)	25.6(3)
C4	7718.5(12)	2201.3(13)	10945.2(11)	32.1(4)
C31A	-805.0(13)	-564.3(12)	1683.2(11)	30.7(4)
C29	7414.3(12)	6043.0(11)	9107.1(11)	28.4(4)
C29A	3528.7(12)	4731.1(12)	6257.1(12)	32.4(4)
C21	5170.5(13)	2113.7(12)	11919.9(11)	28.6(4)
C41	7279.1(11)	600.0(11)	7732.5(10)	25.2(3)
C10	8131.6(13)	4266.7(15)	11045.5(12)	40.8(5)
C30	5789.5(13)	5904.0(12)	8578.6(12)	32.6(4)
C23	5646.4(12)	5083.1(11)	8642.5(11)	27.5(4)
C6	4090.6(12)	771.7(12)	8144.8(12)	31.3(4)
C14	3621.3(13)	2518.3(14)	7656.8(12)	36.5(4)
C11	6795.6(14)	4569.4(12)	11498.2(13)	35.8(4)
C26A	-2245.3(12)	2651.9(12)	3993.6(12)	30.5(4)
C32A	789.0(14)	1760.2(12)	996.8(11)	33.5(4)
C16	4627.2(14)	231.2(12)	8599.2(14)	38.5(4)
C28A	4194.2(12)	3069.6(12)	3838.0(12)	32.0(4)
C50	7330.6(14)	764.6(14)	8623.0(11)	37.2(4)
F22A	786(6)	2571(2)	1088(4)	55.1(14)
C51	7666.1(13)	-186.0(14)	7442.3(14)	41.9(5)
C53	4786.3(13)	2354.0(12)	6152.1(11)	32.7(4)
C46	10425.0(12)	3341.1(12)	8986.3(12)	32.4(4)
C47	7335.8(15)	4600.0(16)	5952.1(13)	46.9(5)
F23A	227(4)	1325(4)	212(2)	51.8(13)
C15	3450.1(14)	3238.5(13)	9015.5(13)	36.3(4)
C9A	686.1(13)	2428.9(13)	6764.0(11)	34.5(4)
C48	6375.2(13)	4591.2(16)	6836.7(13)	42.2(5)
B1A	946.2(12)	2342.1(11)	3985.5(11)	19.1(3)
C12	8502.5(15)	2452.6(18)	11767.1(13)	50.5(6)
C13	7230.8(16)	1249.6(14)	10674.4(13)	42.3(5)
C17	3100.0(14)	285.7(14)	7647.8(15)	45.9(5)
F24A	1622(4)	1666(6)	1008(5)	77.4(18)
F22B	1575(6)	2370(6)	1335(5)	73(3)
F23B	178(6)	2209(9)	689(7)	93(2)
F24B	859(10)	1193(3)	409(5)	72(3)
F22C	1303(10)	1269(9)	702(10)	35(3)
F23C	55(7)	1652(11)	350(7)	40(3)
F24C	1229(11)	2537(6)	1274(9)	35(3)
F17C	3020(11)	4546(11)	6700(8)	94(5)
F18C	4366(6)	4898(10)	6693(8)	65(4)
F16C	3318(13)	5499(7)	6180(7)	72(3)
F17A	4051(5)	4453(6)	6823(6)	47.4(18)

F18A	4016(4)	5481(4)	6300(6)	60(2)
F16A	2845(5)	4944(6)	6515(7)	31.3(14)
F5C	-3(7)	2743(9)	6692(9)	41.6(9)
F6C	933(8)	2113(7)	7382(6)	35(2)
F4C	1421(7)	3219(7)	7125(8)	31.3(8)
F4B	1454(6)	3071(6)	7292(6)	41(2)
F5B	65(9)	2893(9)	6582(11)	41.6(9)
F6B	496(4)	1979(4)	7195(4)	30.3(13)
F13C	4450(12)	2342(7)	3728(14)	45(4)
F14C	3762(12)	3115(12)	3056(9)	39(4)
F15C	4936(9)	3736(8)	4115(10)	63(4)
F13B	5053(9)	3239(12)	4371(11)	58(4)
F14B	3980(11)	2215(6)	3423(10)	34(3)
F15B	4202(13)	3485(11)	3306(9)	54(4)

Table 3 Anisotropic Displacement Parameters ($Å^2×10^3$) for c020717_4_2. The Anisotropic displacement factor exponent takes the form: $-2\pi^2[h^2a^{*2}U_{11}+2hka^*b^*U_{12}+...]$.

Atom	U_{11}	U_{22}	U_{33}	U_{23}	U_{13}	U_{12}
Pd1	17.66(6)	19.20(6)	16.09(6)	6.93(4)	7.40(4)	4.20(4)
Cu1	17.39(10)	17.54(11)	14.82(11)	3.91(9)	6.34(8)	2.39(8)
P1	20.60(18)	28.6(2)	17.18(19)	9.14(16)	6.94(15)	7.79(16)
P2	18.90(18)	21.74(19)	20.94(19)	5.46(16)	8.00(15)	2.40(15)
F1A	37.8(6)	32.3(6)	52.4(7)	25.6(5)	25.2(5)	11.2(5)
F19A	38.0(6)	34.0(6)	31.4(6)	8.6(5)	14.9(5)	-7.4(5)
F2A	72.4(8)	32.5(6)	45.2(7)	16.1(5)	30.0(6)	26.6(6)
O2	22.3(5)	28.0(6)	28.8(6)	11.6(5)	11.8(5)	3.4(5)
F4A	39.7(18)	34.5(16)	26.2(18)	9.6(14)	18.6(15)	13.9(13)
F3A	21.1(5)	49.3(7)	104.4(11)	44.9(8)	20.3(6)	16.9(5)
F7A	95.7(10)	31.3(6)	30.1(6)	13.8(5)	23.0(7)	5.3(6)
O1	28.9(6)	33.3(6)	19.5(6)	12.1(5)	9.6(5)	8.8(5)
F20A	74.2(9)	20.0(5)	81.6(10)	6.6(6)	51.2(8)	5.2(6)
F10A	33.5(6)	50.1(8)	100.3(12)	27.4(8)	37.7(7)	17.3(6)
F8A	59.1(8)	28.0(6)	55.8(8)	17.9(6)	-18.9(6)	-10.2(5)
N2	15.3(6)	18.2(6)	15.3(6)	3.3(5)	4.6(5)	1.0(5)
F13A	13(5)	36.1(18)	42(4)	22.2(18)	15(3)	18.2(18)
F21A	58.9(8)	64.5(9)	29.0(6)	12.1(6)	-7.4(6)	-36.1(7)
F9A	77.7(10)	46.3(8)	151.3(16)	60.8(10)	83.7(11)	45.4(7)
F14A	38(5)	29(4)	48(3)	25(3)	31(3)	6(3)
F16B	37(4)	34(6)	43(5)	-5(3)	0(3)	18(4)
N1	16.5(6)	16.2(6)	15.6(6)	2.9(5)	5.0(5)	2.6(5)
F11A	41.4(7)	43.4(7)	76.7(10)	0.5(7)	27.4(7)	-11.4(6)
F12A	38.1(7)	142.7(16)	70.1(10)	74.6(11)	26.0(7)	13.5(8)
C18	15.9(6)	17.2(7)	13.8(7)	4.7(6)	3.0(5)	2.8(5)
F15A	22(2)	70(5)	45(3)	1(3)	16.4(17)	-4(3)
C7	17.9(7)	23.5(8)	16.4(7)	4.1(6)	7.6(6)	5.4(6)

C1	18.3(7)	22.7(8)	14.7(7)	5.4(6)	7.3(6)	4.2(6)
F5A	48(2)	58.1(19)	41(2)	26.9(17)	32.4(18)	24.4(17)
C25	16.6(7)	18.4(7)	18.4(7)	2.9(6)	7.7(6)	0.5(6)
C10A	20.7(7)	21.0(7)	14.4(7)	4.5(6)	4.8(6)	5.3(6)
C31	18.0(7)	20.8(8)	20.2(8)	3.9(6)	6.3(6)	2.0(6)
F17B	57(6)	44(3)	21(2)	9(2)	1(4)	19(4)
C27	16.9(7)	16.1(7)	17.4(7)	2.9(6)	6.5(6)	2.4(5)
C18A	25.8(8)	20.2(8)	17.2(7)	4.3(6)	6.4(6)	6.8(6)
F6A	31.2(19)	139(7)	27(2)	-15(4)	6.2(16)	21(3)
C13A	21.1(7)	21.7(8)	17.9(7)	5.1(6)	7.3(6)	5.3(6)
C8	27.9(8)	20.5(8)	29.1(9)	12.6(7)	15.8(7)	9.9(6)
C6A	15.6(7)	22.2(8)	19.4(8)	6.7(6)	4.2(6)	2.6(6)
C19	25.3(8)	19.1(7)	18.6(8)	6.0(6)	9.0(6)	6.0(6)
C36	18.2(7)	24.0(8)	24.3(8)	2.8(7)	2.9(6)	0.3(6)
C33	21.6(7)	18.8(7)	17.9(7)	4.1(6)	6.9(6)	6.3(6)
C2	27.1(8)	21.4(8)	22.9(8)	11.2(6)	14.6(7)	9.3(6)
C20A	20.7(7)	26.9(8)	26.2(8)	12.8(7)	8.3(6)	7.1(6)
C26	19.3(7)	25.9(8)	19.2(8)	3.6(6)	9.6(6)	3.2(6)
C11A	20.8(7)	19.7(7)	19.8(8)	8.7(6)	5.1(6)	5.6(6)
C34	18.7(7)	18.1(7)	17.9(7)	3.7(6)	6.3(6)	4.2(6)
C32	18.6(7)	23.0(8)	20.5(8)	7.5(6)	8.1(6)	2.7(6)
C28	19.8(7)	23.4(8)	17.6(7)	1.7(6)	7.9(6)	3.6(6)
C42	17.4(7)	22.9(8)	22.7(8)	4.6(7)	3.9(6)	1.7(6)
C21A	22.6(7)	22.3(8)	22.3(8)	8.7(6)	3.4(6)	5.2(6)
C3A	15.9(7)	25.2(8)	27.0(8)	11.7(7)	6.5(6)	5.5(6)
C23A	26.3(8)	22.3(8)	20.9(8)	10.1(6)	8.6(6)	8.7(6)
C22A	19.0(7)	22.4(8)	22.1(8)	7.5(7)	6.2(6)	5.4(6)
C43	19.9(7)	23.5(8)	20.4(8)	8.7(6)	5.9(6)	5.7(6)
C22	23.9(8)	23.1(8)	24.6(8)	9.1(7)	7.4(6)	5.4(6)
C15A	23.3(7)	21.2(8)	20.8(8)	8.0(6)	6.4(6)	5.3(6)
C16A	18.5(7)	23.5(8)	19.7(8)	8.9(6)	6.9(6)	5.7(6)
C4A	15.7(7)	23.7(8)	21.3(8)	7.0(6)	6.4(6)	4.0(6)
C17A	23.1(7)	17.3(7)	21.7(8)	6.9(6)	6.3(6)	4.5(6)
C24A	27.3(8)	23.5(8)	25.0(8)	7.7(7)	9.0(7)	9.3(6)
C12A	17.5(7)	20.2(7)	20.4(8)	6.9(6)	5.5(6)	7.0(6)
C44	22.2(8)	18.8(8)	33.5(9)	3.7(7)	6.3(7)	-3.0(6)
C49	24.5(8)	20.2(8)	31.0(9)	7.1(7)	11.0(7)	0.3(6)
C30A	24.2(8)	22.1(8)	18.0(8)	5.5(6)	6.6(6)	7.8(6)
C37	22.7(8)	19.7(8)	22.8(8)	2.1(7)	-0.7(6)	3.0(6)
C2A	20.6(8)	32.1(9)	37.6(10)	19.3(8)	12.9(7)	9.3(7)
C14A	22.2(7)	21.0(7)	19.0(8)	6.1(6)	5.8(6)	3.8(6)
C40	28.0(8)	21.3(8)	26.0(8)	10.9(7)	9.7(7)	6.7(6)
C19A	20.5(7)	28.2(8)	20.4(8)	6.9(7)	7.2(6)	5.0(6)
F18B	35(3)	46(5)	45(4)	-11(3)	10(3)	-16(3)
C9	28.2(8)	22.7(8)	27.0(9)	12.3(7)	13.8(7)	11.0(6)
C27A	19.3(7)	26.0(8)	27.4(9)	12.4(7)	3.8(6)	4.5(6)
C38	23.2(8)	21.0(8)	30.0(9)	9.8(7)	8.0(7)	2.4(6)

C25A	24.5(8)	27.3(8)	21.3(8)	6.5(7)	8.4(6)	10.9(7)
C1A	20.6(7)	24.8(8)	21.6(8)	8.4(7)	5.9(6)	5.9(6)
C5	20.9(8)	33.4(9)	24.8(9)	11.0(7)	5.9(6)	5.5(7)
C52	27.7(8)	28.5(9)	21.3(8)	7.2(7)	4.6(7)	7.0(7)
C20	32.2(9)	25.0(8)	40.1(10)	18.6(8)	22.5(8)	11.6(7)
C8A	22.9(7)	22.2(8)	20.2(8)	6.6(6)	5.7(6)	5.6(6)
C39	23.5(8)	23.6(8)	21.8(8)	8.7(7)	4.1(6)	3.2(6)
C45	29.1(9)	35.6(10)	32.2(10)	17.6(8)	2.1(7)	3.3(7)
C24	42.1(10)	32.2(9)	40.3(10)	25.3(8)	29.0(9)	20.4(8)
C3	24.4(8)	34.1(9)	19.3(8)	6.4(7)	4.2(6)	0.3(7)
C35	46(1)	21.0(8)	33.6(10)	10.8(7)	18.3(8)	11.9(7)
C7A	25.0(8)	32.9(9)	19.4(8)	9.1(7)	8.1(6)	8.4(7)
C5A	24.6(8)	34.6(9)	23.4(8)	15.7(7)	9.5(7)	9.7(7)
C4	31.0(9)	47.3(11)	22.6(9)	12.0(8)	10.2(7)	21.0(8)
C31A	33.4(9)	29.0(9)	24.7(9)	4.6(7)	10.7(7)	-3.1(7)
C29	31.8(9)	22.5(8)	29.4(9)	7.1(7)	11.0(7)	2.2(7)
C29A	24.3(8)	34.1(10)	28.9(9)	2.8(8)	3.5(7)	3.0(7)
C21	39.7(10)	31.7(9)	28.8(9)	19.0(8)	19.9(8)	17.7(8)
C41	23.2(8)	26.4(8)	23.5(8)	10.0(7)	2.8(6)	5.8(6)
C10	29.6(9)	56.0(13)	29(1)	13.4(9)	6.6(8)	-8.2(9)
C30	36.8(10)	30.1(9)	37.5(10)	13.8(8)	15.2(8)	18.7(8)
C23	25.1(8)	28.7(9)	30.9(9)	10.0(7)	10.9(7)	9.7(7)
C6	28.2(9)	26.8(9)	33.8(10)	0.0(8)	13.9(8)	1.7(7)
C14	31.6(9)	50.6(12)	28(1)	18.5(9)	7.7(8)	5.8(8)
C11	40.2(10)	27.9(9)	34.3(10)	6.0(8)	10.5(8)	4.9(8)
C26A	24.2(8)	34.5(10)	35.7(10)	13.3(8)	12.0(7)	7.9(7)
C32A	48.5(11)	27.4(9)	24.3(9)	9.7(7)	13.2(8)	2.9(8)
C16	40.4(10)	24.6(9)	52.5(13)	7.9(9)	22.5(10)	8.5(8)
C28A	25.6(8)	36.8(10)	35.4(10)	12.2(8)	13.2(7)	5.5(7)
C50	37.3(10)	42.5(11)	24.4(9)	11.9(8)	0.9(8)	4.3(8)
F22A	113(4)	24.3(15)	46(3)	19.2(16)	46(3)	15(2)
C51	28.7(9)	44.2(12)	45.7(12)	9.1(10)	3.5(8)	18.7(9)
C53	40.7(10)	26.2(9)	26.0(9)	7.5(7)	2.8(8)	13.6(8)
C46	24.9(8)	28.9(9)	34.4(10)	4.1(8)	1.9(7)	9.1(7)
C47	44.8(12)	62.6(14)	29.6(11)	23.8(10)	6.2(9)	-4(1)
F23A	81(3)	43(3)	19.1(14)	8.5(16)	12.8(19)	-12(2)
C15	40.6(10)	34.3(10)	37.8(11)	14.5(9)	12.6(9)	18.0(8)
C9A	41.2(10)	43.6(11)	24.7(9)	13.8(8)	13.9(8)	18.5(8)
C48	26.8(9)	60.0(14)	30.9(10)	7.4(10)	1.7(8)	15.6(9)
B1A	20.5(8)	18.5(8)	17.9(8)	5.8(7)	6.4(7)	4.3(6)
C12	43.1(12)	77.1(17)	28.5(10)	10.5(11)	4.1(9)	39.0(12)
C13	54.4(13)	43.1(12)	39.7(11)	19.9(10)	18(1)	29(1)
C17	32.8(10)	33.2(11)	51.0(13)	-9.4(10)	9.8(9)	-2.6(8)
F24A	60(3)	137(5)	92(5)	81(4)	57(3)	46(3)
F22B	90(5)	77(5)	40(3)	15(4)	29(4)	-33(4)
F23B	117(5)	112(6)	92(6)	91(5)	35(4)	49(5)
F24B	144(8)	36(2)	42(5)	1(3)	63(5)	-9(5)

F22C	51(7)	35(6)	30(8)	8(5)	31(6)	9(5)
F23C	58(5)	40(7)	22(5)	20(5)	4(4)	10(5)
F24C	60(8)	19(4)	31(6)	11(4)	25(7)	0(5)
F17C	107(9)	102(10)	40(6)	-18(6)	41(7)	-40(8)
F18C	33(4)	64(9)	53(7)	-16(6)	-16(4)	12(5)
F16C	95(9)	47(5)	51(6)	-4(4)	2(6)	37(6)
F17A	32(3)	67(5)	24.6(18)	-1(3)	-8(2)	25(3)
F18A	64(4)	38(3)	52(3)	-11.2(19)	20(4)	-25(3)
F16A	24.8(15)	32(4)	26(2)	-4(2)	3.3(13)	9.9(19)
F5C	48(2)	58.1(19)	41(2)	26.9(17)	32.4(18)	24.4(17)
F6C	44(6)	47(5)	19(4)	14(4)	12(5)	21(5)
F4C	39.7(18)	34.5(16)	26.2(18)	9.6(14)	18.6(15)	13.9(13)
F4B	36(3)	56(4)	14(3)	-3(2)	-1(2)	6(2)
F5B	48(2)	58.1(19)	41(2)	26.9(17)	32.4(18)	24.4(17)
F6B	32(3)	46(3)	26(3)	23(3)	15(3)	19(3)
F13C	24(9)	64(5)	69(11)	34(6)	27(7)	25(6)
F14C	40(8)	45(9)	50(5)	28(6)	32(4)	5(6)
F15C	43(6)	66(7)	71(8)	0(6)	38(5)	-14(5)
F13B	20(3)	85(8)	59(4)	8(4)	12(3)	14(4)
F14B	29(6)	39(2)	43(5)	13(2)	21(4)	19(2)
F15B	56(8)	59(7)	81(7)	46(6)	47(6)	21(5)

Table 4 Bond Lengths for c020717_4_2.

Atom	Atom	Length/Å	Atom	Atom	Length/Å
Pd1	P1	2.2789(4)	C32	C39	1.522(2)
Pd1	P2	2.2815(4)	C42	C49	1.388(2)
Pd1	C1	2.0626(15)	C21A	C27A	1.390(2)
Pd1	C2	2.0152(15)	C21A	C1A	1.387(2)
Cu1	C18	1.9123(15)	C21A	C29A	1.492(3)
Cu1	C7	2.0827(15)	C3A	C4A	1.395(2)
Cu1	C1	2.0263(15)	C3A	C2A	1.498(2)
P1	O1	1.6497(12)	C3A	C5A	1.389(2)
P1	C3	1.8210(18)	C23A	C17A	1.392(2)
P1	C4	1.8323(18)	C23A	C30A	1.386(2)
P2	O2	1.6467(12)	C23A	C32A	1.496(2)
P2	C5	1.8231(17)	C22A	C16A	1.395(2)
P2	C6	1.8272(18)	C22A	C30A	1.388(2)
F1A	C2A	1.3340(19)	C22A	C31A	1.494(2)
F19A	C31A	1.335(2)	C43	C52	1.528(2)
F2A	C2A	1.344(2)	C43	C53	1.531(2)
O2	C8	1.384(2)	C22	C29	1.391(2)
F4A	C9A	1.340(6)	C16A	C12A	1.401(2)
F3A	C2A	1.3398(19)	C17A	C12A	1.403(2)
F7A	C24A	1.327(2)	C12A	B1A	1.640(2)
O1	C9	1.392(2)	C44	C38	1.386(2)

F20A	C31A	1.337(2)	C49	C40	1.384(2)
F10A	C26A	1.327(2)	C37	C45	1.531(3)
F8A	C24A	1.317(2)	C37	C46	1.533(2)
N2	C18	1.3600(19)	C14A	C19A	1.384(2)
N2	C25	1.4453(19)	C19A	C25A	1.389(2)
N2	C26	1.387(2)	C19A	C26A	1.501(2)
F13A	C28A	1.357(7)	F18B	C29A	1.330(7)
F21A	C31A	1.338(2)	C9	C21	1.391(2)
F9A	C24A	1.322(2)	C5	C14	1.529(2)
F14A	C28A	1.339(7)	C5	C15	1.527(3)
F16B	C29A	1.296(9)	C20	C24	1.386(3)
N1	C18	1.356(2)	C8A	C7A	1.391(2)
N1	C27	1.4425(19)	C39	C47	1.528(2)
N1	C28	1.387(2)	C39	C48	1.523(3)
F11A	C26A	1.332(2)	C24	C21	1.389(3)
F12A	C26A	1.321(2)	C3	C10	1.532(2)
F15A	C28A	1.346(7)	C3	C11	1.528(3)
C7	C1	1.227(2)	C35	C29	1.385(3)
C7	C19	1.453(2)	C35	C30	1.384(3)
F5A	C9A	1.446(5)	C7A	C5A	1.387(2)
C25	C31	1.400(2)	C7A	C9A	1.497(3)
C25	C32	1.401(2)	C4	C12	1.529(3)
C10A	C13A	1.399(2)	C4	C13	1.534(3)
C10A	C14A	1.406(2)	C29A	F17C	1.351(9)
C10A	B1A	1.644(2)	C29A	F18C	1.265(8)
C31	C36	1.396(2)	C29A	F16C	1.378(8)
C31	C37	1.522(2)	C29A	F17A	1.329(6)
F17B	C29A	1.380(8)	C29A	F18A	1.341(6)
C27	C33	1.400(2)	C29A	F16A	1.342(6)
C27	C34	1.405(2)	C41	C50	1.532(3)
C18A	C13A	1.397(2)	C41	C51	1.531(3)
C18A	C24A	1.499(2)	C30	C23	1.384(2)
C18A	C25A	1.390(2)	C6	C16	1.529(3)
F6A	C9A	1.262(6)	C6	C17	1.529(3)
C8	C2	1.395(2)	C32A	F22A	1.302(4)
C8	C20	1.391(2)	C32A	F23A	1.359(4)
C6A	C4A	1.401(2)	C32A	F24A	1.333(4)
C6A	C8A	1.402(2)	C32A	F22B	1.349(6)
C6A	B1A	1.647(2)	C32A	F23B	1.360(5)
C19	C22	1.396(2)	C32A	F24B	1.256(5)
C19	C23	1.402(2)	C32A	F22C	1.335(11)
C36	C44	1.383(2)	C32A	F23C	1.324(8)
C33	C40	1.393(2)	C32A	F24C	1.264(9)
C33	C41	1.520(2)	C28A	F13C	1.295(12)
C2	C9	1.390(2)	C28A	F14C	1.397(11)
C20A	C15A	1.398(2)	C28A	F15C	1.362(10)
C20A	C27A	1.380(2)	C28A	F13B	1.344(10)

C20A	C28A	1.500(2)	C28A	F14B	1.351(10)
C26	C28	1.344(2)	C28A	F15B	1.321(10)
C11A	C15A	1.399(2)	C9A	F5C	1.243(9)
C11A	C1A	1.406(2)	C9A	F6C	1.329(8)
C11A	B1A	1.647(2)	C9A	F4C	1.474(9)
C34	C42	1.393(2)	C9A	F4B	1.392(7)
C34	C43	1.525(2)	C9A	F5B	1.331(9)
C32	C38	1.394(2)	C9A	F6B	1.280(5)

Table 5 Bond Angles for c020717_4_2.

Atom	Atom	Atom	Angle/°	Atom	Atom	Atom	Angle/°
P1	Pd1	P2	158.201(15)	C14A	C19A	C26A	118.73(15)
C1	Pd1	P1	100.09(4)	C25A	C19A	C26A	120.32(15)
C1	Pd1	P2	101.71(4)	C2	C9	O1	118.55(14)
C2	Pd1	P1	79.39(5)	C2	C9	C21	122.67(16)
C2	Pd1	P2	79.51(5)	C21	C9	O1	118.73(15)
C2	Pd1	C1	165.81(6)	C20A	C27A	C21A	118.07(15)
C18	Cu1	C7	151.40(6)	C44	C38	C32	120.87(15)
C18	Cu1	C1	173.88(6)	C19A	C25A	C18A	117.87(15)
C1	Cu1	C7	34.71(6)	C21A	C1A	C11A	122.46(15)
O1	P1	Pd1	105.48(5)	C14	C5	P2	110.65(12)
O1	P1	C3	100.45(7)	C15	C5	P2	109.24(12)
O1	P1	C4	102.48(7)	C15	C5	C14	111.96(16)
C3	P1	Pd1	121.19(6)	C24	C20	C8	117.69(16)
C3	P1	C4	108.13(9)	C7A	C8A	C6A	122.70(15)
C4	P1	Pd1	116.08(6)	C32	C39	C47	112.21(14)
O2	P2	Pd1	105.52(5)	C32	C39	C48	110.26(14)
O2	P2	C5	100.65(7)	C48	C39	C47	110.55(17)
O2	P2	C6	101.71(8)	C20	C24	C21	122.14(16)
C5	P2	Pd1	121.76(6)	C10	C3	P1	111.27(14)
C5	P2	C6	108.76(9)	C11	C3	P1	109.13(12)
C6	P2	Pd1	115.25(6)	C11	C3	C10	111.51(16)
C8	O2	P2	114.57(10)	C30	C35	C29	120.14(16)
C9	O1	P1	114.30(10)	C8A	C7A	C9A	119.10(16)
C18	N2	C25	124.90(13)	C5A	C7A	C8A	120.53(16)
C18	N2	C26	111.47(13)	C5A	C7A	C9A	120.37(15)
C26	N2	C25	123.43(12)	C7A	C5A	C3A	118.07(15)
C18	N1	C27	124.28(13)	C12	C4	P1	113.35(14)
C18	N1	C28	111.70(12)	C12	C4	C13	111.02(17)
C28	N1	C27	123.78(13)	C13	C4	P1	109.07(13)
N2	C18	Cu1	129.15(11)	F19A	C31A	F20A	106.44(15)
N1	C18	Cu1	127.17(11)	F19A	C31A	F21A	106.41(15)
N1	C18	N2	103.68(12)	F19A	C31A	C22A	113.26(15)
C1	C7	Cu1	70.13(10)	F20A	C31A	F21A	106.33(16)
C1	C7	C19	171.15(16)	F20A	C31A	C22A	111.54(15)

C19	C7	Cu1	118.71(11)	F21A	C31A	C22A	112.39(15)
Cu1	C1	Pd1	133.58(8)	C35	C29	C22	120.10(16)
C7	C1	Pd1	151.25(13)	F16B	C29A	F17B	105.8(8)
C7	C1	Cu1	75.16(10)	F16B	C29A	C21A	115.3(8)
C31	C25	N2	118.72(13)	F16B	C29A	F18B	109.3(7)
C31	C25	C32	123.50(14)	F17B	C29A	C21A	108.4(7)
C32	C25	N2	117.74(13)	F18B	C29A	F17B	103.3(6)
C13A	C10A	C14A	115.88(14)	F18B	C29A	C21A	113.7(6)
C13A	C10A	B1A	124.58(14)	F17C	C29A	C21A	111.3(5)
C14A	C10A	B1A	119.43(13)	F17C	C29A	F16C	101.0(8)
C25	C31	C37	122.17(14)	F18C	C29A	C21A	118.7(6)
C36	C31	C25	116.70(14)	F18C	C29A	F17C	108.9(8)
C36	C31	C37	121.13(14)	F18C	C29A	F16C	107.1(7)
C33	C27	N1	117.60(13)	F16C	C29A	C21A	108.2(5)
C33	C27	C34	123.52(14)	F17A	C29A	C21A	112.3(5)
C34	C27	N1	118.79(13)	F17A	C29A	F18A	107.0(4)
C13A	C18A	C24A	119.40(14)	F17A	C29A	F16A	105.9(5)
C25A	C18A	C13A	121.03(15)	F18A	C29A	C21A	112.7(4)
C25A	C18A	C24A	119.56(14)	F18A	C29A	F16A	105.1(5)
C18A	C13A	C10A	121.85(15)	F16A	C29A	C21A	113.4(5)
O2	C8	C2	118.85(14)	C24	C21	C9	117.84(17)
O2	C8	C20	118.36(15)	C33	C41	C50	111.02(14)
C20	C8	C2	122.76(16)	C33	C41	C51	110.67(14)
C4A	C6A	C8A	115.65(14)	C51	C41	C50	110.92(15)
C4A	C6A	B1A	124.47(14)	C35	C30	C23	120.41(16)
C8A	C6A	B1A	119.73(14)	C30	C23	C19	119.91(16)
C22	C19	C7	120.47(14)	C16	C6	P2	108.33(14)
C22	C19	C23	119.41(15)	C16	C6	C17	111.34(17)
C23	C19	C7	120.12(15)	C17	C6	P2	112.72(13)
C44	C36	C31	121.29(15)	F10A	C26A	F11A	104.88(15)
C27	C33	C41	122.89(14)	F10A	C26A	C19A	113.50(15)
C40	C33	C27	117.07(14)	F11A	C26A	C19A	112.10(15)
C40	C33	C41	120.00(14)	F12A	C26A	F10A	107.29(17)
C8	C2	Pd1	121.17(12)	F12A	C26A	F11A	106.03(17)
C9	C2	Pd1	121.36(12)	F12A	C26A	C19A	112.46(15)
C9	C2	C8	116.85(14)	F22A	C32A	C23A	114.4(3)
C15A	C20A	C28A	119.20(16)	F22A	C32A	F23A	105.1(3)
C27A	C20A	C15A	121.08(15)	F22A	C32A	F24A	106.4(4)
C27A	C20A	C28A	119.71(15)	F23A	C32A	C23A	113.1(2)
C28	C26	N2	106.67(13)	F24A	C32A	C23A	112.1(2)
C15A	C11A	C1A	115.58(14)	F24A	C32A	F23A	104.9(4)
C15A	C11A	B1A	124.98(14)	F22B	C32A	C23A	112.8(4)
C1A	C11A	B1A	119.09(14)	F22B	C32A	F23B	101.5(5)
C27	C34	C43	121.89(13)	F23B	C32A	C23A	109.6(3)
C42	C34	C27	116.62(14)	F24B	C32A	C23A	115.8(3)
C42	C34	C43	121.49(14)	F24B	C32A	F22B	107.5(5)
C25	C32	C39	122.58(14)	F24B	C32A	F23B	108.6(5)

C38	C32	C25	117.14(14)	F22C	C32A	C23A	109.4(7)
C38	C32	C39	120.27(14)	F23C	C32A	C23A	110.2(6)
C26	C28	N1	106.48(14)	F23C	C32A	F22C	104.5(6)
C49	C42	C34	121.41(15)	F24C	C32A	C23A	114.2(8)
C27A	C21A	C29A	118.81(15)	F24C	C32A	F22C	108.0(7)
C1A	C21A	C27A	120.69(16)	F24C	C32A	F23C	110.0(7)
C1A	C21A	C29A	120.40(15)	F13A	C28A	C20A	113.6(5)
C4A	C3A	C2A	119.87(15)	F14A	C28A	F13A	105.3(6)
C5A	C3A	C4A	121.08(15)	F14A	C28A	F15A	107.1(6)
C5A	C3A	C2A	119.04(15)	F14A	C28A	C20A	112.2(5)
C17A	C23A	C32A	120.11(15)	F15A	C28A	F13A	104.5(6)
C30A	C23A	C17A	120.90(15)	F15A	C28A	C20A	113.4(6)
C30A	C23A	C32A	118.98(15)	F13C	C28A	C20A	120.7(11)
C16A	C22A	C31A	121.05(14)	F13C	C28A	F14C	106.2(11)
C30A	C22A	C16A	121.07(15)	F13C	C28A	F15C	109.9(9)
C30A	C22A	C31A	117.80(15)	F14C	C28A	C20A	105.6(10)
C34	C43	C52	112.95(13)	F15C	C28A	C20A	112.0(8)
C34	C43	C53	111.84(13)	F15C	C28A	F14C	100.1(7)
C52	C43	C53	109.04(13)	F13B	C28A	C20A	110.5(10)
C29	C22	C19	120.02(15)	F13B	C28A	F14B	106.0(8)
C20A	C15A	C11A	122.01(15)	F14B	C28A	C20A	108.5(8)
C22A	C16A	C12A	122.15(14)	F15B	C28A	C20A	115.9(10)
C3A	C4A	C6A	121.91(15)	F15B	C28A	F13B	108.0(9)
C23A	C17A	C12A	122.46(15)	F15B	C28A	F14B	107.5(9)
F7A	C24A	C18A	112.02(14)	F4A	C9A	F5A	97.5(5)
F8A	C24A	F7A	105.57(15)	F4A	C9A	C7A	113.2(5)
F8A	C24A	F9A	106.73(16)	F5A	C9A	C7A	110.1(3)
F8A	C24A	C18A	113.34(14)	F6A	C9A	F4A	113.9(5)
F9A	C24A	F7A	105.65(15)	F6A	C9A	F5A	105.1(4)
F9A	C24A	C18A	112.93(14)	F6A	C9A	C7A	115.1(4)
C16A	C12A	C17A	115.52(14)	F5C	C9A	C7A	120.1(7)
C16A	C12A	B1A	123.56(14)	F5C	C9A	F6C	116.0(7)
C17A	C12A	B1A	120.61(14)	F5C	C9A	F4C	101.0(7)
C36	C44	C38	120.46(15)	F6C	C9A	C7A	113.3(5)
C40	C49	C42	120.20(15)	F6C	C9A	F4C	97.3(6)
C23A	C30A	C22A	117.86(15)	F4C	C9A	C7A	104.5(6)
C31	C37	C45	110.92(14)	F4B	C9A	C7A	111.2(5)
C31	C37	C46	112.33(14)	F5B	C9A	C7A	111.7(8)
C45	C37	C46	109.82(14)	F5B	C9A	F4B	101.6(7)
F1A	C2A	F2A	106.29(14)	F6B	C9A	C7A	114.6(3)
F1A	C2A	F3A	105.85(14)	F6B	C9A	F4B	105.7(4)
F1A	C2A	C3A	112.86(14)	F6B	C9A	F5B	111.2(8)
F2A	C2A	C3A	113.18(14)	C10A	B1A	C6A	109.04(13)
F3A	C2A	F2A	105.63(15)	C10A	B1A	C11A	112.29(13)
F3A	C2A	C3A	112.42(14)	C11A	B1A	C6A	103.99(12)
C19A	C14A	C10A	122.38(15)	C12A	B1A	C10A	104.21(12)
C49	C40	C33	121.17(15)	C12A	B1A	C6A	114.33(13)

C14A	C19A	C25A	120.95(15)	C12A	B1A	C11A	113.15(13)

Table 6 Hydrogen Atom Coordinates (Å×10^4) and Isotropic Displacement Parameters (Å^2×10^3) for c020717_4_2.

Atom	*x*	*y*	*z*	U(eq)
H13D	844.58	4004.29	3834.34	24
H36	10060.3	4904.67	9230.66	30
H26	8333.01	2515.35	6285.29	26
H28	7164.92	1145.99	5768.79	25
H42	3903.14	93.41	5712.73	27
H43	5426.64	1639.61	5449.58	25
H22	7793.22	4981.19	9364.87	29
H15D	2476.62	2295.07	3449.71	26
H16D	-101.82	639.17	3156.43	24
H4A	1340.75	756.63	4180.1	24
H17D	1185.76	2527.82	2582.46	25
H44	9586.63	6013.65	8764.16	33
H49	4289.72	-819.89	6484.81	31
H30A	-217.78	256.72	807.76	26
H37	9145.56	2642.64	8163.32	30
H14D	-790.7	2033.1	4021.13	25
H40	5769.12	-570.08	7401.7	29
H27A	4441.29	4253.43	5257.88	29
H38	8310.36	5718.73	7587.96	30
H25A	-1716.54	4178.98	3818.29	29
H1A	1886.86	3753.08	5335.58	27
H5	2762.56	2027.64	8184.45	32
H52A	4104.08	524.91	4567.32	40
H52B	3970.53	1464.13	4536.3	40
H52C	3512.75	1012.73	5048.53	40
H20	3102.2	1182.91	10586.99	33
H8A	638.76	2822.29	5441.95	27
H39	6916.79	3594.55	6335.24	29
H45A	9200.76	3581.08	9767.85	50
H45B	9180.47	2570.84	9460.49	50
H45C	8313.12	2927.51	9058.87	50
H24	3966.66	1596.63	11984.41	37
H3	7862.55	4058.22	12045.15	33
H35	6761.76	6945.74	8764.19	38
H5A	1089.18	874.39	6377.9	31
H4	7987.98	2275.57	10524.87	39
H29	8017.36	6375.42	9270.31	34
H21	5518.12	2273.72	12488.14	34
H41	7662.11	1117.03	7707.51	30
H10A	8589.2	3911.7	11067.73	61

H10B	8439.73	4876.53	11326.41	61
H10C	7778.36	4185	10471.61	61
H30	5280.75	6140.04	8374.81	39
H23	5041.19	4759.16	8487.16	33
H6	4387.2	890.81	7754.8	38
H14A	4260.52	2826.07	7840.28	55
H14B	3219.43	2858.98	7412.86	55
H14C	3525.86	1955.86	7246.97	55
H11A	6447.12	4546.43	10939.56	54
H11B	7120.49	5166.35	11825.43	54
H11C	6376.06	4362.96	11748.45	54
H16A	5273.22	530.58	8861.08	58
H16B	4571.55	-332.88	8208.82	58
H16C	4380.95	149.6	9019.12	58
H50A	7095.5	1278.96	8799.98	56
H50B	7968.16	855.93	8976.16	56
H50C	6961.1	264.07	8662.66	56
H51A	7299.96	-701.73	7461.07	63
H51B	8301.32	-91.93	7801.87	63
H51C	7644.57	-267.29	6878.39	63
H53A	4248.23	2243.91	6308.24	49
H53B	4701.69	2748.66	5828.06	49
H53C	5330.93	2615.57	6647.5	49
H46A	10679.02	3486.61	8592.4	49
H46B	10599.71	2816.43	9080.06	49
H46C	10664.69	3818.98	9505.87	49
H47A	7514.75	5231.83	6177	70
H47B	6786.59	4427.1	5458.76	70
H47C	7834.94	4374.77	5810.38	70
H15A	3330.98	3127.19	9486.02	54
H15B	2990.77	3526.69	8760.45	54
H15C	4060.97	3610.27	9201.45	54
H48A	6225.08	4319.73	7216.38	63
H48B	5831.44	4465.17	6346.09	63
H48C	6580.17	5217.71	7105.65	63
H12A	8848.73	3039.72	11894.33	76
H12B	8908.3	2048.41	11734.22	76
H12C	8253.12	2430.69	12199.77	76
H13A	6978.84	1153.5	11086.71	63
H13B	7668.51	883.11	10617.38	63
H13C	6733.62	1103.93	10146.24	63
H17A	2797.19	157.98	8018.41	69
H17B	3091.03	-255.72	7249.53	69
H17C	2776.83	643.5	7356.8	69

Table 7 Atomic Occupancy for c020717_4_2.

Atom	*Occupancy*	Atom	*Occupancy*	Atom	*Occupancy*
F4A	0.494(3)	F13A	0.494(3)	F14A	0.494(3)
F16B	0.346(3)	F15A	0.494(3)	F5A	0.494(3)
F17B	0.346(3)	F6A	0.494(3)	F18B	0.346(3)
F22A	0.494(3)	F23A	0.494(3)	F24A	0.494(3)
F22B	0.346(3)	F23B	0.346(3)	F24B	0.346(3)
F22C	0.160(3)	F23C	0.160(3)	F24C	0.160(3)
F17C	0.160(3)	F18C	0.160(3)	F16C	0.160(3)
F17A	0.494(3)	F18A	0.494(3)	F16A	0.494(3)
F5C	0.160(3)	F6C	0.160(3)	F4C	0.160(3)
F4B	0.346(3)	F5B	0.346(3)	F6B	0.346(3)
F13C	0.160(3)	F14C	0.160(3)	F15C	0.160(3)
F13B	0.346(3)	F14B	0.346(3)	F15B	0.346(3)

3.3.3. Crystal structure for [($^{i\text{Pr}}$POCOP)Pd$^{\text{II}}$(CCPh)•Ag$^{\text{I}}$(IPr)]BF4, [**2**]BF_4:

Crystal Data for $C_{61}H_{88}AgBF_4N_2O_4P_2Pd$ (M =1276.35 g/mol): triclinic, space group P-1 (no. 2), a = 11.22300(10) Å, b = 12.2171(3) Å, c = 23.2541(3) Å, α = 78.442(2)°, β = 83.5370(10)°, γ = 89.622(2)°, V = 3103.51(9) Å^3, Z = 2, T = 100.0(1) K, μ(CuKα) = 5.819 mm^{-1}, $Dcalc$ = 1.366 g/cm^3, 114002 reflections measured (7.386° ≤ 2Θ ≤ 159.51°), 13209 unique (R_{int} = 0.0575, R_{sigma} = 0.0267) which were used in all calculations. The final R_1 was 0.0365 (I > 2σ(I)) and wR_2 was 0.0983 (all data).

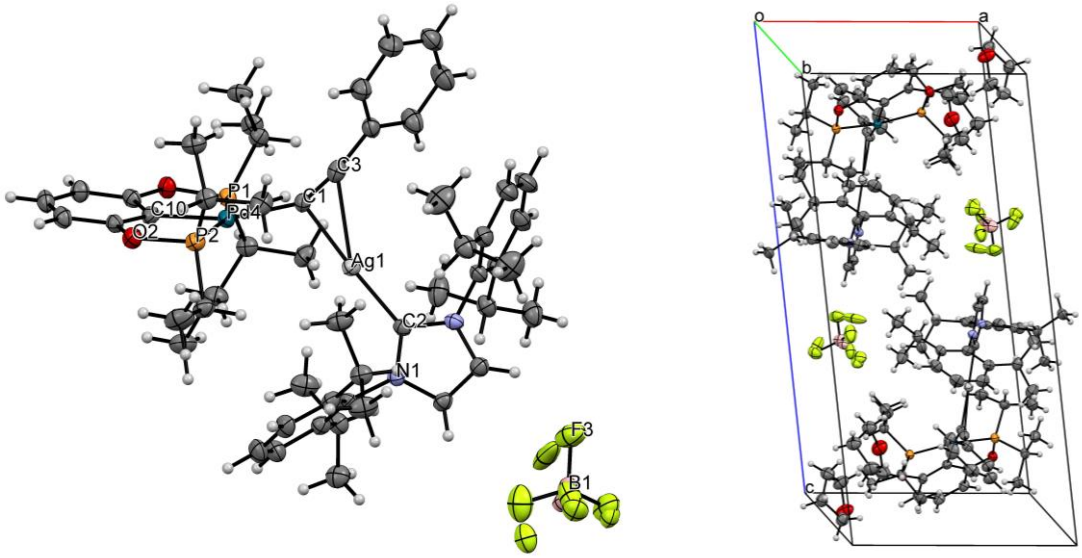

Figure SI-91: Representation of crystal structure from different perspectives. Colors-code: grey/carbon, red/oxygen, light-orange/phosphorus, light-gray/Ag, yellow/fluorine, pink/boron, blue/nitrogen, teal/palladium. *Left)* XRD structure (ORTEP 50% probability ellipsoids), hydrogens and co-crystallizing molecules omitted for clearity. *Right)* representation of the unit cell, crystal packing.

Table 1 Crystal data and structure refinement for c060917_2_1.

Identification code	c060917_2_1
Empirical formula	$C_{61}H_{88}AgBF_4N_2O_4P_2Pd$
Formula weight	1276.35
Temperature/K	100.0(1)
Crystal system	triclinic
Space group	P-1
a/Å	11.22300(10)
b/Å	12.2171(3)
c/Å	23.2541(3)
α/°	78.442(2)
β/°	83.5370(10)
γ/°	89.622(2)
Volume/Å^3	3103.51(9)
Z	2
ρ_{calc}g/cm^3	1.366
μ/mm^{-1}	5.819
F(000)	1328.0
Crystal size/mm^3	0.182 × 0.134 × 0.014
Radiation	CuKα (λ = 1.54184)
2Θ range for data collection/°	7.386 to 159.51

Index ranges	$-14 \le h \le 14$, $-12 \le k \le 15$, $-29 \le l \le 29$
Reflections collected	114002
Independent reflections	13209 [R_{int} = 0.0575, R_{sigma} = 0.0267]
Data/restraints/parameters	13209/108/747
Goodness-of-fit on F^2	1.068
Final R indexes [I>=2σ (I)]	R_1 = 0.0365, wR_2 = 0.0962
Final R indexes [all data]	R_1 = 0.0406, wR_2 = 0.0983
Largest diff. peak/hole / e $Å^{-3}$	1.54/-0.96

Table 2 Fractional Atomic Coordinates ($\times 10^4$) and Equivalent Isotropic Displacement Parameters ($Å^2 \times 10^3$) for c060917_2_1. U_{eq} is defined as 1/3 of of the trace of the orthogonalised U_{IJ} tensor.

Atom	*x*	*y*	*z*	U(eq)
Ag1	6589.4(2)	6468.2(2)	7032.4(2)	23.71(6)
Pd4	6024.7(2)	4564.9(2)	8425.8(2)	21.83(6)
P1	4014.2(6)	4501.4(6)	8686.2(3)	23.09(14)
P2	7975.8(6)	4037.5(6)	8383.1(3)	25.25(15)
O1	3763.6(16)	3430.7(17)	9245.8(9)	27.3(4)
F4	7212(15)	8663(14)	3016(7)	56(4)
O2	7996.6(17)	2895.6(18)	8899.2(9)	28.6(4)
N1	7511.2(19)	6222.3(19)	5719.1(10)	23.0(5)
F1	9182(10)	8381(15)	3150(5)	47(2)
N2	6776(2)	7821(2)	5772.5(10)	24.3(5)
O2A	2064(3)	7901(2)	8168.0(13)	57.1(7)
C2	7001(2)	6818(2)	6113.2(11)	22.1(5)
O1A	1504(3)	968(2)	10275.8(12)	55.9(7)
C10	5874(2)	3152(2)	9045.9(11)	24.7(5)
C6	7592(2)	6839(2)	5146.1(12)	26.2(6)
C1	6114(2)	6203(2)	7972.5(11)	23.7(5)
C19	9076(2)	4918(3)	8609.6(13)	28.9(6)
C7	7965(2)	5107(2)	5869.1(11)	23.6(5)
C8	7135(3)	7846(3)	5179.2(12)	28.1(6)
C5	5918(3)	8316(2)	8084.8(13)	29.3(6)
C21	6884(2)	2546(2)	9205.6(12)	24.1(5)
C41	6818(3)	1622(3)	9662.8(13)	30.0(6)
C25	7689(3)	3138(3)	6013.7(14)	33.4(6)
C13	7197(2)	4203(3)	5905.1(12)	26.5(6)
C22	4788(2)	2811(2)	9380.8(12)	24.9(5)
C9	6283(3)	8750(2)	6011.2(12)	26.3(6)
C15	5057(3)	8965(2)	5986.9(13)	28.6(6)
C27	10008(2)	5999(3)	5892.1(13)	29.1(6)
C29	4238(3)	8198(3)	5765.6(14)	30.9(6)
C17	3334(2)	5663(3)	8980.3(12)	27.3(6)
C20	8648(3)	3556(3)	7725.4(13)	30.5(6)
C42	4671(3)	1893(3)	9842.8(13)	29.2(6)

C3	6033(2)	7192(3)	7977.1(12)	28.8(6)
C26	5864(2)	4332(3)	5847.2(13)	30.1(6)
C14	9191(2)	4999(3)	5939.5(12)	27.5(6)
C44	8887(3)	3002(3)	6093.9(14)	36.8(7)
C18	3052(2)	4157(3)	8163.6(13)	28.6(6)
C28	9625(3)	3913(3)	6063.0(13)	33.4(7)
C16	7049(3)	9393(3)	6248.2(13)	31.2(6)
C54	5708(3)	1301(3)	9978.1(14)	32.2(6)
C35	3014(3)	5140(3)	7643.4(13)	34.8(7)
C37	8562(3)	5221(3)	9192.6(14)	35.6(7)
C36	3480(3)	3081(3)	7966.4(15)	36.0(7)
C33	2002(3)	5461(3)	9199.8(13)	32.5(6)
C38	9416(3)	5956(3)	8131.7(14)	37.7(7)
C31	8380(3)	9150(3)	6245.4(15)	37.3(7)
C34	4045(3)	5921(3)	9465.4(14)	35.0(7)
C11	6664(3)	8680(3)	8453.0(14)	37.3(7)
C23	6515(3)	9717(3)	8599.2(16)	44.4(8)
C2A	272(3)	2411(3)	9885.7(16)	41.7(8)
C30	4610(3)	9880(3)	6214.9(15)	36.1(7)
C45	5439(3)	3657(3)	5421.3(15)	39.0(7)
C46	5142(3)	4012(3)	6458.3(15)	39.8(7)
F2	7743(4)	7174(5)	3686(4)	63(2)
C47	10158(3)	6220(3)	6504.9(14)	38.4(7)
C49	3322(3)	8823(3)	5387.4(16)	42.3(8)
C39	7839(3)	2628(3)	7622.9(16)	43.6(8)
C43	5620(3)	10411(3)	8374.2(16)	41.5(8)
C32	6537(3)	10276(3)	6479.5(15)	39.0(7)
C12	5021(3)	9021(3)	7863.1(16)	41.0(8)
C48	11232(3)	5868(3)	5549.8(15)	40.9(8)
C51	5341(3)	10525(3)	6453.1(16)	42.0(8)
C3A	756(3)	1838(3)	9385.8(16)	46.3(9)
C1A	1158(3)	2062(3)	10333.1(17)	44.5(8)
C50	3626(3)	7362(3)	6290.0(17)	47.2(9)
F3	7926(5)	8921(7)	3859(2)	58.6(19)
C24	4891(3)	10068(3)	8003.8(18)	46.5(8)
C4A	1485(4)	884(3)	9680.2(17)	49.0(9)
C7A	677(4)	9303(3)	7919.4(17)	49.9(9)
C52	8866(4)	9291(4)	6810.7(18)	58.2(11)
C8A	1587(4)	8553(3)	7667.8(17)	49.6(9)
C6A	1296(4)	9573(4)	8422.2(19)	56.3(10)
C40	9943(3)	3185(4)	7764.3(16)	47.6(9)
C53	9083(3)	9877(4)	5707.5(18)	57.2(11)
C5A	1981(4)	8527(4)	8626.1(17)	56.3(10)
B1	8019(10)	8285(8)	3426(4)	42(2)
F1A	9057(12)	8400(17)	3294(8)	55(3)
F4A	7291(18)	8642(15)	2913(8)	36(2)
F3A	7309(11)	8145(11)	3905(2)	88(5)

B1A	7873(13)	8028(10)	3362(5)	36(3)
F2A	7869(4)	6901(5)	3347(4)	41.5(19)

Table 3 Anisotropic Displacement Parameters ($Å^2×10^3$) for c060917_2_1. The Anisotropic displacement factor exponent takes the form: $-2\pi^2[h^2a^{*2}U_{11}+2hka^*b^*U_{12}+...]$.

Atom	U_{11}	U_{22}	U_{33}	U_{23}	U_{13}	U_{12}
Ag1	21.78(10)	26.66(11)	22.88(10)	-5.80(7)	-2.04(7)	3.88(7)
Pd4	18.75(10)	23.71(11)	22.91(10)	-4.42(7)	-2.49(7)	4.09(7)
P1	19.0(3)	25.5(4)	24.6(3)	-4.8(3)	-2.6(2)	4.6(2)
P2	19.7(3)	30.8(4)	25.8(3)	-7.2(3)	-2.4(2)	4.7(3)
O1	21.5(9)	28.5(11)	29.9(10)	-1.8(8)	-1.9(7)	5.4(8)
F4	54(5)	75(5)	42(6)	-11(3)	-16(4)	35(4)
O2	21.9(9)	33.6(11)	30(1)	-5.2(8)	-3.9(7)	8.4(8)
N1	22.1(10)	23.0(12)	24.9(11)	-6.1(9)	-4.5(8)	4.9(9)
F1	45(3)	50(4)	44(4)	-12(3)	2(2)	13(2)
N2	24.2(11)	23.8(12)	26.5(11)	-9.3(9)	-2.4(9)	4.0(9)
O2A	63.7(17)	47.6(16)	61.0(17)	-7.1(13)	-18.8(14)	13.2(13)
C2	21.0(12)	21.2(13)	25.0(12)	-6.3(10)	-3.4(10)	2.9(10)
O1A	80(2)	41.5(15)	49.5(15)	-6.7(12)	-27.6(14)	17.6(14)
C10	25.8(13)	27.0(15)	21.8(12)	-5.0(11)	-4.6(10)	2.8(11)
C6	24.6(13)	31.0(15)	22.5(13)	-5.1(11)	-1.7(10)	3.6(11)
C1	24.8(12)	22.0(14)	22.2(12)	0.1(10)	-2.1(10)	1.6(10)
C19	20.6(12)	34.7(16)	32.0(14)	-7.8(12)	-3.8(11)	1.9(11)
C7	24.6(13)	25.7(14)	21.2(12)	-6.4(10)	-2.6(10)	8.9(11)
C8	28.5(14)	29.1(15)	26.3(13)	-4.9(11)	-2.6(11)	2.4(11)
C5	32.8(14)	23.3(15)	29.8(14)	-2.5(11)	0.0(11)	1.6(11)
C21	24.8(13)	22.2(14)	26.3(13)	-5.7(10)	-5(1)	4.6(10)
C41	28.6(14)	26.1(15)	35.7(15)	-4.3(12)	-9.7(11)	5.6(11)
C25	36.1(16)	26.9(16)	37.0(16)	-5.5(12)	-5.0(12)	2.5(12)
C13	24.8(13)	29.7(15)	24.5(13)	-4.8(11)	-1.5(10)	3.3(11)
C22	22.2(12)	23.1(14)	30.2(14)	-6.7(11)	-4.9(10)	4.6(10)
C9	30.4(14)	20.3(14)	28.1(13)	-5.8(11)	-0.9(11)	2.3(11)
C15	29.9(14)	24.5(15)	30.2(14)	-4.7(11)	0.6(11)	3.5(11)
C27	22.4(13)	35.7(17)	30.7(14)	-9.4(12)	-4.0(11)	1.8(11)
C29	26.0(13)	28.8(16)	37.8(16)	-6.2(12)	-4.5(11)	7.0(11)
C17	22.9(13)	31.8(16)	26.3(13)	-5.6(11)	-0.4(10)	5.5(11)
C20	28.7(14)	38.4(17)	25.7(14)	-10.1(12)	-1.9(11)	6.9(12)
C42	26.6(13)	28.8(16)	30.9(14)	-2.8(12)	-4.2(11)	0.9(11)
C3	25.1(13)	32.6(17)	25.9(13)	1.2(11)	-3.5(10)	-0.8(11)
C26	24.4(13)	29.9(16)	36.1(15)	-6.6(12)	-3.6(11)	1.6(11)
C14	24.5(13)	35.3(16)	22.6(13)	-6.0(11)	-2.8(10)	4.7(11)
C44	39.5(17)	29.1(17)	39.8(17)	-1.6(13)	-5.9(13)	13.2(13)
C18	23.4(13)	33.2(16)	30.6(14)	-8.8(12)	-4.2(11)	1.5(11)
C28	26.4(14)	39.8(18)	33.4(15)	-5.4(13)	-5.8(11)	14.4(13)
C16	36.1(15)	25.2(15)	31.7(15)	-5.3(12)	-2.5(12)	-1.0(12)

C54	37.1(16)	23.7(15)	34.6(15)	0.5(12)	-9.9(12)	1.6(12)
C35	32.0(15)	42.6(19)	29.3(15)	-3.8(13)	-7.5(12)	4.5(13)
C37	30.4(15)	42.9(19)	35.5(16)	-12.6(14)	-3.5(12)	0.9(13)
C36	35.7(16)	36.4(18)	38.8(17)	-14.0(14)	-5.6(13)	-1.1(13)
C33	25.1(14)	39.8(18)	33.2(15)	-9.4(13)	-3.1(11)	8.2(12)
C38	33.1(16)	42.5(19)	35.9(16)	-3.2(14)	-5.6(13)	-6.2(14)
C31	35.0(16)	32.9(17)	45.2(18)	-8.6(14)	-7.6(13)	-3.1(13)
C34	29.8(14)	43.1(19)	36.6(16)	-19.0(14)	-3.8(12)	7.9(13)
C11	42.0(17)	33.1(17)	38.8(17)	-7.7(13)	-12.5(14)	5.7(14)
C23	52(2)	40(2)	44.7(19)	-13.0(15)	-11.1(16)	-0.3(16)
C2A	35.9(17)	41(2)	49.2(19)	-9.9(15)	-8.3(14)	5.6(14)
C30	36.3(16)	27.1(16)	43.5(17)	-7.4(13)	1.2(13)	9.0(13)
C45	34.6(16)	44(2)	40.6(17)	-11.1(15)	-9.5(13)	3.0(14)
C46	28.3(15)	47(2)	46.5(19)	-17.9(15)	3.8(13)	-5.1(14)
F2	43(2)	63(3)	76(5)	8(3)	-13(2)	5(2)
C47	29.5(15)	54(2)	35.7(16)	-19.2(15)	-3.5(12)	3.0(14)
C49	42.5(18)	37.4(19)	46.6(19)	-2.4(15)	-14.8(15)	7.1(15)
C39	47.4(19)	49(2)	37.8(17)	-18.7(16)	-0.3(14)	1.3(16)
C43	48.6(19)	26.5(17)	48.5(19)	-9.4(14)	1.7(15)	0.0(14)
C32	50.3(19)	26.0(16)	42.3(18)	-11.2(13)	-3.7(14)	-2.6(14)
C12	39.8(17)	32.3(18)	53(2)	-8.1(15)	-16.6(15)	6.0(14)
C48	28.5(15)	58(2)	38.9(17)	-18.4(16)	3.6(13)	-6.1(15)
C51	54(2)	25.5(17)	47.6(19)	-15.2(14)	3.0(15)	6.3(14)
C3A	49(2)	48(2)	39.1(18)	-1.9(16)	-6.0(15)	14.4(17)
C1A	41.6(18)	45(2)	49(2)	-13.0(16)	-10.0(15)	5.1(15)
C50	40.9(18)	44(2)	52(2)	8.4(16)	-16.3(16)	-9.2(15)
F3	54(3)	86(4)	42(2)	-26(2)	-12.0(18)	33(3)
C24	45.0(19)	32.4(19)	64(2)	-10.0(16)	-12.5(17)	10.8(15)
C4A	60(2)	41(2)	53(2)	-15.0(17)	-25.5(18)	15.6(17)
C7A	56(2)	47(2)	46(2)	-5.8(17)	-12.1(17)	12.0(18)
C52	46(2)	79(3)	50(2)	-10(2)	-15.9(17)	-5(2)
C8A	54(2)	48(2)	47(2)	-7.9(17)	-8.9(17)	6.4(17)
C6A	67(3)	53(3)	52(2)	-16.7(19)	-10.4(19)	7(2)
C40	33.7(17)	73(3)	40.8(18)	-22.6(18)	-4.0(14)	19.3(17)
C53	40(2)	74(3)	53(2)	-7(2)	3.0(17)	-5.1(19)
C5A	56(2)	70(3)	39.1(19)	-1.2(18)	-4.9(17)	8(2)
B1	42(5)	46(4)	37(4)	-6(3)	-10(3)	23(4)
F1A	54(6)	35(4)	82(10)	-9(6)	-40(5)	2(5)
F4A	37(4)	39(4)	29(4)	0(3)	-5(3)	8(4)
F3A	118(7)	114(9)	23(2)	-6(3)	1(3)	82(7)
B1A	40(5)	44(5)	25(4)	-10(4)	-5(4)	17(4)
F2A	26(2)	39(3)	58(4)	-2(2)	-9(2)	4.1(18)

Table 4 Bond Lengths for c060917_2_1.

Atom	Atom	Length/Å	Atom	Atom	Length/Å

Ag1	C2	2.093(3)	C9	C15	1.404(4)
Ag1	C1	2.151(3)	C9	C16	1.396(4)
Pd4	P1	2.2672(7)	C15	C29	1.517(4)
Pd4	P2	2.2754(7)	C15	C30	1.397(4)
Pd4	C10	2.010(3)	C27	C14	1.512(4)
Pd4	C1	2.064(3)	C27	C47	1.529(4)
P1	O1	1.651(2)	C27	C48	1.532(4)
P1	C17	1.822(3)	C29	C49	1.528(4)
P1	C18	1.824(3)	C29	C50	1.524(5)
P2	O2	1.650(2)	C17	C33	1.530(4)
P2	C19	1.831(3)	C17	C34	1.535(4)
P2	C20	1.830(3)	C20	C39	1.529(5)
O1	C22	1.402(3)	C20	C40	1.527(4)
F4	B1	1.397(10)	C42	C54	1.398(4)
O2	C21	1.391(3)	C26	C45	1.527(4)
N1	C2	1.357(3)	C26	C46	1.534(4)
N1	C6	1.387(3)	C14	C28	1.396(4)
N1	C7	1.442(3)	C44	C28	1.378(5)
F1	B1	1.384(9)	C18	C35	1.529(4)
N2	C2	1.359(4)	C18	C36	1.533(4)
N2	C8	1.388(4)	C16	C31	1.521(4)
N2	C9	1.441(4)	C16	C32	1.393(5)
O2A	C8A	1.428(5)	C31	C52	1.520(5)
O2A	C5A	1.426(5)	C31	C53	1.523(5)
O1A	C1A	1.416(5)	C11	C23	1.380(5)
O1A	C4A	1.412(4)	C23	C43	1.389(5)
C10	C21	1.395(4)	C2A	C3A	1.522(5)
C10	C22	1.389(4)	C2A	C1A	1.518(5)
C6	C8	1.342(4)	C30	C51	1.374(5)
C1	C3	1.213(4)	F2	B1	1.393(9)
C19	C37	1.526(4)	C43	C24	1.376(5)
C19	C38	1.527(4)	C32	C51	1.380(5)
C7	C13	1.389(4)	C12	C24	1.386(5)
C7	C14	1.405(4)	C3A	C4A	1.514(5)
C5	C3	1.446(4)	F3	B1	1.384(9)
C5	C11	1.397(4)	C7A	C8A	1.514(5)
C5	C12	1.396(4)	C7A	C6A	1.516(6)
C21	C41	1.383(4)	C6A	C5A	1.508(6)
C41	C54	1.389(4)	F1A	B1A	1.390(11)
C25	C13	1.397(4)	F4A	B1A	1.383(11)
C25	C44	1.382(4)	F3A	B1A	1.381(10)
C13	C26	1.521(4)	B1A	F2A	1.385(11)
C22	C42	1.385(4)			

Table 5 Bond Angles for c060917_2_1.

Atom	Atom	Atom	Angle/°	Atom	Atom	Atom	Angle/°
C2	Ag1	C1	176.57(10)	C9	C15	C29	121.8(3)
P1	Pd4	P2	159.90(3)	C30	C15	C9	116.7(3)
C10	Pd4	P1	79.81(8)	C30	C15	C29	121.4(3)
C10	Pd4	P2	80.20(8)	C14	C27	C47	110.7(3)
C10	Pd4	C1	165.48(11)	C14	C27	C48	112.1(3)
C1	Pd4	P1	96.31(8)	C47	C27	C48	110.7(2)
C1	Pd4	P2	103.58(8)	C15	C29	C49	113.4(3)
O1	P1	Pd4	105.74(7)	C15	C29	C50	109.2(3)
O1	P1	C17	103.27(12)	C50	C29	C49	111.4(3)
O1	P1	C18	102.04(13)	C33	C17	P1	112.8(2)
C17	P1	Pd4	118.02(10)	C33	C17	C34	111.7(2)
C17	P1	C18	107.41(13)	C34	C17	P1	109.73(19)
C18	P1	Pd4	118.03(10)	C39	C20	P2	107.8(2)
O2	P2	Pd4	105.12(7)	C40	C20	P2	113.2(2)
O2	P2	C19	100.91(12)	C40	C20	C39	112.2(3)
O2	P2	C20	101.86(13)	C22	C42	C54	117.6(3)
C19	P2	Pd4	118.63(10)	C1	C3	C5	170.8(3)
C20	P2	Pd4	118.62(10)	C13	C26	C45	112.5(3)
C20	P2	C19	108.54(14)	C13	C26	C46	109.8(2)
C22	O1	P1	114.11(17)	C45	C26	C46	110.9(3)
C21	O2	P2	114.88(16)	C7	C14	C27	122.3(3)
C2	N1	C6	111.4(2)	C28	C14	C7	116.8(3)
C2	N1	C7	125.1(2)	C28	C14	C27	120.9(3)
C6	N1	C7	123.4(2)	C28	C44	C25	120.8(3)
C2	N2	C8	111.5(2)	C35	C18	P1	110.2(2)
C2	N2	C9	123.3(2)	C35	C18	C36	112.4(3)
C8	N2	C9	125.2(2)	C36	C18	P1	109.8(2)
C5A	O2A	C8A	108.4(3)	C44	C28	C14	121.0(3)
N1	C2	Ag1	133.7(2)	C9	C16	C31	121.6(3)
N1	C2	N2	103.8(2)	C32	C16	C9	116.7(3)
N2	C2	Ag1	122.55(19)	C32	C16	C31	121.7(3)
C4A	O1A	C1A	108.3(3)	C41	C54	C42	121.4(3)
C21	C10	Pd4	121.0(2)	C16	C31	C53	110.0(3)
C22	C10	Pd4	121.6(2)	C52	C31	C16	112.9(3)
C22	C10	C21	117.0(3)	C52	C31	C53	110.9(3)
C8	C6	N1	106.8(2)	C23	C11	C5	120.7(3)
Pd4	C1	Ag1	116.48(13)	C11	C23	C43	119.8(3)
C3	C1	Ag1	94.0(2)	C1A	C2A	C3A	102.2(3)
C3	C1	Pd4	149.5(2)	C51	C30	C15	121.1(3)
C37	C19	P2	108.4(2)	C24	C43	C23	120.1(3)
C37	C19	C38	111.9(3)	C51	C32	C16	121.3(3)
C38	C19	P2	111.5(2)	C24	C12	C5	120.0(3)
C13	C7	N1	118.9(2)	C30	C51	C32	120.6(3)
C13	C7	C14	123.5(3)	C4A	C3A	C2A	104.3(3)
C14	C7	N1	117.5(3)	O1A	C1A	C2A	105.4(3)
C6	C8	N2	106.5(2)	C43	C24	C12	120.5(3)

C11	C5	C3	119.5(3)	O1A	C4A	C3A	108.1(3)
C12	C5	C3	121.4(3)	C8A	C7A	C6A	101.2(3)
C12	C5	C11	118.9(3)	O2A	C8A	C7A	105.2(3)
O2	C21	C10	118.7(2)	C5A	C6A	C7A	103.5(3)
C41	C21	O2	119.1(2)	O2A	C5A	C6A	107.7(3)
C41	C21	C10	122.2(3)	F1	B1	F4	110.2(12)
C21	C41	C54	118.6(3)	F1	B1	F2	110.1(10)
C44	C25	C13	120.8(3)	F1	B1	F3	108.5(8)
C7	C13	C25	117.2(3)	F2	B1	F4	108.8(10)
C7	C13	C26	122.8(3)	F3	B1	F4	109.9(10)
C25	C13	C26	119.9(3)	F3	B1	F2	109.3(8)
C10	C22	O1	118.4(2)	F4A	B1A	F1A	108.9(14)
C42	C22	O1	118.6(2)	F4A	B1A	F2A	111.4(12)
C42	C22	C10	123.1(3)	F3A	B1A	F1A	110.3(11)
C15	C9	N2	118.0(3)	F3A	B1A	F4A	110.3(13)
C16	C9	N2	118.4(3)	F3A	B1A	F2A	107.7(9)
C16	C9	C15	123.6(3)	F2A	B1A	F1A	108.3(12)

Table 6 Hydrogen Atom Coordinates (Å×10^4) and Isotropic Displacement Parameters (Å^2×10^3) for c060917_2_1.

Atom	*x*	*y*	*z*	U(eq)
H6	7902.47	6601.41	4804.74	31
H19	9801.7	4482.07	8676.76	35
H8	7071.12	8442.13	4865.94	34
H41	7502.02	1223.1	9757.11	36
H25	7205.58	2514.23	6032.19	40
H27	9626.37	6652.98	5674.36	35
H29	4742.1	7774.45	5518.4	37
H17	3400.52	6321.29	8658.12	33
H20	8645.54	4180.8	7387.36	37
H42	3929.4	1676.95	10055.53	35
H26	5722.85	5122.83	5690.76	36
H44	9198.05	2286.53	6169.68	44
H18	2237.65	4020.43	8367.19	34
H28	10425.4	3803.65	6125.38	40
H54	5652.63	680.25	10285.88	39
H35A	2656.02	5768.46	7782.71	52
H35B	2546.64	4932.45	7359.65	52
H35C	3814.76	5337.07	7461.29	52
H37A	7882.44	5692.53	9129.24	53
H37B	9163.7	5609.01	9340.87	53
H37C	8317.55	4551.14	9474.27	53
H36A	4286.76	3189.23	7776.25	54
H36B	2965.24	2900.31	7694.55	54
H36C	3454.28	2481.45	8304.81	54

H33A	1564.39	5427.4	8871.72	49
H33B	1706.17	6061.34	9383.9	49
H33C	1898.07	4767.95	9481.47	49
H38A	9791.51	5733.33	7782.3	57
H38B	9962.46	6416.99	8271.03	57
H38C	8706.68	6368.42	8041.58	57
H31	8490.57	8368.61	6209.76	45
H34A	3985.95	5294.01	9791.25	52
H34B	3721.84	6568.46	9597.99	52
H34C	4871.35	6060.8	9310.43	52
H11	7268.25	8219.36	8601.21	45
H23	7010.73	9949.93	8847.49	53
H2AA	270.39	3216.59	9754.71	50
H2AB	-534.23	2148.96	10047.04	50
H30	3803.46	10054.71	6205.24	43
H45A	5900.86	3871.2	5042.13	58
H45B	4606.4	3798.62	5381.8	58
H45C	5540.59	2874.86	5572.2	58
H46A	5278.86	3243.21	6625.16	60
H46B	4304.02	4115.59	6420.71	60
H46C	5392.43	4476.69	6711.74	60
H47A	9384.44	6327.11	6706.57	58
H47B	10646.86	6877.99	6465.14	58
H47C	10535.03	5592.07	6727.69	58
H49A	2770.64	9195.5	5627.14	63
H49B	2890.7	8301.95	5226.05	63
H49C	3731.22	9364.68	5071.35	63
H39A	7799.18	2016.38	7956.35	65
H39B	8162.16	2373.44	7273.38	65
H39C	7048.84	2910.13	7574.48	65
H43	5513.4	11107.47	8474.06	50
H32	7010.33	10706.75	6655.29	47
H12	4510.55	8787.47	7621.14	49
H48A	11664.2	5285.08	5775.46	61
H48B	11679.48	6557.77	5481.12	61
H48C	11117.73	5679.39	5178.09	61
H51	5026.65	11135.86	6598	50
H3AA	105.93	1561.19	9209.4	56
H3AB	1255.12	2348.42	9081.93	56
H1AA	1848.62	2565.28	10248.61	53
H1AB	785.13	2063.2	10729.95	53
H50A	4222.67	6985.22	6519.19	71
H50B	3175.24	6824.66	6149.49	71
H50C	3096.29	7749.42	6531.7	71
H24	4307.02	10543.57	7846.52	56
H4AA	1127.43	174.3	9659.16	59
H4AB	2296	926.06	9481.26	59

H7AA	-82.62	8915.37	8061.98	60
H7AB	546.54	9972.15	7630.57	60
H52A	8793.67	10056.62	6850.72	87
H52B	9694.76	9087.25	6795.57	87
H52C	8416.43	8819.53	7143.09	87
H8AA	1205.75	8077.04	7452.29	60
H8AB	2215.69	8993.77	7403.14	60
H6AA	1833.93	10212.9	8286.06	68
H6AB	715.14	9724.75	8737.22	68
H40A	10423.77	3797.87	7815	71
H40B	10247.8	2946.92	7407.45	71
H40C	9970.82	2575.73	8094.95	71
H53A	8818.87	9715.38	5354.4	86
H53B	9922.18	9725.19	5711.27	86
H53C	8949.3	10650.67	5717.68	86
H5AA	2775.89	8719.84	8704.05	68
H5AB	1565.72	8090.68	8986.83	68

Table 7 Atomic Occupancy for c060917_2_1.

Atom	*Occupancy*	Atom	*Occupancy*	Atom	*Occupancy*
F4	0.571(12)	F1	0.571(12)	F2	0.571(12)
F3	0.571(12)	B1	0.571(12)	F1A	0.429(12)
F4A	0.429(12)	F3A	0.429(12)	B1A	0.429(12)
F2A	0.429(12)				

3.3.4. Crystal structure for [(^{iPr}POCOP)Pd^{II}(CCPh)•Ag^{I}(IPr)]OTf, [**2**]OTf:

Comment: The crystals cracked (burst) at 200 K after a few hours; that's why the crystals were subjected to an additional prior step in order to get XRD data. The crystals were annealed at 20°C, bubbles forming presumably from Et_2O domains within the crystal. After cooling down, a good measurement could be untertaken. Disorder was observed on the co-crystallized THF molecule (special position, 2 orientations) as well as on the anion (2 orientations). In total half a unit of THF was observed.

Crystal Data for $C_{56}H_{76}AgF_3N_2O_{5.5}P_2PdS$ (M =1230.45 g/mol): triclinic, space group P-1 (no. 2), a = 13.06490(10) Å, b = 13.77990(10) Å, c = 18.7504(2) Å, α = 73.4020(10)°, β = 79.1420(10)°, γ = 71.1830(10)°, V = 3044.85(5) Å^3, Z = 2, T = 200.0(1) K, μ(CuKα) = 6.222 mm^{-1}, $Dcalc$ = 1.342 g/cm^3, 63178 reflections measured (7.188° ≤ 2Θ ≤ 159.192°), 12961 unique (R_{int} = 0.0423, R_{sigma} = 0.0285) which were used in all calculations. The final R_1 was 0.0314 (I > 2σ(I)) and wR_2 was 0.0939 (all data).

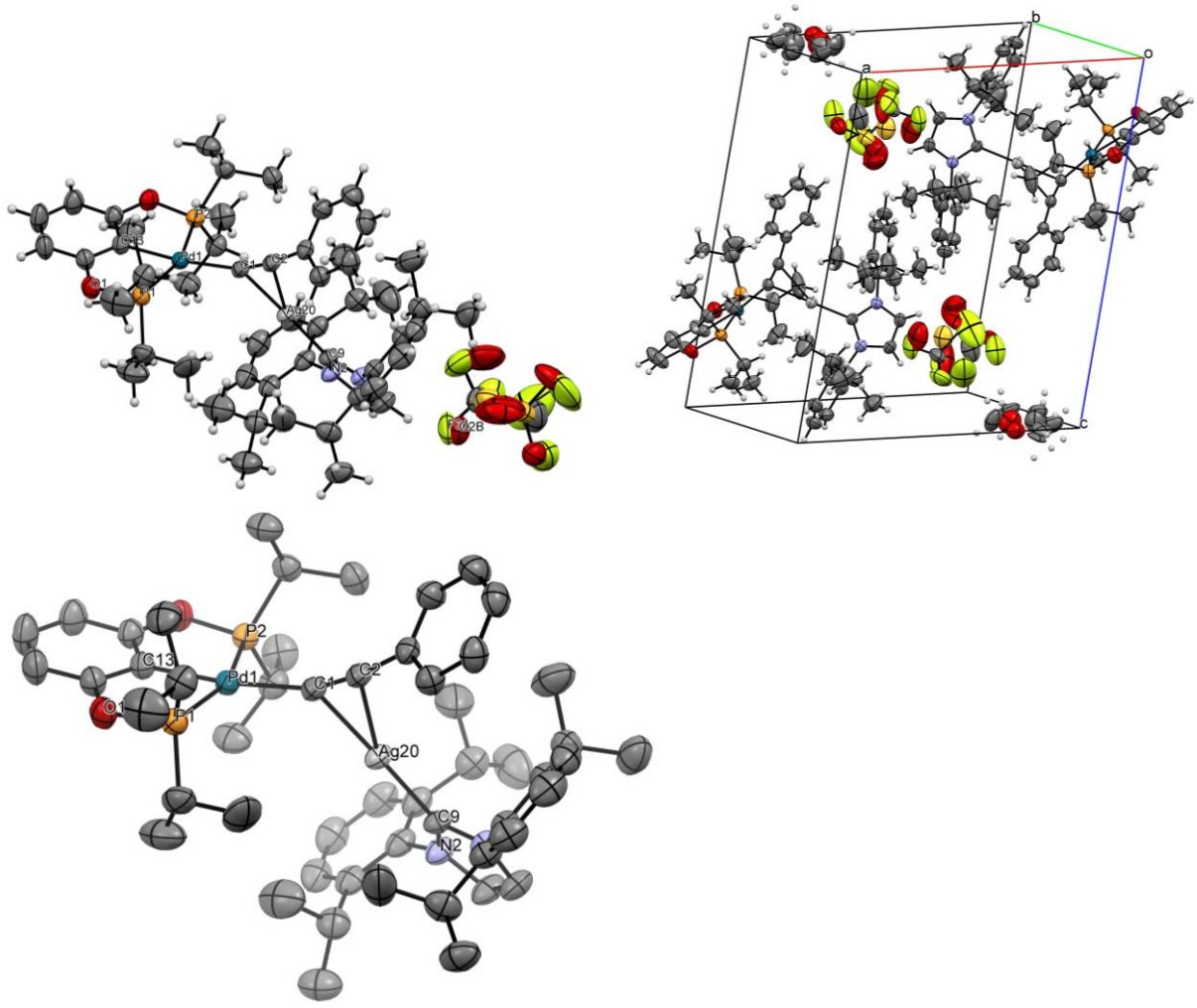

Figure SI-92: Representation of crystal structure from different perspectives. Colors-code: grey/carbon, red/oxygen, light-orange/phosphorus, dark-orange/Cu, yellow/fluorine, orange/sulfur, blue/nitrogen, teal/palladium. *Left)* XRD structure (ORTEP 50% probability ellipsoids), hydrogens and co-crystallizing molecules omitted for clearity. *Right)* representation of the unit cell, crystal packing.

Table 1 Crystal data and structure refinement for c040219_2_1.

Identification code	c040219_2_1
Empirical formula	$C_{56}H_{76}AgF_3N_2O_{5.5}P_2PdS$
Formula weight	1230.45
Temperature/K	200.0(1)
Crystal system	triclinic

Space group	P-1
a/Å	13.06490(10)
b/Å	13.77990(10)
c/Å	18.7504(2)
α/°	73.4020(10)
β/°	79.1420(10)
γ/°	71.1830(10)
Volume/Å^3	3044.85(5)
Z	2
ρ_{calc}g/cm^3	1.342
μ/mm^{-1}	6.222
F(000)	1272.0
Crystal size/mm^3	0.149 × 0.146 × 0.108
Radiation	CuKα (λ = 1.54184)
2Θ range for data collection/°	7.188 to 159.192
Index ranges	-16 ≤ h ≤ 16, -17 ≤ k ≤ 17, -23 ≤ l ≤ 18
Reflections collected	63178
Independent reflections	12961 [R_{int} = 0.0423, R_{sigma} = 0.0285]
Data/restraints/parameters	12961/305/801
Goodness-of-fit on F^2	1.051
Final R indexes [I>=2σ (I)]	R_1 = 0.0314, wR_2 = 0.0920
Final R indexes [all data]	R_1 = 0.0341, wR_2 = 0.0939
Largest diff. peak/hole / e Å^{-3}	0.63/-0.64

Table 2 Fractional Atomic Coordinates (×10^4) and Equivalent Isotropic Displacement Parameters (Å^2×10^3) for c040219_2_1. U_{eq} is defined as 1/3 of of the trace of the orthogonalised U_{IJ} tensor.

Atom	*x*	*y*	*z*	U(eq)
Ag20	2564.1(2)	3070.7(2)	3028.7(2)	36.46(6)
Pd1	478.3(2)	1878.8(2)	2782.8(2)	32.18(6)
P1	1239.4(5)	95.8(5)	3026.5(4)	39.66(13)
P2	-653.2(5)	3495.7(4)	2318.3(3)	35.75(12)
O1	593.4(16)	-344.8(14)	2571.0(11)	50.2(4)
O2	-1513.6(15)	3272.1(14)	1884.7(10)	44.5(4)
N1	4620.8(16)	3731.4(16)	2987.1(11)	38.2(4)
N2	4034.3(17)	4403.0(17)	1914.4(11)	42.4(5)
C1	1241.7(18)	2269.7(18)	3478.8(13)	34.5(5)
C2	1419.5(19)	2409.8(18)	4050.7(13)	36.3(5)
C3	1477(2)	2524.7(19)	4785.1(13)	37.7(5)
C4	2359(2)	1929(2)	5184.9(15)	46.9(6)
C5	2374(3)	1998(2)	5904.4(17)	54.2(7)
C6	1508(3)	2663(3)	6234.3(17)	56.4(7)
C7	632(3)	3278(3)	5838.9(18)	59.9(8)
C8	613(2)	3214(2)	5121.3(16)	49.5(6)
C9	3820.1(18)	3789.6(18)	2594.8(13)	36.1(5)

C10	5311(2)	4310(2)	2556.6(16)	49.9(6)
C11	4943(2)	4728(2)	1883.4(16)	52.1(7)
C12	-988(3)	4830(2)	3244.2(17)	54.0(7)
C13	-435(2)	1473.2(19)	2223.8(13)	38.4(5)
C14	-1577(2)	4267(2)	2938.1(14)	42.5(5)
C15	-22(2)	4372(2)	1577.9(15)	47.3(6)
C16	1001(3)	-632(2)	3991.1(17)	55.5(7)
C17	2655(2)	-446(2)	2695(2)	59.6(8)
C18	-1307(2)	2221(2)	1876.2(14)	42.8(5)
C19	-268(2)	427(2)	2216.3(15)	45.4(6)
C21	-2116(3)	3552(2)	3568.4(17)	58.2(7)
C22	-818(3)	5411(2)	1229.4(18)	61.5(8)
C23	620(3)	3762(3)	991.7(18)	64.2(8)
C24	-219(3)	-365(3)	4223.2(19)	65.7(8)
C25	1512(4)	-1809(3)	4122(3)	94.9(14)
C26	2839(3)	-3(3)	1859(3)	89.9(13)
C27	3370(3)	-195(4)	3132(3)	97.9(16)
C28	-1996(3)	1956(3)	1530.3(18)	56.7(7)
C29	-930(3)	126(3)	1879(2)	61.7(8)
C30	-1791(3)	898(3)	1540(2)	69.2(9)
C31	4707.3(19)	3227(2)	3771.5(14)	39.6(5)
C32	3405(2)	4747(2)	1281.8(14)	43.5(6)
C33	5375(2)	2194(2)	3971.8(16)	47.5(6)
C34	4153(2)	3824(2)	4287.7(15)	45.4(6)
C35	3719(2)	4139(2)	752.2(15)	48.1(6)
C36	2591(2)	5706(2)	1205.9(15)	48.5(6)
C37	5470(3)	1760(3)	4734.0(18)	59.7(8)
C38	5973(3)	1561(3)	3404(2)	62.1(8)
C39	4283(3)	3341(3)	5043.7(16)	55.9(7)
C40	3466(2)	4961(2)	4053.6(18)	53.4(7)
C41	3165(3)	4542(3)	111.1(16)	57.2(7)
C42	4598(3)	3093(3)	861.8(17)	57.7(7)
C43	2287(3)	6360(3)	1785.6(18)	56.7(7)
C44	2070(3)	6059(3)	552.6(17)	58.6(7)
C45	4937(3)	2327(3)	5255.0(17)	64.5(9)
C46	7128(3)	927(3)	3560(2)	71.3(9)
C47	5336(4)	840(4)	3355(4)	109.2(19)
C48	3969(3)	5711(3)	4240(3)	87.5(13)
C49	2307(3)	5106(3)	4431(3)	89.7(13)
C50	2363(3)	5495(3)	18.5(17)	61.5(8)
C51	5418(3)	2990(3)	182(2)	80.1(11)
C52	4096(4)	2184(3)	1124(3)	96.3(14)
C53	2294(5)	7497(3)	1442(3)	100.9(16)
C54	1219(4)	6292(5)	2222(3)	102.8(16)
S1A	6385.4(12)	7217.7(12)	2610.5(8)	61.3(5)
F1A	5496(5)	8158(4)	1362(3)	113.9(18)
F2A	4631(5)	7204(7)	2160(5)	118(3)

F3A	6101(7)	6447(6)	1584(4)	101(2)
O1A	6336(9)	6248(8)	3129(4)	105(4)
O2A	5780(9)	8140(8)	2880(4)	118(4)
O3A	7450(5)	7215(5)	2225(4)	73.1(16)
C1A	5614(5)	7281(5)	1873(4)	64.2(15)
S1B	5839(2)	6973(2)	2329(2)	91.7(12)
F1B	6023(8)	8752(8)	1534(7)	190(5)
F2B	7484(8)	7685(8)	1978(7)	130(4)
F3B	6140(14)	8423(14)	2681(9)	209(8)
O1B	6338(13)	6259(11)	2997(7)	146(7)
O2B	6251(13)	6561(15)	1672(8)	157(7)
O3B	4711(8)	7469(12)	2445(9)	137(6)
C1B	6436(9)	8021(8)	2097(7)	107(3)
O1C	2345(7)	-149(7)	9958(5)	73(2)
C1C	1184(11)	354(12)	10027(8)	68(4)
C2C	1024(17)	1454(12)	9922(14)	101(5)
C3C	1972(14)	1574(14)	9866(11)	91(5)
C4C	2854(13)	667(11)	9739(12)	95(5)
O1D	2264(15)	636(13)	9804(11)	102(5)
C1D	1338(14)	315(15)	10232(8)	62(5)
C2D	481(19)	1244(16)	10005(14)	96(6)
C3D	744(16)	2046(17)	9745(11)	82(5)
C4D	1916(17)	1770(15)	9640(16)	97(8)

Table 3 Anisotropic Displacement Parameters ($Å^2×10^3$) for c040219_2_1. The Anisotropic displacement factor exponent takes the form: $-2\pi^2[h^2a^{*2}U_{11}+2hka^*b^*U_{12}+...]$.

Atom	U_{11}	U_{22}	U_{33}	U_{23}	U_{13}	U_{12}
Ag20	32.55(9)	37.98(9)	37.91(10)	-3.89(7)	-3.21(7)	-13.75(7)
Pd1	31.79(9)	29.74(9)	35.27(9)	-7.49(6)	-5.74(6)	-8.24(6)
P1	37.6(3)	30.5(3)	49.4(3)	-8.9(2)	-6.1(3)	-7.4(2)
P2	36.8(3)	31.7(3)	37.6(3)	-6.0(2)	-8.6(2)	-7.6(2)
O1	54.2(11)	37.5(9)	63.1(12)	-17.8(8)	-12.2(9)	-10.4(8)
O2	44.6(9)	41.0(9)	48.4(10)	-7.1(7)	-18.0(8)	-8.7(7)
N1	33.6(10)	40.0(10)	39.0(10)	-1.8(8)	-6.2(8)	-13.3(8)
N2	39.9(11)	49.3(12)	37.8(10)	-1.1(9)	-4.9(8)	-20.2(9)
C1	31.5(11)	33.6(11)	39.5(12)	-7.3(9)	-4.1(9)	-12.0(9)
C2	32.8(11)	35.7(11)	41.5(12)	-6.6(9)	-2.2(9)	-14.6(9)
C3	39.6(12)	39.6(12)	38.0(12)	-7.3(9)	-4.1(9)	-18.7(10)
C4	47.7(14)	44.5(13)	48.0(14)	-11.0(11)	-10.6(11)	-9.5(11)
C5	63.4(18)	51.1(15)	52.8(16)	-9.7(13)	-23.0(14)	-15.3(13)
C6	71(2)	63.5(18)	44.7(15)	-16.6(13)	-10.5(14)	-26.4(15)
C7	54.7(17)	73(2)	54.3(17)	-28.1(15)	-2.2(13)	-12.2(15)
C8	41.3(13)	60.1(16)	48.8(14)	-18.1(12)	-8.3(11)	-10.7(12)
C9	32.6(11)	38.5(11)	34.8(11)	-3.6(9)	-0.4(9)	-13.4(9)
C10	38.4(13)	59.3(16)	53.0(15)	-1.4(12)	-8.6(11)	-23.9(12)

C11	47.3(15)	61.7(17)	46.8(14)	4.4(12)	-4.2(11)	-30.5(13)
C12	61.3(17)	46.2(14)	56.8(16)	-19.0(12)	-11.9(13)	-9.6(13)
C13	40.2(12)	41.8(12)	37.7(12)	-12.4(10)	-6.6(9)	-13.6(10)
C14	40.2(13)	37.9(12)	46.2(13)	-11.3(10)	-8.3(10)	-3.9(10)
C15	51.9(15)	42.6(13)	46.1(14)	-2.6(11)	-6.2(11)	-18.1(11)
C16	61.3(17)	47.3(15)	55.4(16)	-0.6(12)	-12.3(13)	-19.1(13)
C17	43.1(15)	42.3(14)	89(2)	-23.5(15)	3.8(14)	-5.2(12)
C18	44.3(13)	46.1(13)	41.7(13)	-12.2(11)	-10.3(10)	-13.3(11)
C19	50.5(14)	41.5(13)	48.4(14)	-15.8(11)	-8.4(11)	-12.5(11)
C21	54.4(17)	56.1(17)	55.9(17)	-13.4(13)	7.7(13)	-12.4(13)
C22	77(2)	47.3(15)	52.6(16)	3.4(13)	-15.2(15)	-16.9(15)
C23	69(2)	63.1(19)	51.9(17)	-7.6(14)	9.3(15)	-21.8(16)
C24	70(2)	72(2)	57.2(18)	-8.3(15)	3.0(15)	-35.3(17)
C25	111(3)	45.4(18)	101(3)	8.4(19)	-7(3)	-10(2)
C26	78(3)	71(2)	104(3)	-25(2)	35(2)	-21(2)
C27	38.2(17)	90(3)	175(5)	-61(3)	-22(2)	0.5(18)
C28	58.8(17)	57.5(17)	61.1(17)	-15.7(14)	-25.4(14)	-14.7(14)
C29	72(2)	54.4(17)	74(2)	-28.9(15)	-16.3(16)	-22.3(15)
C30	78(2)	67(2)	81(2)	-26.0(17)	-35.7(19)	-23.5(17)
C31	35.4(11)	44.1(13)	40.2(12)	-5.2(10)	-7.2(9)	-15.5(10)
C32	42.9(13)	51.5(14)	36.3(12)	2.9(10)	-5.9(10)	-24.4(11)
C33	40.0(13)	45.1(14)	51.2(15)	-1.6(11)	-8.7(11)	-10.6(11)
C34	41.7(13)	50.0(14)	46.4(14)	-8.3(11)	-7.7(11)	-17.0(11)
C35	50.0(15)	55.9(15)	39.7(13)	-2.2(11)	-3.3(11)	-25.6(12)
C36	46.5(14)	51.8(15)	47.0(14)	-1.2(12)	-8.8(11)	-20.8(12)
C37	53.6(17)	55.4(17)	57.7(17)	7.6(14)	-16.1(14)	-11.6(13)
C38	56.5(18)	50.0(16)	68.2(19)	-12.5(14)	-10.0(15)	0.5(13)
C39	58.8(17)	73(2)	40.7(14)	-11.8(13)	-5.6(12)	-27.4(15)
C40	52.9(16)	48.7(15)	58.7(17)	-17.0(13)	-6.4(13)	-11.0(12)
C41	67.1(19)	71.0(19)	39.7(14)	-7.7(13)	-6.1(13)	-32.7(16)
C42	62.1(18)	60.6(17)	50.5(16)	-10.6(13)	-3.1(13)	-21.7(14)
C43	56.7(17)	56.3(17)	54.8(16)	-7.8(13)	-10.4(13)	-15.4(14)
C44	55.1(17)	58.5(17)	57.9(17)	3.8(14)	-20.4(14)	-18.1(14)
C45	64.2(19)	80(2)	44.4(15)	8.3(15)	-16.6(14)	-28.0(17)
C46	48.8(17)	51.6(17)	101(3)	-10.7(17)	0.5(17)	-8.5(14)
C47	65(2)	105(3)	182(5)	-89(4)	-36(3)	3(2)
C48	64(2)	61(2)	147(4)	-37(2)	-14(2)	-19.6(17)
C49	47.8(19)	66(2)	147(4)	-24(2)	1(2)	-12.0(16)
C50	67.9(19)	72(2)	46.2(15)	1.6(14)	-21.2(14)	-28.3(16)
C51	69(2)	84(3)	75(2)	-16(2)	11.7(18)	-19(2)
C52	98(3)	60(2)	116(4)	-9(2)	18(3)	-30(2)
C53	143(4)	67(2)	98(3)	-27(2)	18(3)	-47(3)
C54	99(3)	134(4)	101(3)	-62(3)	35(3)	-64(3)
S1A	58.1(9)	66.1(10)	53.5(8)	-26.3(6)	-12.3(6)	4.7(6)
F1A	132(4)	124(4)	84(3)	18(3)	-59(3)	-46(3)
F2A	58(3)	135(6)	163(6)	-33(4)	-23(3)	-28(3)
F3A	119(5)	122(4)	109(4)	-71(3)	12(3)	-73(4)

O1A	95(7)	125(7)	47(3)	7(3)	11(3)	-2(5)
O2A	125(6)	126(6)	83(4)	-66(4)	-28(4)	38(5)
O3A	58(3)	92(5)	75(3)	-34(3)	-15(2)	-11(3)
C1A	65(3)	80(4)	52(3)	-17(3)	-19(3)	-21(3)
S1B	69.2(16)	68.6(15)	127(3)	-30.8(17)	-7.4(18)	-0.7(12)
F1B	162(9)	121(7)	242(10)	72(7)	-64(8)	-56(6)
F2B	89(5)	112(8)	204(12)	-66(7)	-23(6)	-21(5)
F3B	166(13)	194(13)	306(14)	-195(13)	-57(11)	31(10)
O1B	80(9)	75(8)	200(12)	19(8)	-7(9)	39(6)
O2B	88(7)	200(14)	265(14)	-177(12)	28(8)	-69(8)
O3B	67(6)	96(8)	208(16)	-22(8)	-4(7)	12(5)
C1B	94(6)	72(6)	168(10)	-42(6)	-41(7)	-15(5)
O1C	94(6)	62(4)	68(5)	-14(4)	-11(4)	-31(4)
C1C	95(7)	88(7)	40(7)	-37(6)	-13(6)	-30(6)
C2C	94(8)	69(7)	126(13)	-4(9)	-23(10)	-18(6)
C3C	127(9)	87(8)	67(11)	-13(8)	-29(8)	-36(7)
C4C	84(8)	67(7)	123(12)	8(7)	3(9)	-41(6)
O1D	119(9)	71(8)	121(11)	-33(8)	0(9)	-29(7)
C1D	91(9)	77(8)	28(8)	-9(6)	-34(6)	-24(7)
C2D	101(9)	73(9)	80(11)	8(8)	7(10)	-13(7)
C3D	91(9)	77(8)	61(9)	3(8)	-5(8)	-20(7)
C4D	110(9)	70(8)	71(14)	15(9)	22(10)	-21(8)

Table 4 Bond Lengths for c040219_2_1.

Atom	Atom	Length/Å	Atom	Atom	Length/Å
Ag20	C1	2.250(2)	C32	C35	1.399(4)
Ag20	C2	2.354(2)	C32	C36	1.393(4)
Ag20	C9	2.103(2)	C33	C37	1.395(4)
Pd1	P1	2.2777(6)	C33	C38	1.511(4)
Pd1	P2	2.2715(6)	C34	C39	1.400(4)
Pd1	C1	2.056(2)	C34	C40	1.517(4)
Pd1	C13	2.018(2)	C35	C41	1.402(4)
P1	O1	1.6460(19)	C35	C42	1.514(4)
P1	C16	1.824(3)	C36	C43	1.522(4)
P1	C17	1.818(3)	C36	C44	1.400(4)
P2	O2	1.6523(18)	C37	C45	1.371(5)
P2	C14	1.813(3)	C38	C46	1.515(4)
P2	C15	1.822(3)	C38	C47	1.517(6)
O1	C19	1.395(3)	C39	C45	1.371(5)
O2	C18	1.390(3)	C40	C48	1.534(5)
N1	C9	1.358(3)	C40	C49	1.521(5)
N1	C10	1.386(3)	C41	C50	1.380(5)
N1	C31	1.445(3)	C42	C51	1.510(5)
N2	C9	1.350(3)	C42	C52	1.515(5)
N2	C11	1.384(3)	C43	C53	1.516(5)

N2	C32	1.450(3)	C43	C54	1.495(5)
C1	C2	1.217(3)	C44	C50	1.364(5)
C2	C3	1.448(3)	S1A	O1A	1.423(9)
C3	C4	1.389(4)	S1A	O2A	1.436(8)
C3	C8	1.398(4)	S1A	O3A	1.441(6)
C4	C5	1.383(4)	S1A	C1A	1.827(6)
C5	C6	1.377(5)	F1A	C1A	1.294(8)
C6	C7	1.383(5)	F2A	C1A	1.322(8)
C7	C8	1.379(4)	F3A	C1A	1.332(9)
C10	C11	1.338(4)	S1B	O1B	1.466(10)
C12	C14	1.526(4)	S1B	O2B	1.443(10)
C13	C18	1.387(3)	S1B	O3B	1.414(9)
C13	C19	1.391(3)	S1B	C1B	1.768(11)
C14	C21	1.527(4)	F1B	C1B	1.296(11)
C15	C22	1.523(4)	F2B	C1B	1.293(11)
C15	C23	1.531(4)	F3B	C1B	1.305(12)
C16	C24	1.522(5)	O1C	C1C	1.449(13)
C16	C25	1.507(5)	O1C	C4C	1.411(13)
C17	C26	1.515(5)	C1C	C2C	1.421(12)
C17	C27	1.525(5)	C2C	C3C	1.28(2)
C18	C28	1.389(4)	C3C	C4C	1.444(13)
C19	C29	1.381(4)	O1D	C1D	1.442(16)
C28	C30	1.390(5)	O1D	C4D	1.437(17)
C29	C30	1.383(5)	C1D	C2D	1.421(13)
C31	C33	1.394(4)	C2D	C3D	1.21(2)
C31	C34	1.395(4)	C3D	C4D	1.442(13)

Table 5 Bond Angles for c040219_2_1.

Atom	Atom	Atom	Angle/°	Atom	Atom	Atom	Angle/°
C1	Ag20	C2	30.56(8)	C29	C30	C28	121.6(3)
C9	Ag20	C1	178.60(9)	C33	C31	N1	118.8(2)
C9	Ag20	C2	150.32(9)	C33	C31	C34	123.5(2)
P2	Pd1	P1	159.44(2)	C34	C31	N1	117.6(2)
C1	Pd1	P1	100.69(6)	C35	C32	N2	117.6(2)
C1	Pd1	P2	99.63(6)	C36	C32	N2	118.1(2)
C13	Pd1	P1	79.50(7)	C36	C32	C35	124.1(2)
C13	Pd1	P2	79.94(7)	C31	C33	C37	116.6(3)
C13	Pd1	C1	171.84(9)	C31	C33	C38	122.7(3)
O1	P1	Pd1	105.85(7)	C37	C33	C38	120.7(3)
O1	P1	C16	102.40(13)	C31	C34	C39	117.0(3)
O1	P1	C17	102.42(13)	C31	C34	C40	122.5(2)
C16	P1	Pd1	115.95(11)	C39	C34	C40	120.4(3)
C17	P1	Pd1	119.93(10)	C32	C35	C41	116.5(3)
C17	P1	C16	107.85(15)	C32	C35	C42	122.4(2)
O2	P2	Pd1	105.34(7)	C41	C35	C42	121.1(3)

O2	P2	C14	101.39(11)	C32	C36	C43	122.7(2)
O2	P2	C15	103.06(11)	C32	C36	C44	116.3(3)
C14	P2	Pd1	120.92(9)	C44	C36	C43	121.0(3)
C14	P2	C15	108.28(13)	C45	C37	C33	121.3(3)
C15	P2	Pd1	115.25(9)	C33	C38	C46	113.6(3)
C19	O1	P1	114.34(16)	C33	C38	C47	109.8(3)
C18	O2	P2	114.57(15)	C46	C38	C47	110.2(3)
C9	N1	C10	111.3(2)	C45	C39	C34	120.6(3)
C9	N1	C31	125.67(19)	C34	C40	C48	110.6(3)
C10	N1	C31	122.8(2)	C34	C40	C49	111.2(3)
C9	N2	C11	111.5(2)	C49	C40	C48	109.7(3)
C9	N2	C32	127.0(2)	C50	C41	C35	120.6(3)
C11	N2	C32	121.5(2)	C35	C42	C52	110.4(3)
Pd1	C1	Ag20	121.53(11)	C51	C42	C35	113.3(3)
C2	C1	Ag20	79.41(15)	C51	C42	C52	112.1(3)
C2	C1	Pd1	158.77(19)	C53	C43	C36	112.4(3)
C1	C2	Ag20	70.03(15)	C54	C43	C36	110.6(3)
C1	C2	C3	170.8(2)	C54	C43	C53	111.7(4)
C3	C2	Ag20	118.98(15)	C50	C44	C36	121.4(3)
C4	C3	C2	121.4(2)	C37	C45	C39	121.0(3)
C4	C3	C8	118.4(2)	C44	C50	C41	121.2(3)
C8	C3	C2	120.2(2)	O1A	S1A	O2A	114.0(5)
C5	C4	C3	120.9(3)	O1A	S1A	O3A	114.4(5)
C6	C5	C4	120.1(3)	O1A	S1A	C1A	102.9(6)
C5	C6	C7	119.8(3)	O2A	S1A	O3A	116.4(6)
C8	C7	C6	120.4(3)	O2A	S1A	C1A	103.3(4)
C7	C8	C3	120.4(3)	O3A	S1A	C1A	103.2(3)
N1	C9	Ag20	124.67(16)	F1A	C1A	S1A	112.6(4)
N2	C9	Ag20	131.39(17)	F1A	C1A	F2A	107.4(7)
N2	C9	N1	103.93(19)	F1A	C1A	F3A	111.7(6)
C11	C10	N1	106.5(2)	F2A	C1A	S1A	110.0(5)
C10	C11	N2	106.8(2)	F2A	C1A	F3A	106.4(7)
C18	C13	Pd1	121.05(18)	F3A	C1A	S1A	108.6(5)
C18	C13	C19	117.2(2)	O1B	S1B	C1B	104.1(10)
C19	C13	Pd1	121.57(19)	O2B	S1B	O1B	112.4(8)
C12	C14	P2	111.06(19)	O2B	S1B	C1B	99.4(9)
C12	C14	C21	111.5(2)	O3B	S1B	O1B	115.4(8)
C21	C14	P2	109.55(18)	O3B	S1B	O2B	118.4(9)
C22	C15	P2	114.1(2)	O3B	S1B	C1B	104.3(8)
C22	C15	C23	111.9(2)	F1B	C1B	S1B	111.1(8)
C23	C15	P2	108.2(2)	F1B	C1B	F3B	107.2(10)
C24	C16	P1	108.7(2)	F2B	C1B	S1B	111.5(8)
C25	C16	P1	113.9(3)	F2B	C1B	F1B	111.6(10)
C25	C16	C24	111.4(3)	F2B	C1B	F3B	111.2(11)
C26	C17	P1	109.6(2)	F3B	C1B	S1B	103.9(12)
C26	C17	C27	112.6(4)	C4C	O1C	C1C	106.8(10)
C27	C17	P1	108.5(2)	C2C	C1C	O1C	107.6(13)

C13	C18	O2	118.9(2)	C3C	C2C	C1C	106.3(16)
C13	C18	C28	122.4(3)	C2C	C3C	C4C	114.1(17)
C28	C18	O2	118.6(2)	O1C	C4C	C3C	102.5(13)
C13	C19	O1	118.5(2)	C4D	O1D	C1D	104.9(13)
C29	C19	O1	119.1(2)	C2D	C1D	O1D	100.7(15)
C29	C19	C13	122.4(3)	C3D	C2D	C1D	116(2)
C18	C28	C30	117.9(3)	C2D	C3D	C4D	108(2)
C19	C29	C30	118.4(3)	O1D	C4D	C3D	104.8(17)

Table 6 Hydrogen Atom Coordinates (Å×10^4) and Isotropic Displacement Parameters (Å^2×10^3) for c040219_2_1.

Atom	*x*	*y*	*z*	U(eq)
H4	2947.81	1478.02	4965.93	56
H5	2970.46	1593.32	6165.68	65
H6	1511.73	2699.85	6721.46	68
H7	52.57	3736.63	6058.31	72
H8	21.59	3631.98	4859	59
H10	5911.38	4391.1	2706.12	60
H11	5240.02	5155.38	1473.57	63
H12A	-365.82	4324.78	3470.5	81
H12B	-1471.86	5168.21	3611.99	81
H12C	-755.23	5351.9	2842.52	81
H14	-2146.27	4804.52	2650.1	51
H15	501.12	4542.5	1799	57
H16	1321.77	-376.71	4307.58	67
H17	2815.49	-1215.18	2794.04	71
H21A	-2430.32	3169.22	3358.83	87
H21B	-2674.92	3975.43	3856.41	87
H21C	-1580.7	3063.25	3886.16	87
H22A	-1371.72	5269.13	1037.16	92
H22B	-436.33	5815.15	828.87	92
H22C	-1147.86	5804.83	1602.57	92
H23A	1147.99	3138.97	1225.49	96
H23B	984.04	4201.32	606.17	96
H23C	130.86	3562.61	775.95	96
H24A	-515.19	386.07	4156.51	98
H24B	-353.27	-709.43	4739.76	98
H24C	-558.07	-601.81	3919.61	98
H25A	1303.58	-2065.57	3762.17	142
H25B	1269.29	-2150.53	4617.63	142
H25C	2289.37	-1960.56	4069	142
H26A	2388.06	-199.36	1607.75	135
H26B	3588.9	-281.43	1685.41	135
H26C	2656.59	753.54	1752.51	135
H27A	3202.28	557.21	3052.93	147

H27B	4120.91	-477.19	2963.39	147
H27C	3236.69	-506.07	3656	147
H28	-2575.41	2469.87	1299.46	68
H29	-799.92	-579.33	1880.56	74
H30	-2244.04	703.99	1312.87	83
H37	5904.8	1071.37	4891.89	72
H38	6008.05	2059.42	2914.39	74
H39	3922.53	3711.08	5405.76	67
H40	3442.73	5144.45	3510.75	64
H41	3338.86	4162.61	-254.98	69
H42	4995.63	3058.1	1266.67	69
H43	2840.35	6047.62	2137.91	68
H44	1513.92	6689.59	481.37	70
H45	5019.19	2019.44	5759.12	77
H46A	7510.3	1384.2	3617.57	107
H46B	7489.1	612.82	3150.5	107
H46C	7114.97	380.88	4011.79	107
H47A	5285.86	343.26	3829.32	164
H47B	5699.89	465.34	2976.4	164
H47C	4618.1	1254.77	3230.03	164
H48A	3983.15	5551.6	4771.8	131
H48B	3541.62	6427.62	4068.33	131
H48C	4697.39	5622.06	3997.06	131
H49A	1984.62	4656.56	4295.8	135
H49B	1889.51	5829.24	4270.33	135
H49C	2314.83	4922.4	4963.95	135
H50	2015.48	5758.68	-415.83	74
H51A	5061.06	3006.92	-226.35	120
H51B	5977.26	2332.43	295.35	120
H51C	5735.26	3564.67	45.95	120
H52A	3588.74	2274.9	1559.36	144
H52B	4657.69	1530.49	1246.58	144
H52C	3723.73	2171.94	733.17	144
H53A	2989.74	7511.21	1166.98	151
H53B	2160.49	7861.53	1831.64	151
H53C	1736.56	7837.28	1110.23	151
H54A	649.65	6639.06	1900.31	154
H54B	1085.71	6629.98	2626.66	154
H54C	1236.68	5563.6	2420.11	154
H1CA	849.15	232.57	9653.3	82
H1CB	856.88	65.89	10518.86	82
H2CA	675.79	1848.82	9470.7	121
H2CB	569.35	1699.53	10344.12	121
H3CA	2053.31	1729.22	10321.41	109
H3CB	2024.75	2179.07	9455.99	109
H4CA	3145.9	767.35	9216.09	115
H4CB	3434.6	522.12	10043.12	115

H1DA	1256.8	-285.38	10100.55	75
H1DB	1386.14	145.73	10766.21	75
H2DA	127.47	1135.88	9634.53	115
H2DB	-52.7	1338.94	10434.11	115
H3DA	461.7	2512.41	10083.07	98
H3DB	451.53	2409.57	9270.15	98
H4DA	2170.53	2070.29	9129.8	116
H4DB	2187.94	2023.34	9978.37	116

Table 7 Atomic Occupancy for c040219_2_1.

Atom	*Occupancy*	Atom	*Occupancy*	Atom	*Occupancy*
S1A	0.582(3)	F1A	0.582(3)	F2A	0.582(3)
F3A	0.582(3)	O1A	0.582(3)	O2A	0.582(3)
O3A	0.582(3)	C1A	0.582(3)	S1B	0.418(3)
F1B	0.418(3)	F2B	0.418(3)	F3B	0.418(3)
O1B	0.418(3)	O2B	0.418(3)	O3B	0.418(3)
C1B	0.418(3)	O1C	0.2912(17)	C1C	0.2912(17)
H1CA	0.2912(17)	H1CB	0.2912(17)	C2C	0.2912(17)
H2CA	0.2912(17)	H2CB	0.2912(17)	C3C	0.2912(17)
H3CA	0.2912(17)	H3CB	0.2912(17)	C4C	0.2912(17)
H4CA	0.2912(17)	H4CB	0.2912(17)	O1D	0.2088(17)
C1D	0.2088(17)	H1DA	0.2088(17)	H1DB	0.2088(17)
C2D	0.2088(17)	H2DA	0.2088(17)	H2DB	0.2088(17)
C3D	0.2088(17)	H3DA	0.2088(17)	H3DB	0.2088(17)
C4D	0.2088(17)	H4DA	0.2088(17)	H4DB	0.2088(17)

3.3.5. Crystal structure for [($^{i\text{Pr}}$POCOP)Pd$^{\text{II}}$(CCPh)•Ag$^{\text{I}}$(IPr)]BArF, [**2**]BArF:

Comment: The $BArF^-$ anion shows disorder.

Crystal Data for $C_{85}H_{84}AgBF_{24}N_2O_2P_2Pd$ (M =1908.56 g/mol): triclinic, space group P-1 (no. 2), a = 15.70660(10) Å, b = 16.49960(10) Å, c = 18.15710(10) Å, α = 105.2690(10)°, β = 107.8080(10)°, γ = 97.3030(10)°, V = 4209.95(5) Å^3, Z = 2, T = 100.0(1) K, μ(Cu Kα) = 4.836 mm^{-1}, $Dcalc$ = 1.506 g/cm^3, 163544 reflections measured (5.396° ≤ 2Θ ≤ 160.242°), 17959 unique (R_{int} = 0.0418, R_{sigma} = 0.0205) which were used in all calculations. The final R_1 was 0.0257 (I > 2σ(I)) and wR_2 was 0.0627 (all data).

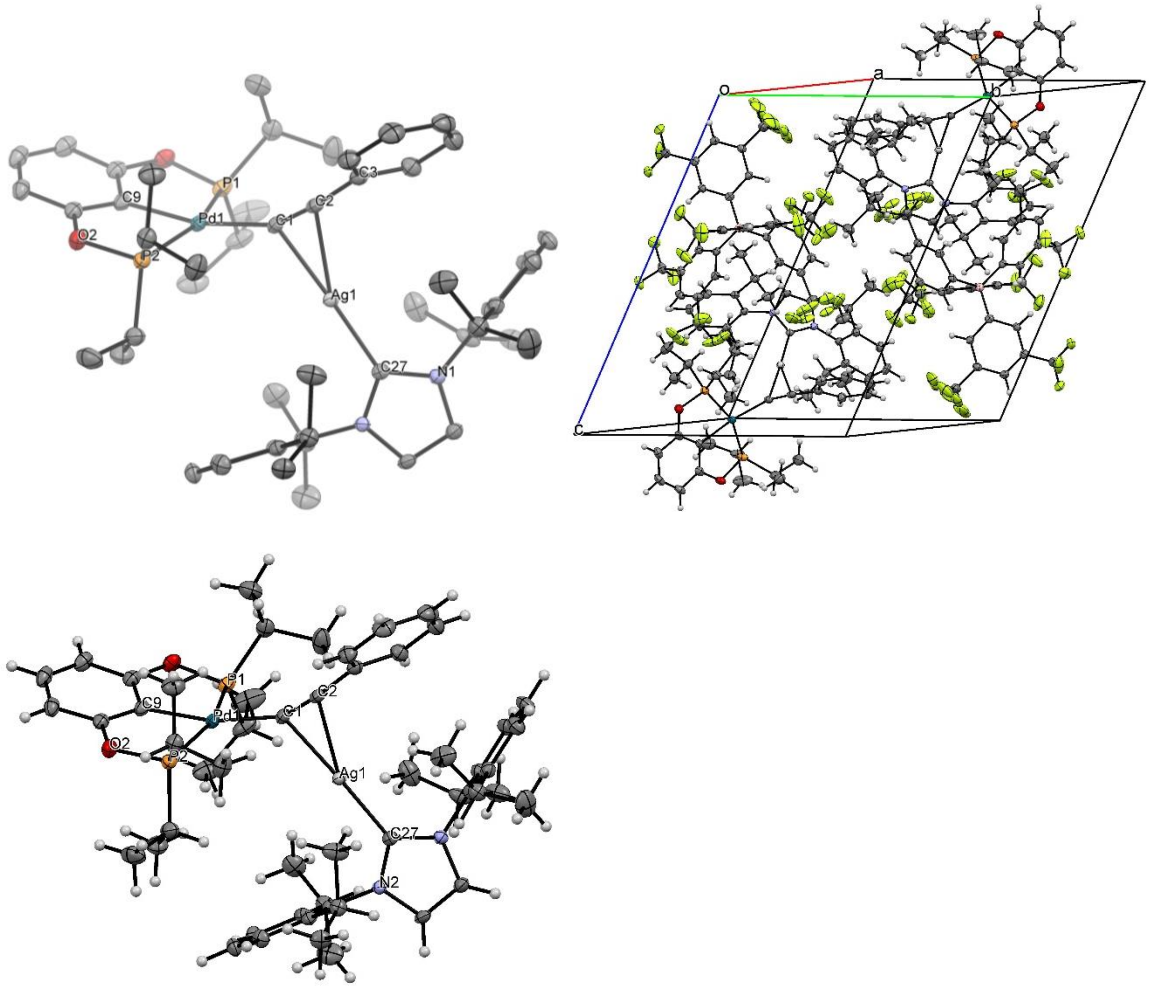

Figure SI-93: Representation of crystal structure from different perspectives. Color-code: grey/carbon, red/oxygen, light-orange/phosphorus, gray/Ag, yellow/fluorine, pink/boron, blue/nitrogen, teal/palladium. *Left)* XRD structure (ORTEP 50% probability ellipsoids), hydrogens and co-crystallizing molecules omitted for clearity. *Right)* representation of the unit cell, crystal packing.

Table 1 Crystal data and structure refinement for c120819_2_1.

Identification code	c120819_2_1
Empirical formula	$C_{85}H_{84}AgBF_{24}N_2O_2P_2Pd$
Formula weight	1908.56
Temperature/K	100.0(1)
Crystal system	triclinic
Space group	P-1
a/Å	15.70660(10)
b/Å	16.49960(10)

c/Å	18.15710(10)
α/°	105.2690(10)
β/°	107.8080(10)
γ/°	97.3030(10)
Volume/Å^3	4209.95(5)
Z	2
ρ_{calc}g/cm^3	1.506
μ/mm^{-1}	4.836
F(000)	1936.0
Crystal size/mm^3	0.306 × 0.145 × 0.113
Radiation	Cu Kα (λ = 1.54184)
2Θ range for data collection/°	5.396 to 160.242
Index ranges	-20 ≤ h ≤ 20, -20 ≤ k ≤ 20, -23 ≤ l ≤ 23
Reflections collected	163544
Independent reflections	17959 [R_{int} = 0.0418, R_{sigma} = 0.0205]
Data/restraints/parameters	17959/692/1248
Goodness-of-fit on F^2	1.043
Final R indexes [I>=2σ (I)]	R_1 = 0.0257, wR_2 = 0.0621
Final R indexes [all data]	R_1 = 0.0268, wR_2 = 0.0627
Largest diff. peak/hole / e Å^{-3}	0.53/-0.62

Table 2 Fractional Atomic Coordinates (×10^4) and Equivalent Isotropic Displacement Parameters (Å^2×10^3) for c120819_2_1. U_{eq} is defined as 1/3 of of the trace of the orthogonalised U_{IJ} tensor.

Atom	*x*	*y*	*z*	U(eq)
Ag1	3391.4(2)	7087.8(2)	1745.0(2)	15.84(3)
Pd1	4419.7(2)	7453.7(2)	184.4(2)	15.44(3)
P1	3167.3(3)	7143.6(3)	-969.9(3)	19.79(9)
P2	5854.3(3)	8125.1(3)	1110.0(3)	18.32(9)
O1	3567.3(9)	7374.7(8)	-1649.0(7)	22.8(3)
O2	6426.6(8)	8480.4(8)	590.9(8)	22.2(3)
N1	2185.7(9)	7116.6(9)	2832.1(8)	15.8(3)
N2	3207.4(9)	8289.8(9)	3287.6(8)	15.0(3)
C1	3957.0(11)	6672.0(11)	758.0(10)	17.3(3)
C2	3794.1(11)	5996.9(11)	903.3(10)	18.3(3)
C3	3634.0(12)	5158.2(11)	1006.6(10)	19.3(3)
C4	4374.0(14)	4813.8(13)	1344.7(12)	26.6(4)
C5	4211.2(15)	4013.6(13)	1449.8(13)	32.1(4)
C6	3320.0(16)	3551.4(12)	1221.7(13)	31.1(4)
C7	2586.8(14)	3881.7(12)	884.6(12)	28.3(4)
C8	2740.3(13)	4684.1(12)	779.8(12)	23.9(4)
C9	4977.0(12)	7953.9(11)	-506.2(11)	19.0(3)
C10	4491.4(12)	7793.6(11)	-1331.3(11)	20.7(3)
C11	4899.6(14)	8004.0(12)	-1857.3(12)	25.9(4)
C12	5825.5(14)	8406.1(13)	-1529.7(13)	27.3(4)

Table 2 Fractional Atomic Coordinates (×10^4) and Equivalent Isotropic Displacement Parameters (Å^2×10^3) for c120819_2_1. U_{eq} is defined as 1/3 of of the trace of the orthogonalised U_{IJ} tensor.

Atom	*x*	*y*	*z*	U(eq)
C13	6341.8(13)	8595.8(12)	-709.3(12)	24.4(4)
C14	5905.2(12)	8348.8(11)	-217.1(11)	20.0(3)
C15	2348.4(14)	7836.0(14)	-920.8(12)	30.5(4)
C16	1571.8(17)	7641.7(19)	-1742.1(14)	49.8(7)
C17	2861.4(17)	8780.1(15)	-599.8(14)	40.0(5)
C18	2508.9(13)	6041.5(13)	-1529.9(12)	26.1(4)
C19	1871.7(15)	5759.6(17)	-1106.6(14)	40.7(5)
C20	3170.9(15)	5444.0(13)	-1608.5(14)	34.1(5)
C21	5919.4(13)	9126.8(12)	1880.7(12)	26.0(4)
C22	5382.6(15)	9681.8(13)	1444.2(14)	32.6(4)
C23	6906.4(15)	9621.6(15)	2401.2(15)	39.6(5)
C24	6626.1(12)	7535.4(12)	1601.4(11)	23.2(4)
C25	6588.5(15)	6699.6(13)	963.4(13)	32.8(4)
C26	6380.6(14)	7361.5(15)	2305.8(13)	32.2(4)
C27	2882.9(11)	7527.6(10)	2677.2(10)	15.6(3)
C28	2074.2(12)	7616.0(11)	3524.4(11)	20.2(3)
C29	2714.3(12)	8358.1(11)	3810.5(11)	19.5(3)
C30	3917.3(11)	8972.2(10)	3338.6(10)	16.1(3)
C31	4813.0(11)	9082.2(11)	3872.1(10)	17.0(3)
C32	5468.0(12)	9766.7(12)	3920.8(11)	21.3(4)
C33	5240.0(12)	10307.4(12)	3456.5(12)	23.0(4)
C34	4351.4(13)	10170.2(11)	2928.6(11)	22.1(4)
C35	3661.4(12)	9502.1(11)	2857.9(10)	18.3(3)
C36	5071.6(12)	8479.6(11)	4370.9(11)	19.6(3)
C37	5197.7(15)	7641.5(13)	3853.0(12)	31.8(4)
C38	5936.2(13)	8889.7(12)	5127.7(11)	25.5(4)
C39	2680.7(12)	9391.9(12)	2300.8(11)	22.8(4)
C40	2617.3(15)	9211.4(15)	1412.0(12)	34.3(5)
C41	2306.6(14)	10184.5(15)	2582.7(15)	37.5(5)
C42	1680.0(11)	6237.4(11)	2375.1(10)	17.4(3)
C43	896.7(12)	6082.9(11)	1685.8(11)	20.2(3)
C44	440.2(12)	5224.7(12)	1260.1(12)	24.6(4)
C45	744.5(13)	4563.9(12)	1522.1(12)	26.3(4)
C46	1512.4(13)	4737.9(12)	2212.3(12)	24.1(4)
C47	2006.3(12)	5584.3(11)	2658.1(11)	19.3(3)
C48	2864.2(12)	5763.1(12)	3402.1(11)	22.2(4)
C49	2674.2(17)	5408.0(17)	4045.3(14)	43.1(6)
C50	3616.2(14)	5401.6(16)	3147.4(14)	36.5(5)
C51	551.4(13)	6809.0(12)	1399.8(12)	25.2(4)
C52	920.2(15)	6959.5(15)	748.0(14)	36.4(5)
C53	-499.4(14)	6636.6(13)	1073.5(14)	32.7(5)
F1A	9881(5)	7040(6)	3440(7)	29.7(11)
F2A	8565(4)	7088(7)	2690(4)	73(2)
F3A	9746(6)	8078(3)	2964(4)	49.5(13)

Table 2 Fractional Atomic Coordinates ($\times 10^4$) and Equivalent Isotropic Displacement Parameters ($Å^2 \times 10^3$) for c120819_2_1. U_{eq} is defined as 1/3 of of the trace of the orthogonalised U_{IJ} tensor.

Atom	*x*	*y*	*z*	U(eq)
F4A	7634.1(8)	10105.7(8)	4535.6(9)	41.8(3)
F5A	8896.7(8)	10585.3(7)	4411.8(8)	31.3(3)
F6A	8840.1(9)	10693.6(7)	5598.8(8)	36.7(3)
F7A	6009(6)	7848(3)	6628(6)	34.1(13)
F8A	5889(6)	6612(6)	6792(5)	42.1(13)
F9A	4955(4)	6781(4)	5732(4)	43.5(11)
F10B	5988(5)	4542(5)	3814(7)	56(2)
F11B	5907(6)	5521(7)	3239(7)	43(2)
F12B	7138(8)	5078(9)	3564(11)	35(2)
F13A	12145.7(10)	7592.6(14)	5376.2(10)	67.6(5)
F14A	12705.7(10)	8120.4(9)	6666.4(10)	53.0(4)
F15A	12881.1(9)	6894.2(9)	6091.0(11)	54.5(4)
F16A	10944.6(12)	4538.1(10)	6253.3(14)	70.1(6)
F17A	10240.7(12)	4986.8(8)	7046.9(8)	50.1(4)
F18A	9504.9(11)	4418.8(8)	5785.8(9)	54.7(4)
F19A	10229.7(11)	11172.4(8)	8357.6(10)	51.7(4)
F20A	11180.3(8)	10758.9(7)	7790.1(7)	32.3(3)
F21A	11441.6(11)	10862.5(10)	9045.2(8)	59.3(5)
F22A	9268(4)	7448(2)	8929(3)	45.0(12)
F23A	9850(3)	8696(3)	9803(2)	37.8(10)
F24A	8433(3)	8362(4)	9031(3)	59.6(13)
C1A	9051.5(11)	8153.3(11)	5356.0(10)	17.3(3)
C2A	9212.6(12)	7726.6(11)	4649.6(11)	19.6(3)
C3A	9148.9(12)	8065.4(12)	4018.0(11)	21.8(4)
C4A	8938.3(12)	8865.7(12)	4064.4(11)	21.9(4)
C5A	8776.1(11)	9303.3(11)	4757.3(11)	19.5(3)
C6A	8814.5(11)	8947.0(11)	5381.0(11)	17.4(3)
C7A	9304.8(14)	7554.1(13)	3274.5(12)	29.3(4)
C8A	8545.2(12)	10165.2(12)	4825.7(12)	23.5(4)
C9A	8026.6(11)	7093.2(11)	5737.1(10)	17.3(3)
C10A	7382.4(12)	7276.8(11)	6108.1(11)	18.7(3)
C11A	6476.5(12)	6794.9(11)	5774.1(11)	19.9(3)
C12A	6170.4(12)	6129.2(11)	5042.6(11)	21.1(3)
C13A	6789.1(12)	5953.3(11)	4648.3(11)	19.6(3)
C14A	7695.3(12)	6413.2(11)	4995.0(11)	19.2(3)
C15A	5834.1(13)	6994.0(12)	6225.1(12)	25.7(4)
C16A	6452.2(13)	5293.3(13)	3819.3(12)	27.3(4)
C17A	9847.7(12)	7089.4(11)	6081.8(10)	17.2(3)
C18A	10704.8(12)	7435.0(11)	6067.5(10)	18.9(3)
C19A	11393.1(12)	6979.0(12)	6103.5(11)	20.1(3)
C20A	11268.5(12)	6161.0(12)	6179.3(11)	21.6(4)
C21A	10435.8(12)	5812.5(11)	6213.1(10)	19.3(3)
C22A	9737.1(12)	6268.0(11)	6162.6(10)	18.2(3)
C23A	12277.7(13)	7386.2(13)	6055.9(13)	27.8(4)

Table 2 Fractional Atomic Coordinates ($\times 10^4$) and Equivalent Isotropic Displacement Parameters ($Å^2 \times 10^3$) for c120819_2_1. U_{eq} is defined as 1/3 of of the trace of the orthogonalised U_{IJ} tensor.

Atom	*x*	*y*	*z*	U(eq)
C24A	10282.2(13)	4942.3(12)	6318.1(11)	23.0(4)
C25A	9406.4(11)	8343.2(11)	6985.6(10)	17.1(3)
C26A	9947.7(11)	9181.2(11)	7249.3(11)	17.7(3)
C27A	10259.9(11)	9706.3(11)	8060.0(11)	18.7(3)
C28A	10048.4(12)	9420.4(11)	8651.4(11)	19.8(3)
C29A	9529.7(12)	8589.4(11)	8409.6(11)	20.4(3)
C30A	9226.9(12)	8063.6(11)	7601.0(11)	18.5(3)
C31A	10781.0(14)	10618.5(12)	8312.3(12)	27.2(4)
C32A	9286.2(16)	8265.2(13)	9031.5(12)	32.4(4)
B1A	9075.7(13)	7678.5(12)	6051.7(12)	16.7(4)
F10A	7074(6)	4901(7)	3649(8)	42(2)
F11A	5714(4)	4702(4)	3686(4)	45.2(14)
F12A	6167(4)	5682(5)	3243(5)	41.0(16)
F12C	6816(14)	5568(12)	3311(9)	57(5)
F10C	6790(13)	4582(9)	3870(10)	41(4)
F11C	5577(7)	5034(12)	3436(10)	35(4)
F22B	8850(8)	7471(5)	8761(6)	35(2)
F24B	8773(8)	8751(5)	9341(7)	44(2)
F23B	10037(6)	8377(9)	9678(7)	62(3)
F23C	9921(9)	7726(8)	9237(7)	73(3)
F24C	9390(10)	8801(5)	9687(6)	52(3)
F22C	8498(7)	7683(9)	8718(6)	69(3)
F9B	5828(13)	7816(6)	6490(11)	34(2)
F8B	4975(8)	6561(11)	5788(10)	68(4)
F7B	6082(13)	6748(12)	6898(9)	44(3)
F3B	9313(14)	7951(6)	2755(6)	58(3)
F1B	9992(8)	7182(11)	3426(13)	33(3)
F2B	8546(7)	6852(6)	2821(8)	40(2)

Table 3 Anisotropic Displacement Parameters ($Å^2 \times 10^3$) for c120819_2_1. The Anisotropic displacement factor exponent takes the form: $-2\pi^2[h^2a^{*2}U_{11}+2hka^*b^*U_{12}+\ldots]$.

Atom	U_{11}	U_{22}	U_{33}	U_{23}	U_{13}	U_{12}
Ag1	16.47(6)	16.76(6)	13.72(6)	2.96(4)	6.34(5)	3.42(4)
Pd1	15.49(6)	18.52(6)	13.52(6)	5.67(5)	6.06(5)	4.58(5)
P1	18.1(2)	26.8(2)	15.4(2)	7.02(17)	5.79(17)	7.74(17)
P2	16.8(2)	20.8(2)	17.0(2)	5.29(17)	6.42(17)	3.85(16)
O1	24.5(6)	30.1(7)	15.3(6)	9.3(5)	6.4(5)	8.3(5)
O2	19.4(6)	25.9(6)	22.6(6)	9.5(5)	8.7(5)	3.2(5)
N1	14.3(7)	16.8(7)	14.2(7)	3.2(5)	4.2(5)	2.1(5)
N2	13.8(6)	14.6(6)	15.0(7)	2.2(5)	5.0(5)	2.9(5)
C1	16.1(8)	22.3(8)	14.3(8)	5.2(7)	7.1(7)	4.3(6)
C2	16.7(8)	22.8(8)	15.0(8)	2.4(7)	7.5(7)	6.1(7)

Table 3 Anisotropic Displacement Parameters ($Å^2×10^3$) for c120819_2_1. The Anisotropic displacement factor exponent takes the form: $-2π^2[h^2a^{*2}U_{11}+2hka^*b^*U_{12}+...]$.

Atom	U_{11}	U_{22}	U_{33}	U_{23}	U_{13}	U_{12}
C3	23.2(9)	19.2(8)	16.6(8)	4.9(7)	8.9(7)	6.3(7)
C4	25.0(9)	28.0(10)	28.5(10)	8.5(8)	10.5(8)	10.2(8)
C5	38.5(11)	29.8(10)	36.4(11)	15.1(9)	15.8(10)	20.3(9)
C6	48.6(13)	20.0(9)	30.7(11)	10.1(8)	18.6(10)	12.2(9)
C7	32.5(10)	22.3(9)	28.9(10)	7.7(8)	11.4(9)	1.7(8)
C8	24.5(9)	22.1(9)	24.1(9)	7.6(7)	6.9(8)	5.1(7)
C9	24.4(9)	18.8(8)	19.9(9)	9.3(7)	12.3(7)	8.7(7)
C10	24.6(9)	20.7(8)	21.9(9)	9.7(7)	10.8(7)	10.2(7)
C11	36.3(11)	29.3(10)	23.7(9)	16.4(8)	16.0(8)	17.2(8)
C12	36.4(11)	29.0(10)	34.1(11)	21.5(9)	23.1(9)	17.2(8)
C13	26.8(9)	22.8(9)	32.9(10)	14.7(8)	17.0(8)	9.3(7)
C14	24.0(9)	18.4(8)	22.5(9)	9.1(7)	11.2(7)	8.1(7)
C15	28.3(10)	44.8(12)	20.3(9)	8.2(9)	8.6(8)	19.4(9)
C16	42.1(14)	72.8(18)	29.5(12)	7.7(12)	2.5(10)	39.8(13)
C17	50.0(14)	40.4(12)	35.5(12)	14.4(10)	14.5(11)	27.6(11)
C18	21.6(9)	32.9(10)	18.2(9)	6.1(8)	3.5(7)	0.7(8)
C19	27.2(11)	56.6(15)	30.7(12)	13.8(11)	6.7(9)	-6.9(10)
C20	37.9(12)	26.3(10)	31.1(11)	4.1(9)	7.8(9)	5.2(9)
C21	23.0(9)	25.2(9)	25.6(10)	1.4(8)	9.3(8)	4.0(7)
C22	36.0(11)	25.5(10)	38.7(12)	8.1(9)	16.7(10)	10.8(9)
C23	27.9(11)	32.8(11)	41.0(13)	-6.1(10)	6.2(10)	1.1(9)
C24	18.9(9)	28.2(9)	21.6(9)	9.3(8)	5.0(7)	5.4(7)
C25	36.8(11)	31.5(11)	32.8(11)	11.6(9)	11.3(9)	16.6(9)
C26	26.7(10)	46.1(12)	26.1(10)	17.3(9)	7.7(8)	8.0(9)
C27	14.8(8)	17.4(8)	14.1(8)	4.8(6)	4.4(6)	5.0(6)
C28	17.6(8)	23.5(9)	18.0(8)	2.9(7)	8.1(7)	3.4(7)
C29	17.7(8)	22.5(8)	15.5(8)	-0.1(7)	7.4(7)	4.6(7)
C30	16.0(8)	15.1(7)	16.4(8)	2.8(6)	6.7(7)	3.1(6)
C31	16.3(8)	18.3(8)	17.1(8)	5.1(7)	6.7(7)	6.2(6)
C32	14.7(8)	24.1(9)	22.2(9)	6.6(7)	3.4(7)	3.7(7)
C33	19.8(9)	20.6(8)	27.7(10)	8.2(7)	8.8(8)	0.3(7)
C34	23.9(9)	20.6(8)	24.6(9)	11.2(7)	8.8(8)	6.2(7)
C35	18.3(8)	18.0(8)	17.2(8)	3.9(7)	5.5(7)	5.5(6)
C36	18.5(8)	22.0(8)	19.8(9)	9.1(7)	5.7(7)	6.7(7)
C37	40.0(12)	25.7(10)	23.6(10)	6.4(8)	1.1(9)	14.8(9)
C38	26.7(10)	27.8(9)	19.9(9)	8.3(8)	3.5(8)	8.5(8)
C39	19.0(9)	22.9(9)	22.6(9)	7.9(7)	1.6(7)	4.9(7)
C40	34.6(11)	38.0(11)	23.2(10)	11.8(9)	0.1(9)	4.7(9)
C41	23.3(10)	39.0(12)	44.5(13)	9.0(10)	4.1(9)	16.5(9)
C42	16.3(8)	15.9(8)	18.3(8)	2.8(7)	7.2(7)	1.2(6)
C43	17.6(8)	18.8(8)	20.8(9)	3.5(7)	5.2(7)	2.6(7)
C44	17.6(8)	21.8(9)	24.6(9)	1.4(7)	1.2(7)	0.2(7)
C45	20.8(9)	17.0(8)	32.6(10)	2.2(8)	5.2(8)	-1.2(7)
C46	22.6(9)	19.0(8)	29.8(10)	8.1(8)	8.0(8)	4.2(7)

Table 3 Anisotropic Displacement Parameters ($Å^2×10^3$) for c120819_2_1. The Anisotropic displacement factor exponent takes the form: $-2π^2[h^2a^{*2}U_{11}+2hka^*b^*U_{12}+...]$.

Atom	U_{11}	U_{22}	U_{33}	U_{23}	U_{13}	U_{12}
C47	16.9(8)	21.5(8)	19.9(9)	6.2(7)	7.8(7)	3.9(7)
C48	22.2(9)	21.0(8)	21.5(9)	7.5(7)	4.6(7)	4.7(7)
C49	43.9(13)	55.4(15)	27.4(11)	20.7(11)	7.5(10)	-0.3(11)
C50	24.1(10)	46.1(13)	31.3(11)	5.1(10)	2.7(9)	14.1(9)
C51	23.2(9)	18.3(8)	23.7(9)	2.9(7)	-2.1(8)	3.0(7)
C52	30.0(11)	38.0(12)	36.0(12)	20.2(10)	-0.1(9)	1.9(9)
C53	24.9(10)	26.7(10)	35.0(11)	1.9(9)	0.2(9)	9.4(8)
F1A	36(2)	33(2)	33.0(18)	15.5(16)	23.1(19)	16.3(19)
F2A	31.1(17)	128(5)	26.0(18)	-22(3)	-1.0(13)	26(2)
F3A	91(3)	47.3(17)	45(2)	28.8(17)	51(2)	36(2)
F4A	17.0(6)	40.5(7)	76.9(10)	31.6(7)	15.0(6)	14.5(5)
F5A	34.2(6)	28.5(6)	45.8(7)	22.9(5)	22.9(6)	12.2(5)
F6A	52.3(8)	26.6(6)	37.0(7)	10.3(5)	19.6(6)	18.4(6)
F7A	36(3)	30.3(15)	42(2)	6.4(14)	23.7(19)	11.2(12)
F8A	47(3)	49(3)	59(3)	38(2)	38.4(19)	21(2)
F9A	16.4(14)	65(2)	40.1(17)	4.0(16)	8.2(12)	11.9(14)
F10B	67(5)	34(3)	44(4)	-5(2)	15(4)	-20(3)
F11B	28(3)	60(6)	22(2)	-2(3)	-7(2)	21(3)
F12B	22(2)	40(5)	28(3)	-7(3)	2.1(19)	10(3)
F13A	33.8(8)	132.4(16)	58.9(10)	64.6(11)	21.3(7)	10.5(9)
F14A	36.3(7)	40.3(8)	70.6(10)	0.9(7)	24.7(7)	-10.2(6)
F15A	29.7(7)	48.1(8)	103.1(13)	31.4(8)	37.1(8)	18.7(6)
F16A	69.4(11)	43.2(8)	152.7(18)	59.5(10)	78.8(12)	42.3(8)
F17A	92.3(12)	29.8(7)	30.8(7)	14.3(6)	24.2(7)	7.0(7)
F18A	57.9(9)	24.7(6)	50.2(9)	14.5(6)	-18.2(7)	-8.9(6)
F19A	65.1(9)	17.5(6)	83.4(11)	7.9(6)	49.2(9)	7.0(6)
F20A	34.4(6)	29.8(6)	30.9(6)	7.8(5)	16.0(5)	-5.4(5)
F21A	60.3(9)	58.3(9)	26.2(7)	9.0(6)	-6.2(6)	-36.4(8)
F22A	84(4)	21.2(14)	38(3)	14.0(14)	32(3)	7(2)
F23A	59(3)	33(2)	15.2(13)	7.1(13)	10.4(17)	-2.5(18)
F24A	45(2)	103(4)	67(3)	56(3)	40(2)	28(2)
C1A	13.4(8)	18.2(8)	17.3(8)	4.9(7)	2.5(6)	2.6(6)
C2A	18.8(8)	18.9(8)	19.4(9)	5.5(7)	4.9(7)	5.3(7)
C3A	21.5(9)	25.2(9)	18.1(9)	6.4(7)	6.2(7)	6.9(7)
C4A	20.5(9)	27.9(9)	21.2(9)	12.9(8)	7.5(7)	8.1(7)
C5A	13.3(8)	22.0(8)	25.1(9)	10.5(7)	6.3(7)	5.4(7)
C6A	13.0(8)	20.0(8)	18.2(8)	5.1(7)	4.8(6)	3.9(6)
C7A	34.8(10)	34.7(10)	21.7(9)	10.2(8)	10.7(8)	15.0(8)
C8A	17.5(8)	26.8(9)	32.5(10)	15.0(8)	11.3(8)	8.6(7)
C9A	17.5(8)	17.4(8)	18.2(8)	8.7(7)	4.8(7)	6.1(6)
C10A	19.5(8)	18.6(8)	18.6(8)	6.9(7)	6.0(7)	5.9(7)
C11A	19.1(8)	21.7(8)	22.8(9)	10.9(7)	8.3(7)	7.5(7)
C12A	16.0(8)	21.9(8)	23.4(9)	9.7(7)	2.5(7)	4.2(7)
C13A	19.7(8)	18.3(8)	19.1(8)	6.6(7)	3.5(7)	5.5(7)

Table 3 Anisotropic Displacement Parameters ($Å^2×10^3$) for c120819_2_1. The Anisotropic displacement factor exponent takes the form: $-2π^2[h^2a^{*2}U_{11}+2hka*b*U_{12}+...]$.

Atom	U_{11}	U_{22}	U_{33}	U_{23}	U_{13}	U_{12}
C14A	19.0(8)	19.4(8)	19.8(9)	7.1(7)	6.2(7)	6.7(7)
C15A	21.9(9)	29.3(9)	28.7(10)	10.7(8)	11.3(8)	6.0(7)
C16A	21.4(9)	27.8(9)	25.6(10)	2.9(8)	3.8(8)	4.2(7)
C17A	18.7(8)	17.7(8)	12.5(8)	2.8(6)	3.6(6)	4.3(6)
C18A	19.8(8)	18.1(8)	16.8(8)	4.9(7)	4.7(7)	3.8(7)
C19A	17.4(8)	24.8(9)	17.0(8)	6.1(7)	5.4(7)	4.2(7)
C20A	21.2(9)	24.6(9)	20.0(9)	5.9(7)	7.4(7)	10.7(7)
C21A	22.9(9)	18.1(8)	16.3(8)	4.6(7)	6.1(7)	6.6(7)
C22A	18.6(8)	18.8(8)	15.8(8)	3.9(7)	5.6(7)	4.5(7)
C23A	21.7(9)	33.1(10)	32.4(11)	13.3(9)	11.6(8)	8.6(8)
C24A	24.2(9)	22.6(9)	23.0(9)	7.0(7)	8.1(8)	9.3(7)
C25A	15.1(8)	17.8(8)	19.3(8)	6.5(7)	5.3(7)	7.1(6)
C26A	15.6(8)	20.4(8)	18.7(8)	8.0(7)	6.7(7)	4.1(6)
C27A	14.4(8)	19.4(8)	20.8(9)	5.9(7)	4.7(7)	4.0(6)
C28A	21.0(8)	20.6(8)	16.0(8)	4.5(7)	4.9(7)	6.2(7)
C29A	23.3(9)	21.4(8)	19.1(9)	9.4(7)	7.7(7)	7.5(7)
C30A	19.5(8)	14.9(8)	20.1(9)	5.9(7)	5.0(7)	4.6(6)
C31A	29.5(10)	25.4(9)	21.8(9)	3.1(8)	9.8(8)	-3.0(8)
C32A	47.9(12)	25.6(9)	22.2(9)	8.6(8)	11.9(9)	2.1(9)
B1A	16.2(9)	17.5(9)	16.8(9)	5.8(7)	5.6(7)	5.1(7)
F10A	30(3)	37(4)	39(4)	-12(2)	-0.4(18)	19(3)
F11A	35(2)	39(3)	39(3)	-7.7(19)	9(2)	-15.0(19)
F12A	54(4)	38(2)	18.4(16)	4.2(15)	-1(3)	14(3)
F12C	71(9)	61(8)	33(6)	9(5)	25(6)	-8(7)
F10C	46(8)	32(6)	37(7)	0(5)	8(6)	24(6)
F11C	23(4)	40(8)	26(7)	-6(5)	-3(4)	11(5)
F22B	53(6)	24(3)	30(4)	9(3)	23(5)	-3(4)
F24B	67(6)	38(4)	50(5)	17(3)	47(4)	15(4)
F23B	68(5)	79(7)	38(5)	42(5)	1(3)	7(4)
F23C	112(6)	68(5)	61(5)	53(4)	27(5)	35(5)
F24C	91(7)	37(3)	37(4)	7(3)	42(5)	3(5)
F22C	77(5)	79(7)	49(4)	24(5)	34(5)	-20(4)
F9B	38(6)	38(3)	52(6)	29(3)	33(4)	26(3)
F8B	30(4)	87(7)	66(5)	-13(4)	29(3)	-10(4)
F7B	63(7)	53(5)	43(4)	30(4)	37(4)	28(5)
F3B	122(8)	47(3)	35(4)	26(3)	46(5)	43(4)
F1B	18(3)	49(6)	33(4)	8(4)	14(2)	9(3)
F2B	27(3)	37(3)	32(4)	-13(2)	2(2)	4.6(19)

Table 4 Bond Lengths for c120819_2_1.

Atom	Atom	Length/Å	Atom	Atom	Length/Å
Ag1	C1	2.2255(16)	F6A	C8A	1.342(2)

Table 4 Bond Lengths for c120819_2_1.

Atom	Atom	Length/Å	Atom	Atom	Length/Å
Ag1	C2	2.3254(16)	F7A	C15A	1.353(5)
Ag1	C27	2.0873(16)	F8A	C15A	1.328(6)
Pd1	P1	2.2764(5)	F9A	C15A	1.336(5)
Pd1	P2	2.2797(5)	F10B	C16A	1.352(7)
Pd1	C1	2.0515(16)	F11B	C16A	1.313(8)
Pd1	C9	2.0130(16)	F12B	C16A	1.349(9)
P1	O1	1.6496(13)	F13A	C23A	1.328(2)
P1	C15	1.8322(19)	F14A	C23A	1.333(3)
P1	C18	1.821(2)	F15A	C23A	1.322(2)
P2	O2	1.6477(12)	F16A	C24A	1.323(2)
P2	C21	1.8308(19)	F17A	C24A	1.328(2)
P2	C24	1.8188(19)	F18A	C24A	1.319(2)
O1	C10	1.393(2)	F19A	C31A	1.340(2)
O2	C14	1.386(2)	F20A	C31A	1.337(2)
N1	C27	1.356(2)	F21A	C31A	1.333(2)
N1	C28	1.384(2)	F22A	C32A	1.306(4)
N1	C42	1.447(2)	F23A	C32A	1.345(4)
N2	C27	1.352(2)	F24A	C32A	1.369(4)
N2	C29	1.389(2)	C1A	C2A	1.405(2)
N2	C30	1.443(2)	C1A	C6A	1.399(2)
C1	C2	1.224(2)	C1A	B1A	1.646(2)
C2	C3	1.446(2)	C2A	C3A	1.385(2)
C3	C4	1.402(3)	C3A	C4A	1.389(3)
C3	C8	1.396(3)	C3A	C7A	1.500(3)
C4	C5	1.386(3)	C4A	C5A	1.390(3)
C5	C6	1.386(3)	C5A	C6A	1.396(2)
C6	C7	1.379(3)	C5A	C8A	1.495(2)
C7	C8	1.388(3)	C7A	F3B	1.284(7)
C9	C10	1.392(3)	C7A	F1B	1.302(10)
C9	C14	1.391(3)	C7A	F2B	1.409(8)
C10	C11	1.391(2)	C9A	C10A	1.399(2)
C11	C12	1.388(3)	C9A	C14A	1.404(2)
C12	C13	1.388(3)	C9A	B1A	1.644(3)
C13	C14	1.390(2)	C10A	C11A	1.398(2)
C15	C16	1.533(3)	C11A	C12A	1.382(3)
C15	C17	1.527(3)	C11A	C15A	1.498(2)
C18	C19	1.533(3)	C12A	C13A	1.389(2)
C18	C20	1.533(3)	C13A	C14A	1.387(2)
C21	C22	1.532(3)	C13A	C16A	1.495(3)
C21	C23	1.529(3)	C15A	F9B	1.316(10)
C24	C25	1.531(3)	C15A	F8B	1.328(10)
C24	C26	1.528(3)	C15A	F7B	1.350(10)
C28	C29	1.346(2)	C16A	F10A	1.307(7)
C30	C31	1.400(2)	C16A	F11A	1.331(5)
C30	C35	1.402(2)	C16A	F12A	1.359(6)

Table 4 Bond Lengths for c120819_2_1.

Atom	Atom	Length/Å	Atom	Atom	Length/Å
C31	C32	1.392(2)	C16A	F12C	1.365(10)
C31	C36	1.525(2)	C16A	F10C	1.361(10)
C32	C33	1.388(3)	C16A	F11C	1.290(10)
C33	C34	1.380(3)	C17A	C18A	1.404(2)
C34	C35	1.394(2)	C17A	C22A	1.396(2)
C35	C39	1.519(2)	C17A	B1A	1.645(2)
C36	C37	1.528(3)	C18A	C19A	1.389(2)
C36	C38	1.525(3)	C19A	C20A	1.388(3)
C39	C40	1.531(3)	C19A	C23A	1.502(3)
C39	C41	1.531(3)	C20A	C21A	1.386(3)
C42	C43	1.398(2)	C21A	C22A	1.401(2)
C42	C47	1.400(2)	C21A	C24A	1.497(2)
C43	C44	1.394(2)	C25A	C26A	1.403(2)
C43	C51	1.523(2)	C25A	C30A	1.404(2)
C44	C45	1.382(3)	C25A	B1A	1.639(3)
C45	C46	1.380(3)	C26A	C27A	1.392(2)
C46	C47	1.397(3)	C27A	C28A	1.390(2)
C47	C48	1.518(2)	C27A	C31A	1.497(2)
C48	C49	1.525(3)	C28A	C29A	1.384(3)
C48	C50	1.527(3)	C29A	C30A	1.390(2)
C51	C52	1.528(3)	C29A	C32A	1.496(3)
C51	C53	1.533(3)	C32A	F22B	1.286(8)
F1A	C7A	1.339(5)	C32A	F24B	1.346(7)
F2A	C7A	1.287(6)	C32A	F23B	1.336(8)
F3A	C7A	1.374(4)	C32A	F23C	1.448(7)
F4A	C8A	1.346(2)	C32A	F24C	1.231(7)
F5A	C8A	1.335(2)	C32A	F22C	1.325(8)

Table 5 Bond Angles for c120819_2_1.

Atom	Atom	Atom	Angle/°	Atom	Atom	Atom	Angle/°
C1	Ag1	C2	31.12(6)	F2A	C7A	F3A	107.2(4)
C27	Ag1	C1	177.77(6)	F2A	C7A	C3A	114.1(3)
C27	Ag1	C2	151.01(6)	F3A	C7A	C3A	111.6(3)
P1	Pd1	P2	157.797(17)	F3B	C7A	C3A	114.7(5)
C1	Pd1	P1	100.79(5)	F3B	C7A	F1B	112.0(9)
C1	Pd1	P2	101.36(5)	F3B	C7A	F2B	102.2(6)
C9	Pd1	P1	79.43(5)	F1B	C7A	C3A	114.7(10)
C9	Pd1	P2	79.52(5)	F1B	C7A	F2B	103.0(8)
C9	Pd1	C1	165.41(7)	F2B	C7A	C3A	108.7(6)
O1	P1	Pd1	105.36(5)	F4A	C8A	C5A	112.34(15)
O1	P1	C15	102.45(8)	F5A	C8A	F4A	105.92(15)
O1	P1	C18	101.08(8)	F5A	C8A	F6A	106.58(15)
C15	P1	Pd1	116.06(7)	F5A	C8A	C5A	112.97(15)

Table 5 Bond Angles for c120819_2_1.

Atom	Atom	Atom	Angle/°	Atom	Atom	Atom	Angle/°
C18	P1	Pd1	121.39(7)	F6A	C8A	F4A	105.33(15)
C18	P1	C15	107.59(10)	F6A	C8A	C5A	113.09(15)
O2	P2	Pd1	105.43(5)	C10A	C9A	C14A	115.60(16)
O2	P2	C21	101.78(8)	C10A	C9A	B1A	124.69(15)
O2	P2	C24	101.08(8)	C14A	C9A	B1A	119.31(15)
C21	P2	Pd1	115.07(6)	C11A	C10A	C9A	122.04(16)
C24	P2	Pd1	121.94(6)	C10A	C11A	C15A	119.40(16)
C24	P2	C21	108.45(9)	C12A	C11A	C10A	121.00(16)
C10	O1	P1	114.20(11)	C12A	C11A	C15A	119.58(16)
C14	O2	P2	114.43(11)	C11A	C12A	C13A	118.02(16)
C27	N1	C28	111.43(14)	C12A	C13A	C16A	118.97(16)
C27	N1	C42	124.08(14)	C14A	C13A	C12A	120.81(16)
C28	N1	C42	124.25(14)	C14A	C13A	C16A	120.12(16)
C27	N2	C29	111.33(14)	C13A	C14A	C9A	122.45(16)
C27	N2	C30	123.77(14)	F7A	C15A	C11A	111.5(5)
C29	N2	C30	124.66(14)	F8A	C15A	F7A	105.2(5)
Pd1	C1	Ag1	125.43(8)	F8A	C15A	F9A	107.0(5)
C2	C1	Ag1	78.95(11)	F8A	C15A	C11A	113.9(5)
C2	C1	Pd1	155.60(14)	F9A	C15A	F7A	105.6(4)
C1	C2	Ag1	69.93(11)	F9A	C15A	C11A	112.9(4)
C1	C2	C3	174.01(17)	F9B	C15A	C11A	115.2(9)
C3	C2	Ag1	116.05(11)	F9B	C15A	F8B	107.8(8)
C4	C3	C2	120.46(16)	F9B	C15A	F7B	105.5(9)
C8	C3	C2	120.47(16)	F8B	C15A	C11A	112.4(8)
C8	C3	C4	119.06(17)	F8B	C15A	F7B	106.0(8)
C5	C4	C3	119.90(18)	F7B	C15A	C11A	109.3(9)
C6	C5	C4	120.31(18)	F10B	C16A	C13A	111.3(5)
C7	C6	C5	120.29(18)	F11B	C16A	F10B	106.8(5)
C6	C7	C8	119.97(19)	F11B	C16A	F12B	105.9(7)
C7	C8	C3	120.46(18)	F11B	C16A	C13A	114.6(6)
C10	C9	Pd1	121.15(13)	F12B	C16A	F10B	104.5(7)
C14	C9	Pd1	121.18(13)	F12B	C16A	C13A	113.0(8)
C14	C9	C10	116.84(15)	F10A	C16A	C13A	114.1(6)
C9	C10	O1	118.52(15)	F10A	C16A	F11A	108.7(5)
C11	C10	O1	118.72(16)	F10A	C16A	F12A	106.4(6)
C11	C10	C9	122.71(17)	F11A	C16A	C13A	113.3(4)
C12	C11	C10	117.68(18)	F11A	C16A	F12A	104.3(4)
C13	C12	C11	122.24(17)	F12A	C16A	C13A	109.4(4)
C12	C13	C14	117.62(18)	F12C	C16A	C13A	111.0(7)
O2	C14	C9	118.82(15)	F10C	C16A	C13A	109.4(7)
O2	C14	C13	118.28(16)	F10C	C16A	F12C	103.1(9)
C13	C14	C9	122.87(17)	F11C	C16A	C13A	118.1(7)
C16	C15	P1	112.99(14)	F11C	C16A	F12C	107.0(9)
C17	C15	P1	109.39(14)	F11C	C16A	F10C	107.3(9)
C17	C15	C16	110.8(2)	C18A	C17A	B1A	119.22(15)

Table 5 Bond Angles for c120819_2_1.

Atom	Atom	Atom	Angle/°	Atom	Atom	Atom	Angle/°
C19	C18	P1	110.60(15)	C22A	C17A	C18A	115.99(15)
C19	C18	C20	111.51(18)	C22A	C17A	B1A	124.71(15)
C20	C18	P1	109.22(13)	C19A	C18A	C17A	122.29(16)
C22	C21	P2	108.21(14)	C18A	C19A	C23A	118.76(16)
C23	C21	P2	112.89(14)	C20A	C19A	C18A	120.87(16)
C23	C21	C22	111.00(18)	C20A	C19A	C23A	120.37(16)
C25	C24	P2	109.18(13)	C21A	C20A	C19A	117.99(16)
C26	C24	P2	110.56(13)	C20A	C21A	C22A	121.00(16)
C26	C24	C25	111.82(17)	C20A	C21A	C24A	119.75(15)
N1	C27	Ag1	128.84(12)	C22A	C21A	C24A	119.24(16)
N2	C27	Ag1	126.96(12)	C17A	C22A	C21A	121.83(16)
N2	C27	N1	104.16(13)	F13A	C23A	F14A	105.52(18)
C29	C28	N1	106.55(15)	F13A	C23A	C19A	112.08(16)
C28	C29	N2	106.52(15)	F14A	C23A	C19A	112.27(16)
C31	C30	N2	118.83(15)	F15A	C23A	F13A	107.29(18)
C31	C30	C35	123.61(15)	F15A	C23A	F14A	105.46(17)
C35	C30	N2	117.55(15)	F15A	C23A	C19A	113.65(16)
C30	C31	C36	122.18(15)	F16A	C24A	F17A	105.73(17)
C32	C31	C30	116.75(15)	F16A	C24A	C21A	112.97(16)
C32	C31	C36	121.06(15)	F17A	C24A	C21A	112.20(15)
C33	C32	C31	121.30(16)	F18A	C24A	F16A	106.73(17)
C34	C33	C32	120.21(16)	F18A	C24A	F17A	105.35(17)
C33	C34	C35	121.31(16)	F18A	C24A	C21A	113.24(15)
C30	C35	C39	123.03(15)	C26A	C25A	C30A	115.28(16)
C34	C35	C30	116.80(16)	C26A	C25A	B1A	124.07(15)
C34	C35	C39	120.14(16)	C30A	C25A	B1A	120.39(15)
C31	C36	C37	111.28(15)	C27A	C26A	C25A	122.19(16)
C38	C36	C31	113.07(15)	C26A	C27A	C31A	120.94(16)
C38	C36	C37	109.09(15)	C28A	C27A	C26A	121.19(16)
C35	C39	C40	110.95(16)	C28A	C27A	C31A	117.75(16)
C35	C39	C41	110.75(16)	C29A	C28A	C27A	117.73(16)
C40	C39	C41	111.02(17)	C28A	C29A	C30A	120.93(16)
C43	C42	N1	119.06(15)	C28A	C29A	C32A	118.97(16)
C43	C42	C47	123.56(16)	C30A	C29A	C32A	120.10(16)
C47	C42	N1	117.38(15)	C29A	C30A	C25A	122.63(16)
C42	C43	C51	122.32(15)	F19A	C31A	C27A	111.43(16)
C44	C43	C42	116.91(16)	F20A	C31A	F19A	106.21(16)
C44	C43	C51	120.77(16)	F20A	C31A	C27A	112.96(15)
C45	C44	C43	121.02(17)	F21A	C31A	F19A	106.25(17)
C46	C45	C44	120.72(17)	F21A	C31A	F20A	106.81(16)
C45	C46	C47	120.91(17)	F21A	C31A	C27A	112.70(17)
C42	C47	C48	122.85(16)	F22A	C32A	F23A	106.4(3)
C46	C47	C42	116.87(16)	F22A	C32A	F24A	105.4(3)
C46	C47	C48	120.27(16)	F22A	C32A	C29A	114.7(3)
C47	C48	C49	112.19(16)	F23A	C32A	F24A	104.3(3)

Table 5 Bond Angles for c120819_2_1.

Atom	Atom	Atom	Angle/°	Atom	Atom	Atom	Angle/°
C47	C48	C50	110.17(15)	F23A	C32A	C29A	113.5(2)
C49	C48	C50	110.87(18)	F24A	C32A	C29A	111.7(2)
C43	C51	C52	110.89(16)	F22B	C32A	C29A	114.5(5)
C43	C51	C53	112.18(16)	F22B	C32A	F24B	108.3(6)
C52	C51	C53	109.84(17)	F22B	C32A	F23B	109.1(6)
C2A	C1A	B1A	119.64(15)	F24B	C32A	C29A	109.8(4)
C6A	C1A	C2A	115.58(15)	F23B	C32A	C29A	110.7(5)
C6A	C1A	B1A	124.63(15)	F23B	C32A	F24B	103.9(6)
C3A	C2A	C1A	122.68(16)	F23C	C32A	C29A	104.9(4)
C2A	C3A	C4A	120.88(16)	F24C	C32A	C29A	117.5(4)
C2A	C3A	C7A	119.16(16)	F24C	C32A	F23C	105.1(6)
C4A	C3A	C7A	119.96(16)	F24C	C32A	F22C	113.7(6)
C3A	C4A	C5A	117.68(16)	F22C	C32A	C29A	113.2(5)
C4A	C5A	C6A	121.16(16)	F22C	C32A	F23C	100.0(6)
C4A	C5A	C8A	119.05(16)	C9A	B1A	C1A	104.10(13)
C6A	C5A	C8A	119.78(16)	C9A	B1A	C17A	112.58(14)
C5A	C6A	C1A	121.96(16)	C17A	B1A	C1A	108.68(13)
F1A	C7A	F3A	102.6(4)	C25A	B1A	C1A	114.38(14)
F1A	C7A	C3A	112.6(5)	C25A	B1A	C9A	112.91(14)
F2A	C7A	F1A	107.9(5)	C25A	B1A	C17A	104.34(13)

Table 6 Torsion Angles for c120819_2_1.

A	B	C	D	Angle/°	A	B	C	D	Angle/°
Ag1	C2	C3	C4	-110.70(16)	C4A	C3A	C7A	F2A	-85.3(6)
Ag1	C2	C3	C8	68.58(19)	C4A	C3A	C7A	F3A	36.4(4)
Pd1	P1	O1	C10	-8.49(12)	C4A	C3A	C7A	F3B	6.3(10)
Pd1	P1	C15	C16	174.69(16)	C4A	C3A	C7A	F1B	138.0(9)
Pd1	P1	C15	C17	50.76(16)	C4A	C3A	C7A	F2B	-107.4(5)
Pd1	P1	C18	C19	78.46(15)	C4A	C5A	C6A	C1A	2.5(3)
Pd1	P1	C18	C20	-44.63(16)	C4A	C5A	C8A	F4A	92.1(2)
Pd1	P2	O2	C14	4.44(12)	C4A	C5A	C8A	F5A	-27.6(2)
Pd1	P2	C21	C22	-47.82(15)	C4A	C5A	C8A	F6A	-148.80(16)
Pd1	P2	C21	C23	-171.07(14)	C6A	C1A	C2A	C3A	0.4(3)
Pd1	P2	C24	C25	43.35(15)	C6A	C1A	B1A	C9A	88.86(19)
Pd1	P2	C24	C26	-80.07(15)	C6A	C1A	B1A	C17A	-150.94(16)
Pd1	C1	C2	Ag1	178.2(4)	C6A	C1A	B1A	C25A	-34.8(2)
Pd1	C9	C10	O1	8.4(2)	C6A	C5A	C8A	F4A	-87.1(2)
Pd1	C9	C10	C11	-169.01(13)	C6A	C5A	C8A	F5A	153.15(16)
Pd1	C9	C14	O2	-7.1(2)	C6A	C5A	C8A	F6A	32.0(2)
Pd1	C9	C14	C13	170.97(13)	C7A	C3A	C4A	C5A	178.32(17)
P1	O1	C10	C9	1.4(2)	C8A	C5A	C6A	C1A	-178.26(16)
P1	O1	C10	C11	178.91(13)	C9A	C10A	C11A	C12A	-2.2(3)
P2	O2	C14	C9	0.8(2)	C9A	C10A	C11A	C15A	176.67(16)

Table 6 Torsion Angles for c120819_2_1.

A	B	C	D	Angle/°	A	B	C	D	Angle/°
P2	O2	C14	C13	-177.33(13)	C10A	C9A	C14A	C13A	0.2(2)
O1	P1	C15	C16	60.5(2)	C10A	C9A	B1A	C1A	-108.24(18)
O1	P1	C15	C17	-63.44(15)	C10A	C9A	B1A	C17A	134.23(16)
O1	P1	C18	C19	-165.71(14)	C10A	C9A	B1A	C25A	16.4(2)
O1	P1	C18	C20	71.20(14)	C10A	C11A	C12A	C13A	-0.1(3)
O1	C10	C11	C12	-178.77(15)	C10A	C11A	C15A	F7A	34.4(5)
O2	P2	C21	C22	65.61(14)	C10A	C11A	C15A	F8A	-84.5(5)
O2	P2	C21	C23	-57.64(17)	C10A	C11A	C15A	F9A	153.1(4)
O2	P2	C24	C25	-72.85(14)	C10A	C11A	C15A	F9B	48.0(9)
O2	P2	C24	C26	163.73(14)	C10A	C11A	C15A	F8B	172.0(10)
N1	C28	C29	N2	-0.50(19)	C10A	C11A	C15A	F7B	-70.5(9)
N1	C42	C43	C44	179.18(15)	C11A	C12A	C13A	C14A	2.3(3)
N1	C42	C43	C51	-0.4(2)	C11A	C12A	C13A	C16A	-174.24(16)
N1	C42	C47	C46	179.97(15)	C12A	C11A	C15A	F7A	-146.7(4)
N1	C42	C47	C48	-1.2(2)	C12A	C11A	C15A	F8A	94.4(5)
N2	C30	C31	C32	-177.90(15)	C12A	C11A	C15A	F9A	-28.0(4)
N2	C30	C31	C36	2.9(2)	C12A	C11A	C15A	F9B	-133.2(9)
N2	C30	C35	C34	178.57(15)	C12A	C11A	C15A	F8B	-9.1(10)
N2	C30	C35	C39	0.6(2)	C12A	C11A	C15A	F7B	108.3(9)
C2	C3	C4	C5	179.21(17)	C12A	C13A	C14A	C9A	-2.4(3)
C2	C3	C8	C7	-179.53(17)	C12A	C13A	C16A	F10B	-52.2(4)
C3	C4	C5	C6	0.1(3)	C12A	C13A	C16A	F11B	69.1(5)
C4	C3	C8	C7	-0.2(3)	C12A	C13A	C16A	F12B	-169.5(6)
C4	C5	C6	C7	0.3(3)	C12A	C13A	C16A	F10A	-151.6(5)
C5	C6	C7	C8	-0.6(3)	C12A	C13A	C16A	F11A	-26.4(4)
C6	C7	C8	C3	0.6(3)	C12A	C13A	C16A	F12A	89.4(4)
C8	C3	C4	C5	-0.1(3)	C12A	C13A	C16A	F12C	137.2(11)
C9	C10	C11	C12	-1.4(3)	C12A	C13A	C16A	F10C	-109.7(10)
C10	C9	C14	O2	-176.71(15)	C12A	C13A	C16A	F11C	13.2(11)
C10	C9	C14	C13	1.3(3)	C14A	C9A	C10A	C11A	2.0(2)
C10	C11	C12	C13	0.2(3)	C14A	C9A	B1A	C1A	64.12(18)
C11	C12	C13	C14	1.6(3)	C14A	C9A	B1A	C17A	-53.4(2)
C12	C13	C14	O2	175.65(15)	C14A	C9A	B1A	C25A	-171.25(14)
C12	C13	C14	C9	-2.4(3)	C14A	C13A	C16A	F10B	131.2(4)
C14	C9	C10	O1	178.01(15)	C14A	C13A	C16A	F11B	-107.5(5)
C14	C9	C10	C11	0.6(3)	C14A	C13A	C16A	F12B	14.0(7)
C15	P1	O1	C10	113.33(13)	C14A	C13A	C16A	F10A	31.9(5)
C15	P1	C18	C19	-58.71(17)	C14A	C13A	C16A	F11A	157.0(3)
C15	P1	C18	C20	178.20(14)	C14A	C13A	C16A	F12A	-87.2(4)
C18	P1	O1	C10	-135.65(12)	C14A	C13A	C16A	F12C	-39.4(11)
C18	P1	C15	C16	-45.5(2)	C14A	C13A	C16A	F10C	73.7(10)
C18	P1	C15	C17	-169.49(14)	C14A	C13A	C16A	F11C	-163.4(11)
C21	P2	O2	C14	-116.00(12)	C15A	C11A	C12A	C13A	-178.91(16)
C21	P2	C24	C25	-179.38(13)	C16A	C13A	C14A	C9A	174.09(16)
C21	P2	C24	C26	57.19(16)	C17A	C18A	C19A	C20A	-1.9(3)

Table 6 Torsion Angles for c120819_2_1.

A	B	C	D	Angle/°	A	B	C	D	Angle/°
C24	P2	O2	C14	132.27(12)	C17A	C18A	C19A	C23A	177.93(17)
C24	P2	C21	C22	171.66(13)	C18A	C17A	C22A	C21A	-1.0(2)
C24	P2	C21	C23	48.41(18)	C18A	C17A	B1A	C1A	44.1(2)
C27	N1	C28	C29	0.1(2)	C18A	C17A	B1A	C9A	158.85(15)
C27	N1	C42	C43	-89.7(2)	C18A	C17A	B1A	C25A	-78.36(18)
C27	N1	C42	C47	90.8(2)	C18A	C19A	C20A	C21A	0.4(3)
C27	N2	C29	C28	0.7(2)	C18A	C19A	C23A	F13A	-57.8(2)
C27	N2	C30	C31	-101.45(19)	C18A	C19A	C23A	F14A	60.8(2)
C27	N2	C30	C35	79.9(2)	C18A	C19A	C23A	F15A	-179.62(17)
C28	N1	C27	Ag1	178.18(12)	C19A	C20A	C21A	C22A	0.7(3)
C28	N1	C27	N2	0.33(18)	C19A	C20A	C21A	C24A	-178.31(16)
C28	N1	C42	C43	96.3(2)	C20A	C19A	C23A	F13A	122.0(2)
C28	N1	C42	C47	-83.2(2)	C20A	C19A	C23A	F14A	-119.4(2)
C29	N2	C27	Ag1	-178.56(12)	C20A	C19A	C23A	F15A	0.2(3)
C29	N2	C27	N1	-0.66(18)	C20A	C21A	C22A	C17A	-0.4(3)
C29	N2	C30	C31	84.8(2)	C20A	C21A	C24A	F16A	-9.0(3)
C29	N2	C30	C35	-93.9(2)	C20A	C21A	C24A	F17A	110.4(2)
C30	N2	C27	Ag1	6.9(2)	C20A	C21A	C24A	F18A	-130.47(19)
C30	N2	C27	N1	-175.18(14)	C22A	C17A	C18A	C19A	2.1(2)
C30	N2	C29	C28	175.22(15)	C22A	C17A	B1A	C1A	-139.31(16)
C30	C31	C32	C33	-0.4(3)	C22A	C17A	B1A	C9A	-24.5(2)
C30	C31	C36	C37	79.4(2)	C22A	C17A	B1A	C25A	98.26(18)
C30	C31	C36	C38	-157.41(16)	C22A	C21A	C24A	F16A	171.95(18)
C30	C35	C39	C40	-120.16(19)	C22A	C21A	C24A	F17A	-68.6(2)
C30	C35	C39	C41	116.1(2)	C22A	C21A	C24A	F18A	50.5(2)
C31	C30	C35	C34	-0.1(2)	C23A	C19A	C20A	C21A	-179.42(17)
C31	C30	C35	C39	-178.07(16)	C24A	C21A	C22A	C17A	178.64(16)
C31	C32	C33	C34	-0.5(3)	C25A	C26A	C27A	C28A	0.1(3)
C32	C31	C36	C37	-99.8(2)	C25A	C26A	C27A	C31A	-175.72(16)
C32	C31	C36	C38	23.4(2)	C26A	C25A	C30A	C29A	2.6(2)
C32	C33	C34	C35	1.2(3)	C26A	C25A	B1A	C1A	-23.5(2)
C33	C34	C35	C30	-0.9(3)	C26A	C25A	B1A	C9A	-142.35(16)
C33	C34	C35	C39	177.19(17)	C26A	C25A	B1A	C17A	95.08(18)
C34	C35	C39	C40	61.9(2)	C26A	C27A	C28A	C29A	1.1(3)
C34	C35	C39	C41	-61.9(2)	C26A	C27A	C31A	F19A	97.0(2)
C35	C30	C31	C32	0.7(2)	C26A	C27A	C31A	F20A	-22.5(3)
C35	C30	C31	C36	-178.49(16)	C26A	C27A	C31A	F21A	-143.69(18)
C36	C31	C32	C33	178.76(16)	C27A	C28A	C29A	C30A	-0.5(3)
C42	N1	C27	Ag1	3.5(2)	C27A	C28A	C29A	C32A	-179.63(17)
C42	N1	C27	N2	-174.34(14)	C28A	C27A	C31A	F19A	-79.0(2)
C42	N1	C28	C29	174.77(15)	C28A	C27A	C31A	F20A	161.53(16)
C42	C43	C44	C45	1.2(3)	C28A	C27A	C31A	F21A	40.4(2)
C42	C43	C51	C52	94.6(2)	C28A	C29A	C30A	C25A	-1.5(3)
C42	C43	C51	C53	-142.22(18)	C28A	C29A	C32A	F22A	-144.4(4)
C42	C47	C48	C49	123.4(2)	C28A	C29A	C32A	F23A	-21.9(4)

Table 6 Torsion Angles for c120819_2_1.

A	B	C	D	Angle/°	A	B	C	D	Angle/°
C42	C47	C48	C50	-112.6(2)	C28A	C29A	C32A	F24A	95.7(4)
C43	C42	C47	C46	0.5(3)	C28A	C29A	C32A	F22B	-176.1(6)
C43	C42	C47	C48	179.28(16)	C28A	C29A	C32A	F24B	61.7(6)
C43	C44	C45	C46	-0.2(3)	C28A	C29A	C32A	F23B	-52.4(7)
C44	C43	C51	C52	-85.0(2)	C28A	C29A	C32A	F23C	-101.4(7)
C44	C43	C51	C53	38.2(2)	C28A	C29A	C32A	F24C	14.8(9)
C44	C45	C46	C47	-0.7(3)	C28A	C29A	C32A	F22C	150.6(8)
C45	C46	C47	C42	0.6(3)	C30A	C25A	C26A	C27A	-1.9(2)
C45	C46	C47	C48	-178.31(17)	C30A	C25A	B1A	C1A	162.62(15)
C46	C47	C48	C49	-57.8(2)	C30A	C25A	B1A	C9A	43.8(2)
C46	C47	C48	C50	66.2(2)	C30A	C25A	B1A	C17A	-78.76(18)
C47	C42	C43	C44	-1.3(3)	C30A	C29A	C32A	F22A	36.4(4)
C47	C42	C43	C51	179.14(16)	C30A	C29A	C32A	F23A	158.9(3)
C51	C43	C44	C45	-179.26(18)	C30A	C29A	C32A	F24A	-83.5(4)
C1A	C2A	C3A	C4A	1.4(3)	C30A	C29A	C32A	F22B	4.7(7)
C1A	C2A	C3A	C7A	-178.19(17)	C30A	C29A	C32A	F24B	-117.4(6)
C2A	C1A	C6A	C5A	-2.3(2)	C30A	C29A	C32A	F23B	128.4(7)
C2A	C1A	B1A	C9A	-86.37(18)	C30A	C29A	C32A	F23C	79.4(7)
C2A	C1A	B1A	C17A	33.8(2)	C30A	C29A	C32A	F24C	-164.4(8)
C2A	C1A	B1A	C25A	149.95(15)	C30A	C29A	C32A	F22C	-28.6(8)
C2A	C3A	C4A	C5A	-1.3(3)	C31A	C27A	C28A	C29A	177.07(16)
C2A	C3A	C7A	F1A	-29.1(5)	C32A	C29A	C30A	C25A	177.69(17)
C2A	C3A	C7A	F2A	94.3(6)	B1A	C1A	C2A	C3A	176.05(16)
C2A	C3A	C7A	F3A	-144.0(4)	B1A	C1A	C6A	C5A	-177.75(16)
C2A	C3A	C7A	F3B	-174.0(10)	B1A	C9A	C10A	C11A	174.67(15)
C2A	C3A	C7A	F1B	-42.4(9)	B1A	C9A	C14A	C13A	-172.84(15)
C2A	C3A	C7A	F2B	72.3(5)	B1A	C17A	C18A	C19A	179.02(16)
C3A	C4A	C5A	C6A	-0.6(3)	B1A	C17A	C22A	C21A	-177.70(16)
C3A	C4A	C5A	C8A	-179.84(16)	B1A	C25A	C26A	C27A	-176.02(15)
C4A	C3A	C7A	F1A	151.2(4)	B1A	C25A	C30A	C29A	176.94(15)

Table 7 Hydrogen Atom Coordinates (Å×10^4) and Isotropic Displacement Parameters (Å^2×10^3) for c120819_2_1.

Atom	*x*	*y*	*z*	U(eq)
H4	4973.14	5121.79	1498.17	32
H5	4702.53	3785.89	1674.44	39
H6	3215.86	3016.09	1296.21	37
H7	1989.75	3567.04	727.56	34
H8	2244.44	4907.47	556.85	29
H11	4563.81	7879.45	-2409.05	31
H12	6109.42	8553.46	-1871.72	33
H13	6958.05	8878.12	-496.58	29
H15	2071.1	7734.28	-528.21	37

Table 7 Hydrogen Atom Coordinates (Å×10^4) and Isotropic Displacement Parameters (Å^2×10^3) for c120819_2_1.

Atom	*x*	*y*	*z*	U(eq)
H16A	1828.85	7685.62	-2150.28	75
H16B	1190.85	8049.11	-1691.6	75
H16C	1209.26	7068.61	-1898.56	75
H17A	3336.61	8890.59	-81.37	60
H17B	2440.38	9143.65	-536.05	60
H17C	3129.67	8899.59	-979.98	60
H18	2131.37	6019.02	-2079.04	31
H19A	2229.71	5805.32	-557.8	61
H19B	1543.54	5172.47	-1400.75	61
H19C	1442.78	6124.49	-1095.96	61
H20A	3573.36	5648.66	-1858.42	51
H20B	2826.73	4870.21	-1939.95	51
H20C	3527	5439.12	-1076.19	51
H21	5618.32	8980.48	2243.29	31
H22A	5442.34	10226.76	1834.5	49
H22B	4746.39	9391.14	1185.54	49
H22C	5622.7	9775.4	1039.19	49
H23A	7208.74	9783.76	2058.14	59
H23B	7228.45	9261.46	2667.87	59
H23C	6901.5	10130.2	2804.37	59
H24	7252.81	7889.98	1822.98	28
H25A	7035.33	6411.84	1209.08	49
H25B	6719.63	6831.97	519.78	49
H25C	5987.1	6330.7	761.22	49
H26A	5748.31	7063.53	2108	48
H26B	6475.88	7898.87	2720.72	48
H26C	6763.25	7012.73	2531.38	48
H28	1641.8	7467.87	3748.21	24
H29	2807.96	8824.85	4268.27	23
H32	6070.18	9863.68	4271.32	26
H33	5687.38	10763.4	3501.36	28
H34	4210.22	10530.75	2613.78	26
H36	4563.8	8331.92	4553.53	24
H37A	4653.22	7377.71	3377.68	48
H37B	5307.17	7255.4	4167.76	48
H37C	5711.88	7764.75	3688	48
H38A	6459.18	8971.49	4964.89	38
H38B	6014.56	8518.47	5459.54	38
H38C	5879.28	9437.42	5435.13	38
H39	2300.95	8892.93	2334.05	27
H40A	2978.48	9696.04	1363.34	51
H40B	1988.67	9118.41	1068.82	51
H40C	2845.1	8706.62	1246.67	51
H41A	2347.08	10280.5	3138.47	56

Table 7 Hydrogen Atom Coordinates (Å×10⁴) and Isotropic Displacement Parameters (Å²×10³) for c120819_2_1.

Atom	*x*	*y*	*z*	U(eq)
H41B	1676.89	10089.65	2241.3	56
H41C	2661.44	10680.41	2544.97	56
H44	-77.15	5094.82	792.5	29
H45	428.51	3995.86	1230.32	32
H46	1703.62	4285.6	2382.83	29
H48	3085.2	6390.01	3647.45	27
H49A	2207.33	5650.15	4202.65	65
H49B	3226.37	5558.54	4514.62	65
H49C	2469.44	4791.66	3823.64	65
H50A	3416.93	4786.27	2906.18	55
H50B	4164.55	5542.54	3618.69	55
H50C	3739.69	5648.64	2757.31	55
H51	783.5	7338.25	1869.95	30
H52A	1578.94	7112.14	970.01	55
H52B	694.54	7418.91	577.04	55
H52C	718.84	6441.97	287.66	55
H53A	-739.77	6172.91	565	49
H53B	-686.01	7147.02	989.43	49
H53C	-730.57	6481.88	1461.72	49
H2A	9368.38	7194.97	4603.99	23
H4A	8906.89	9100.68	3646.68	26
H6A	8678.58	9245.97	5826.25	21
H10A	7562.18	7733.5	6592.01	22
H12A	5567.98	5808.39	4820.76	25
H14A	8098.57	6265.73	4725.91	23
H18A	10815.34	7988.48	6032.69	23
H20D	11729.86	5855.81	6206.54	26
H22D	9184.17	6016.25	6183.47	22
H26D	10103.09	9393.02	6869.66	21
H28A	10248.48	9775.27	9191.27	24
H30A	8891.99	7504.21	7461.95	22

Table 8 Atomic Occupancy for c120819_2_1.

Atom	*Occupancy*	Atom	*Occupancy*	Atom	*Occupancy*
F1A	0.663(19)	F2A	0.663(19)	F3A	0.663(19)
F7A	0.663(19)	F8A	0.663(19)	F9A	0.663(19)
F10B	0.384(3)	F11B	0.384(3)	F12B	0.384(3)
F22A	0.529(3)	F23A	0.529(3)	F24A	0.529(3)
F10A	0.524(3)	F11A	0.524(3)	F12A	0.524(3)
F12C	0.092(3)	F10C	0.092(3)	F11C	0.092(3)
F22B	0.238(3)	F24B	0.238(3)	F23B	0.238(3)
F23C	0.234(3)	F24C	0.234(3)	F22C	0.234(3)

Table 8 Atomic Occupancy for c120819_2_1.

Atom	*Occupancy*	Atom	*Occupancy*	Atom	*Occupancy*
F9B	0.337(19)	F8B	0.337(19)	F7B	0.337(19)
F3B	0.337(19)	F1B	0.337(19)	F2B	0.337(19)

3.3.6. Crystal structure for [($^{i\text{Pr}}$POCOP)Pd$^{\text{II}}$•(PhCC)Au$^{\text{I}}$(IPr)]BF_4, [**3**]BF_4:

Comment: Complex and anion are lying on the crystallographic mirror plane. A THF molecule shows disorder across the mirror plane. An A alert was noted, coming from a disorder on the position of Au, an alternative position is possible (ca 3%).

Crystal Data for $C_{57}H_{80}AuBF_4N_2O_3P_2Pd$ (M =1293.34 g/mol): monoclinic, space group $P2_1/m$ (no. 11), a = 10.83380(10) Å, b = 15.88720(10) Å, c = 17.4029(2) Å, β = 106.8160(10)°, V = 2867.28(5) Å^3, Z = 2, T = 100.0(1) K, μ(CuKα) = 8.254 mm^{-1}, *Dcalc* = 1.498 g/cm^3, 38250 reflections measured (5.304° ≤ 2Θ ≤ 159.418°), 6366 unique (R_{int} = 0.0601, R_{sigma} = 0.0359) which were used in all calculations. The final R_1 was 0.0427 (I > 2σ(I)) and wR_2 was 0.1109 (all data).

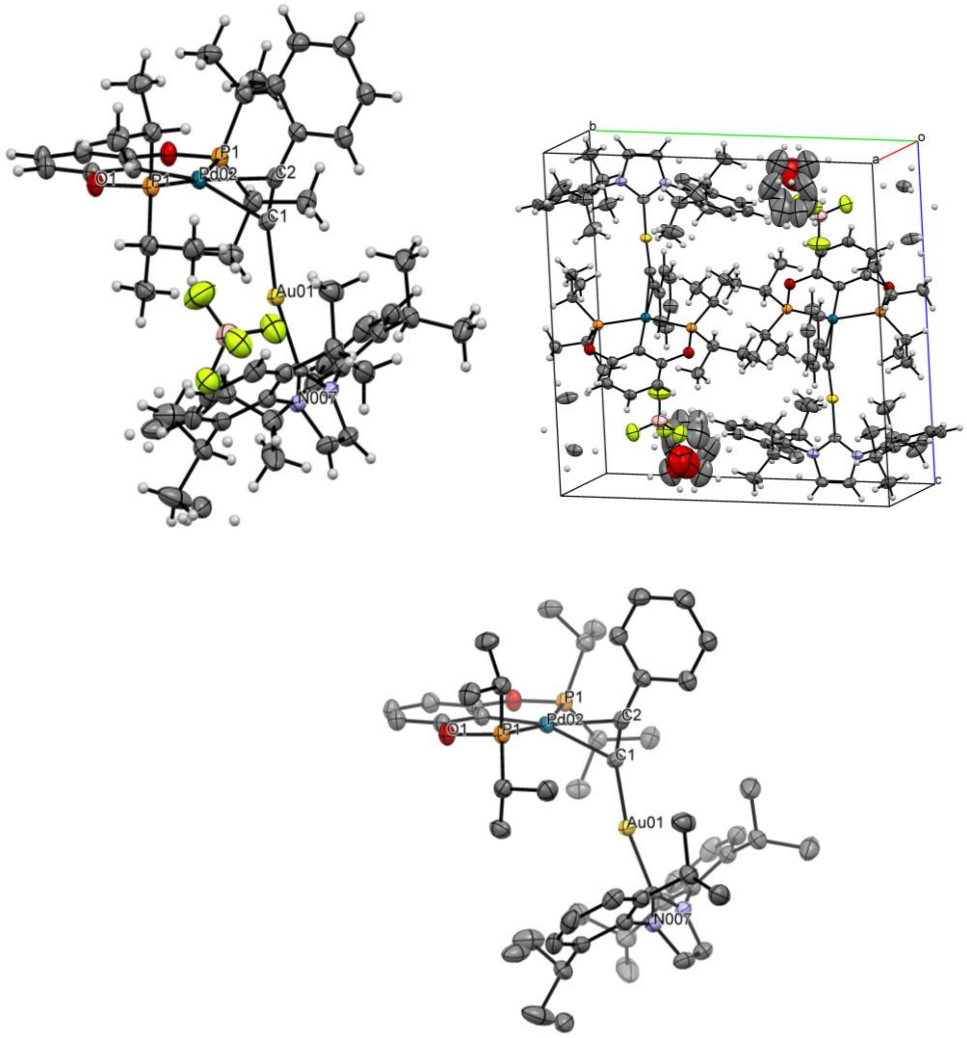

Figure SI-94: Representation of crystal structure from different perspectives. Colors-code: grey/carbon, red/oxygen, light-orange/phosphorus, dark-orange/Cu, yellow/Fluorine, pink/boron, blue/nitrogen, teal/palladium. Left) XRD structure (ORTEP 50% probability ellipsoids), Hydrogens and co-crystallizing molecules omitted for clearity. Right) representation of the unit cell, crystal packing.

Table 1 Crystal data and structure refinement for c240919_1_1.

Identification code	c240919_1_1
Empirical formula	$C_{57}H_{80}AuBF_4N_2O_3P_2Pd$
Formula weight	1293.34

Temperature/K	100.0(1)
Crystal system	monoclinic
Space group	$P2_1/m$
a/Å	10.83380(10)
b/Å	15.88720(10)
c/Å	17.4029(2)
α/°	90
β/°	106.8160(10)
γ/°	90
Volume/Å^3	2867.28(5)
Z	2
ρ_{calc}g/cm^3	1.498
μ/mm^{-1}	8.254
F(000)	1312.0
Crystal size/mm^3	0.138 × 0.063 × 0.033
Radiation	CuKα (λ = 1.54184)
2Θ range for data collection/°	5.304 to 159.418
Index ranges	-12 ≤ h ≤ 13, -20 ≤ k ≤ 20, -21 ≤ l ≤ 22
Reflections collected	38250
Independent reflections	6366 [R_{int} = 0.0601, R_{sigma} = 0.0359]
Data/restraints/parameters	6366/104/396
Goodness-of-fit on F^2	1.077
Final R indexes [I>=2σ (I)]	R_1 = 0.0427, wR_2 = 0.1082
Final R indexes [all data]	R_1 = 0.0475, wR_2 = 0.1109
Largest diff. peak/hole / e Å^{-3}	4.58/-1.91

Table 2 Fractional Atomic Coordinates (×10^4) and Equivalent Isotropic Displacement Parameters (Å^2×10^3) for c240919_1_1. U_{eq} is defined as 1/3 of of the trace of the orthogonalised U_{IJ} tensor.

Atom	*x*	*y*	*z*	U(eq)
Au01	3462.1(2)	2500	7367.3(2)	25.92(9)
Pd02	2537.0(4)	2500	5108.3(3)	23.53(11)
P1	2245.2(10)	1078.6(7)	4870.0(7)	26.8(2)
O1	784(3)	992(2)	4247(2)	31.8(7)
N007	3474(3)	3175(2)	8992(2)	25.9(7)
C1	4005(6)	2500	6363(4)	25.8(12)
C2	4685(6)	2500	5920(4)	27.4(12)
C3	5800(6)	2500	5616(4)	29.2(13)
C4	5684(7)	2500	4800(4)	37.7(16)
C5	6773(7)	2500	4541(5)	44.1(18)
C6	7989(7)	2500	5089(5)	41.8(17)
C7	8110(6)	2500	5902(4)	36.6(15)
C8	7031(6)	2500	6177(4)	32.8(14)
C9	834(6)	2500	4251(4)	28.2(13)
C10	205(4)	1753(3)	3958(3)	28.4(9)

C11	-995(4)	1739(3)	3399(3)	32.5(10)
C12	-1592(6)	2500	3126(4)	33.4(14)
C13	3233(5)	589(3)	4295(3)	33.1(10)
C14	2948(5)	-345(3)	4138(3)	41.3(12)
C15	3036(6)	1066(4)	3505(3)	42.1(12)
C16	2139(4)	354(3)	5663(3)	31.2(9)
C17	3491(5)	170(4)	6224(3)	40.3(11)
C18	1255(5)	730(3)	6113(3)	38.9(11)
C19	3351(5)	2500	8508(3)	25.0(12)
C20	3678(5)	2923(3)	9788(3)	35.5(10)
C21	3350(4)	4036(3)	8724(3)	28.6(9)
C22	4438(4)	4465(3)	8665(3)	30.0(9)
C23	4294(5)	5309(3)	8435(3)	37.8(11)
C24	3093(6)	5694(3)	8270(3)	43.5(12)
C25	2032(5)	5248(4)	8317(3)	41.8(12)
C26	2124(4)	4406(3)	8551(3)	34.5(10)
C27	945(5)	3934(4)	8618(3)	42.2(12)
C28	117(13)	4524(13)	8981(13)	71(6)
C29	145(18)	3643(15)	7801(8)	59(4)
C30	5765(4)	4058(3)	8859(3)	35.3(10)
C31	6726(5)	4545(4)	9527(3)	49.1(14)
C32	6254(5)	4015(5)	8122(4)	51.0(15)
F1	6406(3)	8218(2)	8331(2)	59.3(9)
F2	5273(7)	7500	7231(4)	89(2)
F3	4599(5)	7500	8350(3)	55.1(12)
B1	5647(10)	7500	8028(6)	50(2)
C28A	454(18)	4129(16)	9329(9)	42(5)
C29A	-180(20)	3900(30)	7849(12)	57(8)
O1B	1380(20)	7420(20)	9502(15)	215(9)
C4B	400(30)	7102(16)	8742(18)	153(8)
C3B	-579(16)	7751(12)	8522(12)	112(6)
C2B	-667(16)	8043(15)	9296(15)	122(7)
C1B	555(17)	7972(15)	9865(14)	119(6)

Table 3 Anisotropic Displacement Parameters ($Å^2×10^3$) for c240919_1_1. The Anisotropic displacement factor exponent takes the form: $-2\pi^2[h^2a^{*2}U_{11}+2hka^*b^*U_{12}+...]$.

Atom	U_{11}	U_{22}	U_{33}	U_{23}	U_{13}	U_{12}
Au01	24.23(14)	31.01(15)	22.90(14)	0	7.45(9)	0
Pd02	20.1(2)	25.4(2)	24.7(2)	0	5.79(16)	0
P1	24.1(5)	26.5(5)	28.4(5)	-0.2(4)	5.2(4)	0.0(4)
O1	26.4(15)	28.9(16)	34.9(17)	-0.2(13)	0.8(13)	-0.3(12)
N007	24.1(17)	34(2)	19.8(16)	-1.7(14)	6.5(13)	1.0(14)
C1	24(3)	33(3)	21(3)	0	7(2)	0
C2	26(3)	28(3)	25(3)	0	3(2)	0
C3	26(3)	31(3)	32(3)	0	11(3)	0

C4	26(3)	56(4)	31(3)	0	8(3)	0
C5	39(4)	64(5)	34(4)	0	18(3)	0
C6	30(3)	56(5)	43(4)	0	16(3)	0
C7	26(3)	47(4)	36(4)	0	7(3)	0
C8	29(3)	32(3)	37(4)	0	8(3)	0
C9	22(3)	35(3)	26(3)	0	4(2)	0
C10	27(2)	29(2)	29(2)	-0.2(17)	6.3(17)	0.6(17)
C11	28(2)	33(2)	34(2)	-2.6(19)	5.2(18)	-2.0(18)
C12	24(3)	40(4)	31(3)	0	0(2)	0
C13	30(2)	37(2)	33(2)	-2(2)	9.8(18)	-0.7(19)
C14	45(3)	36(3)	43(3)	-9(2)	12(2)	4(2)
C15	53(3)	42(3)	36(3)	-5(2)	21(2)	1(2)
C16	34(2)	28(2)	30(2)	0.7(18)	7.3(18)	-1.6(18)
C17	39(3)	42(3)	36(3)	7(2)	5(2)	0(2)
C18	42(3)	37(3)	42(3)	-1(2)	19(2)	-9(2)
C19	20(3)	38(3)	21(3)	0	12(2)	0
C20	40(3)	42(3)	25(2)	-5(2)	11.7(19)	-5(2)
C21	27(2)	35(2)	23(2)	-0.5(17)	6.5(16)	-1.5(17)
C22	29(2)	35(2)	25(2)	-3.7(18)	6.0(17)	-2.3(18)
C23	44(3)	38(3)	29(2)	0(2)	7(2)	-6(2)
C24	56(3)	32(3)	34(3)	2(2)	-1(2)	8(2)
C25	36(3)	51(3)	32(2)	-1(2)	0(2)	13(2)
C26	29(2)	49(3)	25(2)	-4(2)	7.9(17)	4(2)
C27	25(2)	66(4)	37(3)	-1(2)	10.4(19)	7(2)
C28	43(6)	106(13)	75(11)	-47(10)	34(7)	-20(7)
C29	56(8)	73(12)	54(6)	-24(6)	27(5)	-29(7)
C30	27(2)	42(3)	37(3)	0(2)	9.7(19)	-2.1(19)
C31	35(3)	70(4)	39(3)	-14(3)	6(2)	1(3)
C32	34(3)	78(4)	43(3)	-16(3)	14(2)	-7(3)
F1	51.7(19)	53(2)	76(3)	-6.9(18)	22.2(18)	-4.8(16)
F2	91(5)	129(6)	44(3)	0	17(3)	0
F3	47(3)	66(3)	54(3)	0	17(2)	0
B1	47(5)	62(6)	41(5)	0	15(4)	0
C28A	28(8)	62(12)	35(7)	4(7)	9(6)	0(7)
C29A	40(10)	100(30)	37(7)	-16(10)	18(6)	-22(11)
O1B	182(14)	200(18)	259(19)	-50(19)	58(11)	100(17)
C4B	169(18)	126(17)	201(19)	-22(14)	110(14)	35(14)
C3B	77(9)	104(17)	186(13)	-10(11)	85(9)	-24(8)
C2B	64(8)	130(14)	187(15)	-67(13)	59(9)	-31(9)
C1B	71(9)	123(14)	184(15)	-31(13)	67(9)	-8(10)

Table 4 Bond Lengths for c240919_1_1.

Atom	Atom	Length/Å	Atom	Atom	Length/Å
Au01	C1	1.999(6)	C13	C15	1.530(7)
Au01	C19	2.023(6)	C16	C17	1.535(7)

Pd02	P1[1]	2.3012(11)	C16	C18	1.523(7)
Pd02	P1	2.3012(11)	C20	C20[1]	1.345(11)
Pd02	C1	2.299(6)	C21	C22	1.390(6)
Pd02	C2	2.347(6)	C21	C26	1.403(6)
Pd02	C9	2.010(6)	C22	C23	1.395(7)
P1	O1	1.645(3)	C22	C30	1.523(6)
P1	C13	1.836(5)	C23	C24	1.391(8)
P1	C16	1.827(5)	C24	C25	1.373(8)
O1	C10	1.388(5)	C25	C26	1.393(8)
N007	C19	1.346(5)	C26	C27	1.515(7)
N007	C20	1.395(6)	C27	C28	1.551(10)
N007	C21	1.439(6)	C27	C29	1.508(10)
C1	C2	1.210(9)	C27	C28A	1.513(12)
C2	C3	1.452(9)	C27	C29A	1.531(13)
C3	C4	1.390(10)	C30	C31	1.528(7)
C3	C8	1.406(9)	C30	C32	1.525(7)
C4	C5	1.379(10)	F1	B1	1.416(7)
C5	C6	1.384(11)	F2	B1	1.328(12)
C6	C7	1.382(11)	F3	B1	1.404(11)
C7	C8	1.386(10)	O1B	C4B	1.53(2)
C9	C10	1.389(5)	O1B	C1B	1.52(2)
C9	C10[1]	1.389(5)	C4B	C3B	1.45(2)
C10	C11	1.380(6)	C3B	C2B	1.45(3)
C11	C12	1.389(6)	C2B	C1B	1.41(2)
C13	C14	1.525(7)			

[1]+X,1/2-Y,+Z

Table 5 Bond Angles for c240919_1_1.

Atom	Atom	Atom	Angle/°	Atom	Atom	Atom	Angle/°
C1	Au01	C19	166.9(2)	C14	C13	P1	112.9(4)
P1	Pd02	P1[1]	157.81(6)	C14	C13	C15	110.7(4)
P1	Pd02	C2	99.73(3)	C15	C13	P1	109.2(3)
P1[1]	Pd02	C2	99.73(3)	C17	C16	P1	110.0(3)
C1	Pd02	P1	101.09(3)	C18	C16	P1	109.1(3)
C1	Pd02	P1[1]	101.09(3)	C18	C16	C17	112.0(4)
C1	Pd02	C2	30.2(2)	N007[1]	C19	Au01	126.2(3)
C9	Pd02	P1	79.48(3)	N007	C19	Au01	126.2(3)
C9	Pd02	P1[1]	79.48(3)	N007	C19	N007[1]	105.6(5)
C9	Pd02	C1	159.9(2)	C20[1]	C20	N007	106.6(3)
C9	Pd02	C2	169.9(2)	C22	C21	N007	119.2(4)
O1	P1	Pd02	104.86(12)	C22	C21	C26	123.2(5)
O1	P1	C13	101.9(2)	C26	C21	N007	117.5(4)
O1	P1	C16	100.75(19)	C21	C22	C23	117.8(4)
C13	P1	Pd02	116.25(16)	C21	C22	C30	122.8(4)

C16	P1	Pd02	121.19(16)	C23	C22	C30	119.4(4)
C16	P1	C13	108.6(2)	C24	C23	C22	120.1(5)
C10	O1	P1	114.5(3)	C25	C24	C23	120.7(5)
C19	N007	C20	110.6(4)	C24	C25	C26	121.5(5)
C19	N007	C21	124.9(4)	C21	C26	C27	122.9(5)
C20	N007	C21	124.5(4)	C25	C26	C21	116.7(5)
Au01	C1	Pd02	122.2(3)	C25	C26	C27	120.4(5)
C2	C1	Au01	160.7(5)	C26	C27	C28	109.4(7)
C2	C1	Pd02	77.1(4)	C26	C27	C29A	115.3(15)
C1	C2	Pd02	72.7(4)	C29	C27	C26	110.3(9)
C1	C2	C3	162.9(6)	C29	C27	C28	109.0(8)
C3	C2	Pd02	124.4(4)	C28A	C27	C26	117.8(8)
C4	C3	C2	122.3(6)	C28A	C27	C29A	109.9(11)
C4	C3	C8	119.7(6)	C22	C30	C31	110.2(4)
C8	C3	C2	118.0(6)	C22	C30	C32	111.7(4)
C5	C4	C3	120.0(7)	C32	C30	C31	109.7(4)
C4	C5	C6	120.6(7)	F1	B1	F1[2]	107.4(7)
C7	C6	C5	119.6(7)	F2	B1	F1	110.9(5)
C6	C7	C8	120.9(7)	F2	B1	F1[2]	111.0(5)
C7	C8	C3	119.1(7)	F2	B1	F3	112.3(8)
C10	C9	Pd02	121.3(3)	F3	B1	F1[2]	107.5(5)
C10[1]	C9	Pd02	121.3(3)	F3	B1	F1	107.5(5)
C10	C9	C10[1]	117.3(6)	C1B	O1B	C4B	101.7(18)
O1	C10	C9	119.3(4)	C3B	C4B	O1B	105.5(18)
C11	C10	O1	118.4(4)	C4B	C3B	C2B	102.7(15)
C11	C10	C9	122.3(4)	C1B	C2B	C3B	109.0(13)
C10	C11	C12	118.5(4)	C2B	C1B	O1B	107.5(17)
C11	C12	C11[1]	121.1(6)				

[1]+X,1/2-Y,+Z; [2]+X,3/2-Y,+Z

Table 6 Hydrogen Atom Coordinates (Å×10⁴) and Isotropic Displacement Parameters (Å²×10³) for c240919_1_1.

Atom	*x*	*y*	*z*	U(eq)
H4	4853.69	2500	4419.5	45
H5	6688.72	2500	3982.69	53
H6	8735.45	2500	4907.44	50
H7	8944.97	2500	6277.2	44
H8	7121.09	2500	6736.13	39
H11	-1402.89	1219.92	3205.82	39
H12	-2421.6	2500	2745.18	40
H13	4159.26	647.93	4612.72	40
H14A	3190.74	-651.45	4648.65	62
H14B	3444.54	-562.21	3790.97	62
H14C	2025.18	-423.3	3873.21	62

H15A	2160.75	964.05	3155.84	63
H15B	3663.89	869.8	3237.12	63
H15C	3155.97	1670.39	3614.55	63
H16	1752.01	-186.71	5409.98	37
H17A	4019.88	-87.19	5915.56	60
H17B	3424.23	-217.2	6648.25	60
H17C	3892.26	696.81	6464.92	60
H18A	1647.33	1243.12	6391.28	58
H18B	1130.14	321.84	6506.19	58
H18C	419.69	867.16	5731.28	58
H20	3794.49	3280.57	10240.8	43
H23	5018.23	5620.83	8390.19	45
H24	3006.53	6272.09	8124.36	52
H25	1215.77	5519.48	8186.34	50
H27	1223.88	3434.89	8976.42	51
H27A	1241.66	3336.55	8706.9	51
H28A	681.96	4843.03	9427.47	107
H28B	-486.27	4186.38	9176.55	107
H28C	-366.41	4914.87	8567.06	107
H29A	-126.34	4131.5	7449.04	88
H29B	-618.72	3343.77	7852.7	88
H29C	658.36	3264.39	7571.61	88
H30	5699.19	3471.29	9051.52	42
H31A	6861.71	5105.87	9331	74
H31B	7548.13	4241.43	9690.3	74
H31C	6384.88	4600.76	9988.26	74
H32A	5636.03	3701.63	7694.52	76
H32B	7091.08	3728.44	8261.86	76
H32C	6350.06	4586.19	7934.85	76
H28D	1105.4	3966.14	9826.11	63
H28E	-342.84	3813.55	9279.95	63
H28F	280	4733.49	9341.34	63
H29D	-526.68	4469.45	7710.05	86
H29E	-863.06	3536.89	7933.5	86
H29F	115.69	3674.77	7410.05	86
H4BA	805.35	7013.67	8307.89	184
H4BB	13.41	6563.29	8846.14	184
H3BA	-1412.42	7519.75	8191.94	135
H3BB	-309.17	8211.45	8221.84	135
H2BA	-956.1	8636.35	9254.58	147
H2BB	-1304.09	7699	9466.03	147
H1BA	472	7715.89	10366.77	143
H1BB	953.27	8534.84	9993.73	143

Table 7 Atomic Occupancy for c240919_1_1.

Atom	*Occupancy*	Atom	*Occupancy*	Atom	*Occupancy*
H27	0.64(3)	H27A	0.36(3)	C28	0.64(3)
H28A	0.64(3)	H28B	0.64(3)	H28C	0.64(3)
C29	0.64(3)	H29A	0.64(3)	H29B	0.64(3)
H29C	0.64(3)	C28A	0.36(3)	H28D	0.36(3)
H28E	0.36(3)	H28F	0.36(3)	C29A	0.36(3)
H29D	0.36(3)	H29E	0.36(3)	H29F	0.36(3)
O1B	0.5	C4B	0.5	H4BA	0.5
H4BB	0.5	C3B	0.5	H3BA	0.5
H3BB	0.5	C2B	0.5	H2BA	0.5
H2BB	0.5	C1B	0.5	H1BA	0.5
H1BB	0.5				

3.3.7. Crystal structure for [($^{i\text{Pr}}$POCOP)Pd$^{\text{II}}$•(PhCC)Au$^{\text{I}}$(IPr)]OTf, [**3**]OTf:

Crystal Data for $C_{55}H_{74}AuCl_2F_3N_2O_5P_2PdS$ (M =1368.42 g/mol): monoclinic, space group $P2_1/m$ (no. 11), a = 10.8130(5) Å, b = 15.7986(8) Å, c = 17.8785(9) Å, β = 107.1730(10)°, V = 2918.0(2) Å^3, Z = 2, T = 100.0(1) K, μ(MoKα) = 3.057 mm^{-1}, *Dcalc* = 1.557 g/cm^3, 71777 reflections measured (3.512° ≤ 2Θ ≤ 61.062°), 9157 unique (R_{int} = 0.0748, R_{sigma} = 0.0543) which were used in all calculations. The final R_1 was 0.0332 (I > 2σ(I)) and wR_2 was 0.0691 (all data).

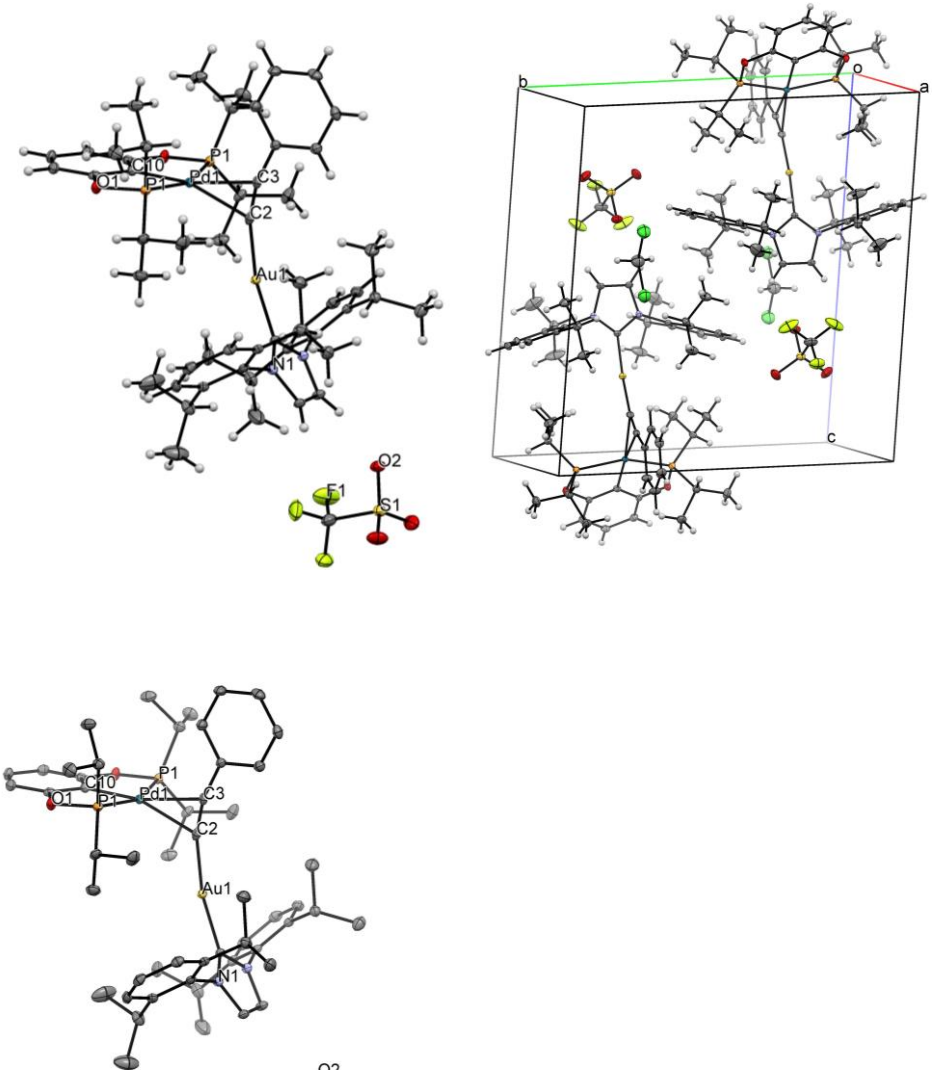

Figure SI-95: Representation of crystal structure from different perspectives. Color-code: grey/carbon, red/oxygen, light-orange/phosphorus, yellow/Au, yellow/fluorine, orange/sulfur, blue/nitrogen, teal/palladium. Left) XRD structure (ORTEP 50% probability ellipsoids), hydrogens and co-crystallizing molecules omitted for clearity. Right) representation of the unit cell, crystal packing.

Table 1 Crystal data and structure refinement for c241016_2_1.

Identification code	c241016_2_1
Empirical formula	$C_{55}H_{74}AuCl_2F_3N_2O_5P_2PdS$
Formula weight	1368.42
Temperature/K	100.0(1)
Crystal system	monoclinic
Space group	$P2_1/m$
a/Å	10.8130(5)
b/Å	15.7986(8)

c/Å	17.8785(9)
α/°	90
β/°	107.1730(10)
γ/°	90
Volume/Å^3	2918.0(2)
Z	2
ρ_{calc}g/cm^3	1.557
μ/mm^{-1}	3.057
F(000)	1380.0
Crystal size/mm^3	0.16 × 0.1 × 0.06
Radiation	MoKα (λ = 0.71073)
2Θ range for data collection/°	3.512 to 61.062
Index ranges	-7 ≤ h ≤ 15, -22 ≤ k ≤ 22, -25 ≤ l ≤ 25
Reflections collected	71777
Independent reflections	9157 [R_{int} = 0.0748, R_{sigma} = 0.0543]
Data/restraints/parameters	9157/0/363
Goodness-of-fit on F^2	1.036
Final R indexes [I>=2σ (I)]	R_1 = 0.0332, wR_2 = 0.0640
Final R indexes [all data]	R_1 = 0.0481, wR_2 = 0.0691
Largest diff. peak/hole / e Å^{-3}	1.65/-1.21

Table 2 Fractional Atomic Coordinates (×10^4) and Equivalent Isotropic Displacement Parameters (Å^2×10^3) for c241016_2_1. U_{eq} is defined as 1/3 of of the trace of the orthogonalised U_{IJ} tensor.

Atom	*x*	*y*	*z*	U(eq)
Au1	6061.5(2)	7500	7604.0(2)	10.31(4)
Pd1	7288.0(2)	7500	9786.8(2)	8.70(6)
P1	7231.9(6)	8929.3(5)	10022.9(4)	11.03(14)
O1	6349.9(17)	9015.7(12)	10628.8(11)	13.2(4)
N1	4502(2)	6820.1(14)	6029.7(14)	10.9(5)
C1	4839(3)	7500	6511(2)	10.4(7)
C2	7581(4)	7500	8565(2)	13.3(8)
C3	8699(3)	7500	9003(2)	11.4(8)
C4	10076(3)	7500	9322(2)	11.7(8)
C5	10709(4)	7500	10119(2)	17.2(9)
C6	12046(4)	7500	10401(3)	20.0(9)
C7	12783(4)	7500	9878(3)	19.9(9)
C8	12171(4)	7500	9082(3)	17.5(9)
C9	10825(3)	7500	8796(2)	14.6(8)
C10	6412(3)	7500	10628(2)	10.9(7)
C11	6066(2)	8249.6(17)	10920.5(16)	11.2(5)
C12	5428(2)	8265.2(19)	11491.9(17)	14.5(6)
C13	5122(4)	7500	11777(2)	15.4(8)
C14	8762(2)	9406.8(18)	10591.2(17)	15.2(6)
C15	8660(3)	10347.6(19)	10754(2)	21.8(7)

C16	9277(3)	8918(2)	11365.5(18)	21.6(7)
C17	6410(3)	9664.6(19)	9256.6(17)	15.2(6)
C18	7258(3)	9853(2)	8717.9(19)	22.8(7)
C19	5098(3)	9290(2)	8800.7(19)	20.9(7)
C20	4583(2)	5952.2(18)	6289.4(16)	12.0(5)
C21	3507(2)	5600.3(19)	6453.0(16)	13.6(6)
C22	3589(3)	4754.3(18)	6678.5(17)	15.3(6)
C23	4693(3)	4283.3(19)	6734.2(17)	17.3(6)
C24	5750(3)	4657.6(19)	6574.1(17)	16.4(6)
C25	5718(2)	5497.9(18)	6345.9(16)	12.0(5)
C26	6875(2)	5875.8(19)	6147.8(17)	15.0(6)
C27	7140(3)	5398(2)	5473.7(18)	23.1(7)
C28	8082(3)	5883(2)	6866.5(19)	24.4(7)
C29	2278(3)	6103(2)	6386.1(19)	19.4(6)
C30	2086(3)	6239(3)	7185(2)	45.7(12)
C31	1093(3)	5694(3)	5828(2)	45.0(11)
C33	3980(2)	7075.1(18)	5257.6(17)	14.1(6)
S1	2446.1(9)	7500	2816.1(6)	16.6(2)
F1	1226(2)	6815.0(17)	3726.2(14)	53.5(7)
F2	-16(2)	7500	2747.8(17)	34.3(7)
O2	3604(3)	7500	3480.7(18)	22.1(7)
O3	2229(2)	8263.7(15)	2361.6(14)	28.9(6)
C34	1153(4)	7500	3274(3)	27.1(11)
Cl1	2315.5(13)	2500	6400.2(9)	40.3(3)
Cl2	1554.7(12)	2500	4691.9(9)	38.2(3)
C32	2873(5)	2500	5568(3)	35.3(12)

Table 3 Anisotropic Displacement Parameters ($Å^2×10^3$) for c241016_2_1. The Anisotropic displacement factor exponent takes the form: $-2\pi^2[h^2a^{*2}U_{11}+2hka^*b^*U_{12}+...]$.

Atom	U_{11}	U_{22}	U_{33}	U_{23}	U_{13}	U_{12}
Au1	10.73(6)	11.32(8)	8.25(8)	0	1.80(5)	0
Pd1	9.09(11)	8.46(15)	8.79(15)	0	3.01(10)	0
P1	12.6(3)	10.0(4)	10.9(4)	1.0(3)	4.3(3)	0.5(2)
O1	18.2(9)	9.9(10)	14.4(11)	1.4(8)	9.1(8)	1.3(7)
N1	12.6(10)	8.8(12)	10.5(12)	-0.1(9)	2.1(8)	-0.2(8)
C1	11.5(15)	11(2)	7.7(19)	0	1.6(13)	0
C2	19.0(17)	12(2)	11(2)	0	7.7(15)	0
C3	15.1(16)	9.6(19)	12(2)	0	7.2(14)	0
C4	11.6(15)	13(2)	10(2)	0	2.3(14)	0
C5	13.6(17)	25(2)	13(2)	0	4.4(15)	0
C6	11.3(16)	33(3)	14(2)	0	0.1(15)	0
C7	10.8(16)	23(2)	23(3)	0	1.2(16)	0
C8	15.2(17)	18(2)	22(2)	0	10.6(16)	0
C9	14.9(17)	16(2)	13(2)	0	3.2(15)	0
C10	10.1(15)	13(2)	10(2)	0	2.9(13)	0

C11	11.7(11)	9.7(14)	10.7(14)	0.1(11)	1.1(9)	-1.4(9)
C12	15.0(12)	14.5(15)	14.2(16)	-2.6(12)	4.3(11)	0.9(10)
C13	16.8(17)	20(2)	12(2)	0	7.4(15)	0
C14	14.3(12)	14.9(15)	15.7(16)	-0.9(12)	3.1(10)	-1.1(10)
C15	22.7(14)	14.2(16)	26.9(19)	-4.4(14)	5.0(13)	-2.6(11)
C16	22.5(14)	19.2(17)	18.0(17)	0.5(13)	-2.0(12)	1.7(11)
C17	21.3(13)	13.3(15)	10.3(15)	2.2(12)	3.6(11)	3.1(10)
C18	33.5(16)	19.9(17)	17.3(17)	5.4(14)	11.0(13)	2.3(13)
C19	21.8(14)	17.2(17)	19.5(17)	1.6(13)	-0.5(12)	5.4(11)
C20	15.5(12)	11.8(14)	7.4(14)	-0.9(11)	1.2(10)	-2.4(10)
C21	13.7(12)	14.9(15)	11.5(15)	-1.7(11)	2.8(10)	-2.5(10)
C22	20.6(13)	12.6(15)	14.3(15)	-1.3(12)	7.6(11)	-5.7(10)
C23	26.7(14)	11.3(15)	12.7(16)	2.6(12)	4.0(11)	1.2(11)
C24	18.2(12)	15.5(15)	14.0(15)	1.1(12)	2.5(10)	3.5(11)
C25	13.0(11)	13.9(14)	8.1(14)	-0.6(11)	1.6(10)	0.1(10)
C26	13.7(12)	15.5(15)	16.1(16)	-1.8(12)	5(1)	0.1(10)
C27	23.1(14)	29.8(19)	18.0(17)	-3.3(14)	8.5(12)	-5.2(13)
C28	16.2(13)	35(2)	20.7(18)	-5.1(15)	3.9(12)	-2.8(12)
C29	16.6(12)	16.2(16)	27.3(18)	-1.4(14)	9.2(12)	0.7(11)
C30	34.2(19)	76(3)	25(2)	-19(2)	5.5(16)	23(2)
C31	21.2(16)	62(3)	45(3)	-21(2)	0.2(16)	10.5(17)
C33	15.7(12)	15.5(15)	8.9(14)	0.0(11)	0(1)	-1.3(10)
S1	15.7(4)	17.4(6)	15.1(6)	0	2.0(4)	0
F1	35.5(11)	83(2)	42.3(15)	34.7(14)	12.4(10)	-5.3(12)
F2	18.5(12)	55(2)	26.8(17)	0	3.0(11)	0
O2	19.2(14)	27.5(19)	15.7(17)	0	-0.8(12)	0
O3	28.1(11)	25.5(14)	28.2(14)	12.7(11)	0.8(10)	-2.0(9)
C34	20(2)	43(3)	16(2)	0	2.0(17)	0
Cl1	47.9(7)	38.0(8)	40.1(9)	0	20.6(6)	0
Cl2	39.4(7)	32.3(8)	39.5(8)	0	6.3(6)	0
C32	35(3)	40(3)	34(3)	0	15(2)	0

Table 4 Bond Lengths for c241016_2_1.

Atom	Atom	Length/Å	Atom	Atom	Length/Å
Au1	C1	2.010(4)	C13	C12[1]	1.389(3)
Au1	C2	1.996(4)	C14	C15	1.525(4)
Pd1	P1[1]	2.3014(7)	C14	C16	1.538(4)
Pd1	P1	2.3014(7)	C17	C18	1.542(4)
Pd1	C2	2.298(4)	C17	C19	1.531(4)
Pd1	C3	2.357(4)	C20	C21	1.396(4)
Pd1	C10	2.001(4)	C20	C25	1.400(4)
P1	O1	1.6467(19)	C21	C22	1.391(4)
P1	C14	1.830(3)	C21	C29	1.522(4)
P1	C17	1.816(3)	C22	C23	1.385(4)
O1	C11	1.388(3)	C23	C24	1.390(4)

N1	C1	1.357(3)	C24	C25	1.386(4)
N1	C20	1.442(4)	C25	C26	1.519(4)
N1	C33	1.388(4)	C26	C27	1.520(4)
C1	N1[1]	1.357(3)	C26	C28	1.538(4)
C2	C3	1.231(5)	C29	C30	1.518(5)
C3	C4	1.428(5)	C29	C31	1.517(4)
C4	C5	1.388(6)	C33	C33[1]	1.343(6)
C4	C9	1.410(5)	S1	O2	1.449(3)
C5	C6	1.384(5)	S1	O3[1]	1.435(2)
C6	C7	1.396(6)	S1	O3	1.435(2)
C7	C8	1.381(6)	S1	C34	1.817(5)
C8	C9	1.393(5)	F1	C34	1.339(3)
C10	C11[1]	1.389(3)	F2	C34	1.335(5)
C10	C11	1.389(3)	C34	F1[1]	1.339(3)
C11	C12	1.392(4)	Cl1	C32	1.762(5)
C12	C13	1.389(3)	Cl2	C32	1.780(5)

[1]+X,3/2-Y,+Z

Table 5 Bond Angles for c241016_2_1.

Atom	Atom	Atom	Angle/°	Atom	Atom	Atom	Angle/°
C2	Au1	C1	167.07(14)	O1	C11	C12	118.2(2)
P1[1]	Pd1	P1	157.76(4)	C10	C11	C12	122.5(3)
P1[1]	Pd1	C3	99.55(2)	C13	C12	C11	118.5(3)
P1	Pd1	C3	99.55(2)	C12	C13	C12[1]	121.0(4)
C2	Pd1	P1[1]	101.121(19)	C15	C14	P1	113.78(19)
C2	Pd1	P1	101.121(19)	C15	C14	C16	110.1(3)
C2	Pd1	C3	30.63(13)	C16	C14	P1	108.7(2)
C10	Pd1	P1[1]	79.52(2)	C18	C17	P1	110.26(19)
C10	Pd1	P1	79.52(2)	C19	C17	P1	108.9(2)
C10	Pd1	C2	160.68(14)	C19	C17	C18	111.7(3)
C10	Pd1	C3	168.69(14)	C21	C20	N1	118.1(2)
O1	P1	Pd1	104.70(8)	C21	C20	C25	123.2(3)
O1	P1	C14	101.84(12)	C25	C20	N1	118.6(2)
O1	P1	C17	101.18(12)	C20	C21	C29	122.6(3)
C14	P1	Pd1	115.97(9)	C22	C21	C20	117.2(2)
C17	P1	Pd1	121.52(10)	C22	C21	C29	120.2(2)
C17	P1	C14	108.43(13)	C23	C22	C21	121.1(3)
C11	O1	P1	114.23(17)	C22	C23	C24	120.0(3)
C1	N1	C20	124.7(2)	C25	C24	C23	121.2(3)
C1	N1	C33	110.8(2)	C20	C25	C26	123.1(3)
C33	N1	C20	124.4(2)	C24	C25	C20	117.2(2)
N1[1]	C1	Au1	126.35(16)	C24	C25	C26	119.6(2)
N1	C1	Au1	126.35(16)	C25	C26	C27	110.5(2)
N1	C1	N1[1]	104.7(3)	C25	C26	C28	111.2(2)

Au1	C2	Pd1	120.57(17)	C27	C26	C28	110.7(2)
C3	C2	Au1	162.1(3)	C30	C29	C21	111.0(3)
C3	C2	Pd1	77.3(3)	C31	C29	C21	112.2(3)
C2	C3	Pd1	72.0(2)	C31	C29	C30	110.9(3)
C2	C3	C4	165.0(4)	C33[1]	C33	N1	106.88(15)
C4	C3	Pd1	123.0(3)	O2	S1	C34	102.9(2)
C5	C4	C3	123.4(3)	O3	S1	O2	114.95(11)
C5	C4	C9	118.5(3)	O3[1]	S1	O2	114.95(11)
C9	C4	C3	118.1(4)	O3	S1	O3[1]	114.5(2)
C6	C5	C4	121.4(4)	O3	S1	C34	103.65(12)
C5	C6	C7	119.8(4)	O3[1]	S1	C34	103.65(13)
C8	C7	C6	119.8(4)	F1[1]	C34	S1	110.8(2)
C7	C8	C9	120.5(4)	F1	C34	S1	110.8(2)
C8	C9	C4	120.0(4)	F1[1]	C34	F1	107.8(4)
C11	C10	Pd1	121.49(17)	F2	C34	S1	112.2(3)
C11[1]	C10	Pd1	121.49(17)	F2	C34	F1	107.5(2)
C11[1]	C10	C11	117.0(3)	F2	C34	F1[1]	107.5(2)
O1	C11	C10	119.2(2)	Cl1	C32	Cl2	111.0(3)

[1]+X,3/2-Y,+Z

Table 6 Torsion Angles for c241016_2_1.

A	B	C	D	Angle/°	A	B	C	D	Angle/°
Au1	C2	C3	Pd1	180.000(6)	C14	P1	O1	C11	-111.77(19)
Au1	C2	C3	C4	0.000(9)	C14	P1	C17	C18	59.7(2)
Pd1	P1	O1	C11	9.40(18)	C14	P1	C17	C19	-177.3(2)
Pd1	P1	C14	C15	-178.02(18)	C17	P1	O1	C11	136.47(19)
Pd1	P1	C14	C16	-54.9(2)	C17	P1	C14	C15	41.1(3)
Pd1	P1	C17	C18	-78.6(2)	C17	P1	C14	C16	164.3(2)
Pd1	P1	C17	C19	44.4(2)	C20	N1	C1	Au1	22.9(4)
Pd1	C2	C3	C4	180.000(6)	C20	N1	C1	N1[1]	-174.76(16)
Pd1	C3	C4	C5	0.000(2)	C20	N1	C33	C33[1]	175.10(19)
Pd1	C3	C4	C9	180.000(2)	C20	C21	C22	C23	-0.3(4)
Pd1	C10	C11	O1	-0.8(4)	C20	C21	C29	C30	-112.5(3)
Pd1	C10	C11	C12	178.4(2)	C20	C21	C29	C31	122.8(3)
P1	O1	C11	C10	-6.6(3)	C20	C25	C26	C27	-118.4(3)
P1	O1	C11	C12	174.15(19)	C20	C25	C26	C28	118.2(3)
O1	P1	C14	C15	-65.0(2)	C21	C20	C25	C24	0.2(4)
O1	P1	C14	C16	58.1(2)	C21	C20	C25	C26	178.4(3)
O1	P1	C17	C18	166.3(2)	C21	C22	C23	C24	0.9(5)
O1	P1	C17	C19	-70.7(2)	C22	C21	C29	C30	68.0(4)
O1	C11	C12	C13	179.0(3)	C22	C21	C29	C31	-56.7(4)
N1	C20	C21	C22	178.0(2)	C22	C23	C24	C25	-1.0(5)
N1	C20	C21	C29	-1.5(4)	C23	C24	C25	C20	0.4(4)
N1	C20	C25	C24	-178.1(2)	C23	C24	C25	C26	-177.8(3)

N1	C20	C25	C26	0.1(4)	C24	C25	C26	C27	59.8(4)
C1	N1	C20	C21	89.9(3)	C24	C25	C26	C28	-63.7(3)
C1	N1	C20	C25	-91.7(3)	C25	C20	C21	C22	-0.3(4)
C1	N1	C33	C33[1]	-0.6(2)	C25	C20	C21	C29	-179.8(3)
C2	C3	C4	C5	180.000(6)	C29	C21	C22	C23	179.2(3)
C2	C3	C4	C9	0.000(7)	C33	N1	C1	Au1	-161.5(2)
C3	C4	C5	C6	180.000(2)	C33	N1	C1	N1[1]	0.9(4)
C3	C4	C9	C8	180.000(2)	C33	N1	C20	C21	-85.2(3)
C4	C5	C6	C7	0.000(3)	C33	N1	C20	C25	93.2(3)
C5	C4	C9	C8	0.000(3)	O2	S1	C34	F1	-59.9(3)
C5	C6	C7	C8	0.000(3)	O2	S1	C34	F1[1]	59.9(3)
C6	C7	C8	C9	0.000(3)	O2	S1	C34	F2	180.000(0)
C7	C8	C9	C4	0.000(3)	O3	S1	C34	F1	-179.9(3)
C9	C4	C5	C6	0.000(3)	O3[1]	S1	C34	F1	60.2(3)
C10	C11	C12	C13	-0.3(4)	O3[1]	S1	C34	F1[1]	179.9(3)
C11[1]	C10	C11	O1	-177.85(18)	O3	S1	C34	F1[1]	-60.2(3)
C11[1]	C10	C11	C12	1.4(5)	O3[1]	S1	C34	F2	-59.93(11)
C11	C12	C13	C12[1]	-0.9(5)	O3	S1	C34	F2	59.93(11)

[1]+X,3/2-Y,+Z

Table 7 Hydrogen Atom Coordinates (Å×10^4) and Isotropic Displacement Parameters (Å^2×10^3) for c241016_2_1.

Atom	*x*	*y*	*z*	U(eq)
H5	10215	7500	10479	21
H6	12462	7500	10950	24
H7	13701	7500	10069	24
H8	12673	7500	8726	21
H9	10412	7500	8248	18
H12	5206	8787	11683	17
H13	4698	7500	12172	19
H14	9399	9338	10288	18
H15A	8403	10659	10258	33
H15B	9501	10556	11079	33
H15C	8010	10433	11030	33
H16A	8717	9026	11697	32
H16B	10160	9107	11637	32
H16C	9283	8311	11256	32
H17	6258	10206	9506	18
H18A	8079	10104	9027	34
H18B	6804	10251	8307	34
H18C	7429	9326	8477	34
H19A	5231	8749	8569	31
H19B	4648	9683	8385	31
H19C	4574	9200	9157	31

H22	2876	4495	6796	18
H23	4727	3704	6882	21
H24	6508	4332	6622	20
H26	6661	6475	5978	18
H27A	7381	4813	5634	35
H27B	7850	5673	5330	35
H27C	6360	5400	5022	35
H28A	7901	6211	7288	37
H28B	8806	6142	6725	37
H28C	8308	5301	7045	37
H29	2386	6672	6170	23
H30A	1951	5691	7407	69
H30B	1329	6600	7132	69
H30C	2856	6512	7533	69
H31A	1240	5607	5318	68
H31B	341	6063	5764	68
H31C	931	5147	6040	68
H33	3680	6717	4814	17
H32A	3416	1993	5579	42
H32B	3416	3007	5579	42

3.3.8. Crystal structure for [(^{iPr}POCOP)Pd^{II} (CCPh)•Au^{I}(IPr)]BArF, [**3**]BArF:

Comment: Disorder on the BArF Anion. Some reflections fell in the beamstop, hence there is a minor alert in the work up of the data. A copper measurement has been performed where this issue did not occur.

Crystal Data for $C_{85}H_{84}AuBF_{24}N_2O_2P_2Pd$ (*M* =1997.65 g/mol): triclinic, space group P-1 (no. 2), *a* = 15.73380(10) Å, *b* = 16.5046(2) Å, *c* = 18.12680(10) Å, *α* = 105.1640(10)°, *β* = 107.8150(10)°, *γ* = 97.3110(10)°, *V* = 4213.93(7) Å^3, *Z* = 2, *T* = 100.00(10) K, μ(Mo Kα) = 2.091 mm^{-1}, *Dcalc* = 1.574 g/cm^3, 140167 reflections measured (4.768° ≤ 2Θ ≤ 69.54°), 31908 unique (R_{int} = 0.0351, R_{sigma} = 0.0340) which were used in all calculations. The final R_1 was 0.0285 (I > 2σ(I)) and wR_2 was 0.0642 (all data).

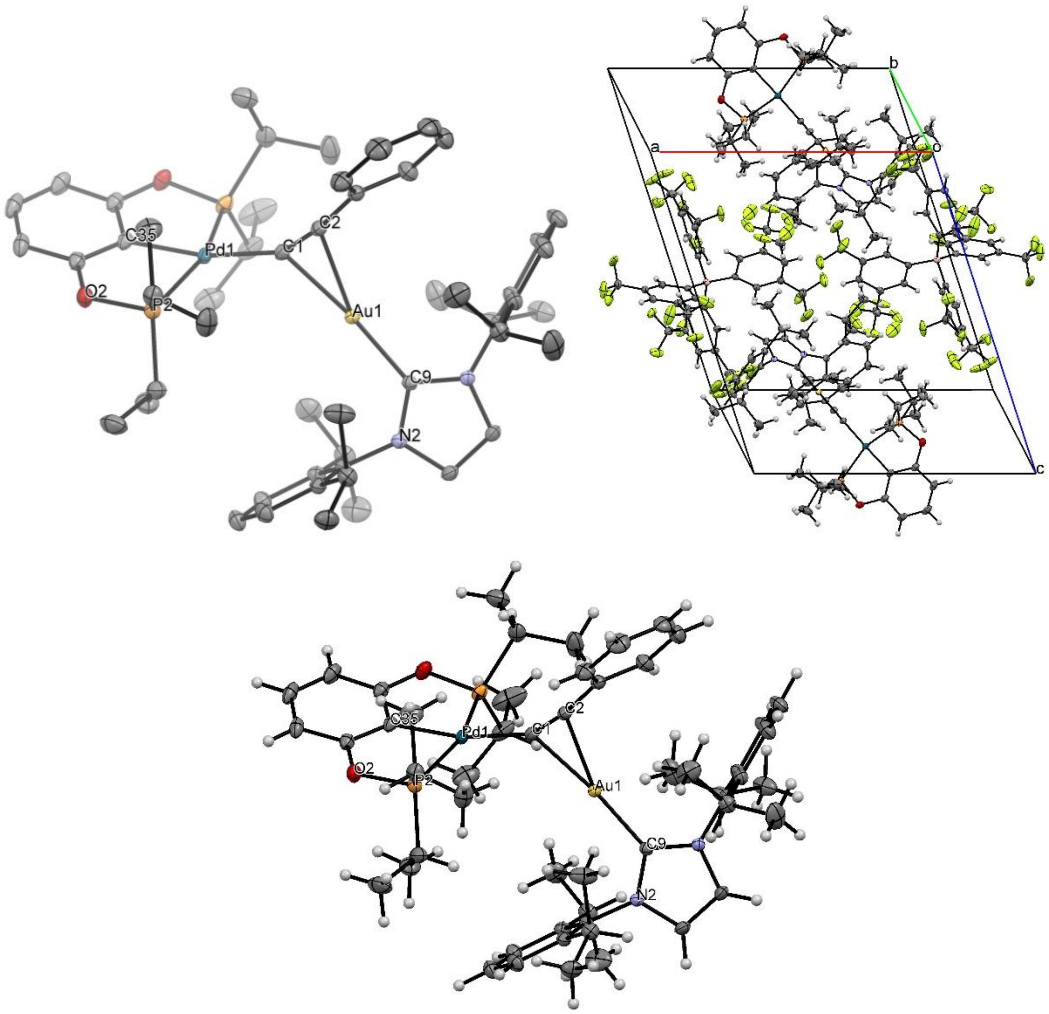

Figure SI-96: Representation of crystal structure from different perspectives. Colors-code: grey/carbon, red/oxygen, light-orange/phosphorus, dark-orange/Cu, yellow/Fluorine, pink/boron, blue/nitrogen, teal/palladium. Left) XRD structure (ORTEP 50% probability ellipsoids), Hydrogens and co-crystallizing molecules omitted for clearity. Right) representation of the unit cell, crystal packing.

Table 1 Crystal data and structure refinement for c061020_2_1.

Identification code	c061020_2_1
Empirical formula	$C_{85}H_{84}AuBF_{24}N_2O_2P_2Pd$
Formula weight	1997.65
Temperature/K	100.00(10)
Crystal system	triclinic

Space group	P-1
a/Å	15.73380(10)
b/Å	16.5046(2)
c/Å	18.12680(10)
α/°	105.1640(10)
β/°	107.8150(10)
γ/°	97.3110(10)
Volume/Å^3	4213.93(7)
Z	2
ρ_{calc}g/cm^3	1.574
μ/mm^{-1}	2.091
F(000)	2000.0
Crystal size/mm^3	0.208 × 0.073 × 0.054
Radiation	Mo Kα (λ = 0.71073)
2Θ range for data collection/°	4.768 to 69.54
Index ranges	-21 ≤ h ≤ 24, -25 ≤ k ≤ 26, -28 ≤ l ≤ 28
Reflections collected	140167
Independent reflections	31908 [R_{int} = 0.0351, R_{sigma} = 0.0340]
Data/restraints/parameters	31908/387/1127
Goodness-of-fit on F^2	1.039
Final R indexes [I>=2σ (I)]	R_1 = 0.0285, wR_2 = 0.0620
Final R indexes [all data]	R_1 = 0.0373, wR_2 = 0.0642
Largest diff. peak/hole / e Å^{-3}	1.75/-0.64

Table 2 Fractional Atomic Coordinates (×10^4) and Equivalent Isotropic Displacement Parameters (Å^2×10^3) for c061020_2_1. U_{eq} is defined as 1/3 of of the trace of the orthogonalised U_{IJ} tensor.

Atom	*x*	*y*	*z*	U(eq)
Au1	3378.8(2)	7065.3(2)	1778.1(2)	12.11(2)
Pd1	4405.1(2)	7477.2(2)	191.3(2)	13.69(2)
P1	3151.2(3)	7145.7(3)	-967.7(3)	18.02(8)
P2	5841.2(3)	8152.0(3)	1108.6(3)	16.90(8)
O1	3545.5(9)	7356.6(9)	-1658.5(8)	21.7(2)
O2	6408.2(8)	8488.1(9)	577.3(8)	21.3(2)
N1	2190.0(9)	7121.8(9)	2816.6(8)	13.9(2)
N2	3222.9(9)	8294.9(9)	3272.1(8)	14.0(2)
C1	3940.4(11)	6731.3(11)	794.3(10)	16.4(3)
C2	3778.9(11)	6048.1(11)	943.5(10)	16.3(3)
C3	3631.0(12)	5196.6(11)	1019.5(10)	16.9(3)
C4	2740.1(13)	4719.0(12)	797.5(12)	21.9(3)
C5	2603.0(14)	3906.8(12)	885.8(13)	27.2(4)
C6	3344.1(16)	3570.7(12)	1198.6(13)	29.3(4)
C7	4226.6(16)	4038.9(14)	1421.3(14)	32.0(4)
C8	4379.7(13)	4850.4(13)	1331.9(12)	25.3(4)
C9	2895.7(10)	7525.8(10)	2670.5(9)	13.1(3)

Table 2 Fractional Atomic Coordinates ($\times 10^4$) and Equivalent Isotropic Displacement Parameters ($Å^2 \times 10^3$) for c061020_2_1. U_{eq} is defined as 1/3 of of the trace of the orthogonalised U_{IJ} tensor.

Atom	*x*	*y*	*z*	U(eq)
C10	2074.7(11)	7631.3(11)	3505.2(10)	18.5(3)
C11	2722.5(11)	8373.7(11)	3790.0(10)	18.1(3)
C12	1688.1(11)	6243.1(10)	2368.1(10)	15.1(3)
C13	898.2(11)	6089.4(11)	1681.6(10)	18.0(3)
C14	442.4(12)	5229.1(12)	1257.3(12)	23.0(3)
C15	750.0(12)	4569.1(12)	1521.0(12)	24.8(4)
C16	1525.1(12)	4745.7(12)	2211.6(12)	22.4(3)
C17	2016.5(11)	5591.7(11)	2653.9(10)	17.7(3)
C18	547.1(12)	6811.3(12)	1396.8(12)	23.6(4)
C19	899.1(15)	6962.5(15)	733.4(14)	34.8(5)
C20	2875.0(12)	5772.0(12)	3398.7(11)	20.2(3)
C21	2683.1(17)	5417.8(18)	4044.7(14)	39.9(5)
C22	3627.6(14)	5409.7(16)	3146.1(13)	33.7(5)
C23	3933.7(10)	8972.5(10)	3322.0(10)	14.0(3)
C24	4825.5(11)	9086.9(10)	3866.8(10)	15.4(3)
C25	5480.9(11)	9774.8(12)	3917.7(11)	20.7(3)
C26	5251.6(12)	10313.6(12)	3447.4(12)	22.4(3)
C27	4365.9(12)	10177.0(11)	2914.9(11)	20.4(3)
C28	3679.3(11)	9502.4(11)	2841.7(10)	16.4(3)
C29	5080.8(12)	8490.6(11)	4374.2(11)	19.0(3)
C30	5225.5(16)	7650.9(13)	3874.2(13)	32.0(4)
C31	5937.3(13)	8913.2(13)	5140.8(11)	25.6(4)
C32	2699.7(12)	9390.6(12)	2277.8(11)	21.6(3)
C33	2316.9(15)	10175.8(16)	2559.6(15)	36.9(5)
C34	2642.2(15)	9218.3(15)	1391.1(12)	32.3(4)
C35	4956.8(11)	7947.5(11)	-517.6(10)	16.6(3)
C36	5885.4(12)	8344.8(11)	-232.8(11)	18.5(3)
C37	6318.3(13)	8574.4(12)	-737.9(13)	23.8(4)
C38	5803.9(14)	8367.5(13)	-1560.3(13)	26.2(4)
C39	4874.6(14)	7964.7(13)	-1881.0(12)	24.5(4)
C40	4470.6(12)	7772.4(11)	-1347.4(11)	19.1(3)
C41	2498.3(12)	6040.8(13)	-1506.5(11)	24.7(4)
C42	1861.2(15)	5776.2(17)	-1078.6(14)	38.3(5)
C43	3157.7(16)	5443.6(14)	-1574.0(14)	33.8(5)
C44	2333.1(14)	7840.7(15)	-929.5(12)	28.7(4)
C45	2845.5(18)	8785.5(15)	-629.0(15)	38.1(5)
C46	1552.9(18)	7632(2)	-1751.5(14)	49.1(7)
C47	6612.4(12)	7568.1(12)	1611.3(11)	22.0(3)
C48	6574.1(15)	6724.4(14)	983.5(13)	31.2(4)
C49	6371.7(14)	7410.5(16)	2326.8(13)	32.2(4)
C50	5910.4(13)	9158.7(12)	1866.7(12)	25.1(4)
C51	5372.6(15)	9710.3(13)	1420.8(15)	32.2(4)
C52	6899.0(15)	9657.8(15)	2384.2(15)	39.1(5)
C53	-505.1(13)	6639.9(13)	1083.2(14)	30.6(4)

Table 2 Fractional Atomic Coordinates ($\times 10^4$) and Equivalent Isotropic Displacement Parameters ($Å^2 \times 10^3$) for c061020_2_1. U_{eq} is defined as 1/3 of of the trace of the orthogonalised U_{IJ} tensor.

Atom	*x*	*y*	*z*	U(eq)
F1A	10257.3(13)	4991.5(9)	7062.0(8)	49.6(4)
F2A	10922.9(13)	4523.1(10)	6238.1(15)	70.0(6)
F3A	9487.1(11)	4417.1(9)	5807.2(10)	53.5(4)
F4A	12689.6(10)	8102.3(10)	6644.1(11)	51.2(4)
F5A	12858.4(9)	6875.3(10)	6066.9(12)	51.5(4)
F6A	12118.8(10)	7572.4(15)	5349.0(11)	65.9(6)
F7A	9865(6)	7046(6)	3417(7)	27.4(13)
F8A	9757(7)	8106(5)	2974(6)	47.8(16)
F9A	8558(4)	7145(10)	2674(5)	70(3)
F10A	8904.3(8)	10602.4(8)	4427.2(8)	30.3(3)
F11A	7638.9(8)	10123.9(9)	4543.9(10)	43.6(4)
F12A	8842.5(10)	10701.8(8)	5613.1(8)	36.8(3)
F13A	7113.2(11)	4981.8(13)	3585.2(11)	49.1(5)
F14A	6049.6(16)	5610.0(13)	3221.8(10)	58.9(6)
F15A	5830.7(19)	4620.0(15)	3712.6(14)	78.5(8)
F16A	4945.3(9)	6690.0(14)	5718.7(11)	64.4(5)
F17A	5943.5(12)	6643.3(11)	6812.8(10)	51.3(4)
F18A	5924.0(10)	7818.0(9)	6551.0(10)	41.6(3)
F19A	8430(2)	8394(3)	9038(2)	93.0(11)
F20A	9188(3)	7442.9(12)	8916.5(15)	65.1(8)
F21A	9806(2)	8661.9(15)	9792.0(11)	56.4(6)
F22A	11189.7(8)	10728.9(8)	7790.3(8)	31.2(3)
F23A	11467.5(11)	10814.8(11)	9045.0(9)	57.5(5)
F24A	10267.6(11)	11161.8(8)	8382.9(11)	50.4(4)
C1A	9834.6(11)	7080.2(10)	6072.8(10)	15.3(3)
C2A	9726.9(11)	6259.5(11)	6158.3(10)	16.7(3)
C3A	10421.5(12)	5803.8(11)	6209.5(10)	17.3(3)
C4A	11254.0(12)	6150.0(11)	6166.8(11)	19.2(3)
C5A	11377.8(11)	6965.4(11)	6089.3(10)	18.3(3)
C6A	10690.3(11)	7426.0(11)	6053.7(10)	17.0(3)
C7A	10273.6(13)	4938.3(12)	6324.3(11)	21.8(3)
C8A	9043.9(11)	8153.2(11)	5351.4(10)	15.5(3)
C9A	9200.3(12)	7728.2(11)	4640.4(10)	18.3(3)
C10A	9138.8(12)	8078.3(12)	4012.6(10)	20.2(3)
C11A	8930.5(12)	8878.8(12)	4065.7(11)	20.4(3)
C12A	8771.3(11)	9310.7(11)	4761.2(11)	17.3(3)
C13A	8808.8(11)	8948.8(11)	5382.4(10)	15.9(3)
C14A	9295.8(14)	7568.6(14)	3267.2(12)	28.5(4)
C15A	8545.2(12)	10176.8(12)	4835.0(12)	22.1(3)
C16A	8018.1(11)	7083.8(10)	5723.9(10)	15.2(3)
C17A	7692.8(11)	6403.7(11)	4981.2(10)	17.3(3)
C18A	6790.2(11)	5939.5(11)	4631.8(10)	18.2(3)
C19A	6167.6(11)	6110.8(11)	5023.1(11)	19.6(3)
C20A	6466.1(11)	6776.1(11)	5754.3(11)	18.7(3)

Table 2 Fractional Atomic Coordinates ($\times 10^4$) and Equivalent Isotropic Displacement Parameters ($Å^2 \times 10^3$) for c061020_2_1. U_{eq} is defined as 1/3 of of the trace of the orthogonalised U_{IJ} tensor.

Atom	*x*	*y*	*z*	U(eq)
C21A	7369.7(11)	7262.7(11)	6091.9(10)	17.3(3)
C22A	6460.8(12)	5283.1(13)	3800.2(12)	26.1(4)
C23A	5819.9(13)	6970.7(13)	6203.1(13)	26.1(4)
C24A	9394.0(11)	8330.7(10)	6982.1(10)	14.9(3)
C25A	9199.3(11)	8050.6(10)	7592.4(10)	16.2(3)
C26A	9503.9(12)	8575.4(11)	8404.1(10)	17.8(3)
C27A	10035.4(11)	9402.2(11)	8647.5(10)	17.5(3)
C28A	10256.1(11)	9686.8(11)	8060.4(10)	16.3(3)
C29A	9944.2(11)	9164.7(11)	7246.1(10)	15.8(3)
C30A	9244.1(16)	8256.2(13)	9025.0(12)	29.7(4)
C31A	10798.3(14)	10591.9(12)	8318.1(12)	25.8(4)
C32A	12255.6(13)	7369.8(13)	6033.2(13)	26.1(4)
B1A	9064.5(12)	7669.0(12)	6043.3(11)	14.8(3)
F19B	8543(6)	7607(5)	8695(3)	56.4(6)
F20B	9925(6)	7885(8)	9356(6)	93.0(11)
F21B	9137(8)	8800(4)	9571(5)	65.1(8)
F14B	6838(10)	5515(8)	3308(7)	78.5(8)
F15B	5625(6)	5026(8)	3407(7)	49.1(5)
F13B	6756(10)	4564(7)	3870(6)	58.9(6)
F8B	9344(13)	7980(5)	2762(6)	65(3)
F7B	9982(6)	7200(8)	3438(9)	32.9(18)
F9B	8549(4)	6860(5)	2804(5)	41.5(16)

Table 3 Anisotropic Displacement Parameters ($Å^2 \times 10^3$) for c061020_2_1. The Anisotropic displacement factor exponent takes the form: $-2\pi^2[h^2a^{*2}U_{11}+2hka^*b^*U_{12}+\ldots]$.

Atom	U_{11}	U_{22}	U_{33}	U_{23}	U_{13}	U_{12}
Au1	12.89(3)	11.96(3)	10.76(3)	2.52(2)	4.60(2)	1.64(2)
Pd1	14.22(5)	16.16(6)	12.19(5)	5.39(4)	6.15(4)	3.07(4)
P1	16.76(18)	25.0(2)	13.17(18)	6.74(16)	5.41(15)	6.11(16)
P2	15.68(18)	17.9(2)	16.13(19)	4.21(15)	6.20(15)	1.60(15)
O1	24.7(6)	29.0(7)	15.1(6)	9.9(5)	8.8(5)	7.5(5)
O2	17.9(5)	24.1(6)	23.1(6)	8.8(5)	9.1(5)	1.7(5)
N1	13.2(6)	15.1(6)	11.8(6)	2.4(5)	4.6(5)	0.6(5)
N2	13.3(6)	13.8(6)	12.4(6)	1.0(5)	4.4(5)	1.3(5)
C1	16.6(7)	19.7(8)	12.9(7)	3.8(6)	6.8(6)	2.9(6)
C2	17.0(7)	17.8(7)	14.3(7)	3.3(6)	7.1(6)	4.9(6)
C3	21.0(7)	14.7(7)	15.8(7)	3.9(6)	8.3(6)	4.2(6)
C4	22.4(8)	18.1(8)	24.0(8)	7.2(7)	6.7(7)	2.8(6)
C5	32.7(10)	19.0(9)	29.7(10)	7.9(7)	12.9(8)	0.5(7)
C6	46.3(12)	15.0(8)	31.3(10)	8.4(7)	18.3(9)	9.8(8)
C7	40.0(11)	26.4(10)	37.5(11)	14.3(9)	16.1(9)	19.3(9)
C8	25.1(9)	23.4(9)	29.1(9)	7.8(7)	10.5(7)	10.2(7)

Table 3 Anisotropic Displacement Parameters ($Å^2×10^3$) for c061020_2_1. The Anisotropic displacement factor exponent takes the form: $-2π^2[h^2a^{*2}U_{11}+2hka*b*U_{12}+...]$.

Atom	U_{11}	U_{22}	U_{33}	U_{23}	U_{13}	U_{12}
C9	11.5(6)	13.1(7)	13.1(7)	3.4(5)	3.3(5)	2.1(5)
C10	17.4(7)	22.1(8)	15.2(7)	1.9(6)	9.0(6)	2.2(6)
C11	16.9(7)	19.9(8)	14.6(7)	-0.5(6)	7.0(6)	2.7(6)
C12	14.5(6)	13.5(7)	15.5(7)	2.4(6)	6.2(6)	-0.3(5)
C13	14.9(7)	17.1(7)	17.3(7)	2.4(6)	3.3(6)	0.4(6)
C14	16.8(7)	19.2(8)	24.2(9)	1.8(7)	1.5(6)	-0.4(6)
C15	19.9(8)	16.0(8)	30.4(10)	2.0(7)	4.8(7)	-1.8(6)
C16	20.0(8)	17.0(8)	29.1(9)	8.3(7)	7.0(7)	2.3(6)
C17	15.5(7)	18.0(8)	18.5(7)	5.2(6)	6.2(6)	1.2(6)
C18	21.2(8)	16.7(8)	22.8(9)	2.8(7)	-2.2(7)	2.7(6)
C19	26.8(10)	38.2(12)	36.8(12)	22.3(10)	1.2(9)	1.6(8)
C20	19.1(7)	21.3(8)	18.7(8)	8.3(6)	3.5(6)	3.1(6)
C21	40.4(12)	53.1(15)	25.1(10)	21.1(10)	7.7(9)	-1.9(10)
C22	23.5(9)	46.0(13)	27.7(10)	8.8(9)	3.4(8)	14.2(9)
C23	14.1(6)	11.2(7)	14.2(7)	1.2(5)	4.5(5)	1.1(5)
C24	14.9(7)	13.9(7)	16.5(7)	3.6(6)	5.4(6)	3.2(5)
C25	14.1(7)	20.7(8)	23.1(8)	5.3(7)	3.4(6)	1.1(6)
C26	19.4(8)	18.7(8)	28.3(9)	7.9(7)	8.6(7)	0.5(6)
C27	22.2(8)	17.6(8)	22.5(8)	8.4(6)	7.8(7)	4.4(6)
C28	16.4(7)	15.8(7)	15.6(7)	4.2(6)	4.4(6)	3.9(6)
C29	18.5(7)	19.4(8)	18.8(8)	7.6(6)	4.5(6)	5.2(6)
C30	42.9(12)	23.0(9)	22.3(9)	5.0(7)	0.0(8)	14.1(8)
C31	27.7(9)	26.1(9)	17.6(8)	5.6(7)	1.9(7)	6.1(7)
C32	18.4(7)	22.8(8)	20.9(8)	9.2(7)	1.3(6)	4.8(6)
C33	24.1(9)	38.5(12)	42.3(13)	7.7(10)	4.2(9)	17.2(9)
C34	32.4(10)	36.6(11)	20.6(9)	10.1(8)	0.3(8)	3.8(9)
C35	20.7(7)	16.8(7)	18.5(7)	9.0(6)	11.6(6)	7.1(6)
C36	22.5(8)	16.2(7)	22.3(8)	9.0(6)	12.0(7)	6.9(6)
C37	26.1(9)	22.6(9)	36.0(10)	16.9(8)	20.8(8)	10.5(7)
C38	37.1(10)	28.1(9)	33.2(10)	21.3(8)	25.6(9)	17.8(8)
C39	34.6(10)	28.7(9)	22.6(9)	16.3(7)	16.9(8)	15.7(8)
C40	24.7(8)	19.2(8)	20.2(8)	10.3(6)	12.0(7)	9.2(6)
C41	20.3(8)	32.2(10)	15.4(8)	5.9(7)	2.2(6)	-1.2(7)
C42	25.7(10)	53.4(15)	27.3(10)	12.8(10)	5.2(8)	-9.4(9)
C43	39.5(11)	24.9(10)	28.5(10)	2.6(8)	7.2(9)	2.8(8)
C44	25.3(9)	44.8(12)	18.0(8)	8.5(8)	7.1(7)	19.2(8)
C45	49.2(13)	37.8(12)	34.9(12)	14.9(10)	16.3(10)	25.9(11)
C46	41.8(13)	73.2(19)	25.7(11)	6.1(11)	0.7(10)	39.0(13)
C47	18.3(7)	27.1(9)	19.7(8)	8.8(7)	4.5(6)	5.0(7)
C48	35.5(11)	29.2(10)	30.8(10)	11.0(8)	10.1(9)	15.2(8)
C49	25.8(9)	48.1(13)	24.5(10)	18.7(9)	6.5(8)	5.9(9)
C50	21.6(8)	22.0(9)	26.9(9)	-0.7(7)	10.4(7)	1.8(7)
C51	35.8(11)	21.6(9)	42.0(12)	7.1(9)	19.1(10)	9.0(8)
C52	27.6(10)	29.7(11)	41.2(13)	-9.4(9)	6.9(9)	-1.6(8)

Table 3 Anisotropic Displacement Parameters ($Å^2×10^3$) for c061020_2_1. The Anisotropic displacement factor exponent takes the form: $-2π^2[h^2a^{*2}U_{11}+2hka*b*U_{12}+...]$.

Atom	U_{11}	U_{22}	U_{33}	U_{23}	U_{13}	U_{12}
C53	22.0(8)	24.1(9)	35.1(11)	2.2(8)	0.8(8)	8.0(7)
F1A	94.0(12)	26.8(7)	27.3(7)	12.6(6)	21.7(8)	2.4(7)
F2A	72.3(11)	41.8(9)	154(2)	60.8(11)	83.2(13)	43.5(8)
F3A	56.6(9)	21.9(7)	50.5(9)	14.4(6)	-18.6(7)	-11.3(6)
F4A	36.5(7)	38.2(8)	68.0(11)	-0.4(7)	26.3(7)	-12.1(6)
F5A	28.8(7)	46.0(9)	97.6(13)	30.0(9)	37.1(8)	17.2(6)
F6A	33.4(8)	128.8(17)	58.0(10)	63.5(11)	22.7(7)	8.5(9)
F7A	38(3)	26(2)	29(3)	14(2)	21(2)	12(2)
F8A	85(4)	50(2)	41(3)	29(2)	48(3)	34(2)
F9A	32.8(19)	119(6)	25(2)	-21(3)	-1.4(14)	31(3)
F10A	35.0(6)	25.9(6)	44.6(7)	22.2(5)	23.5(6)	10.4(5)
F11A	16.2(5)	40.9(8)	83.7(11)	34.0(8)	16.2(6)	14.4(5)
F12A	56.7(8)	24.0(6)	37.2(7)	10.6(5)	22.3(6)	19.3(6)
F13A	28.4(7)	54.4(11)	35.7(9)	-20.2(8)	-3.8(6)	21.3(7)
F14A	82.7(14)	60.9(12)	18.6(7)	2.2(7)	-3.5(8)	42.1(11)
F15A	93.4(17)	53.2(13)	52.6(12)	-21.8(10)	34.7(12)	-48.8(12)
F16A	19.6(6)	101.3(15)	51.6(10)	-6.3(9)	14.0(6)	3.9(7)
F17A	71.9(11)	61.5(10)	64.1(10)	46.6(9)	52.6(9)	36.6(9)
F18A	53.8(8)	33.9(7)	59.1(9)	18.8(7)	42.6(8)	20.1(6)
F19A	73.0(16)	180(3)	107(2)	113(2)	69.7(17)	68.7(19)
F20A	144(3)	21.5(9)	49.1(13)	15.8(8)	61.1(16)	9.7(12)
F21A	85.0(16)	52.7(12)	17.3(8)	12.7(8)	11.5(9)	-19.6(11)
F22A	33.5(6)	28.3(6)	29.7(6)	7.3(5)	15.6(5)	-7.6(5)
F23A	57.4(9)	57.7(10)	24.1(7)	7.3(7)	-6.0(6)	-37.8(8)
F24A	66.9(10)	15.4(6)	79.2(11)	6.8(7)	48.4(9)	5.6(6)
C1A	17.1(7)	14.7(7)	12.6(7)	3.1(5)	4.9(6)	2.1(5)
C2A	17.4(7)	15.5(7)	16.6(7)	4.2(6)	6.4(6)	2.9(6)
C3A	21.4(7)	14.7(7)	16.0(7)	4.6(6)	6.4(6)	5.6(6)
C4A	18.1(7)	20.2(8)	19.1(8)	5.2(6)	6.2(6)	7.1(6)
C5A	16.2(7)	20.9(8)	17.3(7)	5.4(6)	6.4(6)	3.5(6)
C6A	16.3(7)	17.1(7)	17.1(7)	5.5(6)	5.4(6)	3.0(6)
C7A	25.0(8)	18.5(8)	23.4(8)	7.1(7)	8.9(7)	8.8(7)
C8A	13.7(6)	16.4(7)	14.4(7)	4.6(6)	3.0(5)	2.1(5)
C9A	20.5(7)	17.0(8)	17.1(7)	5.1(6)	6.2(6)	4.8(6)
C10A	22.5(8)	24.9(9)	15.1(7)	6.6(6)	7.9(6)	8.2(7)
C11A	20.5(8)	25.8(9)	19.7(8)	12.1(7)	8.4(6)	8.2(7)
C12A	12.4(6)	19.8(8)	22.2(8)	10.2(6)	6.5(6)	4.0(6)
C13A	13.0(6)	17.1(7)	17.5(7)	5.6(6)	5.3(6)	2.8(5)
C14A	36.0(10)	34.9(11)	19.1(8)	10.1(8)	11.5(8)	15.8(8)
C15A	16.5(7)	24.3(9)	33.5(10)	16.9(8)	11.8(7)	8.4(6)
C16A	14.8(7)	14.7(7)	15.4(7)	5.3(6)	3.6(6)	4.0(5)
C17A	15.5(7)	17.7(8)	16.8(7)	4.4(6)	4.2(6)	3.4(6)
C18A	17.5(7)	16.5(7)	16.9(7)	4.4(6)	1.8(6)	3.0(6)
C19A	15.0(7)	20.8(8)	22.1(8)	10.4(7)	3.0(6)	2.8(6)

Table 3 Anisotropic Displacement Parameters ($Å^2×10^3$) for c061020_2_1. The Anisotropic displacement factor exponent takes the form: $-2π^2[h^2a^{*2}U_{11}+2hka*b*U_{12}+...]$.

Atom	U_{11}	U_{22}	U_{33}	U_{23}	U_{13}	U_{12}
C20A	16.7(7)	20.9(8)	21.2(8)	10.0(6)	7.4(6)	5.4(6)
C21A	17.7(7)	17.1(7)	17.3(7)	5.9(6)	5.7(6)	4.5(6)
C22A	19.3(8)	25.8(9)	24.6(9)	1.4(7)	2.7(7)	2.3(7)
C23A	21.1(8)	31.1(10)	30.1(10)	12.4(8)	12.1(7)	6.2(7)
C24A	14.1(6)	15.4(7)	14.7(7)	4.8(6)	3.9(6)	5.2(5)
C25A	18.8(7)	13.0(7)	16.4(7)	5.4(6)	5.3(6)	3.4(6)
C26A	23.0(8)	15.9(7)	15.9(7)	6.7(6)	7.0(6)	5.0(6)
C27A	19.6(7)	16.2(7)	15.5(7)	3.6(6)	5.5(6)	4.4(6)
C28A	15.2(7)	15.5(7)	16.3(7)	3.9(6)	4.5(6)	1.9(5)
C29A	15.1(7)	17.1(7)	15.6(7)	5.2(6)	6.6(6)	2.8(6)
C30A	45.1(11)	23.7(9)	20.7(9)	8.7(7)	13.6(8)	1.3(8)
C31A	29.3(9)	22.1(9)	19.9(8)	1.6(7)	9.3(7)	-5.8(7)
C32A	21.0(8)	29.3(10)	31.6(10)	11.2(8)	12.8(8)	6.3(7)
B1A	15.6(7)	13.3(8)	14.4(8)	3.6(6)	4.8(6)	2.4(6)
F19B	85.0(16)	52.7(12)	17.3(8)	12.7(8)	11.5(9)	-19.6(11)
F20B	73.0(16)	180(3)	107(2)	113(2)	69.7(17)	68.7(19)
F21B	144(3)	21.5(9)	49.1(13)	15.8(8)	61.1(16)	9.7(12)
F14B	93.4(17)	53.2(13)	52.6(12)	-21.8(10)	34.7(12)	-48.8(12)
F15B	28.4(7)	54.4(11)	35.7(9)	-20.2(8)	-3.8(6)	21.3(7)
F13B	82.7(14)	60.9(12)	18.6(7)	2.2(7)	-3.5(8)	42.1(11)
F8B	146(7)	46(3)	34(3)	26(2)	54(4)	45(4)
F7B	18.3(17)	43(4)	33(3)	1(3)	13.9(16)	7(2)
F9B	27.9(18)	43(3)	30(3)	-13.4(17)	0.4(16)	5.3(17)

Table 4 Bond Lengths for c061020_2_1.

Atom	Atom	Length/Å	Atom	Atom	Length/Å
Au1	C1	2.1997(16)	F2A	C7A	1.326(2)
Au1	C2	2.2419(16)	F3A	C7A	1.322(2)
Au1	C9	2.0072(15)	F4A	C32A	1.335(3)
Pd1	P1	2.2789(5)	F5A	C32A	1.325(2)
Pd1	P2	2.2808(4)	F6A	C32A	1.330(2)
Pd1	C1	2.0516(17)	F7A	C14A	1.338(7)
Pd1	C35	2.0099(16)	F8A	C14A	1.384(6)
P1	O1	1.6500(13)	F9A	C14A	1.276(6)
P1	C41	1.820(2)	F10A	C15A	1.336(2)
P1	C44	1.8347(19)	F11A	C15A	1.343(2)
P2	O2	1.6463(13)	F12A	C15A	1.346(2)
P2	C47	1.8200(18)	F13A	C22A	1.314(2)
P2	C50	1.8245(19)	F14A	C22A	1.334(3)
O1	C40	1.396(2)	F15A	C22A	1.320(3)
O2	C36	1.385(2)	F16A	C23A	1.329(2)
N1	C9	1.353(2)	F17A	C23A	1.326(2)

Table 4 Bond Lengths for c061020_2_1.

Atom	Atom	Length/Å	Atom	Atom	Length/Å
N1	C10	1.388(2)	F18A	C23A	1.341(2)
N1	C12	1.444(2)	F19A	C30A	1.334(3)
N2	C9	1.353(2)	F20A	C30A	1.292(3)
N2	C11	1.390(2)	F21A	C30A	1.331(3)
N2	C23	1.441(2)	F22A	C31A	1.336(2)
C1	C2	1.240(2)	F23A	C31A	1.334(2)
C2	C3	1.444(2)	F24A	C31A	1.341(3)
C3	C4	1.399(2)	C1A	C2A	1.398(2)
C3	C8	1.402(2)	C1A	C6A	1.408(2)
C4	C5	1.389(3)	C1A	B1A	1.644(2)
C5	C6	1.383(3)	C2A	C3A	1.397(2)
C6	C7	1.382(3)	C3A	C4A	1.394(2)
C7	C8	1.391(3)	C3A	C7A	1.496(2)
C10	C11	1.355(2)	C4A	C5A	1.385(2)
C12	C13	1.402(2)	C5A	C6A	1.394(2)
C12	C17	1.400(2)	C5A	C32A	1.500(2)
C13	C14	1.398(2)	C8A	C9A	1.407(2)
C13	C18	1.519(2)	C8A	C13A	1.401(2)
C14	C15	1.384(3)	C8A	B1A	1.649(2)
C15	C16	1.387(3)	C9A	C10A	1.389(2)
C16	C17	1.397(2)	C10A	C11A	1.388(3)
C17	C20	1.519(2)	C10A	C14A	1.502(3)
C18	C19	1.531(3)	C11A	C12A	1.389(2)
C18	C53	1.538(3)	C12A	C13A	1.396(2)
C20	C21	1.528(3)	C12A	C15A	1.499(2)
C20	C22	1.529(3)	C14A	F8B	1.288(6)
C23	C24	1.402(2)	C14A	F7B	1.301(8)
C23	C28	1.399(2)	C14A	F9B	1.409(6)
C24	C25	1.396(2)	C16A	C17A	1.406(2)
C24	C29	1.525(2)	C16A	C21A	1.401(2)
C25	C26	1.392(3)	C16A	B1A	1.643(2)
C26	C27	1.381(2)	C17A	C18A	1.387(2)
C27	C28	1.398(2)	C18A	C19A	1.390(2)
C28	C32	1.523(2)	C18A	C22A	1.497(3)
C29	C30	1.531(3)	C19A	C20A	1.382(3)
C29	C31	1.530(3)	C20A	C21A	1.400(2)
C32	C33	1.531(3)	C20A	C23A	1.500(2)
C32	C34	1.529(3)	C22A	F14B	1.319(9)
C35	C36	1.396(2)	C22A	F15B	1.243(8)
C35	C40	1.394(2)	C22A	F13B	1.349(9)
C36	C37	1.394(2)	C24A	C25A	1.404(2)
C37	C38	1.385(3)	C24A	C29A	1.404(2)
C38	C39	1.396(3)	C24A	B1A	1.643(2)
C39	C40	1.388(2)	C25A	C26A	1.393(2)
C41	C42	1.529(3)	C26A	C27A	1.388(2)

Table 4 Bond Lengths for c061020_2_1.

Atom	Atom	Length/Å	Atom	Atom	Length/Å
C41	C43	1.529(3)	C26A	C30A	1.499(3)
C44	C45	1.532(3)	C27A	C28A	1.385(2)
C44	C46	1.533(3)	C28A	C29A	1.395(2)
C47	C48	1.531(3)	C28A	C31A	1.498(2)
C47	C49	1.531(3)	C30A	F19B	1.296(6)
C50	C51	1.537(3)	C30A	F20B	1.359(7)
C50	C52	1.535(3)	C30A	F21B	1.220(6)
F1A	C7A	1.325(2)			

Table 5 Bond Angles for c061020_2_1.

Atom	Atom	Atom	Angle/°	Atom	Atom	Atom	Angle/°
C1	Au1	C2	32.41(6)	C4A	C3A	C7A	119.63(15)
C9	Au1	C1	172.62(6)	C5A	C4A	C3A	117.98(15)
C9	Au1	C2	154.97(6)	C4A	C5A	C6A	121.05(15)
P1	Pd1	P2	157.944(17)	C4A	C5A	C32A	120.50(15)
C1	Pd1	P1	100.73(5)	C6A	C5A	C32A	118.45(16)
C1	Pd1	P2	101.28(5)	C5A	C6A	C1A	121.99(16)
C35	Pd1	P1	79.40(5)	F1A	C7A	F2A	106.02(18)
C35	Pd1	P2	79.62(5)	F1A	C7A	C3A	112.17(15)
C35	Pd1	C1	165.94(7)	F2A	C7A	C3A	113.06(16)
O1	P1	Pd1	105.45(5)	F3A	C7A	F1A	105.39(17)
O1	P1	C41	101.06(8)	F3A	C7A	F2A	106.37(18)
O1	P1	C44	102.53(8)	F3A	C7A	C3A	113.22(15)
C41	P1	Pd1	121.31(6)	C9A	C8A	B1A	119.46(14)
C41	P1	C44	107.83(10)	C13A	C8A	C9A	115.73(15)
C44	P1	Pd1	115.80(7)	C13A	C8A	B1A	124.61(14)
O2	P2	Pd1	105.41(5)	C10A	C9A	C8A	122.32(16)
O2	P2	C47	101.01(8)	C9A	C10A	C14A	118.61(16)
O2	P2	C50	102.01(8)	C11A	C10A	C9A	121.03(16)
C47	P2	Pd1	121.92(6)	C11A	C10A	C14A	120.36(16)
C47	P2	C50	108.43(9)	C10A	C11A	C12A	117.74(16)
C50	P2	Pd1	115.02(6)	C11A	C12A	C13A	121.24(16)
C40	O1	P1	114.12(11)	C11A	C12A	C15A	118.89(16)
C36	O2	P2	114.51(11)	C13A	C12A	C15A	119.87(16)
C9	N1	C10	110.98(13)	C12A	C13A	C8A	121.88(15)
C9	N1	C12	124.36(13)	F7A	C14A	F8A	101.8(5)
C10	N1	C12	124.35(13)	F7A	C14A	C10A	113.7(5)
C9	N2	C11	110.79(13)	F8A	C14A	C10A	110.8(4)
C9	N2	C23	124.48(13)	F9A	C14A	F7A	109.8(6)
C11	N2	C23	124.47(13)	F9A	C14A	F8A	106.2(5)
Pd1	C1	Au1	130.66(8)	F9A	C14A	C10A	113.7(4)
C2	C1	Au1	75.67(10)	F8B	C14A	C10A	114.8(4)
C2	C1	Pd1	153.65(14)	F8B	C14A	F7B	111.3(7)

Table 5 Bond Angles for c061020_2_1.

Atom	Atom	Atom	Angle/°	Atom	Atom	Atom	Angle/°
C1	C2	Au1	71.92(10)	F8B	C14A	F9B	104.1(5)
C1	C2	C3	171.70(17)	F7B	C14A	C10A	113.2(7)
C3	C2	Au1	116.35(11)	F7B	C14A	F9B	102.5(5)
C4	C3	C2	120.18(15)	F9B	C14A	C10A	109.8(4)
C4	C3	C8	119.58(16)	F10A	C15A	F11A	105.99(15)
C8	C3	C2	120.23(16)	F10A	C15A	F12A	106.25(15)
C5	C4	C3	119.89(17)	F10A	C15A	C12A	112.97(15)
C6	C5	C4	120.28(19)	F11A	C15A	F12A	105.46(15)
C7	C6	C5	120.22(18)	F11A	C15A	C12A	112.45(15)
C6	C7	C8	120.46(19)	F12A	C15A	C12A	113.10(15)
C7	C8	C3	119.57(18)	C17A	C16A	B1A	119.28(14)
N1	C9	Au1	127.38(11)	C21A	C16A	C17A	115.56(15)
N1	C9	N2	105.05(13)	C21A	C16A	B1A	124.80(15)
N2	C9	Au1	127.54(11)	C18A	C17A	C16A	122.48(15)
C11	C10	N1	106.53(14)	C17A	C18A	C19A	120.83(16)
C10	C11	N2	106.65(14)	C17A	C18A	C22A	119.99(16)
C13	C12	N1	118.63(14)	C19A	C18A	C22A	119.07(15)
C17	C12	N1	117.66(14)	C20A	C19A	C18A	118.07(16)
C17	C12	C13	123.70(15)	C19A	C20A	C21A	120.96(16)
C12	C13	C18	122.50(15)	C19A	C20A	C23A	119.69(16)
C14	C13	C12	116.75(16)	C21A	C20A	C23A	119.34(16)
C14	C13	C18	120.74(15)	C20A	C21A	C16A	122.04(16)
C15	C14	C13	121.04(17)	F13A	C22A	F14A	105.37(19)
C14	C15	C16	120.66(17)	F13A	C22A	F15A	107.9(2)
C15	C16	C17	120.89(17)	F13A	C22A	C18A	114.27(16)
C12	C17	C20	122.88(15)	F14A	C22A	C18A	111.42(17)
C16	C17	C12	116.93(16)	F15A	C22A	F14A	104.2(2)
C16	C17	C20	120.19(16)	F15A	C22A	C18A	112.97(18)
C13	C18	C19	111.14(16)	F14B	C22A	C18A	112.6(5)
C13	C18	C53	112.23(16)	F14B	C22A	F13B	103.3(8)
C19	C18	C53	109.75(17)	F15B	C22A	C18A	119.5(5)
C17	C20	C21	111.95(16)	F15B	C22A	F14B	106.6(8)
C17	C20	C22	110.36(15)	F15B	C22A	F13B	104.7(7)
C21	C20	C22	110.87(18)	F13B	C22A	C18A	108.6(5)
C24	C23	N2	118.78(14)	F16A	C23A	F18A	105.14(17)
C28	C23	N2	117.38(14)	F16A	C23A	C20A	112.85(17)
C28	C23	C24	123.79(15)	F17A	C23A	F16A	107.97(18)
C23	C24	C29	122.38(14)	F17A	C23A	F18A	104.94(17)
C25	C24	C23	116.57(15)	F17A	C23A	C20A	112.68(16)
C25	C24	C29	121.05(15)	F18A	C23A	C20A	112.65(16)
C26	C25	C24	121.14(16)	C25A	C24A	C29A	115.74(15)
C27	C26	C25	120.53(16)	C25A	C24A	B1A	120.35(14)
C26	C27	C28	120.91(16)	C29A	C24A	B1A	123.67(14)
C23	C28	C32	123.11(15)	C26A	C25A	C24A	122.32(15)
C27	C28	C23	117.06(15)	C25A	C26A	C30A	120.11(16)

Table 5 Bond Angles for c061020_2_1.

Atom	Atom	Atom	Angle/˚	Atom	Atom	Atom	Angle/˚
C27	C28	C32	119.80(15)	C27A	C26A	C25A	120.81(15)
C24	C29	C30	111.86(15)	C27A	C26A	C30A	119.07(16)
C24	C29	C31	112.85(15)	C28A	C27A	C26A	118.01(15)
C31	C29	C30	108.83(15)	C27A	C28A	C29A	121.21(15)
C28	C32	C33	110.87(15)	C27A	C28A	C31A	117.87(15)
C28	C32	C34	111.07(15)	C29A	C28A	C31A	120.83(15)
C34	C32	C33	111.06(17)	C28A	C29A	C24A	121.88(15)
C36	C35	Pd1	121.12(12)	F19A	C30A	C26A	111.57(19)
C40	C35	Pd1	121.38(13)	F20A	C30A	F19A	105.8(3)
C40	C35	C36	116.75(15)	F20A	C30A	F21A	106.1(2)
O2	C36	C35	118.82(15)	F20A	C30A	C26A	115.04(18)
O2	C36	C37	118.43(16)	F21A	C30A	F19A	103.4(2)
C37	C36	C35	122.70(17)	F21A	C30A	C26A	113.92(18)
C38	C37	C36	117.88(18)	F19B	C30A	C26A	112.7(3)
C37	C38	C39	121.94(17)	F19B	C30A	F20B	101.6(6)
C40	C39	C38	117.85(18)	F20B	C30A	C26A	106.2(3)
C35	C40	O1	118.39(14)	F21B	C30A	C26A	115.9(3)
C39	C40	O1	118.73(16)	F21B	C30A	F19B	110.1(6)
C39	C40	C35	122.84(17)	F21B	C30A	F20B	109.3(6)
C42	C41	P1	110.65(15)	F22A	C31A	F24A	106.27(17)
C43	C41	P1	109.40(13)	F22A	C31A	C28A	113.02(15)
C43	C41	C42	111.86(19)	F23A	C31A	F22A	106.77(16)
C45	C44	P1	109.38(14)	F23A	C31A	F24A	106.31(18)
C45	C44	C46	110.7(2)	F23A	C31A	C28A	112.62(17)
C46	C44	P1	112.97(15)	F24A	C31A	C28A	111.38(16)
C48	C47	P2	109.36(13)	F4A	C32A	C5A	112.29(16)
C49	C47	P2	110.59(13)	F5A	C32A	F4A	105.19(17)
C49	C47	C48	111.85(17)	F5A	C32A	F6A	107.22(18)
C51	C50	P2	108.35(14)	F5A	C32A	C5A	113.51(17)
C52	C50	P2	113.08(13)	F6A	C32A	F4A	105.84(19)
C52	C50	C51	110.81(18)	F6A	C32A	C5A	112.21(16)
C2A	C1A	C6A	116.00(15)	C1A	B1A	C8A	108.82(13)
C2A	C1A	B1A	124.77(14)	C16A	B1A	C1A	112.52(13)
C6A	C1A	B1A	119.15(14)	C16A	B1A	C8A	104.16(13)
C3A	C2A	C1A	122.04(15)	C16A	B1A	C24A	113.04(13)
C2A	C3A	C7A	119.47(15)	C24A	B1A	C1A	104.32(13)
C4A	C3A	C2A	120.90(16)	C24A	B1A	C8A	114.13(13)

Table 6 Torsion Angles for c061020_2_1.

A	B	C	D	Angle/˚	A	B	C	D	Angle/˚
Au1	C2	C3	C4	67.07(19)	C2A	C3A	C7A	F1A	-69.9(2)
Au1	C2	C3	C8	-111.63(16)	C2A	C3A	C7A	F2A	170.31(18)
Pd1	P1	O1	C40	-8.08(12)	C2A	C3A	C7A	F3A	49.3(2)

Table 6 Torsion Angles for c061020_2_1.

A	B	C	D	Angle/°	A	B	C	D	Angle/°
Pd1	P1	C41	C42	78.91(16)	C3A	C4A	C5A	C6A	-0.1(3)
Pd1	P1	C41	C43	-44.77(16)	C3A	C4A	C5A	C32A	-179.49(16)
Pd1	P1	C44	C45	51.08(16)	C4A	C3A	C7A	F1A	109.2(2)
Pd1	P1	C44	C46	174.85(17)	C4A	C3A	C7A	F2A	-10.6(3)
Pd1	P2	O2	C36	4.44(12)	C4A	C3A	C7A	F3A	-131.65(19)
Pd1	P2	C47	C48	43.53(16)	C4A	C5A	C6A	C1A	-1.7(3)
Pd1	P2	C47	C49	-80.07(15)	C4A	C5A	C32A	F4A	-119.2(2)
Pd1	P2	C50	C51	-47.88(15)	C4A	C5A	C32A	F5A	-0.1(3)
Pd1	P2	C50	C52	-171.13(15)	C4A	C5A	C32A	F6A	121.7(2)
Pd1	C1	C2	Au1	178.4(3)	C6A	C1A	C2A	C3A	-0.9(2)
Pd1	C35	C36	O2	-6.3(2)	C6A	C1A	B1A	C8A	43.30(19)
Pd1	C35	C36	C37	171.18(13)	C6A	C1A	B1A	C16A	158.20(14)
Pd1	C35	C40	O1	8.3(2)	C6A	C1A	B1A	C24A	-78.90(17)
Pd1	C35	C40	C39	-169.21(14)	C6A	C5A	C32A	F4A	61.3(2)
P1	O1	C40	C35	1.2(2)	C6A	C5A	C32A	F5A	-179.50(18)
P1	O1	C40	C39	178.81(13)	C6A	C5A	C32A	F6A	-57.7(2)
P2	O2	C36	C35	0.4(2)	C7A	C3A	C4A	C5A	-177.77(16)
P2	O2	C36	C37	-177.22(13)	C8A	C9A	C10A	C11A	0.9(3)
O1	P1	C41	C42	-165.20(14)	C8A	C9A	C10A	C14A	-178.60(17)
O1	P1	C41	C43	71.12(15)	C9A	C8A	C13A	C12A	-2.6(2)
O1	P1	C44	C45	-63.16(15)	C9A	C8A	B1A	C1A	34.4(2)
O1	P1	C44	C46	60.6(2)	C9A	C8A	B1A	C16A	-85.82(17)
O2	P2	C47	C48	-72.58(14)	C9A	C8A	B1A	C24A	150.45(15)
O2	P2	C47	C49	163.82(14)	C9A	C10A	C11A	C12A	-1.0(3)
O2	P2	C50	C51	65.64(14)	C9A	C10A	C14A	F7A	-29.1(5)
O2	P2	C50	C52	-57.60(18)	C9A	C10A	C14A	F8A	-143.0(5)
O2	C36	C37	C38	175.12(16)	C9A	C10A	C14A	F9A	97.5(9)
N1	C10	C11	N2	-0.57(19)	C9A	C10A	C14A	F8B	-171.4(9)
N1	C12	C13	C14	178.92(15)	C9A	C10A	C14A	F7B	-42.2(7)
N1	C12	C13	C18	-0.5(2)	C9A	C10A	C14A	F9B	71.7(5)
N1	C12	C17	C16	-179.78(15)	C10A	C11A	C12A	C13A	-0.7(3)
N1	C12	C17	C20	-0.9(2)	C10A	C11A	C12A	C15A	179.97(16)
N2	C23	C24	C25	-177.35(14)	C11A	C10A	C14A	F7A	151.4(5)
N2	C23	C24	C29	3.4(2)	C11A	C10A	C14A	F8A	37.5(5)
N2	C23	C28	C27	177.80(14)	C11A	C10A	C14A	F9A	-82.0(9)
N2	C23	C28	C32	-0.2(2)	C11A	C10A	C14A	F8B	9.0(10)
C2	C3	C4	C5	-178.85(17)	C11A	C10A	C14A	F7B	138.2(6)
C2	C3	C8	C7	178.33(18)	C11A	C10A	C14A	F9B	-107.9(5)
C3	C4	C5	C6	0.5(3)	C11A	C12A	C13A	C8A	2.6(3)
C4	C3	C8	C7	-0.4(3)	C11A	C12A	C15A	F10A	-28.1(2)
C4	C5	C6	C7	-0.4(3)	C11A	C12A	C15A	F11A	91.9(2)
C5	C6	C7	C8	-0.2(3)	C11A	C12A	C15A	F12A	-148.82(16)
C6	C7	C8	C3	0.5(3)	C13A	C8A	C9A	C10A	0.9(2)
C8	C3	C4	C5	-0.1(3)	C13A	C8A	B1A	C1A	-150.82(15)
C9	N1	C10	C11	0.44(19)	C13A	C8A	B1A	C16A	88.96(18)

Table 6 Torsion Angles for c061020_2_1.

A	B	C	D	Angle/°	A	B	C	D	Angle/°
C9	N1	C12	C13	-91.82(19)	C13A	C8A	B1A	C24A	-34.8(2)
C9	N1	C12	C17	88.95(19)	C13A	C12A	C15A	F10A	152.61(16)
C9	N2	C11	C10	0.53(19)	C13A	C12A	C15A	F11A	-87.5(2)
C9	N2	C23	C24	-101.66(18)	C13A	C12A	C15A	F12A	31.9(2)
C9	N2	C23	C28	80.9(2)	C14A	C10A	C11A	C12A	178.51(17)
C10	N1	C9	Au1	177.93(12)	C15A	C12A	C13A	C8A	-178.07(15)
C10	N1	C9	N2	-0.11(18)	C16A	C17A	C18A	C19A	-2.3(3)
C10	N1	C12	C13	95.1(2)	C16A	C17A	C18A	C22A	173.78(16)
C10	N1	C12	C17	-84.1(2)	C17A	C16A	C21A	C20A	2.1(2)
C11	N2	C9	Au1	-178.30(12)	C17A	C16A	B1A	C1A	-52.9(2)
C11	N2	C9	N1	-0.25(18)	C17A	C16A	B1A	C8A	64.76(18)
C11	N2	C23	C24	84.8(2)	C17A	C16A	B1A	C24A	-170.80(14)
C11	N2	C23	C28	-92.73(19)	C17A	C18A	C19A	C20A	2.3(3)
C12	N1	C9	Au1	4.1(2)	C17A	C18A	C22A	F13A	22.9(3)
C12	N1	C9	N2	-173.98(14)	C17A	C18A	C22A	F14A	-96.3(2)
C12	N1	C10	C11	174.30(15)	C17A	C18A	C22A	F15A	146.8(2)
C12	C13	C14	C15	1.6(3)	C17A	C18A	C22A	F14B	-35.9(9)
C12	C13	C18	C19	94.8(2)	C17A	C18A	C22A	F15B	-162.2(8)
C12	C13	C18	C53	-141.87(18)	C17A	C18A	C22A	F13B	77.9(8)
C12	C17	C20	C21	123.2(2)	C18A	C19A	C20A	C21A	-0.1(3)
C12	C17	C20	C22	-112.75(19)	C18A	C19A	C20A	C23A	-178.89(16)
C13	C12	C17	C16	1.0(2)	C19A	C18A	C22A	F13A	-160.9(2)
C13	C12	C17	C20	179.91(16)	C19A	C18A	C22A	F14A	79.9(2)
C13	C14	C15	C16	-0.5(3)	C19A	C18A	C22A	F15A	-37.0(3)
C14	C13	C18	C19	-84.6(2)	C19A	C18A	C22A	F14B	140.3(9)
C14	C13	C18	C53	38.7(2)	C19A	C18A	C22A	F15B	13.9(9)
C14	C15	C16	C17	-0.4(3)	C19A	C18A	C22A	F13B	-105.9(7)
C15	C16	C17	C12	0.2(3)	C19A	C20A	C21A	C16A	-2.1(3)
C15	C16	C17	C20	-178.74(17)	C19A	C20A	C23A	F16A	-22.8(3)
C16	C17	C20	C21	-57.9(2)	C19A	C20A	C23A	F17A	99.8(2)
C16	C17	C20	C22	66.1(2)	C19A	C20A	C23A	F18A	-141.69(18)
C17	C12	C13	C14	-1.9(3)	C21A	C16A	C17A	C18A	0.1(2)
C17	C12	C13	C18	178.66(16)	C21A	C16A	B1A	C1A	134.33(16)
C18	C13	C14	C15	-178.95(18)	C21A	C16A	B1A	C8A	-107.97(17)
C23	N2	C9	Au1	7.4(2)	C21A	C16A	B1A	C24A	16.5(2)
C23	N2	C9	N1	-174.60(14)	C21A	C20A	C23A	F16A	158.38(18)
C23	N2	C11	C10	174.87(15)	C21A	C20A	C23A	F17A	-79.0(2)
C23	C24	C25	C26	-0.1(3)	C21A	C20A	C23A	F18A	39.5(2)
C23	C24	C29	C30	79.7(2)	C22A	C18A	C19A	C20A	-173.89(16)
C23	C24	C29	C31	-157.15(16)	C23A	C20A	C21A	C16A	176.65(16)
C23	C28	C32	C33	115.7(2)	C24A	C25A	C26A	C27A	-1.3(3)
C23	C28	C32	C34	-120.33(19)	C24A	C25A	C26A	C30A	177.52(17)
C24	C23	C28	C27	0.5(2)	C25A	C24A	C29A	C28A	-1.6(2)
C24	C23	C28	C32	-177.52(15)	C25A	C24A	B1A	C1A	-79.80(17)
C24	C25	C26	C27	-0.2(3)	C25A	C24A	B1A	C8A	161.56(14)

Table 6 Torsion Angles for c061020_2_1.

A	B	C	D	Angle/°	A	B	C	D	Angle/°
C25	C24	C29	C30	-99.5(2)	C25A	C24A	B1A	C16A	42.8(2)
C25	C24	C29	C31	23.6(2)	C25A	C26A	C27A	C28A	-0.3(2)
C25	C26	C27	C28	0.6(3)	C25A	C26A	C30A	F19A	-85.5(3)
C26	C27	C28	C23	-0.7(3)	C25A	C26A	C30A	F20A	35.0(3)
C26	C27	C28	C32	177.31(17)	C25A	C26A	C30A	F21A	157.9(2)
C27	C28	C32	C33	-62.2(2)	C25A	C26A	C30A	F19B	-18.6(6)
C27	C28	C32	C34	61.7(2)	C25A	C26A	C30A	F20B	91.8(6)
C28	C23	C24	C25	0.0(2)	C25A	C26A	C30A	F21B	-146.7(7)
C28	C23	C24	C29	-179.32(15)	C26A	C27A	C28A	C29A	0.9(2)
C29	C24	C25	C26	179.19(16)	C26A	C27A	C28A	C31A	177.61(16)
C35	C36	C37	C38	-2.4(3)	C27A	C26A	C30A	F19A	93.4(3)
C36	C35	C40	O1	178.47(14)	C27A	C26A	C30A	F20A	-146.1(3)
C36	C35	C40	C39	0.9(3)	C27A	C26A	C30A	F21A	-23.2(3)
C36	C37	C38	C39	1.8(3)	C27A	C26A	C30A	F19B	160.3(5)
C37	C38	C39	C40	0.0(3)	C27A	C26A	C30A	F20B	-89.3(6)
C38	C39	C40	O1	-178.94(16)	C27A	C26A	C30A	F21B	32.2(7)
C38	C39	C40	C35	-1.4(3)	C27A	C28A	C29A	C24A	0.1(2)
C40	C35	C36	O2	-176.45(15)	C27A	C28A	C31A	F22A	162.47(16)
C40	C35	C36	C37	1.0(2)	C27A	C28A	C31A	F23A	41.4(2)
C41	P1	O1	C40	-135.19(12)	C27A	C28A	C31A	F24A	-78.0(2)
C41	P1	C44	C45	-169.30(14)	C29A	C24A	C25A	C26A	2.2(2)
C41	P1	C44	C46	-45.5(2)	C29A	C24A	B1A	C1A	94.34(17)
C44	P1	O1	C40	113.52(13)	C29A	C24A	B1A	C8A	-24.3(2)
C44	P1	C41	C42	-58.04(17)	C29A	C24A	B1A	C16A	-143.10(15)
C44	P1	C41	C43	178.28(14)	C29A	C28A	C31A	F22A	-20.8(2)
C47	P2	O2	C36	132.20(12)	C29A	C28A	C31A	F23A	-141.94(18)
C47	P2	C50	C51	171.70(13)	C29A	C28A	C31A	F24A	98.7(2)
C47	P2	C50	C52	48.46(19)	C30A	C26A	C27A	C28A	-179.14(17)
C50	P2	O2	C36	-116.04(13)	C31A	C28A	C29A	C24A	-176.55(16)
C50	P2	C47	C48	-179.34(14)	C32A	C5A	C6A	C1A	177.70(16)
C50	P2	C47	C49	57.06(16)	B1A	C1A	C2A	C3A	-177.59(15)
C1A	C2A	C3A	C4A	-0.8(3)	B1A	C1A	C6A	C5A	179.02(15)
C1A	C2A	C3A	C7A	178.29(16)	B1A	C8A	C9A	C10A	176.09(16)
C2A	C1A	C6A	C5A	2.2(2)	B1A	C8A	C13A	C12A	-177.56(15)
C2A	C1A	B1A	C8A	-140.14(16)	B1A	C16A	C17A	C18A	-173.24(15)
C2A	C1A	B1A	C16A	-25.2(2)	B1A	C16A	C21A	C20A	175.04(15)
C2A	C1A	B1A	C24A	97.66(18)	B1A	C24A	C25A	C26A	176.78(15)
C2A	C3A	C4A	C5A	1.3(3)	B1A	C24A	C29A	C28A	-175.94(15)

Table 7 Hydrogen Atom Coordinates (Å×10^4) and Isotropic Displacement Parameters (Å^2×10^3) for c061020_2_1.

Atom	*x*	*y*	*z*	U(eq)
H4	2240.26	4944.85	591.17	26

Table 7 Hydrogen Atom Coordinates (Å×10^4) and Isotropic Displacement Parameters (Å^2×10^3) for c061020_2_1.

Atom	*x*	*y*	*z*	U(eq)
H5	2010.37	3587.53	734.08	33
H6	3248.03	3027.85	1259.1	35
H7	4721.79	3809.71	1632.49	38
H8	4974.71	5161.65	1478.23	30
H10	1638.5	7490.83	3727.54	22
H11	2814.41	8844.3	4243.58	22
H14	-75.73	5098.34	790.46	28
H15	433.95	4001.31	1232.18	30
H16	1720.19	4294.67	2382.55	27
H18	784.05	7340.68	1866.25	28
H19A	680.36	7430.3	574.01	52
H19B	680.69	6449.77	267.61	52
H19C	1556.94	7102.07	942.51	52
H20	3094.95	6398.48	3642.4	24
H21A	2193.36	5635.79	4178.8	60
H21B	3224.38	5595.06	4526.59	60
H21C	2510.92	4799.97	3834.73	60
H22A	3422.6	4796.71	2892.93	51
H22B	4169.08	5537.5	3620.85	51
H22C	3763.52	5667.31	2766.02	51
H25	6080.93	9874.79	4272.01	25
H26	5698.33	10769.22	3492.1	27
H27	4224.43	10538.93	2600.77	24
H29	4569.21	8341.72	4551.25	23
H30A	4698.82	7389.18	3383.39	48
H30B	5309.86	7264.15	4191.07	48
H30C	5758.67	7772.71	3734.65	48
H31A	6465	8994.23	4985.18	38
H31B	6011.93	8549.09	5480.52	38
H31C	5872.26	9461.6	5437.65	38
H32	2321.97	8887.72	2306.36	26
H33A	2350.78	10264.49	3113.77	55
H33B	1689.71	10078.97	2213.51	55
H33C	2670.26	10676.29	2528.33	55
H34A	2889.95	8726.63	1230.39	48
H34B	2987.1	9712.71	1342.95	48
H34C	2013.42	9107.33	1043.27	48
H37	6932.77	8857.35	-529.42	29
H38	6086.19	8500.92	-1908.97	31
H39	4537.01	7829.67	-2434.38	29
H41	2121.25	6007.55	-2060	30
H42A	2213.32	5859.79	-517.91	57
H42B	1556.54	5180.01	-1346.95	57
H42C	1413.71	6122.85	-1102.3	57

Table 7 Hydrogen Atom Coordinates (Å×10^4) and Isotropic Displacement Parameters (Å^2×10^3) for c061020_2_1.

Atom	*x*	*y*	*z*	U(eq)
H43A	3551.43	5634.16	-1837.8	51
H43B	2814.08	4866.43	-1889.42	51
H43C	3521.71	5455.39	-1037.15	51
H44	2061.02	7752.09	-529.29	34
H45A	3336.18	8901.36	-118.58	57
H45B	2430.02	9151.2	-554.32	57
H45C	3091.33	8896.34	-1025.85	57
H46A	1805.38	7652.94	-2167.73	74
H46B	1179.83	8047.47	-1711.06	74
H46C	1184.84	7066.28	-1890.47	74
H47	7237.92	7921.14	1827.46	26
H48A	5969.09	6363.52	775.02	47
H48B	7008.76	6432.83	1239.98	47
H48C	6720.59	6847.94	541.94	47
H49A	6486.97	7951.41	2742.81	48
H49B	6741.38	7050.8	2548.29	48
H49C	5735.86	7130.37	2137.72	48
H50	5611.93	9020.9	2234.54	30
H51A	5604.06	9789	1005.95	48
H51B	5442.09	10261.56	1805.2	48
H51C	4735.65	9425.09	1172.63	48
H52A	7218.43	9307.11	2666.87	59
H52B	6894.05	10176.35	2774.59	59
H52C	7203.03	9802.03	2034.93	59
H53A	-726.51	6481.21	1475.5	46
H53B	-751.8	6179.8	572.47	46
H53C	-693.76	7151.63	1005.69	46
H2A	9175.83	6009.23	6181.91	20
H4A	11712.36	5842.71	6189.68	23
H6A	10800.32	7978.33	6016.19	20
H9A	9350.15	7194.07	4588.86	22
H11A	8898.55	9118.08	3649.6	24
H13A	8673.96	9244.43	5829.59	19
H17A	8098	6259.55	4714.06	21
H19D	5567.78	5786.93	4799.26	23
H21D	7544.82	7718.87	6575.33	21
H25A	8854.93	7495.14	7449.87	19
H27A	10237.35	9754.87	9188.39	21
H29A	10105.14	9374.97	6867.27	19

Table 8 Atomic Occupancy for c061020_2_1.

Atom	*Occupancy*	Atom	*Occupancy*	Atom	*Occupancy*
F7A	0.54(2)	F8A	0.54(2)	F9A	0.54(2)
F13A	0.863(2)	F14A	0.863(2)	F15A	0.863(2)
F19A	0.750(2)	F20A	0.750(2)	F21A	0.750(2)
F19B	0.250(2)	F20B	0.250(2)	F21B	0.250(2)
F14B	0.137(2)	F15B	0.137(2)	F13B	0.137(2)
F8B	0.46(2)	F7B	0.46(2)	F9B	0.46(2)

3.4. Crystal Structure determination Synthesis of [4a]BArF

3.4.1. Crystal structure for $^{Me,but\text{-}3\text{-}en\text{-}1\text{-}yl}$IPrHCl

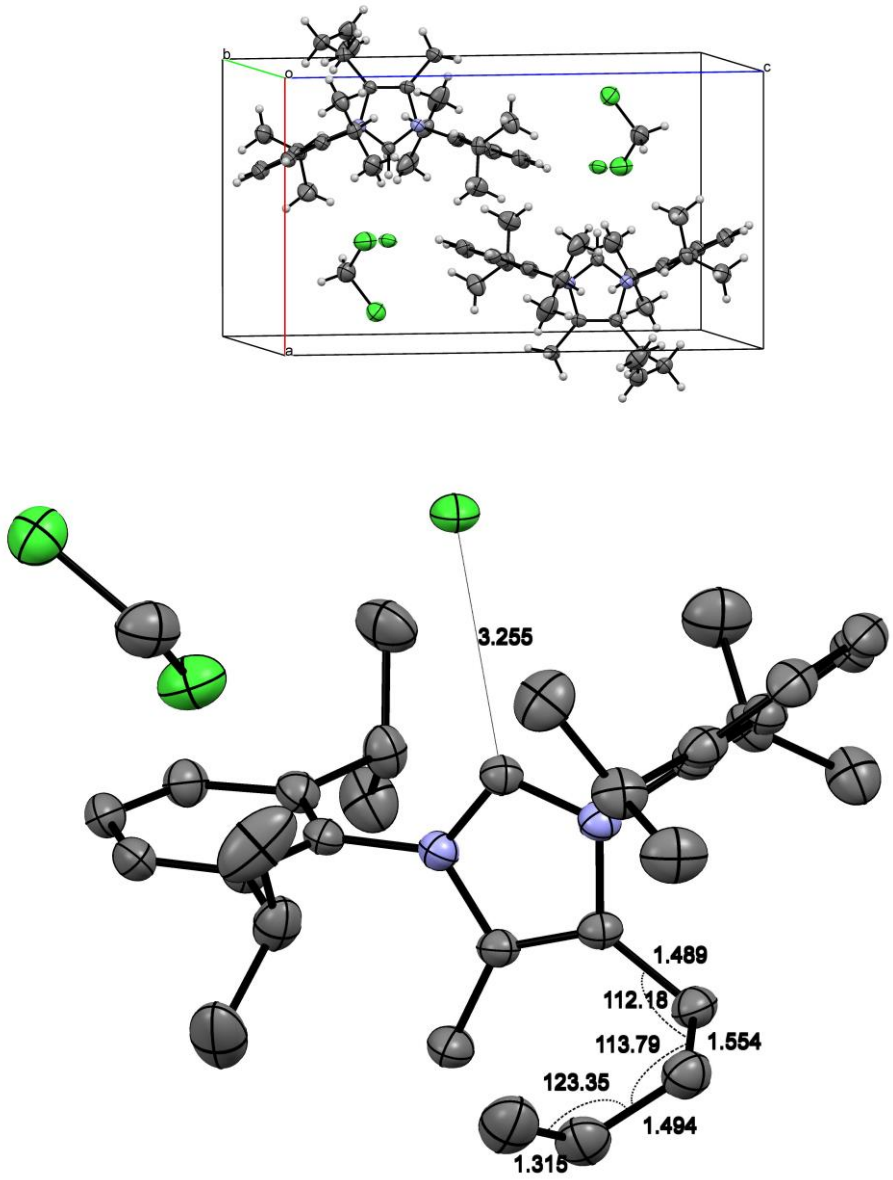

Figure SI-97: Representation of crystal structure from different perspectives. Colors-code: grey/carbon, blue/nitrogen. top) representation of the unit cell, crystal packing. bottom) XRD structure (ORTEP 50% probability ellipsoids), Hydrogens and co-crystallizing molecules omitted for clearity.

Table 1 Crystal data and structure refinement for c300920_2_1.

Identification code	c300920_2_1
Empirical formula	$C_{33}H_{47}Cl_3N_2$
Formula weight	578.07
Temperature/K	100.0(1)
Crystal system	triclinic
Space group	P-1
a/Å	9.6877(2)
b/Å	10.6207(2)
c/Å	16.7100(3)
α/°	105.817(2)
β/°	90.927(2)
γ/°	91.477(2)
Volume/Å^3	1653.17(6)
Z	2
ρ_{calc}g/cm^3	1.161
μ/mm^{-1}	2.669
F(000)	620.0
Crystal size/mm^3	0.161 × 0.119 × 0.086
Radiation	Cu Kα (λ = 1.54184)
2Θ range for data collection/°	5.498 to 159.79
Index ranges	-8 ≤ h ≤ 12, -13 ≤ k ≤ 13, -20 ≤ l ≤ 21
Reflections collected	26801
Independent reflections	7018 [R_{int} = 0.0446, R_{sigma} = 0.0377]
Data/restraints/parameters	7018/0/352
Goodness-of-fit on F^2	1.042
Final R indexes [I>=2σ (I)]	R_1 = 0.0663, wR_2 = 0.1885
Final R indexes [all data]	R_1 = 0.0739, wR_2 = 0.1958
Largest diff. peak/hole / e Å^{-3}	0.76/-0.49

Table 2 Fractional Atomic Coordinates (×10^4) and Equivalent Isotropic Displacement Parameters (Å^2×10^3) for c300920_2_1. U_{eq} is defined as 1/3 of of the trace of the orthogonalised U_{IJ} tensor.

Atom	*x*	*y*	*z*	U(eq)
Cl1	3919.2(6)	7727.7(6)	7555.0(4)	37.38(18)
Cl2	3476.9(8)	1711.1(9)	7247.0(6)	59.8(2)
Cl3	825.8(8)	262.9(8)	6826.8(5)	53.0(2)
C33	2285(4)	601(4)	7492(2)	55.5(8)
N1	8060.9(19)	7604.8(19)	8132.9(12)	26.1(4)
N2	7993.8(19)	6776.6(18)	6805.9(12)	25.5(4)
C1	7217(2)	7208(2)	7469.8(14)	25.7(4)
C2	9432(2)	7427(2)	7888.4(14)	26.6(4)
C3	9385(2)	6913(2)	7045.8(14)	26.9(4)
C4	10504(3)	6543(3)	6434.3(16)	36.6(5)

Table 2 Fractional Atomic Coordinates ($\times 10^4$) and Equivalent Isotropic Displacement Parameters ($Å^2 \times 10^3$) for c300920_2_1. U_{eq} is defined as 1/3 of of the trace of the orthogonalised U_{IJ} tensor.

Atom	*x*	*y*	*z*	U(eq)
C5	10640(2)	7697(2)	8479.2(15)	32.0(5)
C6	11019(3)	6478(3)	8772.7(17)	38.8(6)
C7	11341(3)	5309(3)	8078.6(19)	44.3(6)
C8	10611(4)	4203(3)	7905(2)	55.4(8)
C9	7594(2)	8260(2)	8959.7(14)	28.5(5)
C10	7110(2)	7500(3)	9463.2(15)	33.1(5)
C11	6610(3)	8176(3)	10238.7(16)	38.6(6)
C12	6591(3)	9523(3)	10481.6(16)	39.9(6)
C13	7079(3)	10242(3)	9962.7(16)	36.5(5)
C14	7600(2)	9623(2)	9183.9(14)	30.8(5)
C15	7052(3)	6015(3)	9184.4(17)	38.6(6)
C16	5560(3)	5521(3)	8945(2)	51.2(7)
C17	7656(3)	5404(3)	9837(2)	50.4(7)
C18	8096(3)	10419(2)	8606.0(16)	35.2(5)
C19	6878(4)	11061(4)	8299(2)	57.6(8)
C20	9230(3)	11426(3)	9019.2(19)	46.4(7)
C21	7474(2)	6185(2)	5966.7(14)	27.3(5)
C22	7196(2)	6987(2)	5455.4(15)	30.5(5)
C23	6740(3)	6368(3)	4641.3(15)	34.3(5)
C24	6551(3)	5025(3)	4367.7(15)	34.6(5)
C25	6833(3)	4259(2)	4896.4(16)	34.5(5)
C26	7322(2)	4817(2)	5709.2(15)	31.3(5)
C27	7340(3)	8470(2)	5755.6(16)	34.9(5)
C28	5921(4)	9073(3)	5871(2)	51.3(7)
C29	8203(4)	9038(3)	5170(2)	51.5(7)
C30	7678(3)	3976(3)	6282.4(18)	41.1(6)
C31	8666(5)	2895(3)	5862(2)	65.4(10)
C32	6386(4)	3436(5)	6581(3)	72.6(12)

Table 3 Anisotropic Displacement Parameters ($Å^2 \times 10^3$) for c300920_2_1. The Anisotropic displacement factor exponent takes the form: $-2\pi^2[h^2a^{*2}U_{11}+2hka^*b^*U_{12}+\ldots]$.

Atom	U_{11}	U_{22}	U_{33}	U_{23}	U_{13}	U_{12}
Cl1	23.5(3)	43.0(3)	41.3(3)	3.6(2)	4.1(2)	4.6(2)
Cl2	44.4(4)	65.3(5)	73.5(5)	25.4(4)	-0.2(4)	1.7(3)
Cl3	51.4(4)	57.2(5)	52.2(4)	18.4(3)	0.3(3)	-3.0(3)
C33	53.6(19)	67(2)	51.9(18)	25.7(16)	4.7(14)	10.9(15)
N1	23.8(9)	31.2(9)	24.6(9)	9.5(7)	4.2(7)	1.2(7)
N2	24.5(9)	26.2(9)	25.4(9)	6.1(7)	2.8(7)	2.5(7)
C1	25.0(11)	27.5(10)	25.8(10)	9.3(8)	2.8(8)	1.4(8)
C2	23.3(10)	29.4(11)	28.7(11)	10.5(9)	3.0(8)	2.1(8)
C3	22.4(10)	28.1(11)	29.8(11)	7.0(9)	2.4(8)	3.3(8)
C4	28.5(12)	46.4(14)	32.1(12)	5.3(10)	4.8(9)	4.3(10)

Table 3 Anisotropic Displacement Parameters ($Å^2×10^3$) for c300920_2_1. The Anisotropic displacement factor exponent takes the form: $-2π^2[h^2a^{*2}U_{11}+2hka*b*U_{12}+...]$.

Atom	U_{11}	U_{22}	U_{33}	U_{23}	U_{13}	U_{12}
C5	25.2(11)	39.3(13)	31.5(11)	9.8(10)	0.4(9)	1.5(9)
C6	36.7(13)	44.5(14)	36.4(13)	13.1(11)	-2.0(10)	4.2(11)
C7	46.3(16)	44.2(15)	44.9(15)	15.5(12)	-3.6(12)	12.3(12)
C8	59(2)	41.1(16)	67(2)	15.4(15)	-13.3(16)	8.0(14)
C9	23.2(10)	39.0(12)	23.2(10)	8.2(9)	3.1(8)	2.0(9)
C10	26.2(11)	45.4(14)	29.9(11)	14.1(10)	2.6(9)	1.3(9)
C11	32.8(13)	57.2(16)	28.8(12)	16.6(11)	6.4(10)	-0.8(11)
C12	30.6(13)	59.8(17)	26.2(11)	6.0(11)	6.2(9)	3.7(11)
C13	30.7(13)	43.3(14)	30.8(12)	1.9(10)	2.1(9)	3.8(10)
C14	25.9(11)	38.0(12)	27.5(11)	7.1(9)	2.1(8)	1.4(9)
C15	39.3(14)	44.3(14)	38.1(13)	20.8(11)	8.0(11)	-0.1(11)
C16	49.0(17)	51.6(17)	57.6(18)	23.8(15)	1.5(14)	-11.7(13)
C17	51.1(17)	57.8(18)	53.3(17)	32.8(15)	7.5(13)	7.7(14)
C18	42.0(14)	32.3(12)	31.5(12)	8.7(10)	6.2(10)	3.6(10)
C19	61(2)	61(2)	61(2)	33.0(17)	2.6(16)	10.2(16)
C20	51.5(17)	42.9(15)	44.5(15)	11.6(12)	9.6(13)	-5.5(12)
C21	22.0(10)	32.7(11)	25.3(10)	4.3(9)	3.3(8)	3.8(8)
C22	29.2(12)	32.9(12)	27.9(11)	5.7(9)	5.1(9)	2.1(9)
C23	35.6(13)	41.0(13)	26.8(11)	9.8(10)	1.5(9)	3.5(10)
C24	32.0(12)	41.4(13)	26.4(11)	2.2(10)	0.7(9)	5.1(10)
C25	31.7(12)	31.1(12)	36.1(12)	1.0(10)	1.6(9)	5.0(9)
C26	28.1(11)	31.4(12)	32.9(12)	6.2(9)	1.4(9)	4.4(9)
C27	45.7(14)	30.7(12)	28.8(11)	9.1(9)	-0.3(10)	0.9(10)
C28	54.3(18)	34.1(14)	64.4(19)	10.4(13)	9.6(15)	9.5(12)
C29	63(2)	42.5(16)	49.9(17)	14.9(13)	11.6(14)	-7.3(14)
C30	47.2(15)	33.8(13)	42.9(14)	11.9(11)	-11.6(12)	1.9(11)
C31	91(3)	44.4(17)	58(2)	7.5(15)	-18.1(19)	25.2(17)
C32	65(2)	91(3)	86(3)	68(2)	-24(2)	-22(2)

Table 4 Bond Lengths for c300920_2_1.

Atom	Atom	Length/Å	Atom	Atom	Length/Å
Cl2	C33	1.761(4)	C12	C13	1.383(4)
Cl3	C33	1.751(4)	C13	C14	1.397(3)
N1	C1	1.331(3)	C14	C18	1.522(3)
N1	C2	1.398(3)	C15	C16	1.534(4)
N1	C9	1.453(3)	C15	C17	1.529(4)
N2	C1	1.332(3)	C18	C19	1.528(4)
N2	C3	1.392(3)	C18	C20	1.529(4)
N2	C21	1.447(3)	C21	C22	1.388(3)
C2	C3	1.364(3)	C21	C26	1.401(3)
C2	C5	1.489(3)	C22	C23	1.398(3)
C3	C4	1.488(3)	C22	C27	1.520(3)

Table 4 Bond Lengths for c300920_2_1.

Atom	Atom	Length/Å	Atom	Atom	Length/Å
C5	C6	1.555(4)	C23	C24	1.380(4)
C6	C7	1.493(4)	C24	C25	1.383(4)
C7	C8	1.314(5)	C25	C26	1.395(4)
C9	C10	1.394(3)	C26	C30	1.519(4)
C9	C14	1.392(4)	C27	C28	1.525(4)
C10	C11	1.400(4)	C27	C29	1.530(4)
C10	C15	1.517(4)	C30	C31	1.538(5)
C11	C12	1.378(4)	C30	C32	1.511(5)

Table 5 Bond Angles for c300920_2_1.

Atom	Atom	Atom	Angle/˚	Atom	Atom	Atom	Angle/˚
Cl3	C33	Cl2	113.26(19)	C9	C14	C18	122.5(2)
C1	N1	C2	109.75(18)	C13	C14	C18	120.7(2)
C1	N1	C9	123.42(19)	C10	C15	C16	109.7(2)
C2	N1	C9	126.45(19)	C10	C15	C17	112.7(2)
C1	N2	C3	109.85(19)	C17	C15	C16	111.1(2)
C1	N2	C21	125.28(19)	C14	C18	C19	110.3(2)
C3	N2	C21	124.78(18)	C14	C18	C20	111.7(2)
N1	C1	N2	107.66(19)	C19	C18	C20	111.7(3)
N1	C2	C5	123.9(2)	C22	C21	N2	118.9(2)
C3	C2	N1	106.24(19)	C22	C21	C26	123.7(2)
C3	C2	C5	129.7(2)	C26	C21	N2	117.4(2)
N2	C3	C4	122.2(2)	C21	C22	C23	116.9(2)
C2	C3	N2	106.50(19)	C21	C22	C27	122.6(2)
C2	C3	C4	131.3(2)	C23	C22	C27	120.5(2)
C2	C5	C6	112.2(2)	C24	C23	C22	121.3(2)
C7	C6	C5	113.8(2)	C23	C24	C25	120.2(2)
C8	C7	C6	123.3(3)	C24	C25	C26	121.1(2)
C10	C9	N1	118.7(2)	C21	C26	C30	121.9(2)
C14	C9	N1	117.2(2)	C25	C26	C21	116.8(2)
C14	C9	C10	124.0(2)	C25	C26	C30	121.3(2)
C9	C10	C11	116.5(2)	C22	C27	C28	110.4(2)
C9	C10	C15	122.8(2)	C22	C27	C29	112.0(2)
C11	C10	C15	120.6(2)	C28	C27	C29	110.8(2)
C12	C11	C10	121.2(2)	C26	C30	C31	110.9(3)
C11	C12	C13	120.4(2)	C32	C30	C26	111.0(2)
C12	C13	C14	121.0(3)	C32	C30	C31	112.5(3)
C9	C14	C13	116.8(2)				

Table 6 Torsion Angles for c300920_2_1.

A	B	C	D	Angle/°	A	B	C	D	Angle/°
N1	C2	C3	N2	-0.8(2)	C9	C14	C18	C19	110.0(3)
N1	C2	C3	C4	178.5(2)	C9	C14	C18	C20	-125.1(3)
N1	C2	C5	C6	89.7(3)	C10	C9	C14	C13	-0.3(4)
N1	C9	C10	C11	-177.0(2)	C10	C9	C14	C18	-178.1(2)
N1	C9	C10	C15	0.0(4)	C10	C11	C12	C13	-0.5(4)
N1	C9	C14	C13	176.6(2)	C11	C10	C15	C16	73.8(3)
N1	C9	C14	C18	-1.2(3)	C11	C10	C15	C17	-50.6(3)
N2	C21	C22	C23	177.9(2)	C11	C12	C13	C14	0.0(4)
N2	C21	C22	C27	-3.4(3)	C12	C13	C14	C9	0.4(4)
N2	C21	C26	C25	-179.4(2)	C12	C13	C14	C18	178.2(2)
N2	C21	C26	C30	0.3(3)	C13	C14	C18	C19	-67.7(3)
C1	N1	C2	C3	0.4(2)	C13	C14	C18	C20	57.1(3)
C1	N1	C2	C5	-176.3(2)	C14	C9	C10	C11	-0.2(4)
C1	N1	C9	C10	85.1(3)	C14	C9	C10	C15	176.9(2)
C1	N1	C9	C14	-92.0(3)	C15	C10	C11	C12	-176.6(2)
C1	N2	C3	C2	0.9(2)	C21	N2	C1	N1	176.0(2)
C1	N2	C3	C4	-178.5(2)	C21	N2	C3	C2	-175.8(2)
C1	N2	C21	C22	88.9(3)	C21	N2	C3	C4	4.8(3)
C1	N2	C21	C26	-93.0(3)	C21	C22	C23	C24	1.3(4)
C2	N1	C1	N2	0.2(2)	C21	C22	C27	C28	-106.5(3)
C2	N1	C9	C10	-102.6(3)	C21	C22	C27	C29	129.4(3)
C2	N1	C9	C14	80.3(3)	C21	C26	C30	C31	-127.7(3)
C2	C5	C6	C7	58.1(3)	C21	C26	C30	C32	106.4(3)
C3	N2	C1	N1	-0.7(2)	C22	C21	C26	C25	-1.5(3)
C3	N2	C21	C22	-94.8(3)	C22	C21	C26	C30	178.2(2)
C3	N2	C21	C26	83.2(3)	C22	C23	C24	C25	-1.0(4)
C3	C2	C5	C6	-86.2(3)	C23	C22	C27	C28	72.1(3)
C5	C2	C3	N2	175.7(2)	C23	C22	C27	C29	-51.9(3)
C5	C2	C3	C4	-5.0(4)	C23	C24	C25	C26	-0.5(4)
C5	C6	C7	C8	-117.3(3)	C24	C25	C26	C21	1.7(4)
C9	N1	C1	N2	173.6(2)	C24	C25	C26	C30	-178.0(2)
C9	N1	C2	C3	-172.7(2)	C25	C26	C30	C31	52.0(4)
C9	N1	C2	C5	10.5(3)	C25	C26	C30	C32	-73.9(4)
C9	C10	C11	C12	0.6(4)	C26	C21	C22	C23	0.0(3)
C9	C10	C15	C16	-103.2(3)	C26	C21	C22	C27	178.7(2)
C9	C10	C15	C17	132.4(3)	C27	C22	C23	C24	-177.4(2)

Table 7 Hydrogen Atom Coordinates (Å×10^4) and Isotropic Displacement Parameters (Å^2×10^3) for c300920_2_1.

Atom	*x*	*y*	*z*	U(eq)
H33A	2741.02	-211.79	7464.71	67
H33B	1990.47	957.89	8058.88	67
H1	6257.43	7227.8	7470.08	31

Table 7 Hydrogen Atom Coordinates (Å×10^4) and Isotropic Displacement Parameters (Å^2×10^3) for c300920_2_1.

Atom	*x*	*y*	*z*	U(eq)
H4A	10490.63	5608.87	6209.75	55
H4B	11381.19	6834.55	6706.37	55
H4C	10363.06	6947.29	5992.11	55
H5A	10431.78	8410.16	8959.99	38
H5B	11428.8	7972.25	8211.24	38
H6A	11812.73	6703.58	9150.85	47
H6B	10253.5	6250.18	9079.39	47
H7	12096.25	5366.18	7752.6	53
H8A	9850.25	4121.24	8221.73	66
H8B	10854.69	3503.5	7465.55	66
H11	6285.03	7706.9	10596.37	46
H12	6247.5	9952.65	10997.65	48
H13	7059.32	11150.57	10134.85	44
H15	7604.34	5737.04	8684.22	46
H16A	4992.5	5784	9424.58	77
H16B	5533.61	4583.44	8743.86	77
H16C	5218.66	5887.39	8517.53	77
H17A	8588.07	5728.38	9976.55	76
H17B	7649.61	4468.94	9617.9	76
H17C	7109.88	5630.93	10327.35	76
H18	8491.93	9810.82	8119.85	42
H19A	6192.02	10401.78	8039.17	86
H19B	7192.79	11504.71	7903.1	86
H19C	6484.25	11680.36	8761.84	86
H20A	8863.38	12049.46	9490.45	70
H20B	9556.82	11871.19	8627.06	70
H20C	9980.42	10988.84	9199.57	70
H23	6561.45	6870.73	4277	41
H24	6233	4634.07	3826.49	41
H25	6694.12	3355.34	4706.94	41
H27	7817.22	8699.67	6299.96	42
H28A	5461.78	8927.63	5338.25	77
H28B	6024.96	9997.18	6128.15	77
H28C	5381.28	8674.52	6218.03	77
H29A	9072.01	8612.04	5082.95	77
H29B	8363.04	9959.75	5413.53	77
H29C	7716.19	8896.88	4646.8	77
H30	8165.79	4542.68	6772.39	49
H31A	8229.64	2338.85	5367.27	98
H31B	8888.93	2385.46	6238.25	98
H31C	9497.03	3287.2	5718.98	98
H32A	5851.81	4147.26	6891.21	109
H32B	6636.85	2892.7	6931.35	109
H32C	5848.52	2926.89	6111.17	109

3.4.2. Crystal structure for [($^{Me, but-3-en-1-yl}$IPr)Cu^{I}•Pd^{II}(bhq)$_2$]BArF , [**4a**]BArF:
Comment: none

Crystal Data for $C_{90}H_{72}BCuF_{24}N_4Pd$ (M =1846.26 g/mol): triclinic, space group P-1 (no. 2), a = 12.6056(2) Å, b = 16.5906(2) Å, c = 22.0168(2) Å, α = 104.2570(10)°, β = 105.8030(10)°, γ = 94.5440(10)°, V = 4240.82(10) Å^3, Z = 2, T = 100.0(1) K, μ(CuKα) = 2.900 mm^{-1}, $Dcalc$ = 1.446 g/cm^3, 163181 reflections measured (6.028° ≤ 2Θ ≤ 159.516°), 18092 unique (R_{int} = 0.0522, R_{sigma} = 0.0237) which were used in all calculations. The final R_1 was 0.0561 (I > 2σ(I)) and wR_2 was 0.1196 (all data).

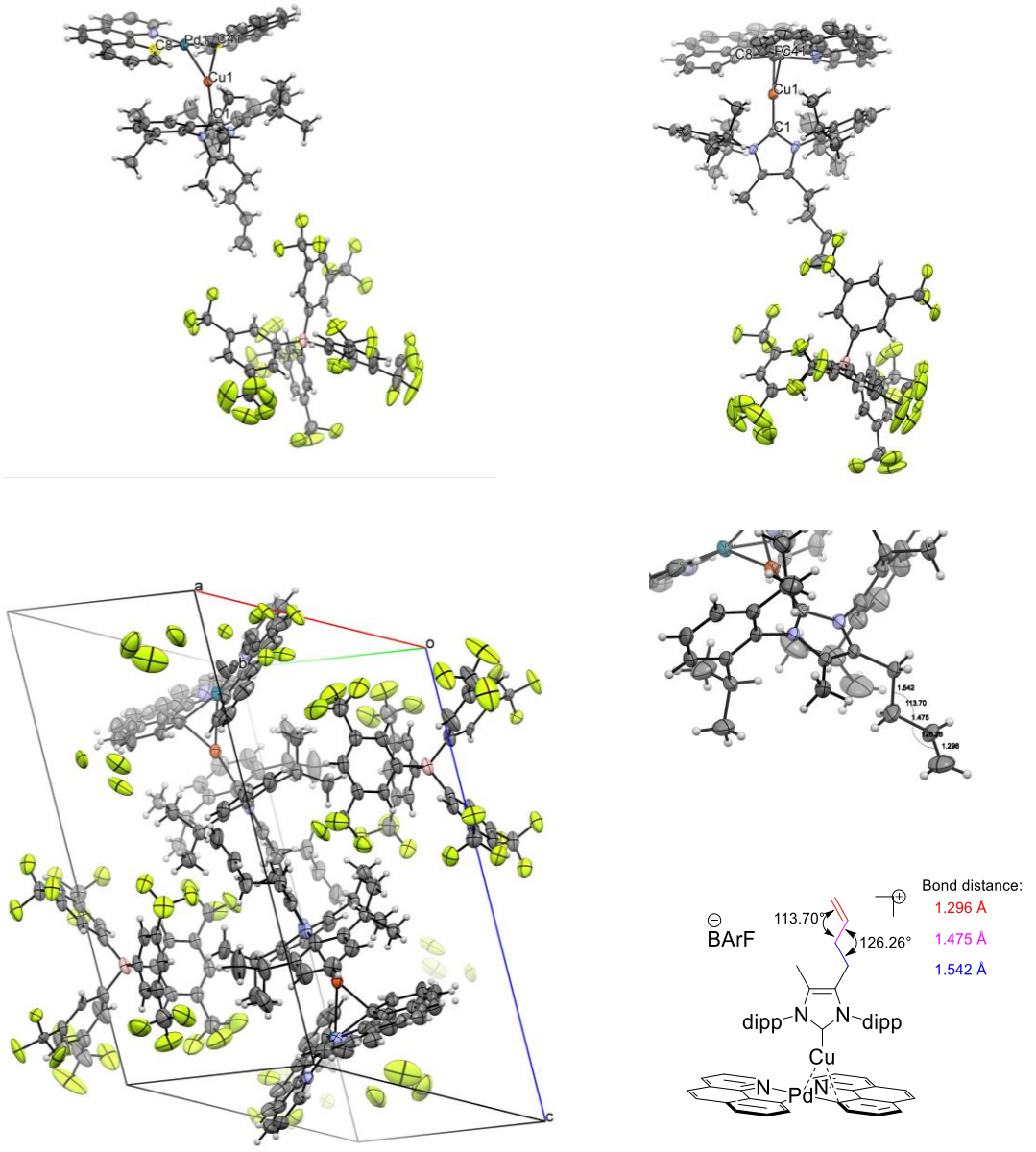

Figure SI-98: Representation of crystal structure from different perspectives. Colors-code: grey/carbon, red/oxygen, light-orange/phosphorus, dark-orange/Cu, yellow/Fluorine, pink/boron, blue/nitrogen, teal/palladium.

Table 1 Crystal data and structure refinement for c160918_1_1.

Identification code	c160918_1_1
Empirical formula	$C_{90}H_{72}BCuF_{24}N_4Pd$
Formula weight	1846.26
Temperature/K	100.0(1)
Crystal system	triclinic
Space group	P-1
a/Å	12.6056(2)
b/Å	16.5906(2)
c/Å	22.0168(2)
α/°	104.2570(10)
β/°	105.8030(10)
γ/°	94.5440(10)
Volume/Å^3	4240.82(10)
Z	2
ρ_{calc}g/cm^3	1.446
μ/mm^{-1}	2.900
F(000)	1872.0
Crystal size/mm^3	0.191 × 0.122 × 0.078
Radiation	CuKα (λ = 1.54184)
2Θ range for data collection/°	6.028 to 159.516
Index ranges	-13 ≤ h ≤ 15, -21 ≤ k ≤ 21, -27 ≤ l ≤ 28
Reflections collected	163181
Independent reflections	18092 [R_{int} = 0.0522, R_{sigma} = 0.0237]
Data/restraints/parameters	18092/948/1383
Goodness-of-fit on F^2	1.141
Final R indexes [I>=2σ (I)]	R_1 = 0.0561, wR_2 = 0.1187
Final R indexes [all data]	R_1 = 0.0584, wR_2 = 0.1196
Largest diff. peak/hole / e Å^{-3}	0.64/-1.08

Table 2 Fractional Atomic Coordinates (×10^4) and Equivalent Isotropic Displacement Parameters (Å^2×10^3) for c160918_1_1. U_{eq} is defined as 1/3 of of the trace of the orthogonalised U_{IJ} tensor.

Atom	*x*	*y*	*z*	U(eq)
Pd1	5031.6(2)	4173.3(2)	8683.2(2)	34.44(7)
Cu1	4764.8(4)	3613.0(3)	7459.2(3)	34.14(12)
N1	6086(2)	3035.3(16)	6579.5(15)	32.7(6)
N2	5293(2)	4047.9(16)	6332.2(14)	30.8(6)
N3	5889(8)	3117(6)	8821(5)	29(2)
N4	5984(2)	5033.6(18)	9581.3(14)	35.4(6)
C1	5409(3)	3590.0(19)	6766.5(18)	32.3(7)
C2	5872(3)	3794(2)	5876.5(18)	34.2(7)
C5	4956(3)	5935(2)	9055(2)	40.7(9)

C7	5684(3)	1634(2)	6693(2)	38.8(8)
C8	4459(3)	5219(2)	8511.8(19)	37.2(8)
C9	5762(3)	5836(2)	9612.1(19)	40.9(9)
C13	4675(3)	4743(2)	6338.9(18)	33.1(7)
C14	5237(3)	5542(2)	6725.7(19)	35.8(8)
C17	4614(3)	1448(2)	6122.7(19)	38.7(8)
C18	6448(3)	5698(2)	7143(2)	40.3(8)
C19	5871(4)	4200(2)	5344(2)	47.2(10)
C21	6367(3)	3143(2)	6032.2(19)	35.2(8)
C22	6401(3)	2399(2)	6905(2)	39.2(8)
C24	2994(3)	3695(2)	5534.3(19)	40.7(8)
C27	3565(3)	4579(2)	5942.4(19)	36.1(8)
C29	2993(3)	5265(2)	5950(2)	43.3(9)
C33	4615(3)	6205(2)	6709(2)	43.8(9)
C36	5997(4)	1028(2)	7025(2)	50.7(10)
C38	3751(3)	5362(3)	7964(2)	47.5(9)
C39	7161(4)	6337(3)	6962(3)	56.9(11)
C41	3879(12)	3214(9)	8000(8)	31(3)
C42	7102(3)	2632(2)	5717(2)	43.0(9)
C43	2370(4)	3283(2)	5907(2)	50.5(10)
C46	3583(3)	1363(2)	6354(2)	45.3(9)
C47	7269(4)	5556(3)	10665(2)	63.4(13)
C48	4680(4)	6750(2)	9058(2)	56.6(12)
C49	4604(4)	667(2)	5579(2)	51.8(10)
C53	6969(4)	1190(3)	7533(3)	62.6(12)
C54	6691(3)	4903(3)	10103.9(19)	45.3(9)
C55	5233(6)	7438(3)	9629(3)	81(2)
C56	6296(4)	6523(3)	10163(2)	58.8(13)
C59	3516(3)	6069(2)	6329(2)	46.7(10)
C60	2222(4)	3665(3)	4859(2)	55.7(11)
C61	8953(3)	2676(3)	5479(3)	55.4(11)
C63	7398(3)	2584(3)	7417(2)	52.8(11)
C64	7081(5)	6366(3)	10686(2)	73.1(16)
C65	3463(4)	6169(3)	7959(3)	62.1(13)
C66	7667(4)	1955(3)	7727(3)	65.8(13)
C67	3917(5)	6843(3)	8499(3)	70.8(16)
C69	8242(4)	3148(3)	5822(3)	64.1(14)
C70	6922(9)	3101(7)	9189(5)	35(2)
C72	5997(6)	7336(3)	10148(3)	84(2)
C73	4098(10)	2427(6)	8135(5)	33(2)
C74	3540(13)	936(8)	8019(7)	50(3)
C75	8155(3)	3429(3)	7627(3)	64.1(13)
C76	6587(4)	5973(4)	7873(2)	69.2(14)
C77	2799(10)	3225(7)	7639(7)	37(3)
C78	5169(10)	2382(6)	8537(5)	34(2)
C79	2202(10)	1768(7)	7539(6)	47(3)
C81	1947(9)	2515(8)	7402(6)	45(3)

C82	9311(4)	2860(4)	5023(3)	77.0(16)
C83	8034(5)	3986(4)	8260(3)	94(2)
C84	5455(12)	1613(5)	8654(5)	42(2)
C86	3281(10)	1704(5)	7897(5)	43(2)
C87	7286(11)	2359(7)	9303(5)	48(3)
C88	4602(13)	894(5)	8385(5)	52(3)
C90	6535(12)	1617(7)	9036(5)	47(3)
C91	9384(4)	3328(4)	7710(4)	111(3)
F1	6041(9)	663(5)	957(5)	39.2(15)
F2	6331.1(18)	683.3(15)	3208.3(14)	59.3(7)
F3	7078(2)	1049.7(15)	4254.1(14)	57.6(6)
F4	11351(2)	-59.1(18)	4566.1(14)	65.1(7)
F5	10938(2)	4777.8(14)	3891.0(14)	62.9(7)
F6	9510(2)	4123.0(15)	4009.4(14)	63.0(7)
F7	9821(2)	-842.4(15)	4399.4(14)	60.5(7)
F8	10696(3)	-1054.9(17)	3673.5(14)	72.3(8)
F9	7112(2)	1956.9(14)	3704.1(16)	65.3(8)
F10	9304(3)	5027.9(15)	3449.8(16)	73.0(8)
F11	5843(13)	-495(6)	240(7)	67(3)
F12	6612(12)	631(8)	141(7)	83(4)
F13	14894(7)	1383(6)	4201(6)	80(3)
F14	13581(10)	1815(6)	4509(5)	72(2)
F15	13308(4)	1703(2)	1293.6(19)	108.8(13)
F16	13165(3)	435(2)	1211.2(19)	105.7(13)
F17	10712(6)	-1391(5)	742(5)	116(4)
F18	9115(7)	-1915(6)	48(5)	161(6)
F19	14652(3)	1233(4)	1810(2)	148(2)
F20	9623(12)	4304(5)	1220(6)	118(5)
F21	14616(9)	2654(4)	4298(4)	96(3)
F22	9529(8)	-2071(5)	1008(7)	138(4)
F23	8253(6)	3378(8)	853(4)	106(3)
F24	9743(11)	3035(6)	741(4)	102(3)
C3	8727(3)	1248(2)	3173(2)	39.8(8)
C4	8310(7)	664(9)	1476(6)	26.5(19)
C6	9702(3)	1026(2)	3031(2)	38.9(8)
C10	13840(3)	1486(2)	2854(2)	42.7(9)
C11	7222(3)	1158(2)	3700(2)	46.7(10)
C12	11487(3)	1360(2)	2611.7(19)	36.7(8)
C15	7662(12)	56(7)	910(6)	33(2)
C16	6533(9)	208(7)	562(6)	26(2)
C20	9896(3)	2276(2)	2438(2)	39.4(8)
C23	14132(3)	1841(2)	4051(2)	47.7(9)
C25	11978(3)	1245(2)	2105(2)	42.2(9)
C26	8298(3)	930(2)	3600(2)	39.3(8)
C28	9732(3)	2503(2)	1851(2)	44.8(9)
C30	9936(3)	2919(2)	2991(2)	39.9(8)
C31	12228(3)	1569(2)	3246.8(19)	37.2(8)

C32	13378(3)	1625(2)	3368(2)	38.8(8)
C34	10204(3)	449(2)	3346(2)	40.2(8)
C35	8825(3)	371(2)	3911(2)	40.9(8)
C37	10399(4)	-449(3)	4103(2)	50.4(10)
C40	9418(3)	607(2)	1800.0(19)	42.9(9)
C80A	9749(14)	-176(7)	1636(8)	47(4)
C85A	9020(8)	-824(6)	1122(5)	28(2)
C62	8071(3)	-667(2)	659(2)	63.2(14)
C15A	7746(18)	114(10)	846(10)	38(3)
C4A	8421(11)	745(14)	1384(9)	26.5(19)
C44	13126(3)	1307(2)	2222(2)	42.9(9)
C45	9789(3)	137(2)	3777(2)	40.4(8)
C50	9783(3)	3733(2)	2961(2)	42.1(9)
C51	9605(3)	3936(2)	2371(2)	47.8(10)
C52	9578(3)	3312(2)	1813(2)	49.1(9)
B1	10138(3)	1327(2)	2469(2)	39.3(9)
C58	9876(4)	4406(2)	3568(2)	50.6(10)
C68	9379(4)	3508(3)	1171(3)	66.2(12)
C71	13581(4)	1182(3)	1648(3)	59.1(12)
C80	9803(12)	-129(7)	1504(8)	70(4)
C85	9206(7)	-730(6)	914(5)	51(3)
C89	9638(7)	-1516(5)	659(6)	86(4)
F1A	6093(15)	606(10)	852(8)	75(5)
F11A	5993(19)	-421(8)	47(9)	69(5)
F12A	6701(17)	785(9)	91(8)	57(3)
F17A	10475(5)	-1612(5)	992(3)	41.3(17)
F18A	8834(6)	-2164(4)	390(3)	51(2)
F22A	9331(5)	-2090(4)	1416(3)	46.8(18)
C16A	6659(14)	270(10)	450(8)	31(3)
C89A	9418(7)	-1656(6)	985(4)	37(2)
F23A	8712(17)	2973(10)	674(6)	141(7)
F24A	10358(9)	3607(13)	1029(8)	129(5)
F20A	9100(20)	4225(9)	1161(11)	155(8)
F21A	13735(13)	2191(10)	4489(7)	95(5)
F13A	15104(6)	2297(8)	4082(4)	73(3)
F14A	14490(12)	1154(7)	4153(8)	86(5)
N3A	5504(10)	3005(8)	8801(6)	45(3)
C41A	3643(13)	3344(9)	7964(9)	43(4)
C77A	2630(10)	3476(8)	7589(8)	42(3)
C81A	1687(10)	2839(9)	7303(6)	56(3)
C79A	1764(12)	2044(9)	7403(6)	62(3)
C86A	2755(13)	1868(6)	7792(5)	53(3)
C73A	3680(11)	2520(7)	8070(6)	43(3)
C74A	2810(14)	1056(6)	7874(5)	64(3)
C88A	3811(17)	886(8)	8229(7)	59(4)
C84A	4774(14)	1520(6)	8534(5)	56(3)
C78A	4671(13)	2342(6)	8480(6)	43(2)

C90A	5777(14)	1404(6)	8924(5)	60(3)
C87A	6666(14)	2049(8)	9221(6)	59(3)
C70A	6474(12)	2847(7)	9143(6)	50(3)

Table 3 Anisotropic Displacement Parameters ($Å^2×10^3$) for c160918_1_1. The Anisotropic displacement factor exponent takes the form: $-2π^2[h^2a^{*2}U_{11}+2hka^*b^*U_{12}+...]$.

Atom	U_{11}	U_{22}	U_{33}	U_{23}	U_{13}	U_{12}
Pd1	35.93(14)	21.92(11)	42.98(14)	4.30(10)	12.46(11)	3.50(9)
Cu1	32.5(3)	24.8(2)	44.8(3)	7.0(2)	13.9(2)	3.49(19)
N1	20.3(13)	23.5(13)	53.8(18)	6.4(12)	13.1(12)	7.4(10)
N2	23.0(13)	21.1(12)	50.1(17)	5.3(11)	17.2(12)	6.4(10)
N3	33(4)	23(4)	36(4)	6(3)	18(4)	12(3)
N4	32.6(15)	32.5(15)	40.1(16)	2.3(12)	17.2(13)	1.6(12)
C1	21.8(15)	22.3(15)	49(2)	3.5(14)	11.1(14)	3.4(12)
C2	28.1(17)	25.0(15)	53(2)	4.6(14)	22.0(15)	7.0(13)
C5	49(2)	27.6(17)	59(2)	11.9(16)	36.0(19)	12.7(15)
C7	37.2(19)	24.6(16)	57(2)	7.1(15)	19.9(17)	12.0(14)
C8	33.8(18)	32.4(17)	54(2)	14.6(16)	23.5(16)	7.6(14)
C9	50(2)	26.5(16)	49(2)	0.1(15)	32.4(18)	-5.1(15)
C13	32.1(17)	23.7(15)	51(2)	10.2(14)	22.2(15)	12.3(13)
C14	33.5(18)	24.7(15)	56(2)	9.8(15)	24.4(16)	8.7(13)
C17	40(2)	21.5(15)	53(2)	3.9(15)	17.8(17)	3.8(14)
C18	33.8(19)	23.4(16)	63(2)	6.8(16)	18.3(17)	3.9(14)
C19	54(2)	33.3(19)	66(3)	12.4(18)	36(2)	13.0(17)
C21	26.5(17)	22.9(15)	58(2)	3.6(14)	21.9(16)	4.6(13)
C22	31.0(18)	27.2(16)	61(2)	11.4(16)	15.3(17)	11.7(14)
C24	30.0(18)	34.8(18)	54(2)	5.7(16)	12.0(16)	7.7(14)
C27	32.0(18)	29.7(17)	51(2)	10.1(15)	20.2(16)	9.6(14)
C29	34.9(19)	38.2(19)	64(2)	16.2(18)	21.7(18)	16.9(16)
C33	44(2)	24.4(16)	70(3)	11.2(17)	29(2)	9.9(15)
C36	56(3)	30.1(19)	71(3)	15.4(19)	25(2)	14.1(17)
C38	39(2)	51(2)	65(3)	24(2)	27.1(19)	17.3(18)
C39	40(2)	56(3)	82(3)	22(2)	28(2)	2.3(19)
C41	27(5)	32(5)	36(5)	4(4)	17(4)	3(4)
C42	36(2)	26.8(17)	72(3)	7.2(17)	29.3(19)	10.5(14)
C43	47(2)	35(2)	63(3)	9.3(18)	13(2)	0.6(17)
C46	42(2)	31.7(18)	61(2)	4.0(17)	21.6(19)	3.2(16)
C47	61(3)	79(3)	39(2)	3(2)	15(2)	-13(2)
C48	86(3)	32.0(19)	78(3)	19(2)	61(3)	21(2)
C49	61(3)	29.7(18)	62(3)	-1.6(18)	28(2)	4.0(18)
C53	63(3)	51(3)	83(3)	33(2)	21(3)	25(2)
C54	39(2)	52(2)	45(2)	6.3(18)	20.1(17)	5.0(17)
C55	157(6)	28(2)	90(4)	14(2)	92(4)	22(3)
C56	90(4)	38(2)	48(2)	-3.7(18)	41(2)	-18(2)
C59	46(2)	33.9(19)	74(3)	19.7(19)	32(2)	22.3(17)

C60	47(2)	56(3)	57(3)	11(2)	11(2)	2(2)
C61	35(2)	46(2)	94(3)	15(2)	35(2)	17.1(17)
C63	33(2)	44(2)	76(3)	16(2)	7(2)	11.1(17)
C64	97(4)	59(3)	49(3)	-11(2)	32(3)	-31(3)
C65	60(3)	73(3)	85(3)	45(3)	45(3)	40(3)
C66	45(3)	64(3)	87(4)	30(3)	6(2)	23(2)
C67	95(4)	61(3)	104(4)	50(3)	73(4)	53(3)
C69	39(2)	47(2)	102(4)	-3(2)	37(2)	6.2(19)
C70	35(5)	35(5)	35(4)	7(4)	12(4)	14(4)
C72	163(6)	25(2)	71(3)	-9(2)	75(4)	-14(3)
C73	40(5)	22(4)	38(5)	1(3)	21(4)	2(4)
C74	72(9)	30(4)	51(8)	4(4)	36(6)	-7(5)
C75	30(2)	56(3)	94(4)	21(3)	-1(2)	2.8(19)
C76	40(2)	93(4)	68(3)	10(3)	21(2)	-5(2)
C77	34(5)	34(5)	40(5)	2(4)	13(4)	5(4)
C78	40(5)	26(4)	43(4)	9(3)	26(4)	5(4)
C79	45(6)	38(5)	54(7)	-7(4)	29(5)	-10(4)
C81	31(5)	44(6)	49(6)	-9(5)	18(4)	-7(4)
C82	42(3)	87(4)	98(4)	16(3)	30(3)	-10(3)
C83	78(4)	68(4)	100(5)	3(3)	-3(3)	-26(3)
C84	69(7)	29(4)	40(5)	11(3)	31(5)	16(4)
C86	45(5)	33(4)	50(5)	-4(3)	28(4)	-5(3)
C87	66(6)	44(5)	40(5)	14(4)	18(5)	29(4)
C88	86(8)	25(4)	61(6)	15(4)	43(5)	8(4)
C90	72(7)	41(5)	46(5)	19(4)	33(5)	28(5)
C91	30(3)	99(5)	201(8)	63(5)	14(4)	9(3)
F1	30(3)	46(3)	43(3)	9(2)	16(3)	14(2)
F2	26.9(11)	47.0(13)	90.2(19)	4.5(12)	8.0(12)	8.2(10)
F3	44.3(14)	48.7(14)	85.4(19)	15.6(13)	29.2(13)	14.8(11)
F4	41.3(14)	77.6(18)	78.0(18)	31.1(15)	9.5(13)	19.6(13)
F5	53.5(15)	36.9(12)	85.8(19)	-3.1(12)	21.3(14)	-1.7(11)
F6	69.3(17)	39.3(13)	91(2)	10.9(13)	47.0(16)	14.1(12)
F7	56.4(15)	49.3(14)	90.7(19)	33.2(14)	29.8(14)	22.9(12)
F8	103(2)	56.3(15)	78.9(19)	27.4(14)	41.7(17)	55.0(16)
F9	49.3(14)	30.2(11)	128(2)	22.4(13)	41.4(15)	19.9(10)
F10	83(2)	38.6(13)	105(2)	18.1(14)	35.4(17)	35.7(13)
F11	30(4)	33(3)	107(8)	7(3)	-20(5)	2(2)
F12	48(4)	155(9)	93(5)	104(6)	30(4)	30(5)
F13	49(4)	126(7)	68(4)	22(5)	12(4)	59(5)
F14	45(3)	96(6)	59(4)	5(4)	7(3)	13(4)
F15	175(4)	86(2)	115(3)	47(2)	96(3)	54(3)
F16	140(3)	63.1(19)	121(3)	-14.0(19)	91(3)	2(2)
F17	59(4)	79(5)	164(8)	-45(5)	26(4)	27(3)
F18	113(6)	140(8)	128(7)	-86(6)	-37(5)	94(6)
F19	54(2)	300(7)	95(3)	41(3)	44(2)	32(3)
F20	193(12)	49(3)	82(5)	28(4)	1(7)	-35(5)
F21	116(7)	53(3)	73(4)	13(3)	-24(4)	-38(4)

F22	116(7)	51(4)	232(12)	24(6)	34(7)	38(4)
F23	82(4)	165(9)	60(4)	31(5)	3(3)	15(5)
F24	154(9)	106(6)	98(6)	62(5)	75(6)	79(6)
C3	27.3(17)	21.6(15)	63(2)	5.2(15)	7.2(16)	6.4(13)
C4	23(2)	22(3)	41(3)	14(2)	16(2)	2(2)
C6	23.7(16)	22.5(15)	60(2)	0.5(15)	4.7(15)	3.0(12)
C10	27.0(18)	25.3(16)	73(3)	8.8(17)	14.0(17)	5.8(13)
C11	32.1(19)	25.7(17)	82(3)	10.3(18)	20(2)	7.3(14)
C12	29.0(17)	23.1(15)	52(2)	2.9(14)	8.5(15)	4.8(13)
C15	23(4)	27(4)	46(5)	9(3)	6(3)	4(3)
C16	23(4)	30(3)	30(4)	13(3)	13(3)	5(3)
C20	21.7(16)	27.8(16)	61(2)	6.2(16)	6.1(16)	3.1(13)
C23	27.2(18)	41(2)	68(2)	15.5(18)	4.7(17)	1.6(15)
C25	34.7(19)	28.5(17)	55(2)	1.8(16)	8.3(17)	7.6(14)
C26	26.6(17)	21.1(15)	65(2)	3.2(15)	13.0(16)	4.1(13)
C28	33.1(19)	29.4(17)	64(3)	6.2(17)	9.5(18)	3.3(14)
C30	24.4(17)	26.0(16)	66(2)	8.4(16)	11.2(16)	6.0(13)
C31	26.0(16)	26.9(16)	55(2)	6.2(15)	10.7(15)	5.1(13)
C32	26.7(17)	24.4(16)	58(2)	5.6(15)	6.3(15)	5.5(13)
C34	24.9(17)	28.2(17)	61(2)	3.0(16)	9.6(16)	6.9(13)
C35	33.6(19)	25.4(16)	60(2)	4.7(16)	15.2(17)	4.1(14)
C37	47(2)	45(2)	63(3)	15(2)	20(2)	19.5(19)
C40	27.3(17)	30.0(17)	62(2)	5.8(16)	3.7(16)	7.3(14)
C80A	27(7)	27(5)	64(8)	-4(5)	-10(5)	3(4)
C85A	13(4)	27(4)	42(5)	0(3)	15(3)	3(3)
C62	36(2)	36(2)	84(3)	-16(2)	-9(2)	10.9(16)
C15A	28(6)	31(6)	55(7)	10(4)	14(4)	8(4)
C4A	23(2)	22(3)	41(3)	14(2)	16(2)	2(2)
C44	37(2)	28.2(17)	63(2)	5.5(16)	19.6(18)	8.1(15)
C45	31.6(18)	26.3(16)	57(2)	5.4(16)	8.4(16)	6.7(14)
C50	27.7(18)	25.4(17)	72(3)	9.7(17)	16.8(18)	5.1(14)
C51	31.8(19)	27.8(17)	82(3)	14.7(18)	13.6(19)	6.7(14)
C52	36(2)	37.5(19)	71(3)	17.2(18)	10.3(19)	4.6(16)
B1	26.4(19)	25.9(18)	57(3)	4.3(17)	5.6(18)	4.5(15)
C58	44(2)	27.7(18)	83(3)	13.1(19)	25(2)	10.9(16)
C68	73(3)	42(2)	79(3)	21(2)	13(2)	4(2)
C71	54(3)	45(2)	81(3)	7(2)	33(2)	9(2)
C80	40(6)	40(5)	96(9)	-8(5)	-14(5)	23(5)
C85	35(4)	36(4)	72(6)	-3(4)	14(4)	10(3)
C89	52(5)	49(5)	112(8)	-29(5)	-6(5)	25(4)
F1A	42(6)	133(10)	45(6)	0(5)	15(5)	50(6)
F11A	42(7)	45(6)	83(9)	-20(5)	-9(5)	17(5)
F12A	62(6)	64(5)	64(6)	39(5)	27(5)	17(4)
F17A	25(3)	49(4)	46(3)	5(3)	8(2)	21(3)
F18A	39(3)	32(3)	51(4)	-18(3)	-8(3)	10(2)
F22A	43(3)	36(3)	67(4)	19(3)	18(3)	17(2)
C16A	29(5)	29(5)	42(7)	7(4)	23(4)	4(4)

C89A	26(4)	35(5)	40(5)	-5(3)	6(3)	5(3)
F23A	174(14)	117(10)	82(7)	22(6)	-8(9)	-80(11)
F24A	91(7)	189(15)	144(11)	112(11)	37(7)	19(7)
F20A	230(20)	111(9)	130(12)	65(10)	17(13)	117(13)
F21A	47(7)	124(12)	65(6)	-42(7)	-10(4)	47(8)
F13A	41(4)	95(7)	62(5)	18(5)	-4(3)	-27(4)
F14A	110(11)	51(4)	71(6)	20(4)	-20(7)	26(5)
N3A	51(6)	33(5)	58(5)	15(4)	23(5)	11(4)
C41A	46(7)	30(5)	46(6)	6(4)	10(6)	-4(5)
C77A	34(5)	42(6)	55(6)	12(5)	23(4)	-2(4)
C81A	36(5)	61(7)	67(6)	8(5)	26(5)	-12(4)
C79A	63(7)	58(7)	54(6)	6(6)	20(5)	-23(5)
C86A	63(8)	38(5)	53(7)	2(4)	25(6)	-17(5)
C73A	48(6)	30(4)	53(5)	7(3)	22(5)	-2(4)
C74A	89(9)	35(4)	67(6)	4(4)	38(6)	-18(5)
C88A	103(11)	19(4)	52(8)	5(4)	29(6)	-9(5)
C84A	85(8)	32(4)	58(6)	12(4)	30(5)	10(4)
C78A	57(6)	22(3)	54(6)	4(3)	28(5)	5(4)
C90A	94(9)	38(5)	59(6)	19(4)	35(6)	20(5)
C87A	87(9)	40(6)	51(6)	11(5)	16(6)	31(6)
C70A	56(6)	32(5)	62(6)	7(4)	23(5)	13(5)

Table 4 Bond Lengths for c160918_1_1.

Atom	Atom	Length/Å	Atom	Atom	Length/Å
Pd1	Cu1	2.5422(6)	F11	C16	1.310(9)
Pd1	N3	2.171(10)	F12	C16	1.314(8)
Pd1	N4	2.106(3)	F13	C23	1.294(8)
Pd1	C8	2.011(3)	F14	C23	1.379(8)
Pd1	C41	2.042(16)	F15	C71	1.307(6)
Pd1	N3A	2.128(12)	F16	C71	1.330(5)
Pd1	C41A	2.122(17)	F17	C89	1.308(9)
Cu1	C1	1.907(4)	F18	C89	1.300(9)
Cu1	C41A	2.105(18)	F19	C71	1.289(6)
N1	C1	1.369(4)	F20	C68	1.302(8)
N1	C21	1.392(5)	F21	C23	1.347(6)
N1	C22	1.439(4)	F22	C89	1.359(10)
N2	C1	1.346(4)	F23	C68	1.374(8)
N2	C2	1.399(4)	F24	C68	1.284(7)
N2	C13	1.440(4)	C3	C6	1.403(5)
N3	C70	1.339(9)	C3	C26	1.390(6)
N3	C78	1.357(10)	C4	C15	1.391(9)
N4	C9	1.371(5)	C4	C40	1.407(9)
N4	C54	1.327(5)	C6	C34	1.408(5)
C2	C19	1.488(5)	C6	B1	1.647(6)
C2	C21	1.358(5)	C10	C32	1.387(6)

C5	C8	1.416(5)	C10	C44	1.381(6)
C5	C9	1.418(6)	C11	C26	1.495(5)
C5	C48	1.423(5)	C12	C25	1.399(5)
C7	C17	1.520(5)	C12	C31	1.395(5)
C7	C22	1.394(5)	C12	B1	1.636(5)
C7	C36	1.404(5)	C15	C16	1.495(9)
C8	C38	1.377(6)	C15	C62	1.393(10)
C9	C56	1.405(5)	C20	C28	1.401(6)
C13	C14	1.397(5)	C20	C30	1.393(5)
C13	C27	1.397(5)	C20	B1	1.641(5)
C14	C18	1.516(5)	C23	C32	1.481(6)
C14	C33	1.402(5)	C23	F21A	1.245(10)
C17	C46	1.529(5)	C23	F13A	1.364(7)
C17	C49	1.528(5)	C23	F14A	1.307(9)
C18	C39	1.532(5)	C25	C44	1.389(5)
C18	C76	1.514(6)	C26	C35	1.390(5)
C21	C42	1.497(4)	C28	C52	1.392(5)
C22	C63	1.393(5)	C30	C50	1.395(5)
C24	C27	1.520(5)	C31	C32	1.392(5)
C24	C43	1.517(6)	C34	C45	1.381(6)
C24	C60	1.526(6)	C35	C45	1.389(5)
C27	C29	1.393(5)	C37	C45	1.488(5)
C29	C59	1.387(5)	C40	C80A	1.389(12)
C33	C59	1.377(6)	C40	C4A	1.412(12)
C36	C53	1.370(6)	C40	B1	1.629(5)
C38	C65	1.417(6)	C40	C80	1.424(10)
C41	C73	1.439(12)	C80A	C85A	1.399(12)
C41	C77	1.382(12)	C85A	C62	1.432(9)
C42	C69	1.542(5)	C85A	C89A	1.496(11)
C47	C54	1.399(6)	C62	C15A	1.389(12)
C47	C64	1.375(7)	C62	C85	1.409(8)
C48	C55	1.435(7)	C15A	C4A	1.386(12)
C48	C67	1.391(7)	C15A	C16A	1.490(13)
C53	C66	1.385(7)	C44	C71	1.503(6)
C55	C72	1.335(9)	C50	C51	1.385(6)
C56	C64	1.392(8)	C50	C58	1.485(6)
C56	C72	1.435(7)	C51	C52	1.387(6)
C61	C69	1.475(5)	C52	C68	1.487(7)
C61	C82	1.297(7)	C68	F23A	1.262(9)
C63	C66	1.396(6)	C68	F24A	1.362(10)
C63	C75	1.523(6)	C68	F20A	1.271(11)
C65	C67	1.365(8)	C80	C85	1.399(11)
C70	C87	1.402(10)	C85	C89	1.493(9)
C73	C78	1.419(11)	F1A	C16A	1.329(11)
C73	C86	1.405(10)	F11A	C16A	1.322(12)
C74	C86	1.411(11)	F12A	C16A	1.307(11)
C74	C88	1.379(12)	F17A	C89A	1.324(9)

C75	C83	1.524(8)	F18A	C89A	1.342(9)
C75	C91	1.537(7)	F22A	C89A	1.346(10)
C77	C81	1.415(10)	N3A	C78A	1.358(10)
C78	C84	1.416(10)	N3A	C70A	1.332(11)
C79	C81	1.388(11)	C41A	C77A	1.385(12)
C79	C86	1.401(10)	C41A	C73A	1.445(12)
C84	C88	1.425(13)	C77A	C81A	1.411(10)
C84	C90	1.390(12)	C81A	C79A	1.397(11)
C87	C90	1.384(11)	C79A	C86A	1.406(11)
F1	C16	1.325(8)	C86A	C73A	1.411(11)
F2	C11	1.353(5)	C86A	C74A	1.408(10)
F3	C11	1.333(5)	C73A	C78A	1.427(12)
F4	C37	1.336(5)	C74A	C88A	1.382(12)
F5	C58	1.347(5)	C88A	C84A	1.427(15)
F6	C58	1.345(5)	C84A	C78A	1.410(11)
F7	C37	1.332(5)	C84A	C90A	1.380(12)
F8	C37	1.353(5)	C90A	C87A	1.377(12)
F9	C11	1.342(4)	C87A	C70A	1.407(11)
F10	C58	1.342(4)			

Table 5 Bond Angles for c160918_1_1.

Atom	Atom	Atom	Angle/˚	Atom	Atom	Atom	Angle/˚
N3	Pd1	Cu1	87.9(3)	F11	C16	C15	112.3(11)
N4	Pd1	Cu1	146.62(8)	F12	C16	F1	105.5(8)
N4	Pd1	N3	96.2(3)	F12	C16	C15	110.0(10)
N4	Pd1	N3A	102.6(3)	C28	C20	B1	120.7(3)
N4	Pd1	C41A	159.4(5)	C30	C20	C28	115.9(3)
C8	Pd1	Cu1	88.42(11)	C30	C20	B1	123.1(4)
C8	Pd1	N3	170.4(3)	F13	C23	F14	101.3(8)
C8	Pd1	N4	82.13(14)	F13	C23	F21	107.7(6)
C8	Pd1	C41	103.9(4)	F13	C23	C32	119.3(6)
C8	Pd1	N3A	174.9(4)	F14	C23	C32	113.5(6)
C8	Pd1	C41A	94.1(4)	F21	C23	F14	97.8(6)
C41	Pd1	Cu1	51.0(4)	F21	C23	C32	114.4(4)
C41	Pd1	N3	80.5(4)	F21A	C23	C32	116.0(8)
C41	Pd1	N4	162.3(4)	F21A	C23	F13A	112.0(8)
N3A	Pd1	Cu1	88.6(3)	F21A	C23	F14A	111.1(12)
C41A	Pd1	Cu1	52.7(5)	F13A	C23	C32	108.6(5)
C41A	Pd1	N3A	80.8(4)	F14A	C23	C32	107.7(7)
C1	Cu1	Pd1	145.86(10)	F14A	C23	F13A	100.2(8)
C1	Cu1	C41A	160.8(5)	C44	C25	C12	122.4(4)
C41A	Cu1	Pd1	53.3(5)	C3	C26	C11	119.5(3)
C1	N1	C21	111.9(3)	C3	C26	C35	121.1(3)
C1	N1	C22	122.2(3)	C35	C26	C11	119.4(4)
C21	N1	C22	125.8(3)	C52	C28	C20	122.4(4)

C1	N2	C2	112.5(3)	C20	C30	C50	122.4(4)
C1	N2	C13	124.7(3)	C32	C31	C12	122.3(4)
C2	N2	C13	122.8(3)	C10	C32	C23	118.8(3)
C70	N3	Pd1	130.5(7)	C10	C32	C31	120.8(4)
C70	N3	C78	118.6(9)	C31	C32	C23	120.4(4)
C78	N3	Pd1	110.4(6)	C45	C34	C6	122.9(3)
C9	N4	Pd1	111.5(3)	C45	C35	C26	117.8(4)
C54	N4	Pd1	130.1(3)	F4	C37	F8	105.4(3)
C54	N4	C9	118.2(3)	F4	C37	C45	112.5(3)
N1	C1	Cu1	125.5(3)	F7	C37	F4	105.8(4)
N2	C1	Cu1	131.1(2)	F7	C37	F8	106.7(3)
N2	C1	N1	103.4(3)	F7	C37	C45	114.0(3)
N2	C2	C19	122.9(3)	F8	C37	C45	111.9(4)
C21	C2	N2	105.9(3)	C4	C40	B1	120.6(7)
C21	C2	C19	131.2(3)	C4	C40	C80	114.2(9)
C8	C5	C9	118.9(3)	C80A	C40	C4A	118.0(12)
C8	C5	C48	122.2(4)	C80A	C40	B1	120.6(8)
C9	C5	C48	118.9(4)	C4A	C40	B1	121.4(10)
C22	C7	C17	122.3(3)	C80	C40	B1	125.1(7)
C22	C7	C36	117.0(4)	C40	C80A	C85A	119.0(14)
C36	C7	C17	120.7(3)	C80A	C85A	C62	122.3(11)
C5	C8	Pd1	111.4(3)	C80A	C85A	C89A	116.1(9)
C38	C8	Pd1	132.1(3)	C62	C85A	C89A	120.2(8)
C38	C8	C5	116.4(3)	C15	C62	C85	119.9(7)
N4	C9	C5	116.0(3)	C15A	C62	C85A	115.5(10)
N4	C9	C56	122.2(4)	C62	C15A	C16A	118.7(15)
C56	C9	C5	121.7(4)	C4A	C15A	C62	121.1(18)
C14	C13	N2	117.8(3)	C4A	C15A	C16A	120.1(12)
C14	C13	C27	124.2(3)	C15A	C4A	C40	122.1(18)
C27	C13	N2	118.0(3)	C10	C44	C25	120.9(4)
C13	C14	C18	122.8(3)	C10	C44	C71	120.3(4)
C13	C14	C33	116.1(3)	C25	C44	C71	118.8(4)
C33	C14	C18	121.1(3)	C34	C45	C35	120.9(3)
C7	C17	C46	111.4(3)	C34	C45	C37	119.0(3)
C7	C17	C49	111.3(3)	C35	C45	C37	120.1(4)
C49	C17	C46	111.2(3)	C30	C50	C58	120.3(4)
C14	C18	C39	111.7(3)	C51	C50	C30	120.4(4)
C76	C18	C14	112.7(3)	C51	C50	C58	119.2(3)
C76	C18	C39	110.1(4)	C50	C51	C52	118.7(4)
N1	C21	C42	124.2(3)	C28	C52	C68	119.8(4)
C2	C21	N1	106.2(3)	C51	C52	C28	120.2(4)
C2	C21	C42	129.5(4)	C51	C52	C68	120.0(4)
C7	C22	N1	117.9(3)	C12	B1	C6	112.0(3)
C63	C22	N1	118.3(3)	C12	B1	C20	105.7(3)
C63	C22	C7	123.8(4)	C20	B1	C6	112.6(3)
C27	C24	C60	113.2(3)	C40	B1	C6	101.7(3)
C43	C24	C27	110.7(3)	C40	B1	C12	112.9(3)

C43	C24	C60	110.7(3)	C40	B1	C20	112.1(3)
C13	C27	C24	121.9(3)	F5	C58	C50	112.4(3)
C29	C27	C13	116.8(3)	F6	C58	F5	105.2(4)
C29	C27	C24	121.3(3)	F6	C58	C50	113.3(3)
C59	C29	C27	120.9(4)	F10	C58	F5	105.9(3)
C59	C33	C14	121.5(3)	F10	C58	F6	106.6(3)
C53	C36	C7	120.8(4)	F10	C58	C50	112.9(4)
C8	C38	C65	122.0(4)	F20	C68	F23	100.0(8)
C73	C41	Pd1	109.5(8)	F20	C68	C52	114.2(7)
C77	C41	Pd1	129.6(8)	F23	C68	C52	109.9(6)
C77	C41	C73	115.7(11)	F24	C68	F20	112.2(9)
C21	C42	C69	112.6(3)	F24	C68	F23	101.9(7)
C64	C47	C54	119.0(5)	F24	C68	C52	116.5(5)
C5	C48	C55	118.2(5)	F23A	C68	C52	117.0(7)
C67	C48	C5	118.3(4)	F23A	C68	F24A	105.9(11)
C67	C48	C55	123.5(4)	F23A	C68	F20A	107.2(13)
C36	C53	C66	120.7(4)	F24A	C68	C52	110.0(6)
N4	C54	C47	122.7(4)	F20A	C68	C52	115.6(12)
C72	C55	C48	122.2(4)	F20A	C68	F24A	99.2(13)
C9	C56	C72	117.8(5)	F15	C71	F16	102.5(5)
C64	C56	C9	117.6(4)	F15	C71	C44	113.9(4)
C64	C56	C72	124.6(5)	F16	C71	C44	112.2(4)
C33	C59	C29	120.5(3)	F19	C71	F15	107.3(5)
C82	C61	C69	126.2(5)	F19	C71	F16	106.5(4)
C22	C63	C66	116.6(4)	F19	C71	C44	113.7(4)
C22	C63	C75	121.6(4)	C85	C80	C40	125.3(11)
C66	C63	C75	121.8(4)	C62	C85	C89	120.0(7)
C47	C64	C56	120.0(4)	C80	C85	C62	116.2(8)
C67	C65	C38	120.4(5)	C80	C85	C89	122.0(8)
C53	C66	C63	121.2(4)	F17	C89	F22	103.2(8)
C65	C67	C48	120.6(4)	F17	C89	C85	113.0(7)
C61	C69	C42	113.7(4)	F18	C89	F17	109.5(8)
N3	C70	C87	122.9(9)	F18	C89	F22	105.7(8)
C55	C72	C56	121.3(5)	F18	C89	C85	114.2(7)
C78	C73	C41	119.0(9)	F22	C89	C85	110.3(8)
C86	C73	C41	122.6(10)	F1A	C16A	C15A	109.2(15)
C86	C73	C78	118.4(9)	F11A	C16A	C15A	114.0(17)
C88	C74	C86	119.8(11)	F11A	C16A	F1A	104.9(11)
C63	C75	C83	110.5(5)	F12A	C16A	C15A	116.9(15)
C63	C75	C91	112.1(4)	F12A	C16A	F1A	105.3(11)
C83	C75	C91	110.4(5)	F12A	C16A	F11A	105.6(11)
C41	C77	C81	123.4(10)	F17A	C89A	C85A	114.5(8)
N3	C78	C73	116.5(8)	F17A	C89A	F18A	105.2(7)
N3	C78	C84	122.0(9)	F17A	C89A	F22A	105.1(7)
C84	C78	C73	121.5(9)	F18A	C89A	C85A	112.0(8)
C81	C79	C86	121.3(9)	F18A	C89A	F22A	105.7(7)
C79	C81	C77	118.7(9)	F22A	C89A	C85A	113.4(7)

C78	C84	C88	117.4(10)	C78A	N3A	Pd1	113.1(7)
C90	C84	C78	117.9(8)	C70A	N3A	Pd1	129.4(8)
C90	C84	C88	124.7(9)	C70A	N3A	C78A	117.5(11)
C73	C86	C74	120.9(9)	Cu1	C41A	Pd1	73.9(5)
C79	C86	C73	118.2(9)	C77A	C41A	Pd1	132.8(9)
C79	C86	C74	120.9(9)	C77A	C41A	Cu1	103.7(8)
C90	C87	C70	118.3(9)	C77A	C41A	C73A	116.4(11)
C74	C88	C84	121.8(9)	C73A	C41A	Pd1	107.5(9)
C87	C90	C84	120.3(9)	C73A	C41A	Cu1	111.8(10)
C26	C3	C6	122.4(3)	C41A	C77A	C81A	122.6(11)
C15	C4	C40	122.4(13)	C79A	C81A	C77A	119.3(10)
C3	C6	C34	115.0(4)	C81A	C79A	C86A	121.4(10)
C3	C6	B1	122.3(3)	C79A	C86A	C73A	117.7(9)
C34	C6	B1	122.3(3)	C79A	C86A	C74A	120.0(10)
C44	C10	C32	117.9(3)	C74A	C86A	C73A	122.3(11)
F2	C11	C26	111.7(3)	C86A	C73A	C41A	122.5(11)
F3	C11	F2	105.9(3)	C86A	C73A	C78A	117.1(10)
F3	C11	F9	107.4(3)	C78A	C73A	C41A	120.3(9)
F3	C11	C26	113.4(3)	C88A	C74A	C86A	118.9(10)
F9	C11	F2	105.0(3)	C74A	C88A	C84A	121.7(11)
F9	C11	C26	112.7(3)	C78A	C84A	C88A	118.0(11)
C25	C12	B1	121.9(3)	C90A	C84A	C88A	124.5(9)
C31	C12	C25	115.6(3)	C90A	C84A	C78A	117.2(10)
C31	C12	B1	122.4(3)	N3A	C78A	C73A	115.9(9)
C4	C15	C16	118.7(9)	N3A	C78A	C84A	122.6(11)
C4	C15	C62	120.7(12)	C84A	C78A	C73A	121.5(10)
C62	C15	C16	120.5(10)	C87A	C90A	C84A	121.7(10)
F1	C16	C15	113.9(9)	C90A	C87A	C70A	116.5(10)
F11	C16	F1	106.7(8)	N3A	C70A	C87A	124.3(11)
F11	C16	F12	108.1(8)				

Table 6 Hydrogen Atom Coordinates (Å×10^4) and Isotropic Displacement Parameters (Å^2×10^3) for c160918_1_1.

Atom	*x*	*y*	*z*	U(eq)
H17	4588.51	1927.69	5936.74	46
H18	6734.48	5163.27	7051.39	48
H19A	5115.84	4215.84	5105.75	71
H19B	6224.47	3881.77	5050.18	71
H19C	6272.39	4763.05	5533.23	71
H24	3580.54	3362.72	5463.35	49
H29	2249.44	5182.08	5696.26	52
H33	4951.31	6747.87	6961.15	53
H36	5538.6	510.55	6900.02	61
H38	3453.18	4915.81	7585.6	57
H39A	7095.94	6143.99	6502.87	85

H39B	7927.96	6396.57	7217.43	85
H39C	6907.29	6871.96	7051.49	85
H42A	6725.67	2411.21	5248.91	52
H42B	7221.53	2158.18	5897.73	52
H43A	2878.19	3281.91	6320.63	76
H43B	2052.7	2714.76	5653.41	76
H43C	1785.63	3593.39	5984.46	76
H46A	3605.18	915.22	6560.7	68
H46B	2922.18	1238.62	5983.42	68
H46C	3572.79	1881.13	6663.56	68
H47	7772.9	5444.49	11019	76
H49A	5242.76	747.01	5430.07	78
H49B	3934.94	578.6	5218.78	78
H49C	4629.1	184.69	5747.34	78
H53	7163.13	782.59	7748.8	75
H54	6807.24	4354.49	10096.95	54
H55	5053.77	7973.24	9638.61	97
H59	3122.02	6519.43	6326.88	56
H60A	1609.69	3955.6	4910.32	84
H60B	1941.11	3088.86	4609.6	84
H60C	2630.27	3930.54	4632	84
H61	9163.8	2200.25	5601.71	66
H64	7478.04	6809.44	11048.69	88
H65	2960.52	6240.45	7586.66	74
H66	8326.92	2051.93	8069.85	79
H67	3714.89	7368.88	8493.14	85
H69A	8117.49	3643.85	5669.67	77
H69B	8635.48	3337.8	6289.27	77
H70	7418.56	3603.27	9377.34	42
H72	6340.8	7800.03	10506.01	101
H74	2996.08	458.56	7852.02	60
H75	7914.94	3710.78	7281.58	77
H76A	6275.6	6480.61	7976.17	104
H76B	7365.99	6073.92	8114.95	104
H76C	6206.55	5538.3	7990.9	104
H77	2621.79	3724.33	7547.28	45
H79	1645.45	1300.5	7389.66	57
H81	1230.79	2549.24	7158.38	54
H82A	9121.66	3329.41	4884.01	92
H82B	9757.6	2522	4834.86	92
H83A	7269.65	4065.59	8195.03	141
H83B	8498.34	4521.76	8378.71	141
H83C	8259.12	3720.03	8606.13	141
H87	8014.99	2366.08	9551.73	58
H88	4765.72	383.6	8459.79	63
H90	6752.21	1119.76	9113.15	57
H91A	9669.89	3128.71	8087.35	166

H91B	9810.91	3862.73	7769.48	166
H91C	9437.94	2931.02	7324.85	166
H3	8354.01	1621.43	2973.53	48
H4	7999.63	1124.97	1647.12	32
H10	14607.19	1512.89	2932.97	51
H25	11519.6	1121.33	1673.24	51
H28	9726.11	2097.32	1472.79	54
H30	10068.08	2800.99	3394.25	48
H31	11943.38	1674.97	3601.74	45
H34	10843.47	270.65	3261.28	48
H35	8540.71	160.72	4198.63	49
H80A	10444.83	-268.49	1864.05	57
H62	7595.79	-1109.14	322.91	76
H62A	7697.97	-1062.02	259.5	76
H4A	8210.56	1275.77	1472.58	32
H51	9506.46	4478.5	2348.94	57
H80	10508.85	-218.63	1720.1	83
H77A	2569.04	4004.77	7522.2	50
H81A	1021.04	2948.05	7050.97	67
H79A	1146.78	1621.56	7208.5	74
H74A	2183.2	640.6	7692.51	77
H88A	3858.2	344.15	8270.17	71
H90A	5854.52	875.54	8989.28	72
H87A	7357.71	1962.35	9460.1	71
H70A	7061.31	3292.71	9342.89	60

Table 7 Atomic Occupancy for c160918_1_1.

Atom	*Occupancy*	Atom	*Occupancy*	Atom	*Occupancy*
N3	0.496(16)	C41	0.496(16)	C70	0.496(16)
H70	0.496(16)	C73	0.496(16)	C74	0.496(16)
H74	0.496(16)	C77	0.496(16)	H77	0.496(16)
C78	0.496(16)	C79	0.496(16)	H79	0.496(16)
C81	0.496(16)	H81	0.496(16)	C84	0.496(16)
C86	0.496(16)	C87	0.496(16)	H87	0.496(16)
C88	0.496(16)	H88	0.496(16)	C90	0.496(16)
H90	0.496(16)	F1	0.585(10)	F11	0.585(10)
F12	0.585(10)	F13	0.585(10)	F14	0.585(10)
F17	0.585(10)	F18	0.585(10)	F20	0.585(10)
F21	0.585(10)	F22	0.585(10)	F23	0.585(10)
F24	0.585(10)	C4	0.585(10)	H4	0.585(10)
C15	0.585(10)	C16	0.585(10)	C80A	0.415(10)
H80A	0.415(10)	C85A	0.415(10)	H62	0.585(10)
H62A	0.415(10)	C15A	0.415(10)	C4A	0.415(10)
H4A	0.415(10)	C80	0.585(10)	H80	0.585(10)
C85	0.585(10)	C89	0.585(10)	F1A	0.415(10)

F11A	0.415(10)	F12A	0.415(10)	F17A	0.415(10)		
F18A	0.415(10)	F22A	0.415(10)	C16A	0.415(10)		
C89A	0.415(10)	F23A	0.415(10)	F24A	0.415(10)		
F20A	0.415(10)	F21A	0.415(10)	F13A	0.415(10)		
F14A	0.415(10)	N3A	0.504(16)	C41A	0.504(16)		
C77A	0.504(16)	H77A	0.504(16)	C81A	0.504(16)		
H81A	0.504(16)	C79A	0.504(16)	H79A	0.504(16)		
C86A	0.504(16)	C73A	0.504(16)	C74A	0.504(16)		
H74A	0.504(16)	C88A	0.504(16)	H88A	0.504(16)		
C84A	0.504(16)	C78A	0.504(16)	C90A	0.504(16)		
H90A	0.504(16)	C87A	0.504(16)	H87A	0.504(16)		
C70A	0.504(16)	H70A	0.504(16)				

Table 8 Solvent masks information for c160918_1_1.

Number	X	Y	Z	Volume	Electron count	Content
1	0.000	0.000	0.000	54.2	17.8	?
2	0.000	0.500	0.000	124.1	22.0	?
3	0.131	0.171	0.464	10.1	0.3	?
4	0.282	0.964	0.389	13.2	0.3	?
5	0.325	0.782	0.753	8.9	0.0	?
6	0.675	0.218	0.247	8.9	0.1	?
7	0.718	0.036	0.611	13.2	0.3	?
8	0.869	0.829	0.536	10.1	0.3	?

4. References

[1] P. Jolliet, M. Gianini, A. von Zelewsky, G. Bernardinelli, and H. Stoeckli-Evans, "Cyclometalated Complexes of Palladium(II) and Platinum(II): cis -Configured Homoleptic and Heteroleptic Compounds with Aromatic C⌒N Ligands," *Inorg. Chem.*, vol. 35, no. 17, pp. 4883–4888, Jan. 1996, doi: 10.1021/ic951466z.

[2] A. Adhikary, J. R. Schwartz, L. M. Meadows, J. A. Krause, and H. Guan, "Interaction of alkynes with palladium POCOP-pincer hydride complexes and its unexpected relation to palladium-catalyzed hydrogenation of alkynes," *Inorg. Chem. Front.*, vol. 1, no. 1, pp. 71–82, 2014, doi: 10.1039/C3QI00073G.

[3] A. Peppas, E. Papadaki, G. Schnakenburg, V. Magrioti, and A. I. Philippopoulos, "Heteroleptic copper(I) complexes incorporating sterically demanding diazabutadiene ligands (DABs). Synthesis, spectroscopic characterization and solid state structural analysis," *Polyhedron*, vol. 171, pp. 412–422, Oct. 2019, doi: 10.1016/j.poly.2019.07.033.

[4] G. R. Fulmer *et al.*, "NMR Chemical Shifts of Trace Impurities: Common Laboratory Solvents, Organics, and Gases in Deuterated Solvents Relevant to the Organometallic Chemist," *Organometallics*, vol. 29, no. 9, pp. 2176–2179, May 2010, doi: 10.1021/om100106e.

[5] M. Solar and N. Trapp, "μCHILL: a lightweight, modular system for handling crystalline samples at low temperatures under inert conditions," *J. Appl. Crystallogr.*, vol. 51, no. 2, pp. 541–548, Apr. 2018, doi: 10.1107/S1600576718003291.

[6] O. V. Dolomanov, L. J. Bourhis, R. J. Gildea, J. A. K. Howard, and H. Puschmann, "OLEX2 : a complete structure solution, refinement and analysis program," *J. Appl. Crystallogr.*, vol. 42, no. 2, pp. 339–341, Apr. 2009, doi: 10.1107/S0021889808042726.

[7] G. M. Sheldrick, "SHELXT - Integrated space-group and crystal-structure determination," *Acta Crystallogr. Sect. A Found. Crystallogr.*, vol. 71, no. 1, pp. 3–8, 2015, doi: 10.1107/S2053273314026370.

[8] G. M. Sheldrick, "Crystal structure refinement with SHELXL," *Acta Crystallogr. Sect. C Struct. Chem.*, vol. 71, no. Md, pp. 3–8, 2015, doi: 10.1107/S2053229614024218.

[9] G. M. Sheldrick, "A short history of SHELX," *Acta Crystallogr. Sect. A Found. Crystallogr.*, vol. 64, no. 1, pp. 112–122, 2008, doi: 10.1107/S0108767307043930.

[10] F. Weigend and R. Ahlrichs, "Balanced basis sets of split valence, triple zeta valence and quadruple zeta valence quality for H to Rn: Design and assessment of accuracy," *Phys. Chem. Chem. Phys.*, vol. 7, no. 18, p. 3297, 2005, doi: 10.1039/b508541a.

[11] M. Dolg, H. Stoll, A. Savin, and H. Preuss, "Energy-adjusted pseudopotentials for the rare earth elements," *Theor. Chim. Acta*, vol. 75, no. 3, pp. 173–194, 1989, doi: 10.1007/BF00528565.

[12] D. Andrae, U. Häussermann, M. Dolg, H. Stoll, and H. Preuss, "Energy-adjustedab initio pseudopotentials for the second and third row transition elements," *Theor. Chim. Acta*, vol. 77, no. 2, pp. 123–141, 1990, doi: 10.1007/BF01114537.

[13] B. Metz, H. Stoll, and M. Dolg, "Hartree-Fock-adjusted pseudopotentials for post-d main group elements: Application to PbH and PbO," *J. Chem. Phys.*, vol. 113, no. 7, pp. 2563–2569, 2000.

[14] K. A. Peterson, D. Figgen, E. Goll, H. Stoll, and M. Dolg, "Systematically convergent basis sets with relativistic pseudopotentials. II. Small-core pseudopotentials and correlation consistent basis sets for the post- d group 16–18 elements," *J. Chem. Phys.*, vol. 119, no. 21, pp. 11113–11123, Dec. 2003, doi: 10.1063/1.1622924.

[15] T. Leininger, A. Nicklass, W. Küchle, H. Stoll, M. Dolg, and A. Bergner, "The accuracy of the pseudopotential approximation: non-frozen-core effects for spectroscopic constants of alkali fluorides XF (X = K, Rb, Cs)," *Chem. Phys. Lett.*, vol. 255, no. 4–6, pp. 274–280, Jun. 1996, doi: 10.1016/0009-2614(96)00382-X.

[16] M. Kaupp, P. v. R. Schleyer, H. Stoll, and H. Preuss, "Pseudopotential approaches to Ca, Sr, and Ba hydrides. Why are some alkaline earth MX 2 compounds bent?," *J. Chem. Phys.*, vol. 94, no. 2, pp. 1360–1366, Jan. 1991, doi: 10.1063/1.459993.

[17] M. Dolg, H. Stoll, and H. Preuss, "Energy-adjusted a b i n i t i o pseudopotentials for the rare earth elements," *J. Chem. Phys.*, vol. 90, no. 3, pp. 1730–1734, Feb. 1989, doi: 10.1063/1.456066.

[18] X. Cao and M. Dolg, "Valence basis sets for relativistic energy-consistent small-core lanthanide pseudopotentials," *J. Chem. Phys.*, vol. 115, no. 16, pp. 7348–7355, Oct. 2001, doi: 10.1063/1.1406535.

[19] S. Grimme, J. Antony, S. Ehrlich, and H. Krieg, "A consistent and accurate ab initio parametrization of density functional dispersion correction (DFT-D) for the 94 elements H-Pu," *J. Chem. Phys.*, vol. 132, no. 15, p. 154104, Apr. 2010, doi: 10.1063/1.3382344.

[20] S. Grimme, S. Ehrlich, and L. Goerigk, "Effect of the damping function in dispersion corrected density functional theory," *J. Comput. Chem.*, vol. 32, no. 7, pp. 1456–1465, May 2011, doi: 10.1002/jcc.21759.

[21] F. Weigend, "Accurate Coulomb-fitting basis sets for H to Rn," *Phys. Chem. Chem. Phys.*, vol. 8, no. 9, p. 1057, 2006, doi: 10.1039/b515623h.

[22] J. C. Kromann, "Calculate Root-mean-square deviation (RMSD) of Two Molecules Using Rotation, GitHub, http://github.com/charnley/rmsd, Version 1.3.2." http://github.com/charnley/rmsd.

[23] W. Kabsch, "A solution for the best rotation to relate two sets of vectors," *Acta Crystallogr. Sect. A*, vol. 32, no. 5, pp. 922–923, Sep. 1976, doi: 10.1107/S0567739476001873.

[24] S. Alvarez, "A cartography of the van der Waals territories," *Dalt. Trans.*, vol. 42, no. 24, p. 8617, 2013, doi: 10.1039/c3dt50599e.

[25] S. Grimme, C. Bannwarth, and P. Shushkov, "A Robust and Accurate Tight-Binding Quantum Chemical Method for Structures, Vibrational Frequencies, and Noncovalent Interactions of Large Molecular Systems Parametrized for All spd-Block Elements (Z = 1–86)," *J. Chem. Theory Comput.*, vol. 13, no. 5, pp. 1989–2009, May 2017, doi: 10.1021/acs.jctc.7b00118.

[26] C. Bannwarth, S. Ehlert, and S. Grimme, "GFN2-xTB—An Accurate and Broadly Parametrized Self-Consistent Tight-Binding Quantum Chemical Method with Multipole Electrostatics and Density-Dependent Dispersion Contributions," *J. Chem. Theory Comput.*, vol. 15, no. 3, pp. 1652–1671, Mar. 2019, doi: 10.1021/acs.jctc.8b01176.

[27] P. Pracht, E. Caldeweyher, S. Ehlert, and S. Grimme, "A Robust Non-Self-Consistent Tight-Binding Quantum Chemistry Method for large Molecules," *ChemRxiv*, no. Md, pp. 1–19, 2019, doi: 10.26434/chemrxiv.8326202.v1.

[28] E. Caldeweyher, C. Bannwarth, and S. Grimme, "Extension of the D3 dispersion coefficient model," *J. Chem. Phys.*, vol. 147, no. 3, p. 034112, Jul. 2017, doi: 10.1063/1.4993215.

[29] E. Caldeweyher *et al.*, "A generally applicable atomic-charge dependent London dispersion correction," *J. Chem. Phys.*, vol. 150, no. 15, p. 154122, Apr. 2019, doi: 10.1063/1.5090222.

[30] S. Grimme and C. Bannwarth, "Ultra-fast computation of electronic spectra for large systems

by tight-binding based simplified Tamm-Dancoff approximation (sTDA-xTB)," *J. Chem. Phys.*, vol. 145, no. 5, p. 054103, Aug. 2016, doi: 10.1063/1.4959605.

[31] V. Ásgeirsson, C. A. Bauer, and S. Grimme, "Quantum chemical calculation of electron ionization mass spectra for general organic and inorganic molecules," *Chem. Sci.*, vol. 8, no. 7, pp. 4879–4895, 2017, doi: 10.1039/C7SC00601B.

[32] S. Grimme, "Exploration of Chemical Compound, Conformer, and Reaction Space with Meta-Dynamics Simulations Based on Tight-Binding Quantum Chemical Calculations," *J. Chem. Theory Comput.*, vol. 15, no. 5, pp. 2847–2862, May 2019, doi: 10.1021/acs.jctc.9b00143.

[33] U. Ekström, L. Visscher, R. Bast, A. J. Thorvaldsen, and K. Ruud, "Arbitrary-Order Density Functional Response Theory from Automatic Differentiation," *J. Chem. Theory Comput.*, vol. 6, no. 7, pp. 1971–1980, Jul. 2010, doi: 10.1021/ct100117s.

[34] G. te Velde *et al.*, "Chemistry with ADF," *J. Comput. Chem.*, vol. 22, no. 9, pp. 931–967, 2001, doi: 10.1002/jcc.1056.